Faculty of Science and Engineering

School of Earth and Planetary Sciences

Compound-specific Sulfur Isotope Study of Petroleum

Nannan He

This thesis is presented for the Degree of

Doctor of Philosophy

of

Curtin University

July 2020

DECLARATION

To the best of my knowledge and belief this thesis contains no material previously published by any other person except where due acknowledgment has been made.

This thesis contains no material which has been accepted for the award of any other degree or diploma in any university.

Signature: Nannan He

Date: 6 July 2020

ABSTRACT

Continuous flow measurement of the stable sulfur isotopic (δ^{34}S) values of individual organic sulfur compounds was shown to be feasible about one decade ago by gas chromatography-inductively coupled plasma mass spectrometry (GC-ICPMS). With on-going development compound specific sulfur isotope analysis (CSSIA) has proved to be a reliable analytical method used in various biogeochemical sulfur studies. Characterisation of sulfur rich (e.g. type IIS) petroleum samples has been one of the more popular applications of CSSIA, with the stable sulfur isotopic values of organic sulfur compounds (δ^{34}S$_{OSC}$) in petroleum often revealing valuable information about the organic sulfur sources and geochemical history of oils. δ^{34}S$_{OSC}$ data has helped to identify major sulfur contribution to oils in several petroleum provinces of the world (e.g. N. America, Middle East and China) and has also been shown to be sensitive to geothermal processes, particularly thermochemical sulfate reduction (TSR). There has been steady uptake of this new analytical technology by petroleum exploration and research groups investigating S-impacted petroleum, yet there is still much to learn about the S-cycle of petroleum systems. The continued development, maturity and petroleum application of CSSIA will help to further illuminate sulfur geochemical processes.

To this end, after a brief evaluation of the δ^{34}S integrity of several common laboratory pretreatment procedures to increase confidence in δ^{34}S based interpretations, the current study conducted CSSIA studies of selected petroleum samples from several prominent petroleum regions of the world. This included biodegraded petroleum from the Athabasca

oil Sands (Canada) and sour gas rich, type-IIS sourced or TSR impacted petroleum from the Bohai Bay and Tarim Basins of China.

The sulfur isotopic integrity of phase transitions accompanying solvent evaporation and column chromatography separation of polarity fractions were briefly evaluated (**Chapter 2**). The concentration and $\delta^{34}S$ dynamics of a mixture of four authentic OSCs (1-dodecanethiol, $C_{12}SH$; 1-octadecanethiol, $C_{18}SH$; benzothiophene, BT; and dibenzothiophene, DBT) dissolved in dichloromethane solvent were monitored during a controlled solvent evaporation experiment. The susceptibility of the OSCs to evaporative loss on solvent volume reduction was consistent with their respective vapor pressures, i.e. $BT > C_{12}SH > DBT > C_{18}SH$. The relatively persistent DBT and $C_{18}SH$ showed no obvious change in their $\delta^{34}S$ values over the 10 hr timeframe of the experiment. However, the more volatile $C_{12}SH$ had shown a small ^{34}S enrichment of up to +3‰ just prior to it was lost at 6.75hrs. BT completely evaporated after 25min preventing a temporal evaluation of its $\delta^{34}S$ value. Nevertheless, the results of the other OSCs suggest the $\delta^{34}S$ values of all but the most volatile petroleum OSCs are relatively stable to large volume solvent evaporation processes.

The OSCs isolated in the aromatic fractions of oils (ZS1C, Qun7) separately isolated on Al_2O_3 and $PdCl_2$ packed columns gave very similar $\delta^{34}S$ values. Higher concentrations of OSCs were obtained with the $PdCl_2$ stationary phase compared to the more traditionally used Al_2O_3, which supported a greater number and precision of $\delta^{34}S_{OSC}$ measurements. The $\delta^{34}S$ values of thioaromatics and caged-S compounds in the ZS1C oil separated using a novel methylation/demethylation method were also measured. The BTs and DBTs in this thioaromatic fraction had very similar $\delta^{34}S$ values to the same compounds in the aromatic fractions obtained with the $PdCl_2$ or Al_2O_3 columns. The thiadiamondoids

isolated in the sulfidic fraction of ZS1C oil by the methlation/demethlation method had similar $\delta^{34}S$ values to the BTs of this oil (both ~40‰ due to incorporation of ^{34}S enriched H_2S reduced from anhydrite). The consistency of $\delta^{34}S_{OSC}$ data measured in the different fractions suggests the $\delta^{34}S$ integrity of petroleum analytes is maintained by each of the separation methods tested.

In **Chapter 3**, the effects of petroleum biodegradation on $\delta^{34}S_{OSC}$ values was investigated. Whilst the $\delta^{34}S_{OSC}$ dynamics associated with thermally matured or TSR impacted oils has been well studied, the S-isotopic behavior of biodegraded oils has not yet received serious attention. After an initial failed attempt to biodegrade the OSCs in the ZS1C oil in laboratory-controlled microcosm experiments (i.e. OSC concentrations had not significantly reduced by 3 months of microcosm treatment), several extracted oils from Peace River (PR) wells of the Athabasca oil sands (Canada) were acquired from the Calgary Organic Geochemistry research team (thank-you Prof. Steve Larter). The oils from two PR wells spanned biodegradation levels (BLs) of 3 to 4 and 5 to 6, respectively. The concentrations of alkylated thioaromatics in the oils were measured by GC-MS to decrease with the progression of biodegradation down both wells. The $\delta^{34}S$ values of several alkyl-BTs measured from one well by GC-ICPMS became more enriched (≤ 6‰) with biodegradation, consistent with a kinetic control on the preferential microbial utilisation of ^{32}S. This result reveals the sensitivity of $\delta^{34}S$ values to moderate–heavy levels of biodegradation (i.e. BLs 5–6). A similar ^{34}S enrichment of alkyl-DBTs was not evident, likely because of the higher S-isotopic stability of these higher MW compounds. The contrasting $\delta^{34}S_{BT}$ and $\delta^{34}S_{DBT}$ results demonstrates the varied isotopic sensitivity of

specific OSCs. Bulk $\delta^{34}S$ values, which reflect the mean behaviour of all the OSCs in the oils, unsuprisingly showed no evidence of the biodegradation gradient in the wells.

In two separate case studies (**Chapter 4**), the CSSIA of S-rich oils and rocks from the Jinxian Sag and Dogpu Depression were conducted to investigate the regional S cycle and origins of the Type IIS sourced and gas rich petroleum reservoirs common throughout the Bohai Bay Basin (China). The $\delta^{34}S$ values in oil and source rock samples from the Zhaolanzhuang (Zh) oil field of the Jinxian Sag spanned a broad range of -5 to $+20‰$. The bitumen and kerogen fractions in the rocks gave almost identical $\delta^{34}S_{OSC}$ values indicating secondary fluids (e.g. via migration) had not impacted the bitumen fraction of the rocks. The broad range of $\delta^{34}S$ values measured in the Jinxian Sag petroleum samples was proposed to be due to temporal variations in the $\delta^{34}S$ of reduced S available for organic sulfurization in a closed system. Kinetic effects determine the H_2S reduced from SO_4^{2-} is slightly depleted in ^{34}S, and in a restricted SO_4^{2-} system the residual SO_4^{2-} would become increasingly enriched and the reduced (H_2S, pyrite) and organic sulfur (OS) pools may in turn become enriched over a similar time profile. This restricted SO_4^{2-}-$\delta^{34}S$ model was consistent with a general trend of more depleted $\delta^{34}S_{OSC}$ values for deeper Zh rocks, i.e. older OS in deeper rocks being produced from initially available reduced S whilst the younger more ^{34}S enriched OS of shallower rock reflect the subsequent input of ^{34}S enriched H_2S which mirrors the ^{34}S enrichment of the SO_4^{2-} pool of a restricted system. It remains undetermined how much this MSR reduced H_2S pool also contributes to the sour gas rich petroleum common to the Jinxian Sag. MSR and TSR have each been separately advocated in the past to be responsible for the high H_2S levels of several Zh oils. Whilst MSR is implicit in the diagenetic mechanism put forward here, it would also seem

plausible that additional externally migrated TSR sourced H_2S contributes to the very high H_2S levels (i.e. ~90%) reported in some reservoirs.

The $\delta^{34}S$ values of OSCs in a suite of 18 oils from the Dongpu Depression (Bohai Bay Basin) showed several differences consistent with five biomarker defined oil families, suggesting good potential for the use of compound specific sulfur isotopes in genetic classification of saline and freshwater lacustrine oil types. Separate correlations between some of the $\delta^{34}S_{OSC}$ data and paleo-environmental (C_{35}-/C_{34}-hopanes), thermal maturity (C_{29} sterane and mDBT parameters) and TSR ($\Delta\delta^{34}S_{BTs-DBTs} = 6–12‰$) indicators suggest each of these factors can also influence the $\delta^{34}S$ signatures of the saline oils in the Dongpu Depression. The over-lapping potential of these controls, therefore, encourages a cautious approach to S-isotopic based oil-source correlations of complex petroleum systems.

In additional case studies, CSSIA complimented by appraisal of selected biomarkers was applied to a suite of oils from three separate regions (i.e. Tazhong Uplift, Tabei Uplift and Southwest Depression) of the Tarim Basin, to help characterize S-rich oils in China's largest oil- and gas-bearing basin (**Chapter 5**). The hydrocarbon composition of most oils indicated they were a mixture of Cambrian (high gammacerane) and Ordovician (V-shaped $C_{27}–C_{29}$ sterane profile) inputs. Multiple charging was also indicated by the co-occurrence of both biodegraded (UCM) and non-biodegraded (low MW n-alkanes) oil signatures. The $\delta^{34}S_{DBTs}$ values (~17–25‰) of the Tazhong oils was inferred to reflect Cambrian strata, consistent with earlier $\delta^{34}S$ (and $\delta^{13}C$) isotopic and biomarker characterization of Tazhong oils by other groups. The very deep (>7000m) ZS1C oil showed very enriched $\delta^{34}S_{OSC}$ values (some exceeding 40‰)—also consistent with previous analyses—which was attributed to TSR. Interestingly, the TSR was shown to have a lesser (possibly negligible) impact on the $\delta^{34}S$ values of OSCs constrained within

the asphaltenes fraction of this oil by the novel application of CSSIA to a hydropyrolysis released asphaltene fraction. Inaugural CSSIA of Tabei oils revealed a relatively narrow range of δ^{34}S values (ave δ^{34}S = 18–23‰) which also correlated with the δ^{34}S values of previously analysed Cambrian source rocks. The Southwest oils were separated into two groups based on their δ^{34}S signatures. One group had relatively depleted δ^{34}S values (ave δ^{34}S$_{DBT}$: <11‰) inferred to represent more significant organic sulfur input from Ordovician rocks, whilst the other group had heavier values (ave δ^{34}S$_{DBT}$: ~22‰) which may reflect the contribution of an additional (i.e. Cambrian) source but may alternatively be influenced by TSR (confirmed to have impacted one of these oils by the GC-MS detection of thiadiamondoids).

In closing (**Chapter 6**) some final comments were provided for context and several recommendations for extending the outcomes of the research of this PhD study were suggested. The significance of newly identified trends of δ^{34}S$_{OSC}$-biodegradation and the source appraisals of Bohai Bay Basin and Tarim Basin oils was briefly reiterated. The new findings about the organic sulfur isotopic behavior of petroleum systems will ultimately assist petroleum exploration endeavors. A poignant observation however, is that most of the outcomes from the current research should be treated cautiously, until confirmed with further studies of a larger range of related or similarly relevant S rich oil samples. Various factors conspire to limit the extent, breadth and reliability of research conducted in this study including (and not limited to) the short research timeframe of PhDs; difficulty acquiring relevant S-rich petroleum samples (Nb. Australian oils typically have a low S content); the technical and time consuming nature of the organic geochemical analyses applied; and the geochemical complexity of S-impacted petroleum systems.

ACKNOWLEDGEMENTS

It's a pleasure for me to thank those who made this thesis possible. First of all, I would like to show my deep gratitude to my supervisor Prof. Kliti Grice, for granting me the opportunity to study in this excellent group and providing exceptional guidance, support, and opportunities for me to present my research in academic conferences during my PhD study. Sincere thanks to A/Prof. Paul Greenwood for being my co-supervisor. He is a very devoted, responsive, motivative and funny person with many brilliant scientific ideas, making my PhD study very productive and priceless. This thesis wouldn't have been possible without his crucial and helpful advices and edits.

Special thanks to Dr. Alex Holman, Dr. Alan Scarlett and Peter Hopper for their technical support during the experimental work. Thanks to Prof. Marco Coolen, Cornelia Wuchter, Chloe Plet, Jaime Cesar Colmenares, Gemma Spaak, Sureyya Kose, Kuldeep Dilip More, Bettina Schaefer, Matthew Campbell, Calum Fox, Danlei Wang, Yalimay Jimenez de Duarte, Darren Shawn Tek-Suen Cheah, Akthar Ekram, Charlie Gurr, Madison Tripp, Takashi Taniwaki and Sohaib Naseer for providing help in my experimental work, giving helpful advices on my research and sharing many memorable moments. Thanks also go to ARC and Curtin University for providing the funding and to all the students and staff at Curtin University who helped me during my PhD study.

The last but not the least, I would like to thank my parents, my husband and my son for their unconditional company and support, which enabled me to complete this challenging journey enjoyably and successfully.

PRIMARY PUBLICATIONS

This thesis is assembled by publications, either accepted, published, submitted and in preparation, which form the individual chapters and are listed below.

Chapter 3

Nannan He, Kliti Grice, Paul F. Greenwood. (2019) The distribution and $\delta^{34}S$ values of organic sulfur compounds in biodegraded oils from Peace River (Alberta Basin, western Canada). Organic Geochemistry 128, 16–25.

Chapter 4

Nannan He, Kliti Grice, Paul F. Greenwood. (2020) Source of organic sulfur in petroleum of the Jinxian Sag (Bohai Bay Basin, China) revealed by compound specific sulfur isotope analysis. Paper in preparation for submission to Organic Geochemistry.

Changwei Ke, Sumei Li, Hongan Zhang, **Nannan He**, Kliti Grice, Tianwu Xu Paul Greenwood. (2020) Compound specific sulfur isotopes of saline lacustrine oils from the Dongpu Depression, Bohai Bay Basin, NE China. Journal of Asian Earth Sciences, 104361.

Chapter 5

Nannan He, Kliti Grice, Guangyou Zhu, Paul F. Greenwood. (2020) δ^{34}S

characteristics of OSCs in oils from Tazhong Uplift, Tabei Uplift and

Southwest Depressions of the Tarim Basin (W. China): Paper in preparation

for submission to Organic Geochemistry.

Nannan He, Kliti Grice, Paul F. Greenwood. (2020) δ^{34}S character of organic sulfur

compounds in the pyrolysis released asphaltene fraction of a TSR impacted

oil. Paper in preparation for submission to Organic Geochemistry.

STATEMENT OF CONTRIBUTION OF OTHERS

The work presented in this thesis was primarily designed, experimentally executed, interpreted, and individual manuscripts were prepared by the first author (Nannan He). Contributions by co-authors are described below.

Chapter 2

Paul F. Greenwood and Kliti Grice assisted with the experimental design and the preparation of the manuscript. Thiophenic$_{m/dm}$ and sulfidic$_{m/dm}$ fractions of the ZS1C oil prepared using a novel methylation/demethylation method were provided by Mr Meng Wang at Petrochina's Research Institute of Petroleum and Exploration Development (RIPED, Beijing, China) for CSSIA. Malcolm T. McCulloch provided the ICPMS equipment and technical expertise.

Chapter 3

Paul F. Greenwood and Kliti Grice assisted with the experimental design and the preparation of the manuscript. Prof. Steve Larter from University of Calgary, Canada provided the samples. Malcolm T. McCulloch provided the ICPMS equipment and technical expertise.

Chapter 4

Paul F. Greenwood and Kliti Grice assisted with the experimental design and the preparation of the manuscript. Prof. Hong Lu from Institute of Geochemistry, China

Academy of Sciences, and Prof. Sumei Li from China University of Petroleum provided the samples. Malcolm T. McCulloch provided the ICPMS equipment and techniqual expertise.

Chapter 5

Paul F. Greenwood and Kliti Grice assisted with the experimental design and the preparation of the manuscript. Prof. Guangyou Zhu from Research Institute of petroleum exploration and development provided the samples. Malcolm T. McCulloch provided the ICPMS equipment and techniqual expertise.

SECONDARY PUBLICATIONS

The following correspond to manuscripts based on research conducted during the preparation of this thesis, and abstracts for conference presentations.

Peer reviewed journal article not part of this thesis:

Pagès, A., Schmid, S. Edwards, D., Barnes, S., **He, N.N.** and Grice, K. (2016) A molecular and isotopic study of paleo-environmental conditions through the middle Cambrian in the Georgina Basin, central Australia. Earth and Planetary Science Letters 447, 21–32.

Zhu, G.Y., Zhang, Y., Zhang, Z.Y., Li, T.T., **He, N.N.**, Grice, K., Neng, Y., Greenwood, P. (2018) High abundance of alkylated diamondoids, thiadiamondoids and thioaromatics in recently discovered sulfur-rich LS2 condensate in the Tarim Basin. Organic Geochemistry, 123, 136–143.

Ji, H., Li, S.M., Greenwood, P., Zhang, H.A., P, X.Q., Xu, T.W., **He, N.N.**, Quan, S. (2018) Geochemical characteristics and significance of heteroatom compounds in lacustrine oils of the Dongpu Depression (Bohai Bay Basin, China) by negative-ion fourier transform ion cyclotron resonance mass spectrometry. Marine and Petroleum Geology, 97, 568–591.

Conference abstracts

He, N.N., Grice, K. and Greenwood, P. δ^{34}S of organic sulfur compounds and the sulfur cycle of petroleum systems. Australian Organic Geochemistry Conference, 4–7 December 2016 in Fremantle, Australia. Oral presentation.

He, N.N., Grice, K. and Greenwood, P. Molecular distributions and δ^{34}S values of organic sulfur compounds in biodegraded oils from Peace River (Alberta Basin, Canada. Australian Organic Geochemistry Conference, 3-7 December 2018 in Canberra, Australia. Oral presentation.

He, N.N., Grice, K. and Greenwood, P. The variation of compound distribution and δ^{34}S values of organic sulfur compounds in biodegraded oils from Peace River, Alberta Basin, Canada. Australian Geoscience Council Convention, 14-18 October 2018 in Adelaide, Australia. Poster presentation.

LIST OF TABLES

LIST OF FIGURES

CONTENTS

CHAPTER 1

Introduction

1.1 Origin of Petroleum

The origin of petroleum has been of considerable intrigue since the 19th century (e.g. Hunt, 1863; Treibs, 1936; Eglinton and Calvin, 1976). It has attracted significant field and experimental attention, from basin appraisal to laboratory analysis and theoretical modelling (e.g. Stinnett, 1982; Tissot and Welte, 1984; Peters et al., 2005). It is now well accepted that petroleum originates from sediments containing organic matter from once-living organisms.

1.1.1 Sources of Sedimentary Organic Matter

Photosynthesis is a key part of the carbon cycle on earth producing new organic compounds. It is the ultimate source of biomass in almost all living organisms and the major source of sedimentary organic matter (OM). Non-photosynthetic biosystems, such as methanotrophic communities (Michaelis et al., 2002), rely on recycling sedimentary carbon originally produced by photosynthetic organisms.

Bacterial and green-plant photosynthesis can be represented by the following generalized reaction:

$$2H_2A + CO_2 \longrightarrow 2A + CH_2O + H_2O$$
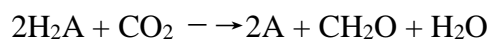
In this reaction, A is O for green plants and cyanobacteria, and is S for sulfur oxidizing bacteria. CH_2O represents OM in the form of carbohydrate. Energy from light is stored in living cells via the reaction above. Because the reaction is initiated by light, photosynthetic

organisms are restricted to the land, and the photic zone (less than ~100m) in lakes and oceans. Higher plants and phototrophic microorganisms are the predominant energy producers in land (e.g. gymnosperms) and aquatic (e.g. phytoplankton) environments.

Sedimentary OM derives from the remains of once living organisms. Archaea, eubacteria and eukarya (eukaryotes or higher organisms) represent the domains of life on earth. All three domains are genomically and biochemically distinct, as a result of early cellular evolution involving horizontal gene transfer from a communal pool (Woese et al., 1978).

Archaeal and eubacterial species are both representative of prokaryotic organisms which are difficult to fully classify/distinguish (cf. eukaryotes) due to their simple morphological structures. They are all simple, single cell organism lacking a cell nucleus. The most significant difference between archaea and eubacteria is that eubacteria (e.g. cyanophyta and some others) are colonial with specialized cells, while none of archaea has this feature.

Eukaryotic microorganisms include algae, protozoa, and fungi (molds and yeasts) as well as higher multicellular organisms. The eukaryotes have a membrane-bound nucleus and complex organelles such as mitochondria and chloroplasts which play important roles in energy generation and photosynthesis, respectively.

Organic matter is typically a minor but important fraction of sediments. The organic composition or type of sediment formed is dependent on the morphological and biochemical make-up of the major source inputs. Common biochemical constituents of organisms include proteins, cellulose, carbohydrates, lipids (i.e. fats, waxes) and lignin. Certain biochemical compounds indicative of specific biological inputs can be directly recognised in sediments (or fossil fuels). For example, steranes in petroleum source rocks or oils originate from the cell membrane sterols of eukaryotes, while hopanoids, which are

precursors of hopane biomarkers of petroleum, originate from the cell membranes of prokaryotes.

1.1.2 Preservation of Organic matter

Sedimentation

After plants and photosynthetic microorganisms die, much of their remains are rapidly mineralized (i.e. the organic components are converted to CO_2). More recalcitrant compounds may survive such diagenetic processes and be preserved as primary or secondary sedimentary products. The amount of organic material surviving diagenesis is influenced by the depositional environment, with oxygen-depleted (anoxic) environments representing the best depositional environments for OM preservation and is typical of the paleo-environments that produced organic-rich, oil-prone petroleum source rocks (Peters et al., 2005). Through earth history, almost all the organic source material of fossil fuels is preserved in marine sediments under oxygenated water along continental coasts. Biological remains can be hydrologically transported to water reservoirs (e.g. the sea or lakes) and eventually sink to the floor of the water body. During this process, numerous microbial alterations (e.g. degradation and mineralization) of OM occur in the water column or upon deposition at the sediment water interface (i.e. on the sea/lake floor).

Diagenesis, Catagenesis and Metagenesis

"Diagenesis" describes the biological, physical, and chemical alteration (such as microbial degradation, polymerization and condensation) of OM and minerals following deposition, and prior to significant burial or other thermal exposure which can act on the OM over long geological time. Diagenetic temperatures typically don't exceed 50 °C, but can lead to the initial formation of sedimentary rocks. The next stage of source rock or kerogen

formation is "catagenesis" which involves thermally mediated reactions, often over long timeframes, such as induced by deep burial. The organic composition of sediments can be thermally altered at subsurface temperatures of 50–150°C producing a large macromolecular fraction referred to by petroleum geochemists as kerogen. With increasing thermal maturity, the kerogen fraction can release hydrocarbons into a relatively free mobile petroleum phase. Subtle structural changes of some biomolecules have been correlated with increasing thermal maturity, such as the partial isomerisation of $5\alpha,14\alpha,17\alpha$ (H)-20R steranes (the isomeric form in living organisms) to $5\alpha,14\alpha,17\alpha$ (H)-20S isomers (Seifert and Moldowan, 1981). Such reactions can be useful for assessing thermal maturity level of sedimentary OM. For example, the C_{29} $\alpha\alpha\alpha$ 20S/(20R+20S) sterane ratio (Peters and Moldowan, 1991) is now an established thermal maturity parameter, increasing in value with increasing thermal maturity to a peak value of ~0.55 at high thermal maturities, corelating with vitrinite reflectance (R_0) values of approximately 1.35%. Numerous other molecular (predominantly hydrocarbon) based thermal maturity parameters have been established from many petroleum geochemical studies to help define thermal maturity of source rocks and oils across the maturity gradient (or oil maturity window) relevant to petroleum formation. At very high geological temperatures, kerogen released petroleum hydrocarbons may undergo cracking to smaller gas phase products in a process termed "metagenesis". Over-mature OM or metagenesis of residual oil in petroleum source rocks and reservoir rocks can lead to the formation of deep gas reservoirs, or more shallow ones through vertical migration. Whereas, structurally significant organic compounds can survive catagenetic conditions (i.e. in deep buried strata for many millions of years) with only minimal structural alteration, the last remaining source diagnostic biomarkers are typically destroyed during metagenesis.

1.1.3 Kerogen and oils types

The organic matter in sedimentary rocks typically consist of kerogen, bitumen and small amounts of hydrocarbon gases. Kerogen is defined as the insoluble fraction in organic solvents (Durand and Monin, 1980) and four separate types have been distinguished based on differences in basic elemental composition and petroleum formation potential (Error! Reference source not found.).

Table 1.1 Kerogen types (modified after Peters and Cassa, 1994).

Kerogen Type	Hydrogen index (mg HC/g TOC)	Atomic O/C	Atomic H/C	Main product at peak maturity
I	>600	0.03–0.1	>1.5	oil
II	300–600	<0.15	1.2–1.5	oil
III	50–200	<0.3	0.7–1.0	gas
IV	<50	<0.3	<0.7	none

Type I kerogen (very oil-prone) is immature and has high oil generation potential, with very high atomic H/C (>1.5) and very low atomic O/C (0.03–0.1) values. This kerogen type comprises hydrogen-rich amorphous alginate and have relatively uniform chemical properties. Aliphatic compounds are the main component, suggesting great contributions from lipids during diagenesis. Sulfur content is generally low.

Type II kerogen (oil prone) has good petroleum generation potential with high atomic H/C (1.2–1.5) and low atomic O/C (~0.15) values. Biological inputs include marine flora (e.g. phytoplankton, zooplankton, bacteria; Peters et al., 2005) which can interact to give the morphological appearance of liptinite macerals. Sulfur content is typically higher than other kerogen types. Exceptionally high organic sulfur (8–14 wt.%, atomic S/C $\geq$ 0.04) contents have been referred to as Type IIS kerogen (Orr, 1986). They can form when OM and metals diagenetically react with hydrogen sulfide (H_2S) or other reduced sulfur

species (e.g. S_x^{2-}, S^0) produced by sulfate-reducing bacteria in anoxic marine sediments. However, in clay-poor carbonate muds, there is insufficient iron or other metals to react with sulfide, resulting in the incorporation of excess sulfide in kerogen. Type IIS kerogens are the most common sulfur-rich kerogens, which usually occur in euxinic marine source rocks and release sulfur-rich oil.

Type III kerogen (gas prone) at high maturity has a propensity for generation of hydrocarbon gases with low H/C (0.7–1.0) and high O/C (up to 0.3) values. It typically derives from terrigenous OM (e.g. plant terpenoids) deposited in deltaic settings. Morphologically it is rich in inertinite macerals formed from higher plant input (e.g. terpenoids, lignin rich woody tissues) and fungal hyphae (Tissort and Welte, 1984; Peters et al., 2005).

Type IV kerogen (inert) is over-mature carbon rich material with negligible hydrocarbon generation potential. It typically has an amorphous carbon morphology.

Three different crude oil types have been distinguished based on the American Petroleum Institute (API) gravity (**Table 1.2**). This physical distinction is also linked to differences in sulfur content and oil types of different geographical locations can be quite varied.

Table 1.2 Classification of oil types by API gravity.

Oil types	API gravity	Content of sulfur
Light oil	> 31.1 °API	< 0.7% sulfur
Medium oil	22.3 – 31.1 °API	> 0.7% sulfur
Heavy oil	< 22.3 °API	> 0.7% sulfur

1.1.4 Petroleum system

Together with the source rock and a cap rock or seal, the sedimentary rock represents a fundamental element of all petroleum systems. The source rock or kerogen is the origin of the oil or gas as described in the previous section. The reservoir rock is the porous, permeable rock layer or layers in which hydrocarbons are accumulated and transmitted. Common sedimentary reservoir rocks are sandstone, carbonate and shale (Peters et al., 2005). The cap rock seals the top and sides so that the hydrocarbons are trapped in the reservoir, while water often seals the bottom part of the reservoir. Anticlines are the most typical formation shape for a reservoir, because its "A" shape help to trap the hydrocarbons in the top of the reservoir (Marshak, 2015). Effective seals are typically formed from impermeable rocks (e.g. some shales, anhydrite, salt).

1.1.5 Secondary alterations of petroleum

Several sedimentary and reservoir processes can cause secondary alteration of the hydrocarbon composition of oils and source rocks. The most significant of these include biodegradation, water washing, thermal alterations (e.g. oil window maturity reactions, metamorphism and thermochemical sulfate reduction) and mixing of different oil charges.

Biodegradation

Biodegradation is a common petroleum alteration occurrence which can degrade petroleum quality and its commercial value. It is limited to reservoirs cooler than approximately 80 °C as most active microbes cannot survive higher temperatures. During biodegradation hydrocarbons are transformed into other chemical products. The effects of biodegradation on the hydrocarbon composition of oils is not only of interest to petroleum explorationists, but has also been studied, optimised and harnessed by ecologists aiming

to limit the impact of petroleum pollution on the environment (Kennicutt, 1988). Petroleum biodegradation is a progressive process in which hydrocarbons are sequentially removed on the basis of varying vulnerabilities to biodegradation. Many dedicated studies of petroleum biodegradation have identified the relative susceptibilities of different hydrocarbon compounds, with several general trends including the preferential removal of lower MW compounds over higher MW compounds, and alkanes over aromatics and moreso asphaltenes and resins. More detailed biodegradation scales (**Table 1.3**) have been proposed on consideration of a large body of research on this topic (e.g. Volkman et al., 1984; Wenger et al., 2002; Greenwood et al., 2008; Larter et al., 2012). Additionally, various molecular based parameters based on the relative abundances or ratios of saturated or aromatic hydrocarbon compounds displaying a different vulnerability to biodegradation have been used to assess the extent to which crude oils have been biodegraded. (e.g. Volkman et al., 1984; Peters and Moldowan 1991; Trolio et al., 1999; Grice et al., 2000; Wenger et al., 2002; Larter et al., 2012).

Table 1.3 Biodegradation scale. Modified from Larter et al. (2012).

Biodegradation level suggested by Wenger et al. (2002)	Biodegradation level suggested by Larter et al. (2012)	Sequential Removal of Hydrocarbons
very slight	1	propane, C_{6-15} n-alkanes, carboxylic acids, C_{15+} n-alkanes, C_{6-15} isoalkanes, methane
slight	2	C_{6-15} isoprenoid alkanes, n-butane, pentanes, BTEX aromatics, naphthalenes
moderate	3	isobutane, ethane, phenanthrenes, dibenzothiophenes, alkylcyclohezanes, C_{15+} isoprenoids, chtysenes, alkylcarzazoles
heavy	4-5	regular steranes, C_{30+} hopanes, C_{27-29} hopanes
severe	6-10	triaromatic steriods, monoaromatic steriods, gammacerane, oleanane, C_{21-22} steranes, tricyclic terpanes, diasteranes, diahopanes, 25-norhopanes

Water Washing

Water washing can preferentially remove hydrocarbons of higher aqueous solubility. The moving formation waters can strip more water-soluble aromatic hydrocarbons, light alkanes and other non-hydrocarbons from oils, and can also impact the bulk physical properties of petroleum accumulations. Water washing can impact hydrocarbons during migration, reservoir storage and potentially during production (Palmer et al., 1984; Peters et al., 2005; Wang et al., 2016). It is a natural in-situ alteration process often co-occurring with biodegradation as formation water also serves to transport microbes to the sediment-water interface where biodegradation functions. It is often difficult to distinguish these two alteration processes (Wang et al., 2016).

Thermal Maturity

Increased thermal exposure during catagenesis can promote a number of reactions which can alter the hydrocarbon composition of petroleum. Thermally controlled petroleum dynamics have been related to the varied generation rate of different kerogen products (e.g. triaromatic steroids; Peters et al., 2005); the varied degradation rate of products (e.g. methyl phenathrene isomers — methylphenanthrene index (MPI); Radke and Welte, 1981) and the secondary generation of new hydrocarbon products (e.g. 20S to 20R sterane isomerisations, Peters and Moldowan, 1991). Many dedicated studies of petroleum samples at different thermal maturity levels have led to the identification of a number of such hydrocarbon compound based thermal maturity parameters sensitive to different regions of the oil maturity window.

At very high temperature (high/over oil window maturity) or metamorphic conditions the residual kerogen typically forms a highly ordered graphitic like structure, though some

amorphic morphology is also possible from some C-precursors (Jehlička et al., 2003; Kouketsu et al., 2014; Mirasol-Robert et al., 2017).

Thermochemical Sulfate Reduction

Thermochemical sulfate reduction (TSR) involves the thermally initiated reaction of petroleum hydrocarbons with mineral sulfates (i.e. anhydrite) which can occur in hot carbonate petroleum reservoirs (typically >80 °C). Sedimentary gypsum ($CaSO_4 \cdot 2H_2O$) and anhydrite ($CaSO_4$) are thermodynamically unstable when hydrocarbons are present (Worden et al., 1996), and TSR can commence at even lower temperature if $MgSO_4$ is present (Gillaizeau et al., 2001; Lu et al., 2011). The sulfate is reduced to sulfide, producing H_2S, and hydrocarbons are oxidized producing CO_2 and OSCs (e.g. thioaromatics, thiadiamondoids). Thiadiamondoids are diagnostic OSCs of TSR (Seewald, 2003; Wei et al., 2007, 2012). The TSR reaction can be simply represented as follows:

$$SO_4^{2-} + Hydrocarbons + H_2O = carbonate + CO_2 + H_2S + S^0 + OSCs + H_2O$$

TSR can significantly degrade the composition and commercial value of petroleum hydrocarbons. Normal and branched alkanes, particularly in the gasoline range, are easily oxidized. The high concentrations of toxic and corrosive H_2S and CO_2 may also lead to higher production costs. High H_2S levels poses the risk of explosions during mining operations and presents many other problems from drilling through transport to processing (Zhang et al., 2005; Zhu et al., 2005).

Oil Mixing

Two or more oils charged from the same or different source rocks may mix together during migration or reservoir accumulation. In such cases the source or alteration event information discernible from specific hydrocarbons parameters (i.e. product ratios) can be

very difficult to interpret from the combined hydrocarbon composition of the mixed oils. But often careful evaluation of distinctive molecular or isotopic features indicative of each of the original or end member oils can help establish the identity or other characteristics (e.g. thermal maturity) of respective petroleum inputs. For example, Jia et al. (2017) distinguished the presence of mixed oils from both the Tabei and Tazhong Uplifts of Tarim Basin (NE China) by measuring the δD and $\delta^{13}C$ values of n-alkane in the individual and mixed oils. The mixed Tabei oils represented charges from the same source but at different maturity stages, while the Tazhong oil was a mixture of differently sourced oils generated at different thermal maturities.

1.2 Petroleum Geochemical Analysis

A large and varied range of geochemical analytical approaches have been developed to characterize the composition and properties of organic sediments, source rocks and crude oils. Several high throughput analytical techniques (e.g. C/H/O content, total organic C, Rock-eval analysis) can help provide a basic screening of the bulk properties of potentially viable petroleum samples. From this initial data a subset of samples can be selected for more sophisticated analysis of the molecular and stable ($\delta^{13}C$, δD) isotopic composition of petroleum samples. More details of several common methods of petroleum analyses follow.

1.2.1 Bulk properties

Bulk properties of sediment, rock and crude oil samples can be revealed by analysis of their major elemental composition (C, H, O, N, S) and measurement of their total organic carbon (TOC) content. The source of petroleum samples can often be inferred from their major element composition (Durand and Monin, 1980). For example, the C/N content of shallow sediments and thermally immature sedimentary rocks can help distinguish

predominant algae (C/N=4–10) or terrigenous (C/N > 20) inputs (Silliman et al., 1996; Meyers, 1994). Atomic H/C and O/C ratios have been widely used to characterize source rocks and coals and can be applied over a wide range of thermal maturities or stages of coalification (van Krevelen, 1961; Stach et al., 1982; Taylor et al., 1998). Plots of these ratios, also known as Van Krevelen diagrams, are frequently employed to determine the different types of kerogen (Tissot et al., 1974). Sulfur is another important component influencing the properties of fossil fuels. The organic sulfur composition of kerogen and oils, which derives from the diagenetic oxidation of reduced S (i.e. H_2S or other sulfides) reacting with organic compounds (i.e. petroleum hydrocarbons) under anoxic conditions, can help distinguish sources and depositional environments (e.g. euxinic versus oxygenated marine environments; Raiswell and Berner, 1985).

TOC is often measured by the combustion of small amounts (1–2g) of ground rock, typically after the removal of inorganic carbon by acid treatments. The carbon dioxide generated by combustion can be analyzed by infrared (IR) or thermal conductivity detectors (TCDs). Some samples can be challenging to analyse including organically lean carbonate-rich rocks and thermally immature OM which is vulnerable to acid destruction (Peters et al., 2005). The TOC content of these samples can often be indirectly determined as the difference between total carbon and inorganic carbon measurements.

Rock-Eval pyrolysis is another useful method which allows inferences of elemental composition whilst also providing a reliable measurement of the thermal maturity level of source rocks/kerogens. Applied to quite small sample amounts (<100 mg), it involves the measurement of total organic carbon (TOC) by summing the carbon in the pyrolyzate with

that obtained by oxidizing the residual organic matter at 600–850 °C (Lafargue et al., 1998; Peters et al., 2005).

1.2.2 Molecular analysis

The molecular composition of petroleum samples can be analysed via a range of analytical methods. Several popular methods use chromatographic separation to help resolve the large hydrocarbon matrix of petroleum samples into simpler fractions or even isolated compounds. Other spectroscopic methods including fourier transform infrared (FTIR) analysis, nuclear magnetic resonance (NMR) analysis and ultra-violet (UV) analysis (Rontani et al., 1985; Cristadoro et al., 2009; Jain et al., 2010) can provide complimentary data about functional groups and carbon bond types.

The major gas range components of petroleum are C_1-C_4 alkanes, while CO_2, N_2, H_2S, H_2, He, and Ar are also occur common trace components. Hydrocarbon gases can be analyzed by GC, often with mass spectrometric detection in a semi-quantitative manner (Maher, 1966; Johansen et al., 1983). Truly quantitative measurements can be provided by flame ionization detectors (FID) or thermal conductivity detectors (TCD; Stadnitskaia et al., 2006; Waseda et al., 2008), but these detectors lack the direct product identification offered by the unique mass spectral signatures of organic compounds.

The higher MW condensate and liquid hydrocarbon composition of petroleum samples are also commonly analysed by GC-MS (Peters et al., 2005). Crude oils include a large number of polar constituents which are incompatible with the generally non-polar nature of GC. Hence, GC-MS is typically constrained to low polarity aliphatic and aromatic fractions of petroleum samples obtained by column chromatographic separation. Various analytical pyrolysis (Larter and Horsfield, 1993; Love et al., 2008) or chemical degradation (Javadli and Klerk, 2012; Demirbas et al., 2015) methods can be used to help

probe the macromolecular kerogen fraction of source rocks — and asphaltene fraction of oils precipitable in excess alkane solvents — to produce smaller fragments which meet the MW limits of GC (<~1000 Da).

A continuing impetus for improved resolution of the multitude of petroleum hydrocarbon constituents has led to the development and application of advanced approaches including high-performance liquid chromatography (HPLC; Kim et al., 2015; Hwang et al., 2017); two-dimensional gas chromatography (GC×GC; Dijkmans et al., 2015; Zhu et al., 2018) and chemical or thermally catalyzed derivatization processes targeting the detection of more polar analytes (Fontanive et al., 2016; Robson et al., 2017).

1.2.3 Isotopic analysis

Stable isotopic analysis of oils and source rocks can complement molecular analysis and provide additional information about the source and history of source rocks and petroleum reservoirs. The isotope ratios of hydrocarbon compounds in petroleum systems are influenced by many variables including source of origin, depositional environment and thermal maturity. Stable carbon ($\delta^{13}C$) isotopic analysis of bulk samples were first applied more than 50 years (Eckelmann et al., 1962; Parker, 1964) and given its straightforward application, quick analysis time and low cost continues to be widely applied for analyses and correlation of petroleum samples (e.g. Yeh et al., 1981) as well as to a broad range of ecological and physiological studies. Bulk δD (Schimmelmann et al., 1999; 2004; 2006) and $\delta^{34}S$ (Cai et al., 2009a; Cai et al., 2015) have also been used to characterise petroleum samples. The bulk δD of oils (which vary widely from approximately –65‰ to –220‰) and the $\delta^{34}S$ values of bulk oils (spanning the broad range of –8‰ to +32‰) having both proved useful for oil-oil correlations (e.g. Thode and Munster, 1970; Gaffney et al., 1980;

Thode 1981; Orr, 1986; Schimmelmann et al., 2004; Faure and Mensing, 2005; O'Sullivan and Kalin, 2008; Cai et al., 2009b).

More sophisticated compound specific isotope analysis (CSIA) of several petroleum elements are now available and quite routinely applied. The isotopic measurement of individual compounds greatly extends bulk isotope analysis which are often limited in resolving isotopically similar or overlapping inputs (e.g. C_3 plants and marine plankton). The organic and petroleum geochemistry communities have rapidly embraced CSIA following the first demonstrations of this capability for $\delta^{13}C$ (Freeman et al., 1990), δD (Sessions et al., 2004) and $\delta^{34}S$ (Amrani et al., 2009).

Genetically linked hydrocarbon biomarkers have similar $\delta^{13}C$ values, the integrity of which is usually maintained during diagenesis (i.e. negligible $\delta^{13}C$ fractionation), so can convey valuable information about the biosynthetic pathways inherent within sedimentary precursors. Compound specific $\delta^{13}C$ analysis has been useful for establishing the sources of OM (e.g. Murray et al., 1994; Grice et al., 2001) and for sample correlation studies (e.g. Kaplan, 1975; Schoell, 1983; Hoefs, 1997) Furthermore, systematic $\delta^{13}C$ fractionations established for common petroleum processes such as thermal maturity (Clayton et al., 1994; Chen et al., 2016), biodegradation (Griebler et al., 2004; Sun et al., 2005) and thermochemical sulfate reduction (e.g. Lu et al., 2011; Cai et al., 2013) are often evident in the $\delta^{13}C$ dynamics measured for specific hydrocarbon compounds in petroleum systems. From a more holistic viewpoint CSIA studies have helped understand many of the biogeochemical cycles on earth (e.g. Canfield and Thamdrup, 1994; Bottcher et al., 2001; Dawson et al., 2007; Maslen et al., 2011; Cai et al., 2015). However, CSIA needs to be carefully applied and interpreted as fractionation could be introduced at any of the many stages from sampling to analysis. Certain laboratory techniques (e.g. methyl

derivatization) may require use of post analysis corrections and data reduction (Whiteman et al., 2019). Another potential problem is the partial GC separation or co-elution of organic compounds. The different chromatographic dynamics of $^{12}CO_2$ (m/z 44) and $^{13}CO_2$ (m/z 45; Peters et al., 2005) can compromise the $\delta^{13}C$ measurement of compounds which are not baseline separated.

Compound specific δD analysis can similarly provide unique information about the biological source and thermal maturity of oils. For example, Dawson et al. (2007) demonstrated that the enrichment of D in pristane and phytane correlates strongly with traditional maturity parameters and that small δD differences between n-alkanes and regular isoprenoids in crude oils and source rocks was an indicator of high maturity.

The $\delta^{34}S$ analysis of the organic sulfur compounds (OSCs) of petroleum samples has been more recently demonstrated (Amrani et al., 2009). The relatively large variance in the $\delta^{34}S$ of OSCs (–20‰ to +40‰) measured in oils across several petroleum regions (e.g. Amrani et al., 2009, 2012; Cai et al., 2015, 2016; Li et al., 2015; Greenwood et al., 2015, 2018) can be attributed to the variable sensitivity and isotopic fractionation of different OSCs to the S-processes impacting petroleum systems (e.g. metabolic behavior, abiotic sulfate reduction, TSR). Further details about the petroleum application of $\delta^{34}S$ are provided in Section 1.4.

1.3 Sulfur Geochemistry

1.3.1 Sulfur Cycle

Sulfur is released into the atmosphere mainly in the form of sulfur dioxide (SO_2) by various processes including the decomposition of organic molecules, volcanic emissions and combustion of fossil fuels. Atmospheric SO_2 can enter terrestrial and marine ecosystems when it is dissolved in precipitation as weak sulfuric acid or directly impacts

the earth via atmospheric dry deposition. Weathered rocks can also release sulfates into terrestrial ecosystems. Mineralisation (i.e. decomposition) of living organisms returns sulfates to the ocean, soil and atmosphere. **Figure 1.1** shows the major routes of S cycling between the atmosphere, land and oceans.
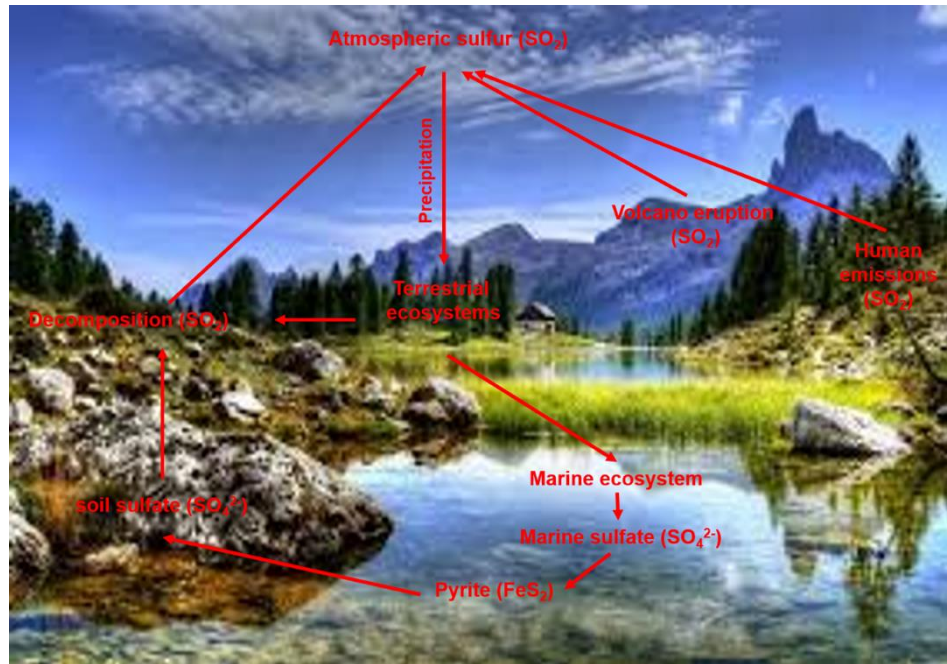
Figure 1.1 The sulfur cycle on Earth.

Geological occurrences of sulfur include many different inorganic (i.e. sulfide minerals) and organic (i.e. in soils, sediments and fossil fuel) forms. Oxidative weathering of sulfides and continental dissolution of evaporate minerals are the main source of oxidized sulfur which largely occurs on Earth as marine sulfate (SO_4^{2-}; Hurtgen, 2012). The SO_4^{2-} of marine shelf systems can be microbially reduced, in a process commonly referred to as microbial sulfate reduction (MSR) via two pathways:

(1) Assimilatory processes, which incorporate S into cell constituents (e.g. cysteine) and cause minor $\delta^{34}S$ fractionation (i.e. $< -3‰$; Kaplan and Rittenberg 1964).

(2) Dissimilatory processes, reducing SO_4^{2-} to H_2S with a large $\delta^{34}S$ fractionation (typically about $-20‰$ but can be as great as $-75‰$). This process involves bacteria and archaea in oxygen-poor environments utilising sulfate as a terminal electron acceptor for the oxidation of organic biochemicals (Canfield, 2001, Detmers et al., 2001, Brunner and Bernasconi, 2005; Canfield, 2010) as outlined by the following simplified reaction:

$$CH_4 + SO_4^{2-} = CO_3^{2-} + H_2S + H_2O$$

The reduced S from dissimilatory MSR can react with iron to form minerals or organic compounds to form organic sulfur. The major iron-sulfide based minerals are mackinawite (FeS), greigite (Fe_3S_4) and pyrite (FeS_2; Rickard and Luther, 2007; Amrani, 2014). Pyrite is the most stable sulfide mineral on Earth and is produced with minimal isotopic fractionation ($\leq 1‰$) of the source sulfide (Butler et al., 2004). The $\delta^{34}S$ of sulfide minerals are generally considered representative of ancient pore-water sulfide and have been used in the reconstruction of atmospheric compositions and redox conditions over Earth's history (Canfield et al., 2000; Fike et al., 2008).

In sedimentary rocks, organic sulfur is the second most abundant reduced S fraction, after pyrite (Anderson & Pratt 1995). Organic sulfurisation processes can lead to both intra- and inter-molecular incorporation of sulfur. The former involves the reaction of HS^- with specific functional groups (e.g. hydroxyl groups) and unsaturated bonds and can produce cyclic-S structures such as thiolanes and thiophenes. Intermolecular sulfurization involves the reactive addition of sulfide and polysulfide (S_x^{2-}) units between organic molecules, resulting in the formation of macromolecules that are cross-linked via $C-S_x-C$ bridges (Kohnen et al., 1990; Sinninghe Damste et al., 1990; Werne et al., 2004; Amrani, 2014), and are concentrated in the macromolecular fractions of source rocks (i.e. kerogen, pyrobitumen) and crude oils (i.e, asphaltenes; Ho et al. 1974, Nelson et al. 1995,

Riboulleau et al. 2000, Walters et al. 2011). A model of the sulfur cycle of sedimentary

systems during early diagenesis is shown in **Figure 1.2** (Amrani et al. 2014).
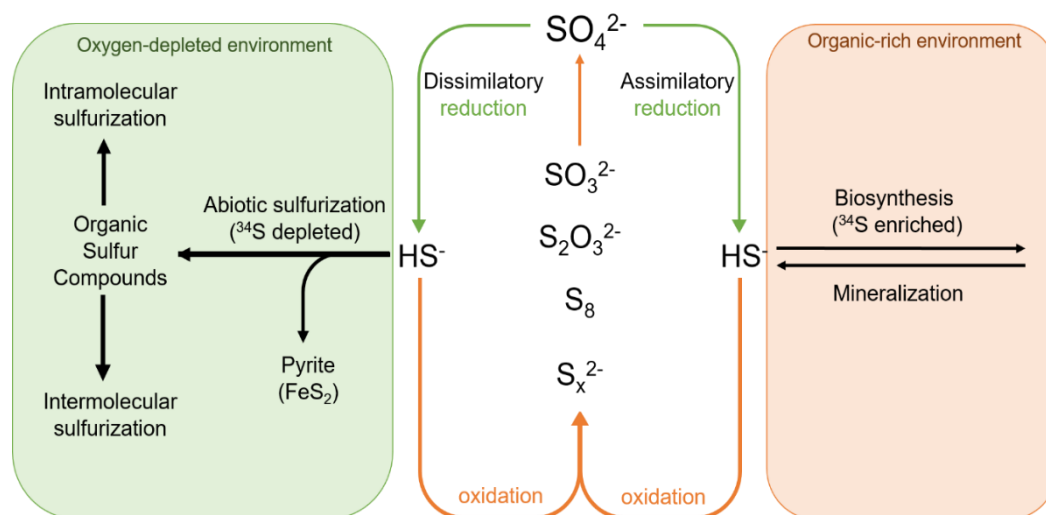
Figure 1.2 Sedimentary sulfur cycle during early diagenesis (modified from Amrani
et al. 2014).

1.3.2 Sulfur content of petroleum

Sulfur is the third most abundant element in petroleum, after carbon and hydrogen. The

average sulfur content varies from 0.03 to 7.9 mass %, with an average of 1% in crude

oils. The total geological resources of petroleum in the Earth are approximately 9.5×10^{10}

tons. The 1% average sulfur content of petroleum globally equates to approximately 10^9

of sulfur or $4–7 \times 10^{10}$ tons of organic sulfur in petroleum reservoirs (Bolshakov, 1986; Orr

and Sinninghe Damste, 1990).

Most of the sulfur in petroleum samples is present as discrete OSCs or macromolecular S_x

bridging units (all with C-S bonding). The hydrogen sulfide and elemental sulfur dissolved

in crude oils are usually a relatively small portion of their total sulfur content (TSR affected

oils being an exception). Sulfur is diagenetically incorporated into type-IIS kerogens and

subsequently oils via reactions between reduced sulfur species and functionalised organic

biomolecules (e.g. amino acids; Krein, 1993; Kok et al., 2000; Amrani and Aizenshtat, 2004). Sulfurisation can increase the geological stability of some hydrocarbon biomarkers (Sinninghe Damste et al., 1990; Kohnen et al., 1991; Adam et al., 1993, 2000).

OSCs are usually the most abundant heteroatom (NSO) compounds in petroleum samples and occur in many structural forms (Sinninghe Damste et al., 1990). These include thiols, sulfides, thiophenes and thiadiamondoids and the structures of several common petroleum OSCs are shown in **Figure 1.3**.
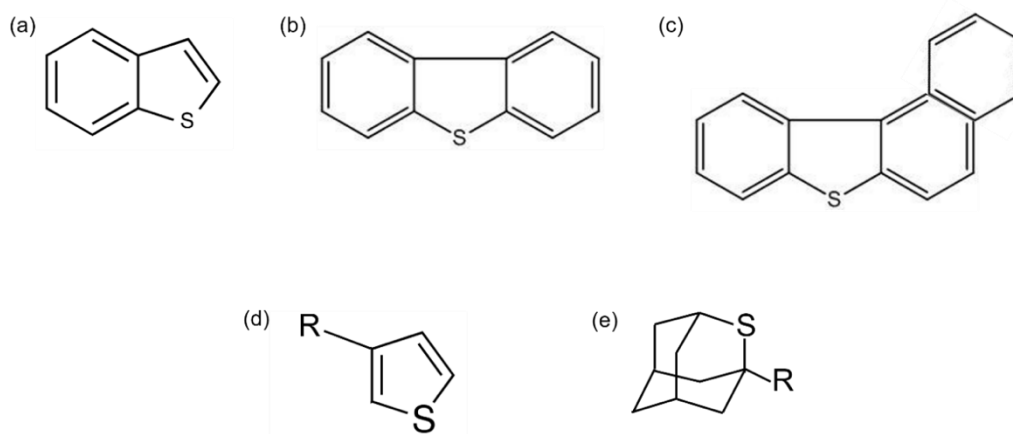
Figure 1.3 The molecular structure of common petroleum OSCs (a) benzothiophene; (b) dibenzothiophene; (c) benzonaphthothiophene; (d) alkyl-thiophene; (e) alkyl-thiaadamantane. R=alkyl substitutions.

Polynuclear thiophenes which have a thiophene unit condensed with one or more aromatic rings, such as benzothiophene (BT; **Figure 1.3a**) and dibenzothiophene (DBT; **Figure 1.3b**) are amongst the most abundant non-hydrocarbons in crude oils (Peters, et al., 2005).

High sulfur petroleum is often undesired by the petroleum industry. For instance, TSR can lead to potentially lethal levels of reservoired H_2S. Sulfur dioxide or sulfuric acid emissions from the combustion and industrial utilisation of S-containing petroleums can also result in the environmental and ecological hazard of acid rain. Robust (and expensive)

desulfurization processes are required during refinement of high S crude oils to reduce the concentrations of corrosive and toxic OSCs (Bolshakov, 1986; Javadli et al., 2012). A better understanding of the geochemical occurrence, structural forms, properties and fate of OSCs in sedimentary environments and petroleum systems will help to design exploration and production strategies to mitigate the detrimental impacts of petroleum S.

1.4 Compound Specific Sulfur Isotope Analysis

The stable isotope value of sulfur ($\delta^{34}S$) is measured using the two most abundant sulfur isotopes of ^{32}S (95.02%) and ^{34}S (4.21%). The two other isotopes of sulfur are ^{33}S (0.75%) and ^{36}S (0.02%; McNamara & Thode 1950; Ding et al. 2001). The $\delta^{34}S$ value is expressed as parts per thousand (‰) deviation against the international standard Vienna Canyon Diablo Troilite (V-CDT) according to the following equation:

$$\delta^{34}S\ (‰) = [(R_{sample} - R_{standard})/R_{standard}] \times 1000$$

where R_{sample} is the $^{34}S/^{32}S$ ratio of the sample analyte. $R_{standard}$ is the $^{34}S/^{32}S$ ratio of V-CDT = 0.044151(Werner and Brand, 2001). A negative $\delta^{34}S$ value implies that the sample is depleted in the heavy isotope relative to the standard, while a positive value means that the sample is isotopically enriched in the heavy isotope relative to V-CDT.

Werne and colleagues conducted the first compound-specific $\delta^{34}S$ analyses on OSC from the sediments of the Cariaco Basin. Seven individual sulfurised isoprenoids were isolated from large (200–250 g) samples by preparative chromatography (prep-HPLC) prior to EA-irMS analysis (Greenwood et al., 2014). Shortly later Amrani et al. (2009) invented continuous flow CSSIA at the sub-nanogram level by using a gas chromatography (GC) coupled to a multi-collector inductively coupled plasma mass spectrometry (MC-ICPMS). This innovative analytical facility interfaces chromatographic separation with subsequent ICPMS measurement of $^{34}S/^{32}S$ ratios. As GC resolved organic compounds elute into the

torch of the ICPMS they are efficiently atomized and ionised by the high energy plasma. The monoatomic $^{32}S^+$ and $^{34}S^+$ species produced from OSCs are directly measured at m/z 32 and m/z 34, respectively. This approach avoids the measurement of oxidized compounds (e.g. SO_2) —such is required for combustion-irMS analysis of $\delta^{13}C$ (i.e. CO_2) — so doesn't require any correction for oxygen isotopes. The high mass resolution (M/ΔM > ~4000) provided by modern multicollector ICPMS (MC-ICPMS) instruments (with grounded interface) sufficiently ensures a sharp separation of monoatomic sulfur and diatomic oxygen ions. The theoretical mass resolution necessary to resolve monatomic sulfur ions (e.g. m/z $^{32}S^+$ = 31.9721 Da) from O_2 ions (m/z $^{16}O_2^+$ = 31.9898 Da) is ~15 mDa. Another convenient contrast to compound specific $\delta^{13}C$ and δD analysis (where baseline separation of hydrocarbon compounds is necessary), is that there is little chromatographic separation of ^{32}S and ^{34}S. Partial integration of the sides of the co-eluting OSC peaks, or of the central most intense part of a peak, can still yield accurate $\delta^{34}S$ measurements. However, good separation of OSCs is still recommended to assist with their identification by complimentary GC-MS analysis.

Only three GC-MC-ICPMS are presently used for CSSIA: The protype instrument developed at Caltech, USA (Amrani et al., 2009) and similar instruments developed at UWA (Greenwood et al., 2015) and Hebrew University, Israel (Said-Ahmad and Amrani, 2013; Gvirtzman et al., 2015). The instrument at UWA was used for the research in this thesis. Photos of this instrument and a schematic of the GC-ICPMS system (after Amrani et al., 2009) are shown in

    (a)

    (b)

Figure 1.4. The UWA instrument consists of an Agilent 6890 GC, interfaced to a Thermo Fisher Scientific Neptune+ MC-ICPMS. The GC is coupled to the ICPMS via a purpose-built transfer line statically heated to high temperatures (~300°C) to keep GC-resolved analytes in the gas phase when being transferred to the ICP torch. The transfer line essentially comprises a deactivated capillary column (id = 0.32 µm) through a 1/8' (3.175 mm) stainless steel tube wrapped in heating ribbon and insulating wool. Flexibility of the transfer line is required to 'tune' the torch position relative to the cone/skimmer orifice (Greenwood et al., 2014). The argon makeup gas (~ 1–2 L/min) of the ICP was pre-heated by passing through a coil of 1/8" SS tubing wrapped in heating tape and maintained at 300

°C to minimize the condensation of analytes as they elute from the capillary column into the torch.

Instrument tuning and subsequent calibration of $\delta^{34}S$ values was achieved with sulfur hexafluoride (SF6) reference gas. The inert, odorless and inexpensive gas was introduced at the end of the analytical column via a simple gas inlet system. The system provides for either pulsed or continuous flow of SF6 diluted in helium to the ICPMS (Amrani et al., 2009). A continuous flow of SF6 is helpful for ICPMS tuning. Pulsed injections of SF6 are injected via micro-volume capillary loops to the carrier gas stream and result in discrete peaks during the analysis of samples which can be used for the anchor point calibration of $\delta^{34}S$ values (Greenwood et al., 2014).

The sensitivity limits for GC-ICPMS analysis of $\delta^{34}S_{OSC}$ values in petroleum and similar samples is about 50 pmol S per analyte peak (precision < 0.5‰; Amrani et al., 2009; Greenwood et al., 2015), although this can often be bettered with optimal analytical conditions (e.g. new or freshly conditioned analytical column and transfer capillary). Precision typically increases (< 0.2‰) with higher analyte concentrations.

To establish the identity and distribution of OSCs (and co-occurring hydrocarbons) all samples are typically analyzed by GC-MS prior to GC-MC-ICPMS. Column chromatography was often used to isolate polarity-based solvent fractions with target OSCs from the abundant hydrocarbon products of oils (e.g. Aromatic fraction for measurement of thioaromatics; $AgNO_3$ isolated sub-fraction for measurement of thiadiamondoids). Hydrocarbons (and many more polar oil compounds) whilst not detected by the ICPMS analysis of S can quickly degrade GC performance.

(a)

(b)
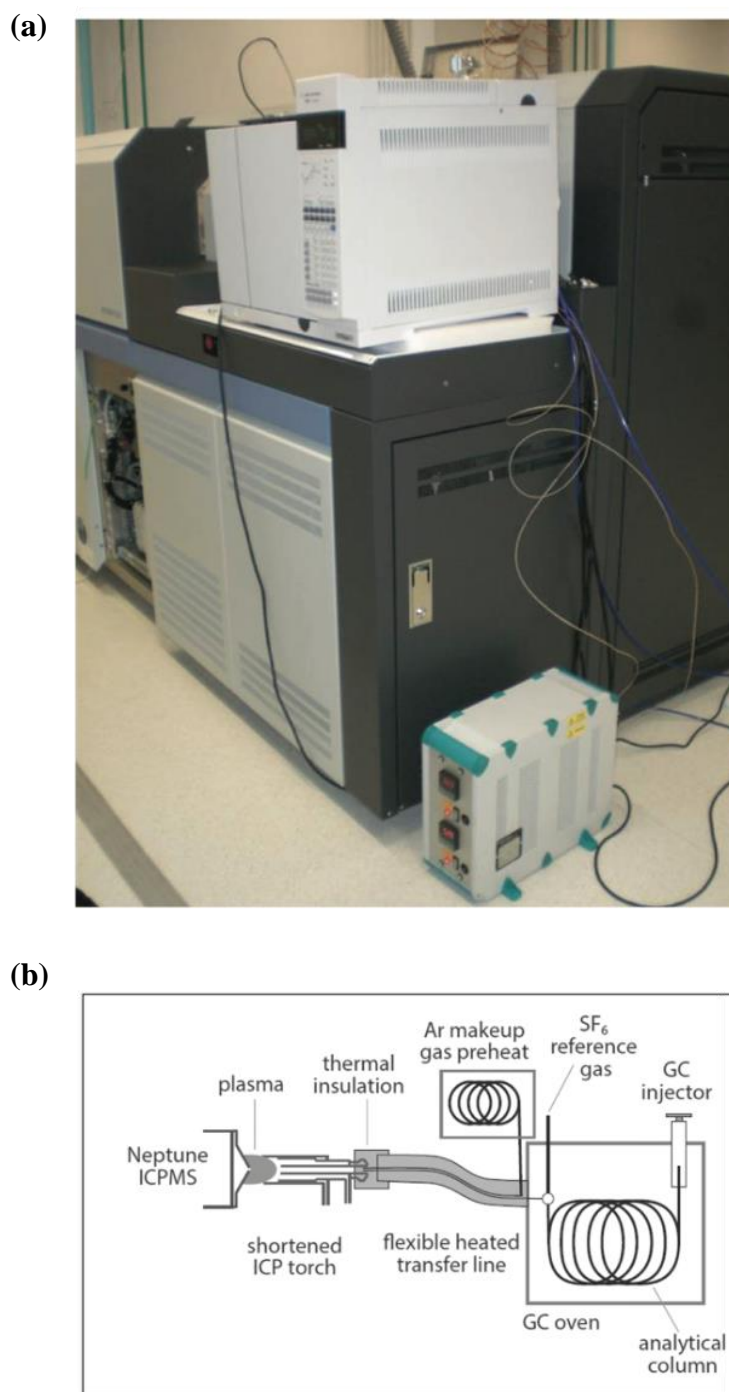
Figure 1.4 (a) GC-ICPMS at the University of Western Australia (Greenwood et al., 2015); (b) Schematic diagram of GC-ICPMS (Amrani et al., 2009).

Petroleum application of CSSIA

Petroleum OSCs generally arise from the organic oxidation of reduced S from dissimilatory MSR (i.e. diagenetic formation) or TSR. MSR produces H_2S generally reflecting a –20‰ fractionation from marine SO_4^{2-} (Engel and Zumberge, 2007), though local depositional factors can influence the metabolic functioning of microbes and the actual ^{34}S fractionation associated with the SO_4^{2-} reduction (Amrani, 2014 and references therein). Laboratory based studies have shown the organic sulfurisation of reduced S occurs with a more modest fractionation of plus several parts per thousand (e.g. ~+3‰ to +6‰; Amrani and Aizenshtat, 2004; Amrani et al., 2008). The $\delta^{34}S$ of diagenetically produced petroleum OSCs across several petroleum regions have shown a large variance (–20‰ to +40‰; Amrani et al., 2009, 2012; Cai et al., 2015, 2016; Li et al., 2015; Ellis et al., 2017; Greenwood et al., 2015, 2018) which has been useful for petroleum correlation studies, extending the useful petroleum correlation capacity that the broad bulk $\delta^{34}S$ values of petroleum (–8‰ to +32‰) have provided for many years (Gaffney et al., 1980; Faure and Mensing, 2005; Cai et al., 2009a). Several examples of $\delta^{34}S_{OSC}$ based petroleum correlation studies include: (1) the correlation of $\delta^{34}S_{DBT}$ values in Lower Paleozoic crude and Lower Cambrian source rocks in the Tarim Basin (Cai et al., 2015, 2016); (2) the $\delta^{34}S$ values of non TSR impacted natural gases of the Sichuan Basin were correlated with mudstones from the Upper Permian Longtan Formation (P_3l) and Wujiaping Formation (P_3w; Cai et al. 2017a, b); and (3) Kurdistan oils (Arabian Platform) were genetically classified by an oil–source rock correlation based on the $\delta^{34}S$ of thioaromatic compounds (Greenwood et al. 2018).

Thermo-chemical sulfate reduction (TSR) can be a significant source of natural H_2S in petroleum systems (Orr et al., 1974; Orr et al., 1977; Krouse et al., 1988), and has a large

impact on petroleum $\delta^{34}S_{OSC}$ values. The $\delta^{34}S$ values of anhydride/gypsum are generally much more enriched than the diagenetically incorporated H_2S of MSR. TSR can lead to significant ^{34}S enrichment of benzothiophene (BT) and thiadiamondoids (TDs), compared to dibenzothiophene (DBT), since the $\delta^{34}S$ values of BTs (reflecting combined $\delta^{34}S$ of diagenetic and TSR sources) is quicker to adopt the $\delta^{34}S$ signature of the mineral SO_4^{2-} source (Amrani et al., 2012) and TDs are exclusively produced by TSR (Gvirtzman et al., 2015). In severely TSR effected oils the $\delta^{34}S$ values of all OSC products may homogenise due to end equilibration with the SO_4^{2-} source (Amrani et al., 2012). The TSR impacted $\delta^{34}S_{OSC}$ trends of low-moderate TSR impacted petroleum relate to OSCs in the bitumen fraction of oils. The corresponding $\delta^{34}S$ behavior of OSCs in the macromolecular fractions of TSR altered petroleum samples (i.e. asphaltene fraction of oils, kerogen of source rocks) has not yet been established.

There have also been several reports that thermal maturity can more modestly alter the $\delta^{34}S$ of petroleum samples. Small changes in the bulk $\delta^{34}S$ values of oils and source rocks with their increasing maturity have been observed (Orr, 1986; Peters et al., 2005). Variations of up to 2‰ were detected among the gas (i.e. H_2S), bitumen and kerogen fractions of source rocks artificially matured by pyrolysis procedures (Idiz et al., 1990; Amrani et al., 2005). The impact of thermal maturity on $\delta^{34}S$ of individual OSCs in source rocks has also been recently investigated. A series of pyrolysis experiments on sulfur-rich source rocks at different temperatures (200–400 °C) and pressures (≤50 psi) showed a small $\delta^{34}S$ enrichment (≤ 4‰) of alkyl-thiophenes and alkyl-thiolanes with increasing maturity (Rosenberg et al., 2017). Ellis et al. (2017) also observed that the $\delta^{34}S$ values of both BTs and DBTs in oils from the Big Horn Basin (USA) generally become heavier

with an increase in thermal maturity, and also homogenised such that the difference between them (i.e. $\Delta\delta^{34}S_{BTs\text{-}DBTs}$) decreased.

1.5 Aims of Thesis

CSSIA is still a relatively new technique and many application areas may be considered at an immature stage of development. Petroleum characterization by CSSIA has attracted some early attention from the petroleum and geochemical research communities and might be considered one of the more advanced CSSIA applications areas. The $\delta^{34}S$ distributions of petroleum OSCs has proved useful for several oil correlation studies and has proved sensitive to increasing thermal exposures, particularly in environments supporting TSR. This PhD research applies CSSIA to selected suites of biodegraded sand oils (Athabasca, Canada) and sour gas rich, type-IIS sourced or TSR impacted petroleum from Bohai Bay Basin and Tarim Basin (both of China). Specific aims include greater understanding of the sources and formation pathways of the organic sulfur present in the S-rich samples selected for study; new information about the $\delta^{34}S_{OSC}$ behavior of biodegraded oils; and further insight into the impacts of TSR on the $\delta^{34}S$ character of oils, including the organic sulfur of different oil fractions. The overarching aims are to extend the petroleum application of CSSIA analyses and further illuminate the sulfur cycle of petroleum systems.

References

Amrani, A. (2014) Organosulfur compounds: Molecular and isotopic evolution from biota to oil and gas. Annual review earth planetary science 42, 733–768.

Amrani, A., Aizenshtat, Z. (2004) Mechanisms of sulfur introduction chemically controlled: $\delta^{34}S$ imprint. Organic Geochemistry 35, 1319–1336.

Amrani, A., Deev, A., Sessions, A.L., Tang, Y.C., Adkins, J.F., Hill, R.J., Moldowan, L.M., Wei, Z.B. (2012) The sulfur-isotopic compositions of benzothiophenes and dibenzothiophenes as a proxy for thermochemical sulfate reduction. Geochimica et Cosmochimica Acta 84, 152–164.

Amrani, A., Lewan, M. D., & Aizenshtat, Z. (2005) Stable sulfur isotope partitioning during simulated petroleum formation as determined by hydrous pyrolysis of Ghareb Limestone, Israel. Geochimica et Cosmochimica Acta 69, 5317–5331.

Amrani, A., Ma, Q., Ahmad, W. S., Aizenshtat, Z., & Tang, Y. (2008) Sulfur isotope fractionation during incorporation of sulfur nucleophiles into organic compounds. Chemical Communications (11), 1356–1358.

Amrani, A., Sessions, A.L., Adkins, J.F. (2009) Compound-specific δ^{34}S analysis of volatile organics by coupled GC/multicollector-ICPMS. Analytical Chemistry 81, 9027–9034.

Anderson, T.F. and Pratt, L.M. (1995) Isotopic evidence for the origin of organic sulfur and elemental sulfur in marine sediments. ACS Symposium Series 612, 378–396.

Bolshakov, G.F. (1986) Organic sulfur compounds of petroleum. Journal of Sulfur Chemistry 5, 103–393.

Bottcher, M.E., Thamdrup, B., Vennemann, T.W. (2001) Oxygen and sulfur isotope fractionation during anaerobic bacterial disproportionation of elemental sulphur. Geochimica et Cosmochimica 65, 1601–1609.

Brunner, B. and Bernasconi, S.M. (2005) A revised isotope fractionation model for dissimilatory sulfate reduction in sulfate reducing bacteria. Geochimica et Cosmochimica Acta 69, 4759–4771.

Butler, I.B., Bottcher, M.E., Rickard, D., Oldroyd, A. (2004) Sulfur isotope partitioning during experimental formation of pyrite via the polysulfide and hydrogen sulfide pathways: Implications for the interpretation of sedimentary and hydrothermal pyrite isotope records. Earth and Planetary Science Letters 228, 495–509.

Cai C., Li K., Anlai M., Zhang C., Xu Z., Worden R.H., Wu G., Zhang B., Chen L. (2009a) Distinguishing Cambrian from Upper Ordovician source rocks: Evidence from sulfur isotopes and biomarkers in the Tarim Basin. Organic Geochemistry 40, 755–776.

Cai, C.F., Zhang, C.M., Cai, L.L., Wu, G.H., Jiang, L., et al. (2009b) Origins of Palaeozoic oils in the Tarim Basin: Evidence from sulfur isotopes and biomarkers. Chemical Geology 268, 197–210.

Cai, C., Zhang, C., He, H., Tang, Y. (2013) Carbon isotope fractionation during methane-dominated TSR in East Sichuan Basin gasfields, China: A review. Marine and Petroleum Geology 48, 100–110.

Cai, C.F., Zhang, C.M., Worden, R.H., Wang, T.K., Li, H.X., et al. (2015) Application of sulfur and carbon isotopes to oil-source rock correlation: A case study from the Tazhong area, Tarim Basin, China. Organic Geochemistry, 83–84, 140–152.

Cai, C., Amrani, A., Worden, R.H., Xiao, Q., Wang, T., Gvirtzman, Z., Li, H., Said-Ahmad, W. and Jia, L. (2016) Sulfur isotopic compositions of individual organosulfur compounds and their genetic links in the Lower Paleozoic petroleum pools of the Tarim Basin, NW China. Geochimica et Cosmochimica Acta 182, 88–108.

Cai, C., Xu, C., He, W., Zhang, C., Li, H. (2017a) Biomarkers and C and S isotopes of the Permian to Triassic solid bitumen and its potential source rocks in NE Sichuan Basin. Geofluids, 2017.

Cai, C., Xiang, L., Yuan, Y., Xu, C., He, W., Tang, Y., Borjigin, T. (2017b) Sulfur and carbon isotopic compositions of the Permian to Triassic TSR and non-TSR altered solid bitumen and its parent source rock in NE Sichuan Basin. Organic Geochemistry 105, 1–12.

Canfield, D.E. (2001) Biogeochemistry of sulfur isotopes. Mineralogy and Geochemistry, 43, 607–636.

Canfield, D.E., Farquhar, J., Zerkle, A.L. (2010) High isotope fractionations during sulfate reduction in a low-sulfate euxinic ocean analog. Geology 38, 415–418.

Canfield, D.E., Habicht, K.S., Thamdrup, B. (2000) The Archean sulfur cycle and the early history of atmospheric oxygen. Science 288, 658–661.

Canfield, D.E., Thamdrup, B. (1994) The production of ^{34}S-depleted sulfide during bacterial disproportionation of elemental sulphur. Science 266, 1973–1975.

Chen, Y., Tian, C., Li, K., Cui, X., Wu, Y., Xia, Y. (2016). Influence of thermal maturity on carbon isotopic composition of individual aromatic hydrocarbons during anhydrous closed-system pyrolysis. Fuel 186, 466–475.

Clayton, C.J., Bjorøy, M. (1994) Effect of maturity on ^{13}C/^{12}C ratios of individual compounds in North Sea oils. Organic Geochemistry 21, 737–750.

Cristadoro, A., Kulkarni, S.U., Burgess, W.A., Cervo, E.G., Räder, H.J., Müllen, K., Thies, M.C. (2009) Structural characterization of the oligomeric constituents of petroleum pitches. Carbon 47, 2358–2370.

Dawson, D., Grice, K., Alexander, R., Edwards, D. (2007) The effect of source and maturity on the stable isotopic compositions of individual hydrocarbons in sediments and crude oils from the Vulcan Sub-basin, Timor Sea, Northern Australia. Organic Geochemistry 38, 1015–1038.

Demirbas, A., Alidrisi, H., Balubaid, M.A. (2015) API gravity, sulfur content, and desulfurization of crude oil. Petroleum Science and Technology 33, 93–101.

Detmers, J., Brüchert, V., Habicht, K. S., Kuever, J. (2001) Diversity of sulfur isotope fractionations by sulfate-reducing prokaryotes. Applied and Environmental Microbiology 67, 888–894.

Dijkmans, T., Djokic, M.R., van Geem, K.M., Marin, G.B. (2015) Comprehensive compositional analysis of sulfur and nitrogen containing compounds in shale oil using GC× GC-FID/SCD/NCD/TOF-MS. Fuel 140, 398–406.

Ding, T., Valkiers, S., Kipphardt, H., De Bi`ever, P., Taylor, P.D.P., et al. (2001) Calibrated sulfur isotope abundance ratios of three IAEA sulfur isotope

reference materials and V-CDT with a reassessment of the atomic weight of sulfur. Geochimica et Cosmochimica Acta 65, 2433–2437.

Durand, B. and Monin, J.C. (1980) Elemental analysis of kerogens (C, H, O, N, S, Fe). In: Kerogen. Insoluble Organic Matter from Sedimentary Rocks (B. Durand, ed.), Editions Technip, Paris, pp. 113–142.

Eckelmann, W.R., Broecker, W.S., Whitlock, D.W., Allsup, J.R. (1962) Implications of carbon isotopic composition of total organic carbon of some recent sediments and ancient oils. AAPG bulletin 46, 699–704.

Eglinton, G. and Calvin, M. (1967) Chemical fossils. Scientific American 216, 32–43.

Engel, M.H., Zumberge, J.E. (2007) Secular change in the stable sulfur isotope composition of crude oils relative to marine sulfates and sulfides. Book of Abstracts, International Meeting of Organic Geochemistry 2007 (Torquay, UK, September 19–24,). pp. 523–524.

Ellis, G.S., Said-Ahmad, W., Lillis, P.G., Shawar, L., Amrani, A. (2017) Effects of thermal maturation and thermochemical sulfate reduction on compound-specific sulfur isotopic compositions of organosulfur compounds in Phosphoria oils from the Bighorn Basin, USA. Organic Geochemistry 103, 63–78.

Faure, G. and Mensing, T.M. (2005) Isotopes, Principles and Applications, John Wiley & Sons, Hoboken, NJ, 3rd Ed.

Fike, D.A., Grotzinger, J.P. (2008) A paired sulfate-pyrite $\delta^{34}S$ approach to understanding the evolution of the Ediacaran-Cambrian sulfur cycle. Geochimica et Cosmochimica Acta 72, 2636–2648.

Fontanive, F.C., Souza-Silva, É.A., da Silva, J.M., Caramão, E.B., Zini, C.A. (2016) Characterization of sulfur and nitrogen compounds in Brazilian petroleum derivatives using ionic liquid capillary columns in comprehensive two-dimensional gas chromatography with time-of-flight mass spectrometric detection. Journal of Chromatography A 1461, 131–143.

Freeman, K.H., Hayes, J.M., Trendel, J.M., Albrecht, P. (1990) Evidence from carbon isotope measurements for diverse origins of sedimentary hydrocarbons. Nature 343, 254–256.

Gaffney, J.S., Premuzic, E.T., Manowitz, B. (1980) On the usefulness of sulfur isotope ratios in crude oil correlations. Geochimica et Cosmochimica Acta 44, 135–139.

Gillaizeau, B. and Tang, Y. (2001) Reaction mechanistic studies for the thermochemical sulfate reduction. In Abstract for 20th International Meeting on Organic Geochemistry, Nancy, France (p. 81).

Greenwood, P.F., Wibrow, S., George, S.J., Tibbett, M. (2008) Sequential hydrocarbon biodegradation in a soil from arid coastal Australia, treated with oil under laboratory-controlled conditions. Organic Geochemistry 39, 1336–1346.

Greenwood, P.F., Amrani, A., Sessions, A., Raven, M.R., Holman, A., Dror, G., Grice, K., McCulloch, M.T., Adkins, J.F. (2015) Development and Initial Biogeochemical Applications of Compound-Specific Sulfur Isotope Analysis. In: Principles and Practice of Analytical Techniques in Geosciences. The Royal Society of Chemistry, UK.

Greenwood, P.F., Mohammed, L., Grice, K., McCulloch, M., Schwark, L. (2018) The application of compound-specific sulfur isotopes to the oil-source rock correlation of Kurdistan petroleum. Organic geochemistry 117, 22–30.

Grice, K., Alexander, R., Kagi, R.I. (2000) Diamondoid hydrocarbon ratios as indicators of biodegradation in Australian crude oils. Organic Geochemistry 31, 67–73.

Grice, K., Audino, M., Boreham, C.J., Alexander, R., Kagi, R. (2001) Distributions and stable carbon isotopic compositions of biomarkers in torbanites from different palaeogeographical locations. Organic Geochemistry 32, 1195–1210.

Griebler, C., Safinowski, M., Vieth, A., Richnow, H.H., Meckenstock, R.U. (2004). Combined application of stable carbon isotope analysis and specific

metabolites determination for assessing in situ degradation of aromatic hydrocarbons in a tar oil-contaminated aquifer. Environmental science and technology 38(2), 617–631.

Gvirtzman, Z., Said-Ahmed, W., Ellis, G.S., Hill, R.J., Moldowan, J.M., Wei, Z.B., Amrani, A. (2015) Compound-specific sulfur isotope analysis of thiadiamondoids of oils from the Smackover Formation, USA. Geochimica et Cosmochimica Acta 167, 144–161.

Ho, T.Y., Rogers, M.A., Drushel, H.V., Koons, C.B. (1974) Evolution of sulfur compounds in crude oils. AAPG Bulletin 58, 2338–2348.

Hoefs, J. (1997) Stable Isotope Geochemistry. Springer-Verlag, New York.

Hunt T. S. (1863) Report on the Geology of Canada. Canadian Geological Survey report: Progress to 1863.

Hurtgen, M.T. (2012) The Marine Sulfur Cycle, Revisited. Science 337, 305–306.

Hwang, I.H., Youn, J.M., Doe, J.W., Park, T.S., Kang, H.K., Ha, J.H., Na, B.G. (2017) Study on the applicability analysis of HPLC for fuel marker (Unimark 1494DB) in petroleum products. Journal of the Korean Applied Science and Technology 34(4), 1076–1084.

Idiz, E.F., Tannenbaum, E., Kaplan, I.R. (1990) Pyrolysis of high-sulfur Monterey kerogens: Stable isotopes of sulfur, carbon, and hydrogen.

Jain, P.S., Bari, S.B. (2010) Isolation of lupeol, stigmasterol and campesterol from petroleum ether extract of woody stem of Wrightia tinctoria. Asian Journal of Plant Sciences 9(3), 163.

Javadli, R., de Klerk, A. (2012) Desulfurization of heavy oil. Applied Petrochemical Research 1, 3–19.

Jehlička, J., Urban, O., Pokorný, J. (2003) Raman spectroscopy of carbon and solid bitumens in sedimentary and metamorphic rocks. Spectrochimica Acta Part A 59, 2341–2352.

Jia, W.L., Chen, S.S., Zhu, X.X., Peng, P.A., Xiao, Z.Y., 2017. D/H ratio analysis of pyrolysis-released *n*-alkanes from asphaltenes for correlating oils from different sources. Journal of Analytical and Applied Pyrolysis 126, 99–104.

Johansen, N.G., Ettre, L.S., Miller, R.L. (1983) Quantitative analysis of hydrocarbons by structural group type in gasolines and distillates: I. Gas chromatography. Journal of Chromatography A 256, 393–417.

Kaplan, I. R. (1975) Stable isotopes as a guide to biogeochemical processes. Proceedings of the Royal Society of London, 189, 183–211.

Kaplan, I.R. and Rittenberg, S.C. (1964) Microbiological fractionation of sulphur isotopes. Microbiology 34, 195–212.

Kennicutt, M.C., 1988. The effect of biodegradation on crude oil bulk and molecular composition. Oil and Chemical Pollution 4, 89–112.

Kim, D., Jin, J.M., Cho, Y., Kim, E.H., Cheong, H.K., Kim, Y.H., Kim, S. (2015) Combination of ring type HPLC separation, ultrahigh-resolution mass spectrometry, and high field NMR for comprehensive characterization of crude oil compositions. Fuel 157, 48–55.

Kohnen, M.E.L., Damste, J.S.S., van Dalen, A.C.K., Haven, H.L.T., Rullkotter, J., De Leeuw, J.W. (1990) Origin and diagenetic transformations of C_{25} and C_{30} highly branched isoprenoid sulphur compounds: Further evidence for the formation of organically bound sulphur during early diagenesis. Geochimica et Cosmochimica Acta 54, 3053–3063.

Kok, M.D., Schouten, S., Sinninghe Damste, J.S. (2000) Formation of insoluble, nonhydrolyzable, sulfur-rich macromolecules via incorporation of inorganic sulfur species into algal carbohydrates. Geochimica et Cosmochimica Acta 64, 2689–2699.

Kouketsu, Y., Mizukami, T., Mori, H., Endo, S., Aoya, M., Hara, H., Nakamura, D., Wallis, S. (2014) A new approach to develop the Raman carbonaceous material geothermometer for low-grade metamorphism using peak width. Island Arc 23, 33–50.

Krein, E.B. (1993) Organic sulfur in the geosphere: analysis, structure and chemical processes. See Patai & Rappoport 1993, pp. 975–1032.

Krouse, H.R., Viau, C.A., Eliuk, L.S., Ueda, A., Halas, S. (1988) Chemical and isotopic evidence of thermochemical sulphate reduction by light hydrocarbon gases in deep carbonate reservoirs. Nature 333, 415–419.

Lafargue, E., Marquis, F. and Pillot, D. (1998) Rock-Eval 6 applications in hydrocarbon exploration, production, and soil contamination studies. Revue de l'Insitut Francais du Petrole 53, 421–437.

Larter, S., Huang, H., Adams, J., Bennett, B., Snowdon, L.R. (2012) A practical biodegradation scale for use in reservoir geochemical studies of biodegraded oils. Organic Geochemistry 45, 66–76.

Larter, S. R. and Horsreld, B. (1993) Determination of structural components of kerogens by the use of analytical pyrolysis methods. In Organic Geochemistry, eds. M. H. Engel and S. A. Macko, pp. 271–288. Plenum Press, NY.

Li, S., Amrani, A., Pang, X., Yang, H., Said-Ahmad, W., Zhang, B. and Pang, Q. (2015) Origin and quantitative source assessment of deep oils in the Tazhong Uplift, Tarim Basin. Organic Geochemistry 78, pp.1–22.

Love, G.D., Stalvies, C., Grosjean, E., Meredith, W. (2008) Analysis of molecular biomarkers covalently bound within Neoproterozoic sedimentary kerogen. The paleontological Society Papers 14, 67–83.

Lu, H., Greenwood, P., Chen, T., Liu, J., Peng, P.A. (2011) The role of metal sulfates in thermochemical sulfate reduction (TSR) of hydrocarbons: Insight from the yields and stable carbon isotopes of gas products. Organic geochemistry, 42(6), 700–706.

Maher, T.P. (1966) Semi-quantitative analysis of hydrocarbon mixtures by gas chromatography without complete separation of components. Journal of Chromatographic Science 4, 355–362.

Marshak, S. (2015) Earth: Portrait of a Planet, 3rd Ed. New York, NY, U.S.A, W.W. Norton & Company.

Maslen, E., Grice, K., Le Metayer, P., Dawson, D., Edwards, D. (2011) Stable carbon isotopic compositions of individual aromatic hydrocarbons as source and age indicators in oils from western Australian basins. Organic Geochemistry 42, 387–398.

McNamara, J., Thode, H.G. (1950) Comparison of the isotope constitution of terrestrial and meteoritic sulfur. Physical Review Journals 78, 307–308.

Meyers, P. A. (1994) Preservation of elemental and isotopic source identification of sedimentary organic matter. Chemical Geology 144, 289–302.

Michaelis, W., Seifert, R., Nauhaus, K., et al. (2002) Microbial reefs in the Black Sea fueled by anaerobic oxidation of methane. Science 297, 1013–1015.

Mirasol-Robert, A., Grotheer, H., Bourdet, J., Suvorova, A., Grice, K., McCuaig, T.C., Greenwood, P.F. (2017) Evidence and origin of the different types of sedimentary organic matter and its implications on Paleoproterozoic orogenic gold mineralisation Precambrian Research) 299, 319–338.

Murray, A.P., Summons, R.E., Boreham, C.J., Dowling, L.M. (1944) Biomarker and *n*-alkane isotope profiles for Tertiary oils: Relationship to source rock depositional setting. Organic Geochemistry 22, 521–542.

Nelson, B.C., Eglinton, T.I., Seewald, J.S., Vairavamurthy, M.A., Miknis, F.P. (1995) Transformations in organic sulfur speciation duringmaturation ofmonetary shale: Constraints from laboratory experiments. ACS Symposium Series 612, 138–166.

Orr, W.L. (1974) Changes in sulfur content and isotopic ratios of sulfur during petroleum maturation: Study of Big Horn Basin Paleozoic oils. AAPG Bulletin 58, 2295–2318.

Orr, W.L. (1977) Geologic and geochemical controls on the distribution of hydrogen sulfide in natural gas. In Advances in Organic Geochemistry 1975, ed. R Campos and J Goni, Oxford, UK, pp. 571–597.

Orr, W.L. (1986) Kerogen/asphaltene/sulfur relationships in sulfur-rich Monterey oils. Organic Geochemistry 10, 499–516.

Orr, W.L. and Sinninghe Damste, J.S.S. (1990) Geochemistry of Sulfur in Petroleum Systems. ACS Symposium Series 429, 2–29.

O'Sullivan, G. and Kalin, R.M. (2008) Investigation of the range of carbon and hydrogen isotopes within a global set of gasolines. Environmental Forensics 9, pp. 166–176.

Palmer, S.E. (1984) Effect of water washing on $C_{15}+$ hydrocarbon fraction of crude oils from northwest Palawan, Phillipines. American Association of Petroleum Geologists Bulletin 68, 137–149.

Parker, P. L. (1964) The biogeochemistry of the stable isotopes of carbon in a marine bay. Geochimica et Cosmochimica Acta 28, 1155–1164.

Peters, K.E. and Cassa, M.R. (1994) Applied source rock geochemistry. In: The Petroleum System—From Source to Trap (L. B. Magoon and W. G. Dow, eds.), American Association of Petroleum Geologists, Tulsa, OK, pp. 93–117.

Peters, K.E., Moldowan, J.M. (1991) Effects of source, thermal maturity, and biodegradation on the distribution and isomerization of homohopanes in petroleum. Organic Geochemistry 17, 47–61.

Peters, K.E., Walters, C.C., Moldowan, J.M. (2005) The Biomarker Guide. V1: Biomarkers and Isotopes in the Environment and Human History, 2nd Ed. Cambridge University Press, UK.

Pompeckj, J.F. (1901) Die Jura-Ablagerungen zwischen Regensburg und Regenstauf. Geologisches Jahrbuch 14, 139–220 (in German).

Radke, M. and Welte, D.H. (1981) Advances in Organic Geochemistry. Wiley, Chichester, 1983, pp. 504–512.

Raiswell, R. and Berner, R.A. (1985) Pyrite formation in euxinic and semi-euxinic sediments. American Journal of Science 285, 710–724.

Riboulleau, A., Derenne, S., Sarret, G., Largeau, C., Baudin, F., Connan, J. (2000) Pyrolytic and spectroscopic study of a sulphur-rich kerogen from the "Kashpir oil shales" (Upper Jurassic, Russian platform). Organic Geochemistry 31, 1641–1661.

Rickard, D. and Luther, G.W. (2007) Chemistry of Iron Sulfides. Chemical Reviews 107, 514–562.

Robson, W.J., Sutton, P.A., McCormack, P., Chilcott, N.P., Rowland, S.J. (2017) Class type separation of the polar and apolar components of petroleum. Analytical chemistry 89(5), 2919–2927.

Rontani, J. F., Bosser-Joulak, F., Rambeloarisoa, E., Bertrand, J. C., Giusti, G., Faure, R. (1985) Analytical study of Asthart crude oil asphaltenes biodegradation. Chemosphere 14(9), 1413–1422.

Rosenberg, Y.O., Meshoulam, A., Said-Ahmad, W., Shawar, L., Dror, G., Reznik, I. J., Amrani, A. (2017) Study of thermal maturation processes of sulfur-rich source rock using compound specific sulfur isotope analysis. Organic Geochemistry 112, 59–74.

Said-Ahmad, W. and Amrani, A. (2013) A sensitive method for the sulfur isotope analysis of dimethyl sulfide and dimethylsulfoniopropionate in seawater. Rapid Communications in Mass Spectrometry 27(24), 2789–2796.

Schimmelmann, A., Lewan, M.D., Wintsch, R.P. (1999) D/H isotope ratios of kerogen, bitumen, oil, and water in hydrous pyrolysis of source rocks containing kerogen types I, II, IIS, and III. Geochimica et Cosmochimica Acta 63(22), 3751–3766.

Schimmelmann, A., Sessions, A.L., Boreham, C.J., Edwards, D.S., Logan, G.A., Summons, R.E. (2004) D/H ratios in terrestrially sourced petroleum systems. Organic Geochemistry 35(10), 1169–1195.

Schimmelmann, A., Sessions, A.L., Mastalerz, M. (2006) Hydrogen isotopic (D/H) composition of organic matter during diagenesis and thermal maturation. Annual review earth planetary science 34, 501–533.

Schoell, M. (1983) Genetic characteristics of natural gases. American Association of Petroleum Geologists Bulletin 67, 2225–2238.

Seewald, J.S. (2003) Organic-inorganic interactions in petroleum-producing sedimentary basins. Nature 426, 327–333.

Seifert, W.K. and Moldowan, J.M. (1981) Paleoreconstruction by biological markers. Geochimica et Cosmochimica Acta 45, 783–794.

Sessions, A.L., Sylva, S.P., Summons, R.E., Hayes, J.M. (2004) Isotopic exchange of carbon-bound hydrogen over geologic timescales. Geochimica et Cosmochimica Acta 68(7), 1545–1559.

Silliman, J.E., Meyers, P.A. and Bourbonniere, R.A. (1996) Record of postglacial organic matter delivery and burial in sediments of Lake Ontario. Organic Geochemistry 24, 463–472.

Sinninghe Damste, J.S., De Leeuw, J.W. (1990) Analysis, structure and geochemical significance of organically-bound sulphur in the geosphere: State of the art and future research. Organic Geochemistry 16, 1077–1101.

Stach, E., Mackowsky, M.T., Teichmuller, M., et al. (1982) Coal Petrology. Gebruder Borntraeger, Berlin.

Stadnitskaia, A., Ivanov, M.K., Blinova, V., Kreulen, R., van Weering, T.C.E. (2006) Molecular and carbon isotopic variability of hydrocarbon gases from mud volcanoes in the Gulf of Cadiz, NE Atlantic. Marine and Petroleum Geology 23, 281–296.

Stinnett, J. W. (1982) The deep earth gas hypothesis: Big on promises, but evidence looks thin. Synergy 2, 12–20.

Sun, Y.G., Chen, Z.Y., Xu, S.P., Cai, P.X. (2005) Stable carbon and hydrogen isotopic fractionation of individual *n*-alkanes accompanying biodegradation: Evidence

from a group of progressively biodegraded oils. Organic Geochemistry 36, 225–238.

Taylor, G.H., Teichm¨uller, M., Davis, A., et al. (1998) Organic Petrology. Gebruder Borntraeger, Berlin.

Thode, H.G., Munster, J. (1970) Sulfur isotope abundances and genetic relations of oil accumulations in Middle East Basin. The American Association of Petroleum Geologists Bulletin 54, 627–637.

Thode, H.G. (1981) Sulfur isotope ratios in petroleum research and exploration: Walliston Basin. The American Association of Petroleum Geologists Bulletin 65, 1527–1537.

Tissot, B.P. and Welte, D.H. (1984) Petroleum Formation and Occurrence. Springer-Verlag, New York.

Tissot, B.P., Durand, B., Espitali´e, J. and Combaz, A. (1974) Influence of the nature and diagenesis of organic matter in formation of petroleum. American Association of Petroleum Geologists Bulletin 58, 499–506.

Treibs, A. (1936) Chlorophyll and hemin derivatives in organic mineral substances. Angewandte Chemie 49, 682–686.

Trolio, R., Grice, K., Fisher, S.J., Alexander, R., Kagi, R.I. (1999) Alkyl-biphenyls and alkyl-diphenylmethanes as indicators of petroleum biodegradation. Organic Geochemistry 30, 1241–1253.

van Krevelen, D.W. (1961) Coal. Elsevier, New York.

Volkman, J.K., Alexander, R., Kagi, R.I., Rowland, S.J., Sheppard, P.N. (1984) Biodegradation of aromatic hydrocarbons in crude oils from the Barrow sub-basin of Western Australia. Organic Geochemistry 6, 619–632.

Walters, C.C., Qian, K., Wu, C., Mennito, A.S., Wei, Z. (2011) Proto-solid bitumen in petroleum altered by thermochemical sulfate reduction. Organic Geochemistry, 42, 999–1006.

Wang, G., Xue, Y., Wang, D., Shi, S., Grice, K. and Greenwood, P.F. (2016) Biodegradation and water washing within a series of petroleum reservoirs of the Panyu Oil Field. Organic geochemistry 96, 65–76.

Waseda, A. and Iwano, H. (2008) Characterization of natural gases in Japan based on molecular and carbon isotope compositions. Geofluids 8, 286–292.

Wei, Z., Moldowan, J.M., Fago, F., Dahl, J.E., Cai, C., Peters, K.E. (2007) Origins of thiadiamondoids and diamondoidthiols in petroleum. Energy Fuels 21, 3431–3436.

Wei, Z., Walters, C.C., Moldowan, J.M., Mankiewicz, P.J., Pottorf, R.J., et al. (2012) Thiadiamondoids as proxies for the extent of thermochemical sulfate reduction. Organic Geochemistry 44, 53–70.

Wenger, L.M., Davis, C.L., Isaksen, G.H. (2002) Multiple controls on petroleum biodegradation and impact on oil quality. SPE Reservoir Evaluation and Engineering 5, 375–383.

Werne, J.P., Hollander, D.J., Lyons, T.W., Damste, J.S.S. (2004) Organic sulfur biogeochemistry: Recent advances and future research directions. Geological Society of America, Special Paper 379, 135–149.

Werne, J.P., Lyons, T.W., Hollander, D.J., Schouten, S., Hopmans, E.C., Sinninghe Damste, J.S. (2008) Investigating pathways of diagenetic organic matter sulfurization using compound-specific sulfur isotope analysis. Geochimica et Cosmochimica Acta 72, 3489–3502.

Werner, R.A., Brand, W.A. (2001) Referencing strategies and techniques in stable isotope ratio analysis. Rapid Communications in Mass Spectrometry 15, 501–519.

Whiteman, J.P., Smith, E.A.E., Besser, A.C., Newsome, S.D. (2019) Diversity, 11, 8.

Woese, C.R., Magrum, L.J. and Fox, G.E. (1978) Archaebacteria. Journal of Molecular Evolution, 11, 245–252.

Worden, R.H., Smalley, P.C. (1996) H$_2$S-producing reactions in deep carbonate gas reservoirs: Khuff Formation, Abu Dhabi. Chemical Geology 133, 157–171.

Yeh, H.W., Epstein, S. (1981) Hydrogen and carbon isotopes of petroleum and related organic matter. Geochimica et Cosmochimica Acta 45, 753–762.

Zhang, S.C., Zhu, G.Y., Liang, Y.B., Dai, J.X., Liang, H.B., Li, M.W. (2005) Geochemical characteristics of the Zhaolanzhuang sour gas accumulation and thermochemical sulfate reduction in the Jixian Sag of Bohai Bay Basin. Organic Geochemistry 36, 1717–1730.

Zhu, G.Y., Zhang, S.C., Liang, Y.B., Dai, J.X., Li, J. (2005) Isotopic evidence of TSR origin for natural gas bearing high H$_2$S contents within the Feixianguan Formation of the northeastern Sichuan Basin, southwestern China. Science in China Series D: Earth Sciences 48, 1960–1971.

Zhu, G., Zhang, Y., Zhang, Z., Li, T., He, N., Grice, K., Greenwood, P. (2018) High abundance of alkylated diamondoids, thiadiamondoids and thioaromatics in recently discovered sulfur-rich LS2 condensate in the Tarim Basin. Organic Geochemistry 123, 136–143.

CHAPTER 2

Potential $\delta^{34}S$ Fractionation of Common Laboratory Procedures

2.1 Introduction

The accuracy of experimental data is fundamental to scientific interpretations. However, some experimental measurements can distort (randomly or subjectively) the physical or chemical properties of analytes leading to imprecise characterisation. Organic-matter rich sediments and fossil fuels are often subject to various laboratory preparations (e.g. extraction, fractionation, derivatisation) prior to molecular analyses by sophisticated spectroscopic techniques such as gas or liquid chromatography coupled with mass spectrometry. The potential for molecular or isotopic error or bias needs to be robustly established for all analytical steps.

It is especially important to establish the viability of pre-treatment procedures on their initial application to new analytical technologies such as compound-specific sulfur isotope analysis (CSSIA). The present study evaluates the potential $\delta^{34}S$ fractionation of two common laboratory procedures: (i) Large scale solvent evaporation; (ii) Column chromatography separation of polarity based saturate (SAT) and aromatic (ARO) fractions with Al_2O_3 or $PdCl_2$ stationary phases, and a preliminary comparison of separating thiophenic and sulfidic fractions with a traditional silver nitrate ($AgNO_3$) stationary phase or via a novel methylation/demethylation procedure.

2.1.1 Solvent Evaporation

Solvents are used in many sample pre-preparation techniques, including extraction of soluble components (e.g. Soxhlet, ultrasonication), separation of major fractions (e.g. column chromatography, molecular sieving) and compound purification processes (e.g. preparative GC and high-performance liquid chromatography, HPLC). Large amounts of excess solvent are typically evaporated at various stages of these procedures, introducing the potential for chemical change as volatile components are sequentially removed based on their respective vapour pressures. Sometimes, Rayleigh distillation occurs in evaporation, because the greater loss of more volatile components can lead to compounds losing more of their lighter isotopes, leaving a residual compound with a greater proportion of heavier isotopes.

Huang et al. (1999) and Poulson and Drever (1999) observed the isotopic fractionation of organic and chlorinated compounds dissolved in trichloroethane (TCE) and dichloromethane (DCM) on reduction of solvent volume, with a $\delta^{13}C$ depletion of 1.6–3.6‰; a δD depletion of 27‰; and a $\delta^{37}Cl$ enrichment of 8–9‰. Wang et al. (2001) similarly observed increasing δD fractionation ($\leq 14\%$) of soluble low molecular-weight (MW) n-alkanes with progressive solvent vaporization. Xiao et al. (2012) reported significant (>1‰) $\delta^{13}C$ enrichment of C_6–C_8 light hydrocarbons with 70% evaporative loss. The $\delta^{13}C$ value of organic solvents can also change with an up to 2‰ enrichment of benzene and toluene observed with progressive evaporation (Shin et al. 2010). These previous studies indicate the isotopic integrity of organic compounds is best maintained

by avoiding evaporative losses where possible at all stages of collection, storage and analytical pre-preparation of samples.

The full impact of solvent reduction/evaporation processes on the $\delta^{34}S$ values of OSCs had not been robustly evaluated at the commencement of this PhD research. Rosenberg et al. (2017) subsequently reported on a similar investigation of the $\delta^{34}S$ fractionation of volatile OSCs (i.e. butythiol, dm-thiophene, BT, DBT — at up to 96% solvent evaporation) and the current results will be compared to the outcomes of this separate study.

2.1.2 Separation of Bulk Fractions

Column chromatography is a common technique used in studies for molecular analysis of petroleum. Certain compounds can be separated from a mixture based on the adsorption of the solutes of a solution over a stationary phase. In traditional column chromatography, the stationary phase in a glass column can be silica gel or aluminium oxide (Al_2O_3). Saturated and aromatic hydrocarbon fractions are well known to be sequentially eluted with *n*-hexane solvent and a *n*-hexane/dichloromethane solvent mixture, respectively. Liberti et al. (1965) reported column chromatography can affect the $\delta^{13}C$ of individual organic compounds due to partitioning between the stationary and mobile phases during sorption and desorption.

Alternative column types have been used in some geochemical studies targeting the isolation of specific compounds. For example, $AgNO_3$-impregnated silica gel, long used to separate saturated and unsaturated hydrocarbons, can also separate thiadiamondoids (TDs) from other OSCs such as BTs and DBTs (Lawrence, 1968; Wei et al., 2007; Wei et al., 2012; Gvirtzman et al., 2015). Some DBTs and TDs can co-elute after GC separations. The $\delta^{34}S$ measurement of partially resolved OSCs might be possible, but not

of fully co-eluting peaks. The removal of hydrocarbons prior to GC-ICPMS analysis is also beneficial to limit GC column degradation.

Sripada et al. (2005) developed an efficient separation method for polycyclic aromatic sulfur heterocycles (PASHs) using a palladium (II)-complex stationary phase. This method was also used by Moustafa et al. (2011) to separate the OSCs in petroleum condensate and volatile oils. Wang et al. (2014) reported a novel approach for selective separation of thiophenic/DBTs and sulfidic/TDs from hydrocarbons and sulfomium salts in oil by methylation of the sulfur compounds using silver tetrafluoroborate ($AgBF_4$) and methyl Iodide (CH_3I). The products were subsequently demethylated using 7-azaindole and 4-dimethylaminopytidine. However, the potential impact of the palladium (II)-complex in column chromatography on $\delta^{34}S$ of OSCs is unknown.

2.2 Materials and experiments

Two series of experiments were undertaken to separately verify if $\delta^{34}S$ fractionation of dissolved OSCs occurs during (i) solvent evaporation and (ii) column chromatography isolation of polarity-based fractions with different stationary phases ($AgNO_3$, $PdCl_2$) or procedures (methylation/demethylation).

2.2.1 Solvent evaporation experiments

Four authentic OSCs were evaluated: BT (C_8H_6S), DBT ($C_{12}H_8S$), 1-dodecanethiol ($C_{12}H_{26}S$), 1-octadecanethiol ($C_{18}H_{38}S$). All were commercially sourced from Sigma-Aldrich (>98% purity). The four OSCs and squalane ($C_{30}H_{62}$) were each combined at a concentration of 155 µg/mL in a mixture dissolved in dichloromethane (DCM). Squalane

was used as a high MW internal standard to help quantify the extent of evaporative loss of the OSCs.

Aliquots of the standard mixture were transferred to twelve 2 mL vials. Each of the vials was simultaneously evaporated in a fume hood with an air velocity of 3×10^3 cm/min at ambient temperature (~24 ± 1 °C). No nitrogen gas was used. Complete evaporation of the solution was achieved after 10 hr. The residual mix was dissolved in additional DCM (100μL) prior to GC-MS and GC-ICPMS analysis (operational details described below).

2.2.2 Fractionation procedures

Two crude oils from the Tarim Basin, China were used for these experiments. One oil (ZS1C) rich in sulfidic/TD compounds had been severely impacted by TSR, whilst the second oil (Qun 7) had no pre-TSR history. Both oils contained high concentrations of thioaromatics/DBTs.

Column chromatography separation of sulfidic and thioaromatic fractions was separately conducted (and compared) using (1) silica/$AgNO_3$ and aluminium oxide (Al_2O_3); and (2) $PdCl_2$ stationary phases as described below:

Silica/AgNO_3 and Al_2O_3 Columns

(1) Small columns filled (5.5 cm) with just silica gel was used for the Qun 7 oil, whereas $AgNO_3$-impregnated silica gel was used with the ZS1C oil (to also separate TDs). One drop of the crude oils was added to the top of each column.

(2) SATs, AROs and POLAR fractions were separately isolated from Qun7 by successive elutions (4mL) of pure *n*-hexane; 30% DCM in hexane; and 50% DCM in methanol. SAT, ARO and SULFIDIC fractions were separately isolated from ZS1C oil by sequential elution using hexane, DCM, and acetone,

respectively. The respective SAT, ARO and SULFIDIC fractions were each molecularly characterised by GC-MS.

(3) Prior to CSSIA the ARO fractions were further separated on an Al_2O_3 column (5 cm) to isolate OSCs from the typically more abundant hydrocarbons. A series of six ARO subfractions were obtained by eluting with *n*-hexane mixed with different concentrations of DCM as indicated in Error! Reference source not found.. The ARO sub-fractions were separately analysed by GC-MS and the fraction in which the OSCs were most concentrated was analysed by GC-ICPMS.

Table 2.1 Sub-fractions obtained from aluminium oxide column.

Sub-fractions	Solvent used	Compounds obtained
AF0	*n*-hexane, 2mL	SATs
AF1	5% DCM in *n*-hexane, 2mL	Mono-ARO (1 ring) and unresolved complex mixture (UCM)
AF2	10% DCM in *n*-hexane, 2mL	Di-AROs (2 rings)
AF3	50% DCM in *n*-hexane, 2mL	Tri-AROs (3 rings)
AF4	Pure DCM, 2mL	Polycyclic aromatic hydrocarbons (PAHs) ($\geq$ 3 rings)
AF5	50% DCM in methanol, 2mL	The remaining compounds on the column

PdCl₂ Column

The PdCl$_2$ column method of Moustafa et al. (2011) was used and is briefly described below:

(1) Pd(II)-mercaptopropano silica gel (MPS) was prepared by refluxing silica gel with 3-mercaptopropanotrimethoxysilane (3-trimethoxysilyl-1-propanethiol) in toluene. The MPS was dried and then treated with aqueous palladium

chloride solution (0.01M) for 12h to generate palladium bonded silica gel. It was rinsed with water, *iso*propanol and cyclohexane, successively, and then dried in a vacuum desiccator at room temperature before use.

(2) The oil samples were first separated into two fractions on a 3cm silica gel column by successive elutions with *n*-cyclohexane (40 mL) and a *n*-cyclohexane:DCM mix (3:1; 40 ml), respectively.

(3) The *n*-cyclohexane (CH) fraction was further separated on a Pd(II)-mercaptopropanol silica gel column (1.5g) into four sub-fractions by elution with the different CH/DCM solvent mixes listed in **Table 2.2**.

Table 2.2 Sub-fractions obtained from PdCl$_2$ column.

Sub-fractions	Solvent used	Compounds obtained
F1	*n*-cyclohexane:DCM (9:1), 40mL	Sulfur-free fraction
F2	*n*-cyclohexane:DCM (2:1) with 1% *iso*-propanol, 40mL	PASHs
F3	*n*-cyclohexane:DCM (2:1) with 1.5% iso-propanol saturated with NH$_3$, 40mL	Sulfides
F4	*n*-cyclohexane:DCM (9:1), 40mL	All remaining compounds

(4) All fractions from Step 2 and the first two sub-fractions from Step 3 were analysed by GC-MS.

(5) The second sub-fraction (F2) in which S-PAH compounds were found to be most concentrated was analysed by GC-ICPMS.

2.2.3 Molecular and Compound-Specific Isotope Analysis

Molecular characterisation of the oil fractions by GC-MS analysis was conducted on a HP 6890 GC coupled to a HP 5975B mass selective detector. The GC was fitted with a DB5 fused silica capillary column (60 m×0.25 mm i.d. ×0.25 µm film thickness) and a 1 mL/min helium carrier gas flow was used. The GC oven was temperature programmed from 40 °C to 325 °C at 3 °C/min then held isothermally for 45 min. Electron impact 70eV full scan (*m/z* 50–550) and selected ion recording mass spectral data were simultaneously acquired. Selected ions corresponded to the parent ions of alkylated BT, DBT and TD compounds (i.e. *m/z* 134, 142, 148, 154, 162, 168, 170, 176, 178, 182, 184, 190, 192, 196, 198, 206, 210, 212, 220, 226, 234 and 248). Product assignments were based on correlation of measured and previously reported GC and MS data, with tentative assignment of several specific alkylated BT and DBT isomers based on previously reported GC elution data (Berthou et al., 1984; Depauw and Froment, 1997; Lopez-García et al., 2002).

The $\delta^{34}S$ analysis of the OSCs were performed using an Agilent 6890 GC coupled to a Thermo Neptune Plus multi-collector ICPMS (Greenwood et al., 2015). The OSCs were separated on the GC with a DB-5 MS column (30 m × 0.25 mm i.d. × 0.1 µm film thickness). The GC oven was heated from 100 °C (held for 0.5 min) to an end temperature of 300 °C (held for 15 min) at a rate of 8 °C/min. The argon gas for the plasma torch was pre-heated and introduced co-axially with the analytes from the GC. An SF_6 gas standard of known $\delta^{34}S$ value was used for tuning and calibration of the ICPMS. Two SF_6 pulses were included at both the start and end of all sample analyses to internally calibrate $\delta^{34}S$ measurements. $\delta^{34}S$ results were reported as permil (‰) relative to the international sulfur isotope standard Vienna Canyon Diablo Troilite (VCDT) and typically represent the average of duplicate analyses with their variance expressed as standard variation

(SV±). In this study, the $\delta^{34}S$ data obtained from GC-ICPMS were typically measured

with high precision (<0.2%) and accuracy (<0.3%).

2.3 Results and discussion

2.3.1 Evaporation experiments

Variation in the abundances of the OSCs relative to squalane over the 10 hr evaporation time frame investigated are shown Error! Reference source not found.. The abundance of squalane, a high MW isoprenoid of much lower volatility than the OSCs, was assumed to be relatively stable over 10 hr.

BT was the most vulnerable compound to evaporation and was completely lost by 1 hr. 1-Dodecanethiol was gone by 6.75 hr. DBT and 1-octadecanethiol were only partially removed, their 10 hr levels being 94.7% and 50.3% less, respectively, than at the beginning of the experiment. This evaporation order is consistent with the vapour pressures of the four OSCs (
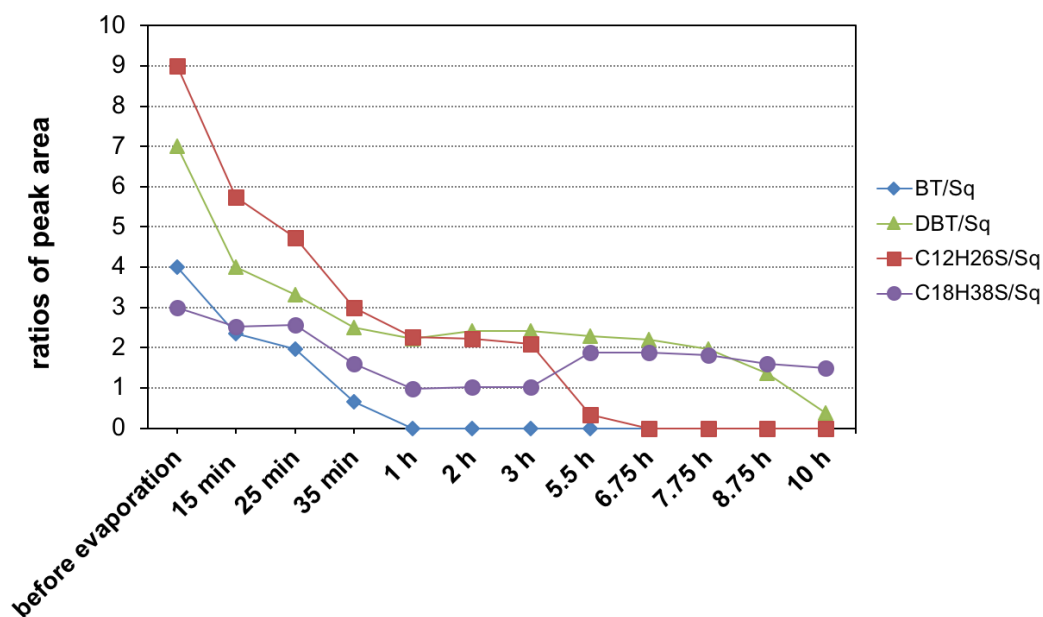
Table 2.3).

Figure 2.1 Temporal changes of ratios of OSCs relative to a squalene (Sq) standard.
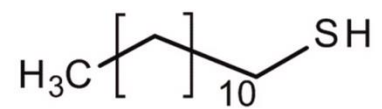
Table 2.3 Vapour pressures of four compounds used in evaporation experiment
(from the website of PubChem).

Compounds	Vapour pressure at 25°C mm Hg
Benzothiophene (C_8H_6S)	2.4×10^{-1}
Dibenzothiophene ($C_{12}H_8S$)	2.05×10^{-4}
1-dodecanethiol ($C_{12}H_{26}S$)	8.5×10^{-3}
1-octadecanethiol ($C_{18}H_{38}S$)	4×10^{-7}

The $\delta^{34}S$ values of the OSCs spanned a broad range from $-7.5‰$ ($C_{12}H_{26}S$) to $13‰$ (DBT). Throughout the evaporation experiments there was little variation in their $\delta^{34}S$ values (**Figure 2.2**). There was an increase of $+3.4‰$ in C_{12}-Thiol (i.e. 5-hr value = $-4.1‰$), but no obvious change in the $\delta^{34}S$ values of the less volatile DBT and C18-Thiol. The single $\delta^{34}S$ measurement for BT did not allow for an evaluation of its potential $\delta^{34}S$ fractionation with progressive evaporation. Similar experiments conducted by Amrani et al. (2013), Rosenberg et al. (2017) and Amrani et al. (2019) showed very small $\delta^{34}S$ fractionation in highly volatile, low MW compounds such as dimethyl sulfide ($-0.5\pm0.2‰$), butyl-thiol ($+1.1‰$), dimethyl-thiophene ($+1.8‰$), and short-chain thiolanes and thiophenes ($< \pm1‰$), but no discernible $\delta^{34}S$ fractionation of BT and DBT. They concluded that $\delta^{34}S$ fractionation even under severe evaporation was negligible ($<2‰$). The present results are generally consistent with negligible $\delta^{34}S$ fractionation of most petroleum OSCs, although certain very volatile OSCs (e.g. low MW alkyl-thiols) might be vulnerable to slightly more significant $\delta^{34}S$ fractionation (needs to be confirmed with further study). The relatively small $\delta^{34}S$ fractionation effect of evaporation is in contrast to more substantial $\delta^{13}C$ and δD changes previously observed for evaporated hydrocarbon compounds (Huang et al., 1999; Poulson and Drever, 1999; Wang et al., 2001). The small relative mass differential between the ^{32}S and ^{34}S atoms [(34–32)/32 = 6.24%, cf. 8.36%

for $\delta^{13}C$ and 99.84% for δD] and heavier atomic weight of sulfur may contribute to the relatively stable $\delta^{34}S$ values of the OSCs investigated.
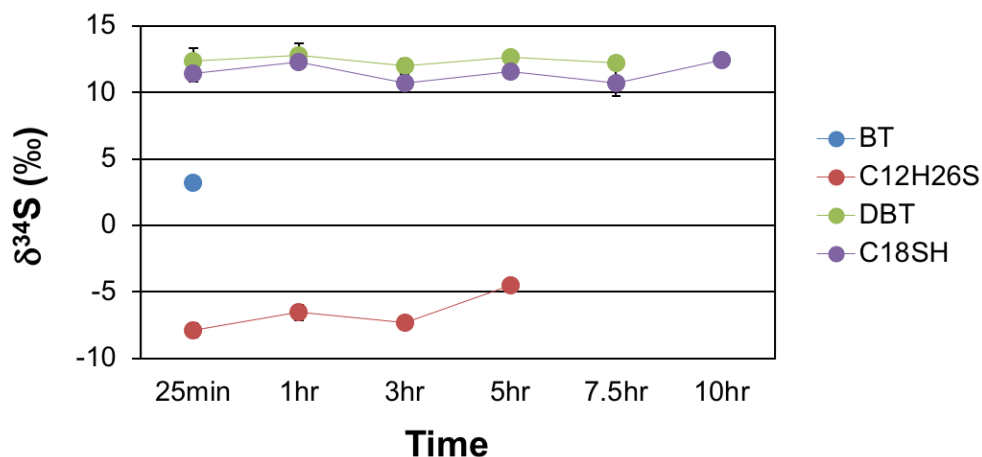
Figure 2.2 $\delta^{34}S$ profiles of OSCs over 10 hr evaporation experiment. Error bars (often smaller than data point) are the SV of duplicate analysis.

2.3.2 OSC Fractionation Procedures

Column Chromatography Fractions — Molecular Distributions

GC-MS of the respective ARO fractions showed the OSCs were most concentrated in the AF3 sub-fraction (AL$_{ARO3}$) of the aluminium column separations and the F2 sub-fraction (Pd$_{CH2}$) of the PdCl$_2$ column separations. The OSC and hydrocarbon product distributions of these two fractions are shown in **Figure 2.3**. The OSCs were generally more selectively isolated in the Pd$_{CH2}$ sub-fraction with fewer potentially co-eluting PAHs (e.g. phenanthrene, pyrene, chrysene) than were detected in AL$_{ARO3}$, particularly of the Qun7 oil.

(a)

(b)

(c)

AL$_{ARO3}$ sub-fraction of Qun 7 oil

(d)
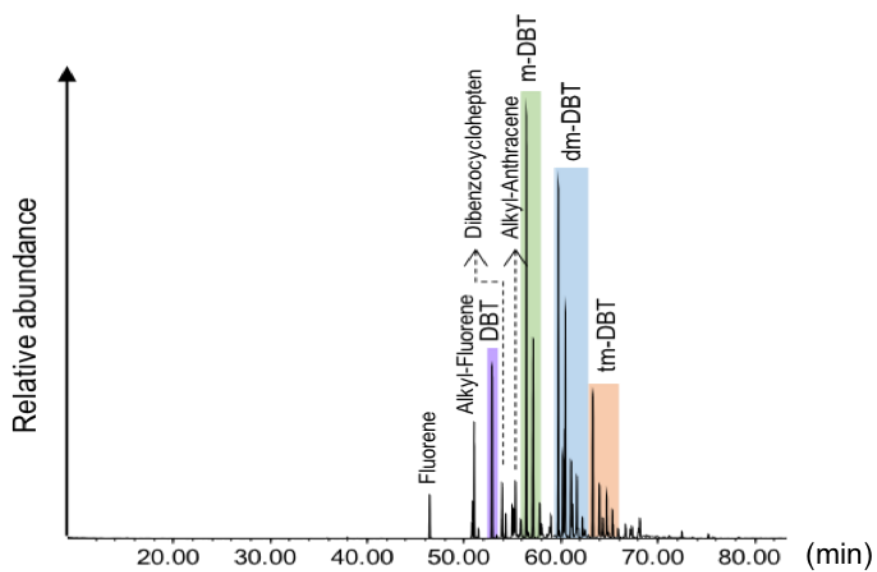
Pd$_{CH2}$ sub-fraction of Qun 7 oil
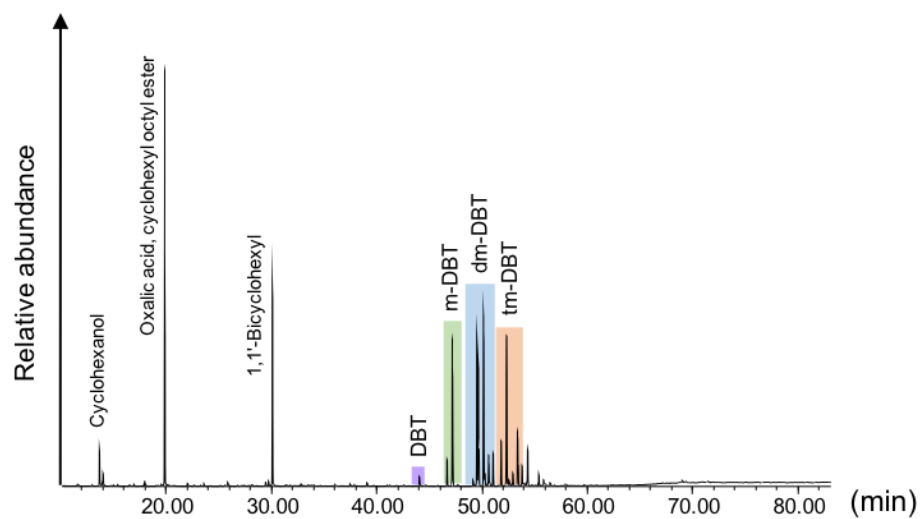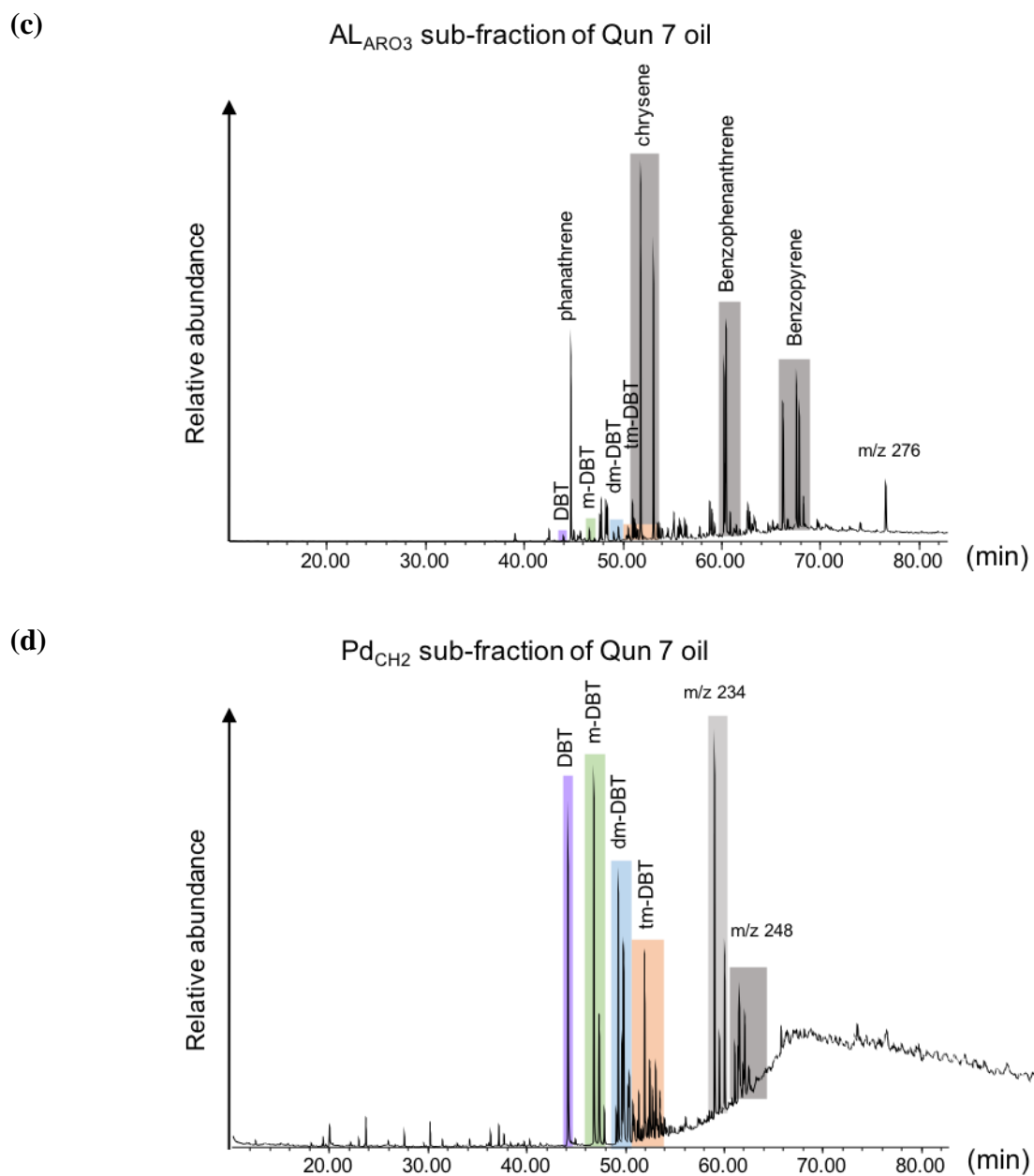
Figure 2.3 TICs from GC-MS analysis of AL$_{ARO3}$ (a and c) and Pd$_{CH2}$ (b and d) fractions of ZS1C and Qun 7 oils.

Column Chromatography Fractions — $\delta^{34}S_{OSC}$ Values

The δ^{34}S values measured for OSCs in the AL_{ARO3} and Pd_{CH2} fractions of the ZS1C and Qun 7 oils are listed in

Table 2.4 and profiled in **Figure 2.4**. The higher concentrations of OSCs isolated from the $PdCl_2$ column allowed for more $\delta^{34}S_{OSC}$ measurements than the AL_{ARO3} fractions. In the Pd_{CH2} fraction of ZS1C the δ^{34}S values of low MW alkyl-BTs ($\leq$ dimethyl) were generally in a narrow range of +40 to +44‰, whilst the higher MW BTs ($C_{3/4}$-BTs) and DBTs showed more depleted values in the range of +32 to +37‰. The reproducibility of measurements was generally < 1‰ (indicated by standard variance/error bars in **Figure 2.4** which were often less than data point size), although a few compounds showed large standard variances (up to 3‰). Low analyte concentrations and other factors (e.g. co-elutions) can reduce the precision of the δ^{34}S measurement.

Some of the $\delta^{34}S_{OSC}$ data of the AL_{ARO3} fraction of ZS1C were very similar to Pd_{CH2} values, whilst others were notably enriched in ^{34}S (**Figure 2.4a**). The $\delta^{34}S_{OSC}$ character of the ZS1C oil has been investigated in several other studies (Li et al., 2015; Cai et al., 2016). Data reported from these two studies, included in **Figure 2.4a** for comparison, are from aromatic fractions separated on alumina columns and is largely consistent with the $\delta^{34}S_{OSC}$ data measured in Pd_{CH2}. The enriched BT outliers presently measured from AL_{ARO3} are hard to rationalize, but are possibly related to the relatively low concentrations of the BT analytes (Nb. BTs << DBTs, and often below GCMS baseline — see **Figure 2.3a**). The

general consistency of the AL_{ARO3} and Pd_{CH2} $\delta^{34}S_{DBT}$ data points suggests there is no systematic ^{34}S enrichment of the more concentrated OSCs in AL_{ARO3}.

For Qun 7 oil, the $\delta^{34}S$ values of BTs in Pd_{CH2} were in the range of +21 to +29‰, and the isotopically lighter DBTs were in range +7 to +15‰. The fewer $\delta^{34}S_{OSC}$ data of AL_{ARO3} were generally consistent with those measured in Pd_{CH2}, which would suggest little isotopic variation/fractionation between both the Al_2O_3 and $PdCl_2$ separation procedures.

A more robust correlation of the $\delta^{34}S$ behaviour and integrity of these methods will obviously require measurement and comparison of a larger data set. Notwithstanding the need for more samples to thoroughly investigate this issue, this initial assessment suggests there is minimal $\delta^{34}S$ fractionation by these column chromatography methods.

Table 2.4 $\delta^{34}S_{OSC}$ data measured in AL_{ARO3} and Pd_{CH2} sub-fractions of ZS1C and Qun 7 oils.

Compounds	ZS1C oil				Qun 7 oil			
	AL$_{ARO3}$		Pd$_{CH2}$		AL$_{ARO3}$		Pd$_{CH2}$	
	Average	S.V.	Average	S.V.	Average	S.V.	Average	S.V.
BT			41.4	0.5				
mBTi			42.4	1.6				
mBTii			40.4	0.8				
mBTiii			41.0	—				
mBTiv			41.0	—				
dmBTi	42.1	—	41.1	0.1				
dmBTii	48.9	—	40.5	0.3			28.5	1.4
dmBTiii	43.3	—	40.8	1.7			25.2	1.1
dmBTiv			39.6	0.2			22.7	0.6
dmBTv			44.2	—	17.5	—		
dmBTvi			43.4	—				
tmBTi	36.9	—	42.7	0.3				
tmBTii	41.3	2.8	36.7	1.4			22.4	0.2
tmBTiii	41.5	—	37.3	0.5	22.1	—	21.4	0.4
tmBTiv			36.0	1.1	22.8	—	22.9	0.1
tmBTv			31.9	2.7			22.8	0.2
tmBTvi	39.5	—	32.1	—			27.6	2.8
temBTi	37.9	1.4	30.9	—				
temBTii	39.5	—	34.1	—				
DBT	38.2	—	36.2	0.1	5.6	0.4	7.3	0.1
mDBTi	37.2	2	35.8	0	12.4	1.3	11.9	0.1
mDBTii	38.6	1.7	34.1	0.2	11.6	—	11.9	0
mDBTiii	36.8	2.5	32.7	—	14.7	—	14.5	0.1
dmDBTi	34.3	—	36.3	0.4			12.1	0.2
dmDBTii	36.9	1.4	32.9	0.8	11.7	—	10.9	0.1
dmDBTiii	34.8	—	34.1	0.4	10.9	—	11.7	0
tmDBTi	33	—	33.3	1	9.7	—	10.2	0
tmDBTii					10.4	—	10.7	0.2
tmDBTiii								

S.V. = Standard variation.

N.D. = Not detected.

(a)

(b)
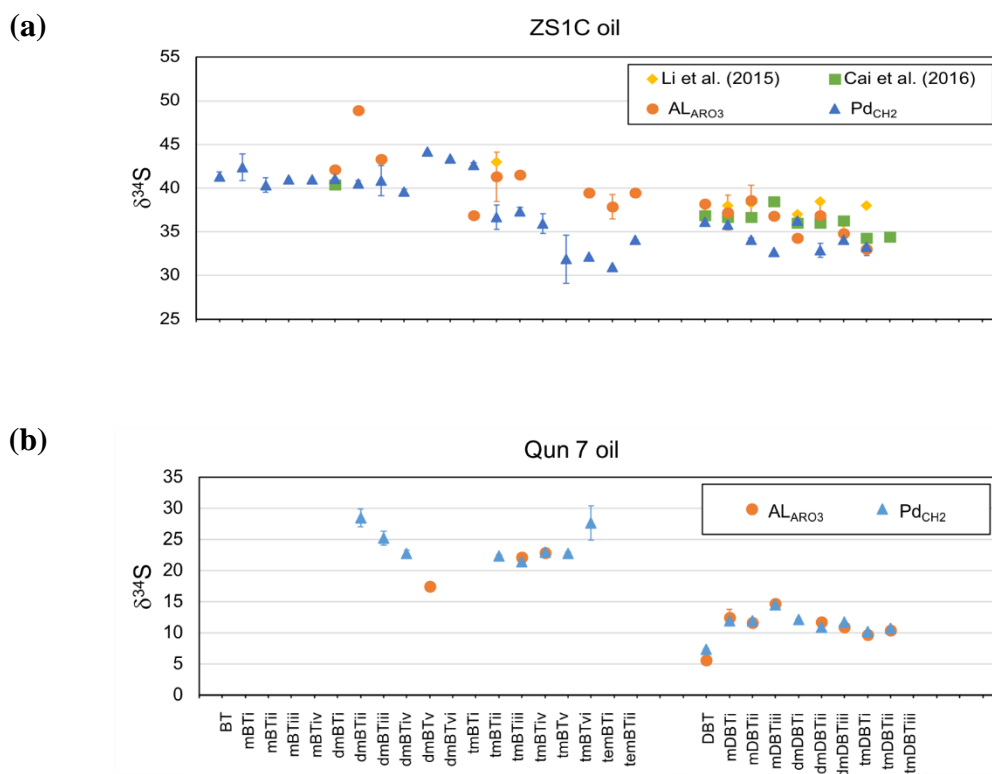
Figure 2.4 The $\delta^{34}S_{OSC}$ profiles of AL_{ARO3} and Pd_{CH2} fractions of (a) ZS1C oil and (b) Qun 7 oil. Error bars (often smaller than data point) are the SV of duplicate analysis. ZS1C $\delta^{34}S_{OSC}$ data previously reported by Li et al. (2015) and Cai et al. (2016) are shown in (a) for comparison.

Thiophenic and Sulfidic Fractions of ZS1C from a Novel

Methylation/Demethylation Method

Wang et al. (2014) developed a novel methylation/demethylation pretreatment method for efficient separation of thiophenic and sulfidic compounds from S-rich oils. In brief, sulfur compounds were methylated to sulfonium salts by $AgBF_4$ and CH_3I, then the polar salts were separated by precipitation from the petroleum matrix. The thiophenic and sulfidic sulfonium salts were sequentially demethylated with 7-azaindole and 4-

dimethylaminopyridine, obtaining original thiophenic and sulfidic compounds, respectively.
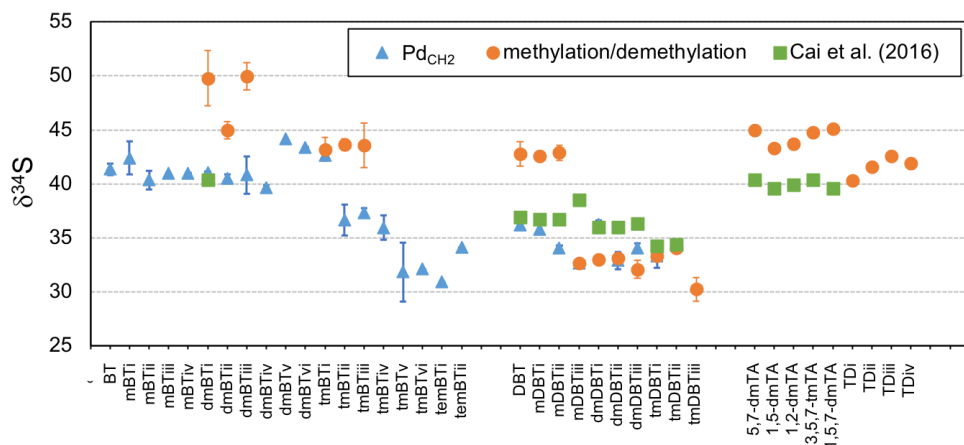
Figure 2.5 $\delta^{34}S$ of alkylated BTs and DBTs in aromatic fraction and alkylated thiadiamondoids (TAs, TDs) in sulfidic fraction of ZS1C oil. The oil was isolated by novel methylation/demethylation method outlined by Wang et al. (2014). Data from Cai et al. (2016) is included for comparison.

It is important to assess whether the significant chemical alteration of the OSCs during this procedure contributes any $\delta^{34}S$ fractionation. Thiophenic$_{m/dm}$ and sulfidic$_{m/dm}$ fractions of the ZS1C oil prepared by Mr Meng Wang at Petrochina's Research Institute of Petroleum and Exploration Development (RIPED, Beijing, China) were provided for CSSIA. The $\delta^{34}S$ values of alkylated BTs and DBTs measured in thiophenic$_{m/dm}$ and alkylated TDs measured in sulfidic$_{m/dm}$ are profiled in **Figure 2.5**. The corresponding $\delta^{34}S$ data of the Pd$_{CH2}$ fraction of ZS1C and the $\delta^{34}S$ values reported in Cai et al. (2016) are also plotted in **Figure 2.5** for comparisons. The thiophenic$_{m/dm}$ fraction seemed to give slightly larger $\delta^{34}S_{BT/DBT}$ values than the Pd$_{CH2}$ fraction (and Cai et al., 2016). The $\delta^{34}S_{TD}$ values of the sulfidic$_{m/dm}$ fraction, like the corresponding $\delta^{34}S_{BTs}$ values, were relatively enriched ($\geq 40‰$) which would be consistent with the incorporation of ^{34}S enriched H_2S from TSR of anhydrite. Cai et al. (2016) also showed TDs were enriched in ^{34}S compared

to DBTs. Obviously to investigate the $\delta^{34}S$ reliability of this novel separation method, more experiments are needed for assessment and comparison in future.

2.4 Conclusions

The effects of common organic geochemistry laboratory practices of solvent evaporation and liquid chromatography separation procedures on the $\delta^{34}S$ values of petroleum OSCs has been preliminarily investigated. Large volume solvent evaporation (i.e. through to dryness) had little impact on the $\delta^{34}S$ value of authentic DBT and $C_{18}SH$ compounds, with an enrichment up to 3‰ detected in the higher volatility $C_{12}SH$. The stable sulfur isotopic values of all but the most volatile OSCs common to petroleum would seem more stable to evaporative processes than previously measured for the $\delta^{13}C$ and δD values of petroleum hydrocarbons, likely due to their higher atomic mass and the lower relative mass difference of the primary isotopes.

There appeared no systematic difference in the $\delta^{34}S$ values of DBTs in the aromatic fractions of two oils isolated by column chromatography with either an Al_2O_3 or a $PdCl_2$ stationary phase. The latter ($PdCl_2$) provided higher concentrations of OSCs which supported greater $\delta^{34}S$ precision and numbers of OSCs that could be isotopically measured. Low analyte concentrations may account for the relatively enriched $\delta^{34}S$ values of several alkylated BTs/DBTs in the AL_{ARO3} fractions measured here. The $\delta^{34}S$ values of some, but not all, thioaromatics and caged-S compounds in the ZS1C oil separated using a novel methylation/demethylation method (Wang et al., 2014) were generally similar to the aromatic fractions from Al_2O_3 and $PdCl_2$ column chromatography.

This preliminary assessment of the $\delta^{34}S_{OSC}$ integrity of these basic laboratory procedures are based on a very limited number of experiments and should serve as only a general

guide. A much larger data set from more samples and experiments will be needed to investigate this issue more systematically.

References

Amrani, A., Said-Ahmad, W., Shaked, Y., Kiene, R.P. (2013) Sulfur isotope homogeneity of oceanic DMSP and DMS. Proceedings of the National Academy of Sciences, 110(46), 18413–18418.

Amrani, A., Rosenberg, Y. O., Meshoulam, A., Said-Ahmad, W., Turich, C., Luu, N., Lacksier, T., Stankiewicz, A., Feinstein, S., Shurki, A. (2019) Sulfur isotopic composition of gas-phase organic sulfur compounds provides insights into the thermal maturation of organic-rich rocks. Geochimica et Cosmochimica Acta, 259, 91–108.

Cai, C., Amrani, A., Worden, R.H., Xiao, Q., Wang, T., Gvirtzman, Z., Li, H.X., Said-Ahmad, W., Jia, L. (2016) Sulfur isotopic compositions of individual organosulfur compounds and their genetic links in the Lower Paleozoic petroleum pools of the Tarim Basin, NW China. Geochimica et Cosmochimica Acta 182, 88–108.

Gvirtzman, Z., Said-Ahmad, W., Ellis, G.S., Hill, R.J., Moldowan, J.M., Wei, Z.B., Amrani, A. (2015) Compound-specific sulfur isotope analysis of thiadiamondoids of oils from the Smackover Formation, USA. Geochimica et Cosmochimica Acta 167, 144–161.

Huang, L., Sturchio, N.C., Abrajano, T., Heraty, L.J., Holt, B.D. (1999) Carbon and chlorine isotope fractionation of chlorinated aliphatic hydrocarbons by evaporation. Organic Geochemistry 30, 777–785.

Lawrence, B.M. (1968) The use of silver nitrate impregnated silica gel layers in the separation of monoterpene hydrocarbons. Journal of Chromatography 38, 535–537.

Li, S.M., Amrani, A., Pang, X.Q., Yang, H.J., Said-Ahmad, W., Zhang, B.S. (2015) Origin and quantitative source assessment of deep oils in the Tazhong Uplift, Tarim Basin. Organic Geochemistry 78, 1–22.

Liberti, A., Cartoni, G.P. and Bruner, F. (1965) Isotope effect in gas chromatography. In: Gas Chromatography 1964 (A. Goldup, et.), Elsevier, Amsterdam, pp. 301–312.

Moustafa, N.E., Anderson, J.T. (2011) Analysis of polycyclic aromatic sulfur heterocycles in Egyptian petroleum condensate and volatile oils by gas chromatography with atomic emission detection. Fuel Processing Technology 92, 547–555.

Poulson, S.R., Drever, J.I. (1999) Stable isotope (C, Cl, and H) fractionation during vaporization of trichloroethelene. Environmental Science and Technology 33, 3689–3694.

Rosenberg, Y.O., Meshoulam, A., Said-Ahmed, W., Shawar, L., Dror, G., Reznik., I.J., Feinstein., S., Amrani A. (2017) Study of thermal maturation processes of sulfur rich source rock using specific sulfur isotope analysis. Organic Geochemistry 112, 59–74.

Shin, W.J., Lee, K.S. (2010) Carbon isotope fractionation of benzene and toluene by progressive evaporation. Rapid Communications in Mass Spectrometry 24, 1636–1640.

Sripada, K., Andersson, J.T. (2005) Liquid chromatographic properties of aromatic sulfur heterocycles on a Pd(II)-containing stationary phase for petroleum analysis. Analytical and Bioanalytical Chemistry 382, 735–741.

Wang, L., Huang, Y.S. (2001) Hydrogen isotope fractionation of low molecular weight *n*-alkanes during progressive vaporization. Organic Geochemistry 32, 991–998.

Wang, M., Zhao, S.Q., Chung, K.H., Xu, C.M., Shi, Q. (2014) Approach for selective separation of thiophenic and sulfidic sulfur compounds from petroleum by methylation/demethylation. Analytical Chemistry 87, 1083–1088.

Wei, Z.B., Moldowan, J.M., Fago, F., Dahi, J.E., Cai. C.F., Peters, K.E. (2007) Origins of Thiadiamondoids and Diamondoidthiols in Petroleum. Energy Fuels 21, 3431–3436.

Wei, Z.B., Walters, C.C., Moldowan, M., Mankiewicz, P.J., Pottorf, R.J., Xiao, Y.T., Maze, W., Nguyen, P.T.H., Madincea, M.E., Phan, N.T., Peters, K.E. (2012) Thiadiamondoids as proxies for the extent of thermochemical sulfate reduction. Organic Geochemistry 44, 53–70.

Xiao, Q., Sun, Y.G., Zhang, Y.D., Chai, P.X. (2012) Stable carbon isotope fractionation of individual light hydrocarbons in the C_6–C_8 range in crude oil as induced by natural evaporation: Experimental results and geological implications. Organic Geochemistry 50, 44–56.

CHAPTER 3

The effect of biodegradation on the distributions and

$\delta^{34}S$ values of petroleum organic sulfur compounds

Introduction

Biodegradation can significantly alter the composition of oils, often reducing the quality and commercial value of hydrocarbon reservoirs. Detailed information about the occurrence of biodegradation and its impact on the hydrocarbon composition of oils were given in the Introduction chapter (Section 1.1.5). The extent to which oils have been affected by biodegradation can often be precisely estimated by scaled biodegradation levels (BLs) related to removal of increasingly susceptible hydrocarbon classes (e.g. Peters et al., 2005), specific hydrocarbon compound ratios (e.g. Volkman et al., 1984; Larter et al., 2012); and from $\delta^{13}C$ or δD fractionation of hydrocarbon compounds (James and Burns, 1984; Pallasser, 2000; Masterson et al., 2001; George et al., 2002; Sun et al., 2005; Wilkes et al., 2008; Asif et al., 2009). Compared to the wealth of available information about the biodegradation of petroleum hydrocarbons, the effects of biodegradation on the composition and $\delta^{34}S$ behavior of organic sulfur compounds (OSCs) are not nearly as well understood. To learn more about the effects of biodegradation on the organic sulfur content of oils the following two studies were undertaken:

(1) The biodegradation of a S-rich oil was attempted in laboratory-controlled microcosm experiments. A heavily TSR-impacted oil (ZS1C) with high concentrations of thioaromatic and thiadiamondoid compounds was selected and exposed to an active soil microbial community for a total period of 3 months. Soil

microflora has previously been shown to biodegrade petroleum hydrocarbons in a similar sequential order to reservoir oil (Greenwood et al., 2008).

However, since the microcosm induced biodegradation had not progressed sufficiently to have impacted the OSCs detected in the recovered oil this approach was not continued. Instead, a suite of naturally biodegraded petroleum samples was assessed for a separate investigation of the biodegradation behavior of petroleum OSCs. The experimental and results of microcosm induced biodegradation are described in Appendix 1.

(2) The second approach involved the analysis of several S-rich oils spanning biodegradation gradients (BLs of 3–6) from the Peace River region of the Athabasca Oil Sands (Canada). The Athabasca Oil Sands of Canada represents one of the few global petroleum regions where the impacts of biodegradation on S-rich oils have been recognized and studied at some length. Much of the organic geochemistry research of these oils has been undertaken by the Calgary Organic Geochemistry research team led by Prof. Steve Larter. One of their studies (Marcano et al., 2013) included details of the progressive biodegradative reduction of methyl-DBTs in a suite of 4 oils from a Peace River Well. For the present study of biodegradation impacts on the S-isotopic character of real oils, Prof. Larter was approached and kindly provided 4 oils from each of two Peace River wells reflecting similar biodegradation gradients. The successful outcomes from the analysis of these oils resulted in a publication in Organic Geochemistry (He et al., 2019) and a full copy of this paper follows.

The distribution and δ^{34}S values of organic sulfur compounds in

biodegraded oils from Peace River (Alberta Basin, W. Canada)

Nannan He, Kliti Grice, Paul F. Greenwood

Abstract

The heavy sulfur-rich oils of the Peace River oil sands were formed by severe anaerobic biodegradation. To investigate the impacts of biodegradation on organic sulfur compounds (OSCs) we have measured the distribution and $\delta^{34}S$ values of alkylated thioaromatics detected in four oils from each of two Peace River wells (A and B). The fluid composition of the Peace River oil sands can be highly complex due to the variable contributions of sources, thermal maturity and secondary alteration. Nevertheless, a previous multi-molecular investigation of samples from well B oils (PR2 oil-leg of Marcano et al., 2013, Organic Geochemistry 59, 114–132) indicated that the oils had biodegradation levels (BLs) of 5–6, with biodegradation increasing down the oil column. The hydrocarbon composition of oils isolated from well A were biodegraded to a lesser degree than well B (i.e. the presence of isoprenoids and high molecular weight (MW) n-alkanes suggests BLs of ~3–4). The concentrations of C_1–C_3 alkylated benzothiophenes (BTs) and C_1–C_3 alkylated dibenzothiophenes (DBTs) declined sharply through both wells consistent with increased biodegradation, although other alteration impacts (e.g. water washing) might also contribute. The rates of decrease recorded for selected isomers showed variable responses (e.g. 3&4-mBT > 2-mBT; 4-eDBT > 1,3-dmDBT) which implies different susceptibilities to biodegradation and which may contribute additional useful molecular parameters for evaluating the BL of biodegraded S-rich petroleum. The S-isotopic measurements showed a ^{34}S enrichment in several alkyl-BTs down the oil leg in well B, with their $\delta^{34}S$ values increasing by up to 6‰, consistent with the microbial utilisation of ^{32}S (n.b. the $\delta^{34}S$ values of alkyl-BTs were not measured in well A oils because of low aromatic sub-fraction concentrations). In contrast, there was little variation in the $\delta^{34}S$ values of alkyl-DBTs down both wells indicating negligible S-isotopic fractionation of these OSCs in the deeper more biodegraded oils, possibly because of their higher MW and

resistance to biodegradation. The $\delta^{34}S_{DBT}$ (and bulk $\delta^{34}S$) values of the well B oils were generally slightly enriched than the well A oils probably due to differences in the relative contribution of the major Devonian and Jurassic source rocks.

Introduction

Biodegradation is one of the major alteration events to impact crude oils and can significantly alter the fluid properties and commercial viability of petroleum reservoirs. The initial removal of low MW volatile liquid components can lead to increased fluid density, viscosity and corrosiveness (Volkman et al., 1984; Kennicutt, 1988; Wenger et al., 2002; Peters et al., 2005; Larter et al., 2012). Changes to the chemical composition and physical properties of biodegraded oils arise from the sequential removal of compounds with a varied susceptibility to biodegradation. Numerous studies have identified consistent differences in the resistance of certain hydrocarbon compounds to microbial attack, including isomers of the same compound (e.g. Alexander et al., 1983; Fedorak and Westlake, 1984; Volkman et al., 1984; Moldowan et al., 1992; Trolio et al., 1999; van Aarssen et al., 1999; Grice et al., 2000), and these observations have evolved into a widely applied biodegradation scale (Peters et al., 2005). For instance, the initial loss of low MW n-alkanes is recognised at a biodegradation level (BL) of 1, whereas more resistant high MW polycyclic hydrocarbons survive to more advanced stages of biodegradation (e.g. BLs of 6–9).

The consideration of a range of different biodegradation indicators can be instructive given the large variety of petroleum sources, charging and alteration histories (e.g. thermal maturity, migration). The biodegradation behaviour of organic sulfur compounds (OSCs) may help to evaluate the biodegradation levels of heavy sulfur-rich oils often devoid of many of the aliphatic and aromatic hydrocarbons used in traditional biodegradation

parameters. The correlation value of OSCs, useful for identifying relationships between Type II-S sourced petroleum (Amrani et al., 2005; Cai et al., 2009), will also be strengthened by a better understanding of their specific vulnerability to biodegradation.

The microbial biodegradation of OSCs has attracted modest attention compared to the large interest in the microbial degradation of petroleum hydrocarbons. Shi et al. (2017) recently reported the biodegradation of alkylated DBTs in oils from the Bohai Bay Basin (China) to be synchronous with the later stage removal of n-alkanes and observed varied biodegradation susceptibility for several different alkyl-DBT isomers. Biodegradation of Prudhoe Bay oil (Alaska) by cultured soil microbes showed the resistance of thioaromatics to biodegradation increased with their MW (i.e. more rings or methyl substituents; Fedorak and Westlake, 1984). Larter et al. (2012) included a 4-score assessment of alkyl-thiophenic behavior in a robust multi-hydrocarbon and OSC parameter-based biodegradation scale coined "Modular Analysis and Numerical Classification of Oils" (Manco). This multi parameter-based system was necessary to reliably quantify the biodegradation level of the Peace River (PR) oil sands. The complex nature of these heavy S-rich oils can mask the behavior of traditional biomarker parameters.

Several studies on the environmental toxicology impacts of OSCs monitored the fate (e.g. S metabolites) of OSCs on aerobic degradation of authentic S compounds or S oils by cultured microbes (e.g. Pseudomonas strains; Bayona et al., 1986; Fedorak and Peakman, 1992; Kropp et al., 1994a, 1994b, 1996, 1997; Fedorak et al., 1996). Kropp et al. (1994b) for example, showed methylated BTs were transformed by Pseudomonas into sulfoxide, sulfone or dione products, with the distribution of these product groups dependent on the isomeric form of the mBT substrate (i.e. methyl substituent on benzene or thiophene ring). The slightly enriched $\delta^{34}S$ values measured for the aromatic fraction compared to the polar fraction of more biodegraded Athabasca and Mannville oils (W. Canada) were attributed

to preferential removal of low MW aromatics (Méhay et al., 2009), but might also reflect the transformation of some aromatics into more polar compounds.

The $\delta^{34}S$ values of OSCs may potentially also be sensitive to biodegradation with a kinetic control on the microbial utilisation of S substrates likely to result in their ^{34}S enrichment. This would be analogous to the ^{13}C or ^2H enrichment observed for some biodegraded hydrocarbons due to preferential microbial utilisation of the lighter isotopes (Guthrie et al., 2000; Pond et al., 2002; Sun et al., 2005; Kinnaman et al., 2007; Wilkes et al., 2008; Asif et al., 2009). Rosenberg et al. (2017) reported little $\delta^{34}S$ variance between C_1–C_3 BTs (and several alkyl-DBTs) in oils from the Dead Sea petroleum system thought to be lightly biodegraded based on differences in gasoline and n-alkane distributions, although the biodegradation alteration of the thioaromatic compounds in these oils was not established.

To investigate further the anaerobic biodegradation behaviour of OSCs we have measured the relative abundance and $\delta^{34}S$ values of alkylated thiophenic products in moderate to heavily biodegraded oils from two wells from the PR oil sands reservoir of NW Alberta, Canada. Our study includes the first detailed investigation of the potential fractionation of the S isotopes of OSCs subjected to biodegradation.

Experimental

Samples

Four reservoir core extracted oils from each of two wells (A and B) from the PR oil sands reservoir (Lower Cretaceous Manville Group, Alberta Basin) were used in this study. The samples come from 20–30 m sections of the respective cores and will be referred to as oils A1–A4 (well A) and B1–B4 (well B), respectively. Well B corresponds to the PR2 oil leg studied by Marcano et al. (2013) and well A is from the same geographic locale. These

oils (20–100 mg) represent the last remaining PR samples from several previous studies by the Petroleum Reservoir Group at the University of Calgary (e.g. Adams et al., 2006, 2012; Larter et al., 2008; Marcano et al., 2013).

Aliphatics susceptible to anaerobic biodegradation (i.e. n-alkanes) had been largely removed from all of the PR oils studied by Marcano et al. (2013) whereas aromatic and thioaromatic hydrocarbons were more persistent. Oil biodegradation typically increases down the PR oil columns, consistent with biodegradation focused mainly at the oil-water transition zone (Head et al., 2003; Larter et al., 2003; Bennett et al., 2013).

Hydrocarbon parameters measured from PR and other W. Canadian oil sands have not always reflected traditional biodegradation trends (Bennett and Larter, 2008; Larter et al., 2012; Marcano et al., 2013) due to the impact of several major compositional variables. In addition to biodegradation, differences in source, thermal maturity and reservoir compartmentalization can contribute to compositional variability (Adams et al., 2006; 2012; Larter et al., 2008, 2012). Nevertheless, on consideration of a number of biodegradation sensitive molecular parameters, the well B oils were assessed to have experienced heavy biodegradation consistent with BLs = 5–6 (Marcano et al., 2013). The ultimate Manco number (MN2) values of the four well B oils range from 955 to 961 (**Error! Reference source not found.**; Marcano et al., 2013). MN2 values were not available for the well A oils, but these oils were recovered from depths similar to the well B oils and the petroleum column has similar biodegradation related geochemical and oil viscosity gradients which are typical of the PR oil sands as described elsewhere (Adams et al., 2012; Marcano et al., 2013).

Molecular and $\delta^{34}S$ analysis

Saturated and aromatic hydrocarbon fractions of all samples were isolated from the oils (~20 mg) by liquid chromatography on activated silica gel and separately analysed by gas chromatography-mass spectrometry (GC-MS). A sub-fraction (ArF3) of the aromatic fraction of the oils in which thioaromatic compounds were most concentrated was obtained by sequential elution of the aromatic fraction on an activated aluminium oxide (Al_2O_3) column with gradually more polar (i.e. more DCM) solvent mixes of *n*-hexane and DCM. The $\delta^{34}S$ values of OSCs were measured by GC inductively coupled plasma (ICP) MS analysis of ArF3 which was sometimes taken to very low solvent volumes to enhance the ^{32}S and ^{34}S signal intensities of low concentration analytes. Laboratory experiments (by us and others, e.g. Amrani et al., 2013) with standard samples have detected no discernible S isotopic fractionation with solvent/sample evaporation.

GC-MS analysis of the oil fractions was conducted with a HP 6890 GC coupled to a HP 5973 mass selective detector. The compounds were chromatographically separated on a DB-5 fused silica capillary column (60 m × 0.25 mm i.d.) with 1 mL/min helium carrier gas. The GC oven was temperature programmed from 40 °C to 325 °C at 3 °C/min then held isothermally at the final temperature for 45 min. Deuterated terphenyl (98% purity, Sigma-Aldrich, USA) was added as an internal standard to the aromatic fractions to assist quantification. Electron impact (70 eV) full scan (*m/z* 50–550) and selected (parent) ion recording mass spectral data were acquired simultaneously. Assignment of alkyl-BT and alkyl-DBT isomers was based on the correlation of measured and previously reported GC and MS data (Berthou et al., 1984; Depauw and Froment, 1997; López García et al., 2002).

The $\delta^{34}S$ analysis of the OSCs was achieved using an Agilent 6890 GC coupled to a Thermo Neptune Plus multi-collector ICPMS following previously reported protocols

(Greenwood et al., 2018). In brief, the OSCs were separated on the GC with a DB-5 MS column (30 m $\times$ 0.25 mm i.d. $\times$ 0.1 μm film thickness). The GC oven was heated from 100 °C (held for 0.5 min) to an end temperature of 300 °C (held for 15 min) at a rate of 8 °C/min. The argon (Ar) gas for the plasma torch was pre-heated and introduced co-axially with the analytes from the GC. An SF6 gas standard of known $\delta^{34}S$ value was used for tuning and calibration of the ICPMS. Two SF6 pulses were included at both the start and end of all sample analyses to internally calibrate $\delta^{34}S$ measurements. $\delta^{34}S$ results are reported as per mil (‰) relative to the international sulfur isotope standard Vienna Canyon Diablo Troilite (VCDT) and represent the average of duplicate analyses with their variance expressed as standard variation (SV±). A $\delta^{34}S$ precision of < 0.2‰ is typical achieved by GC-ICPMS analysis of standard OSCs ($\geq$ 50 pmol sulfur; Greenwood et al., 2014) and the duplicate analysis of the PR samples mostly gave $\delta^{34}S_{OSC}$ values with a standard variance < 0.5‰.

Results and discussion

Hydrocarbon composition and evidence of biodegradation levels

Few low MW aliphatic hydrocarbons were detected by GC-MS analysis of the saturate fractions of well A oils, but they did contain higher MW n-alkanes (C_{27}–C_{35}) and several isoprenoid compounds. All of the well B oils were generally devoid of n-alkanes and isoprenoids and a more advanced biodegradation of the deeper samples was also indicated by sterane alteration. Marcano at al. (2013) previously assessed well B oils (i.e. PR2 oil leg) to have BLs = 5–6. The presence of high MW n-alkanes and isoprenoid alkanes in well A oils indicated they had not been biodegraded to the same extent and had BLs ~3–4.

High abundances of aromatic hydrocarbons, including a number of S-aromatics (see Section 3.2), were detected by GC-MS analysis of the aromatic fractions of all oils. Evidence of biodegradation included a notable change in the alkylated naphthalene composition of oils from both wells and additional alteration of alkylated phenanthrenes in well B. Biodegradation-sensitive di- to tetramethyl-naphthalene isomer ratios have been widely used to assess the biodegradation levels of petroleum samples (Solanas and Pares, 1984; Volkman et al., 1984; Rowland et al., 1986; Fisher et al., 1996, 1998; Ahmed et al., 1999; Peters et al., 2005; Greenwood et al., 2008). The DMNR and TMNR values (**Error! Reference source not found.**) measured from most oils indicated a decline down both wells consistent with the enhanced biodegradation of dimethyl-naphthalene (dmN) and trimethyl-naphthalene (tmN) isomers susceptible to biodegradation compared to isomers more resistant to biodegradation. Relatively constant TeMNR values (**Error! Reference source not found.**) reflected less change in the distributions of tetramethyl-naphthalenes.

The persistence of methylnaphthalenes (mN) and dmN in all oils was surprising given the quite advanced biodegradation levels of the oils. mNs are highly susceptible to biodegradation, normally being removed or substantially altered by BL= 2 (Peters et al., 2005). Similarly, alteration of dmN and tmN usually occurs across BLs 2–5 with the dmNs typically absent at BLs $\geq$ 6 (i.e. BL of well B oils). The mNs and dmNs detected in all oils may derive from multiple oil charges. The influences of different sources, depositional conditions or multiple charging of single sources are major contributors to the highly complex nature of Albertan oil sand deposits such as Peace River (e.g. Deroo et al., 1977; Leenheer, 1984; Creaney and Allan, 1990; Adams et al., 2006, 2012). The TMNR profile of both well A and well B oils, nevertheless, reflected a distinctive gradient consistent with

the transition of BLs 3–6 and was therefore used as a correlation parameter for assessing the alteration levels of the OSCs in the biodegraded PR oils (Section 3.2).

Methyl-phenanthrenes (mPs) are typically more resistant to biodegradation than the lower MW alkyl-naphthalenes (Peters et al., 2005). The distribution of these isomers showed little variance in well A (MPI = 1.2–1.4, **Error! Reference source not found.**), but they were clearly altered in well B (MPI = 0.7–4.8). MPI is a common indicator of thermal maturity (Radke et al., 1982; Radke, 1988), but the alteration of mPs in Peace River oils of similar maturity (e.g. well B) can be attributed to biodegradation (Marcano et al., 2013). Molecular-based maturity parameter values measured from the well A and B oils showed generally similar values (i.e. MNR, TA/(TA+MA), $C_{29}H/C_{30}H$; **Error! Reference source not found.**).

.

Table 3.1 Molecular biodegradation and thermal maturity parameters from GC-MS analysis of PR oils.

Parameter	Well A				Well A			
	A1	A2	A3	A4	B1	B2	B3	B4
MN2	-	-	-	-	955	961	966	966
MDR	0.9	0.9	0.9	0.9	1.9	1.4	0.2	0.3
MNR	0.9	0.7	1.0	1.2	1.0	1.3	0.8	0.8
DMNR	3.8	4.0	3.7	2.9	4.0	2.4	1.4	1.3
TMNR	4.6	2.0	0.5	0.4	5.8	1.9	0.6	0.2
TeMNR	2.9	2.4	4.0	3.0	1.8	1.8	1.6	2.0
MPI-1	1.2	1.4	1.3	1.2	0.7	1.1	3.5	4.8
$C_{29}H/C_{30}H$	0.7	0.7	0.7	0.8	0.7	0.8	0.8	0.8
TA/(TA+MA)	0.2	0.2	0.2	0.1	0.2	0.2	0.2	0.2

MN2 = ultimate Manco numbers for Well B samples (PR2 oils) reported by Marcano et al., 2013.

MDR = methyldibenzothiophene ratio (4-mDBT/1-mDBT; Bennett et al., 2007; Punanova and Vinogradova, 2015)

MNR = methylnaphthalene ratio (2-mN/1-mN; Radke et al., 1982b)

DMNR = Dimethylnaphthalene ratio (1,6-dmN/1,5-dmN; Fisher et al., 1998)

TMNR = Trimethylnaphthalene ratio (1,3,6-tmN/1,2,4-tmN; Fisher et al., 1998)

TeMNR = Tetramethylnaphthalene (1,3,6,7-temN/1,3,5,7-temN; Fisher et al., 1998)

MPI-1 = Methylphenanthrene Index ($1.5 \times$ (2-mP + 3-mP)/(P + 1-mP + 9-mP); Radke et al., 1982a; Radke et al., 1988)

$C_{29}H/C_{30}H$ = 30-*nor*hopane/C_{30} hopane (Peters et al., 2005)

TA/(TA+MA) = C_{26}–C_{28} triaromatic steroids/(C_{27}–C_{29} monoaromatic steroids + C_{26}–C_{28} triaromatic steroids) (Mackenzie et al., 1981)

Biodegradation of thioaromatic compounds

All oil samples showed prominent series of thioaromatics, and several samples also trace concentrations of alkylated naphthothiophenes and alkyl-benzonaphthothiophenes. Sample B1 generally showed the highest thioaromatic concentrations; the distributions of alkyl-BTs and alkyl-DBTs in this oil are highlighted by the selected ion chromatograms in **Figure 3.1** . Isomeric assignments are consistent with the GC elution orders reported by López García et al. (2002), although product identifications may be considered tentative. Lower abundance and less expansive S aromatic product distributions were evident in the deeper, more biodegraded B2–B4 oils. Apart from generally lower OSC concentrations, the well A oils showed similar thioaromatic distributions to the Well B oils and a similar trend of decreasing abundance with depth.
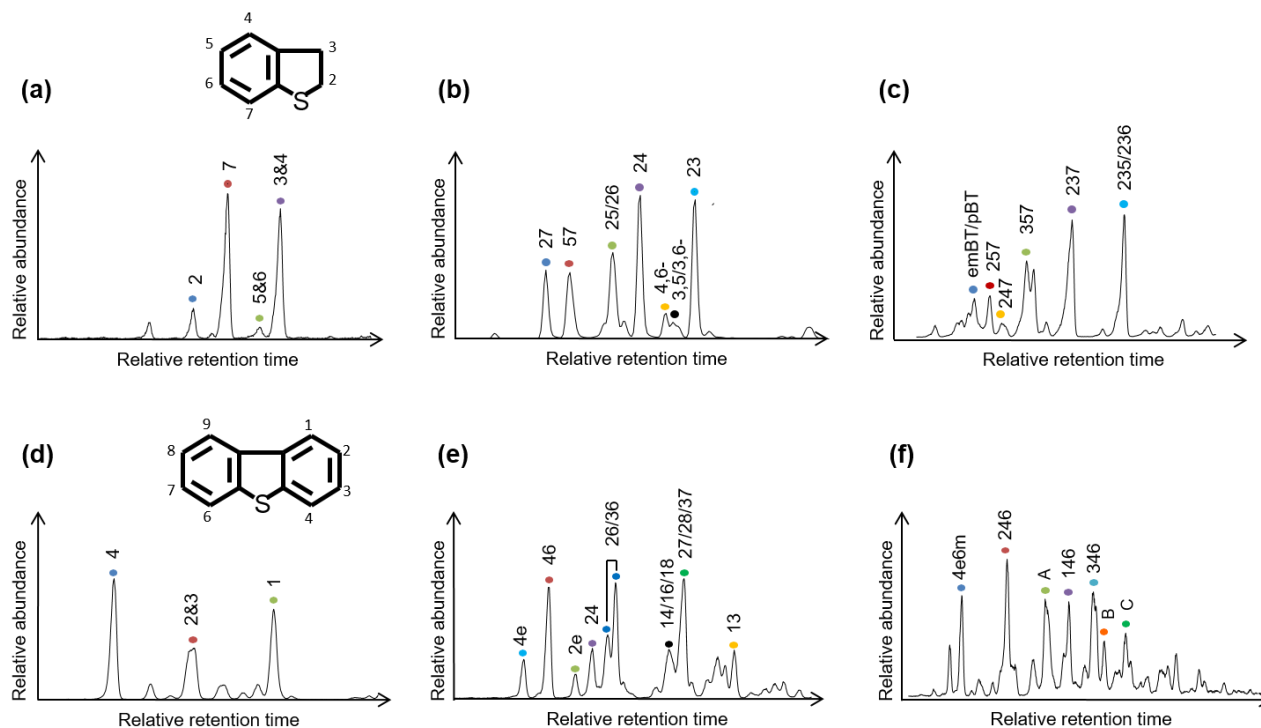
Figure 3.1 Selected ion chromatogram from GC-MS analysis of oil B1: (a) *m/z* 148 highlighting the mBTs; (b) *m/z* 162 of C_2-BTs; (c) *m/z* 176 of C_3-BTs; (d) *m/z* 198 of mDBTs; (e) *m/z* 212 of C_2-DBTs; and (f) *m/z* 226 of C_3-DBTs. Isomer assignments based on GC elution order reported by López García et al., 2002 (A–C = unassigned C_3-DBT isomers). Structures of BT and DBT are included with alkyl substitution positions numbered.

Concentration profiles

The oil sample concentrations of the alkyl-BTs and alkyl-DBTs declined down both wells (**Figure 3.2**). This decrease in concentration is consistent with biodegradative loss, although other alteration factors (e.g. water washing, diffusion, dilution from multiple charging or mixing) can also contribute to a concentration gradient. There were some variations in the rates at which the concentrations of different product groups decreased with increasing well depth likely due to structurally related differences in their diffusion and metabolic utilisation as well as possible variations in charging. A dominance of charge over degradation can be characterised by linear concentration gradients (Adams, 2008), as evident for several OSCs in each of well A (e.g. mDBTs) and Well B (e.g. 4,6-dmBT; and the co-eluting 2,3,5- and 2,3,6-tmBT). Metabolic preferences can additionally contribute to the varied profiles evident between many isomer products (i.e. with similar diffusion properties).

Most alkyl-BTs showed a particularly sharp drop in concentration between the two uppermost samples (i.e. A1 to A2; B1 to B2) and a generally exponential profile for the four oils of each well (**Figure 3.2a–c**). The concentrations of several dmBT and tmBT compounds showed a more gradual (~linear) decrease down well B. The decrease in concentration of alkyl-DBTs down wells A and B was generally less than the alkyl-BTs with linear and sometimes logarithmic-like gradients evident for different isomers (**Figure 3.2d–f**).
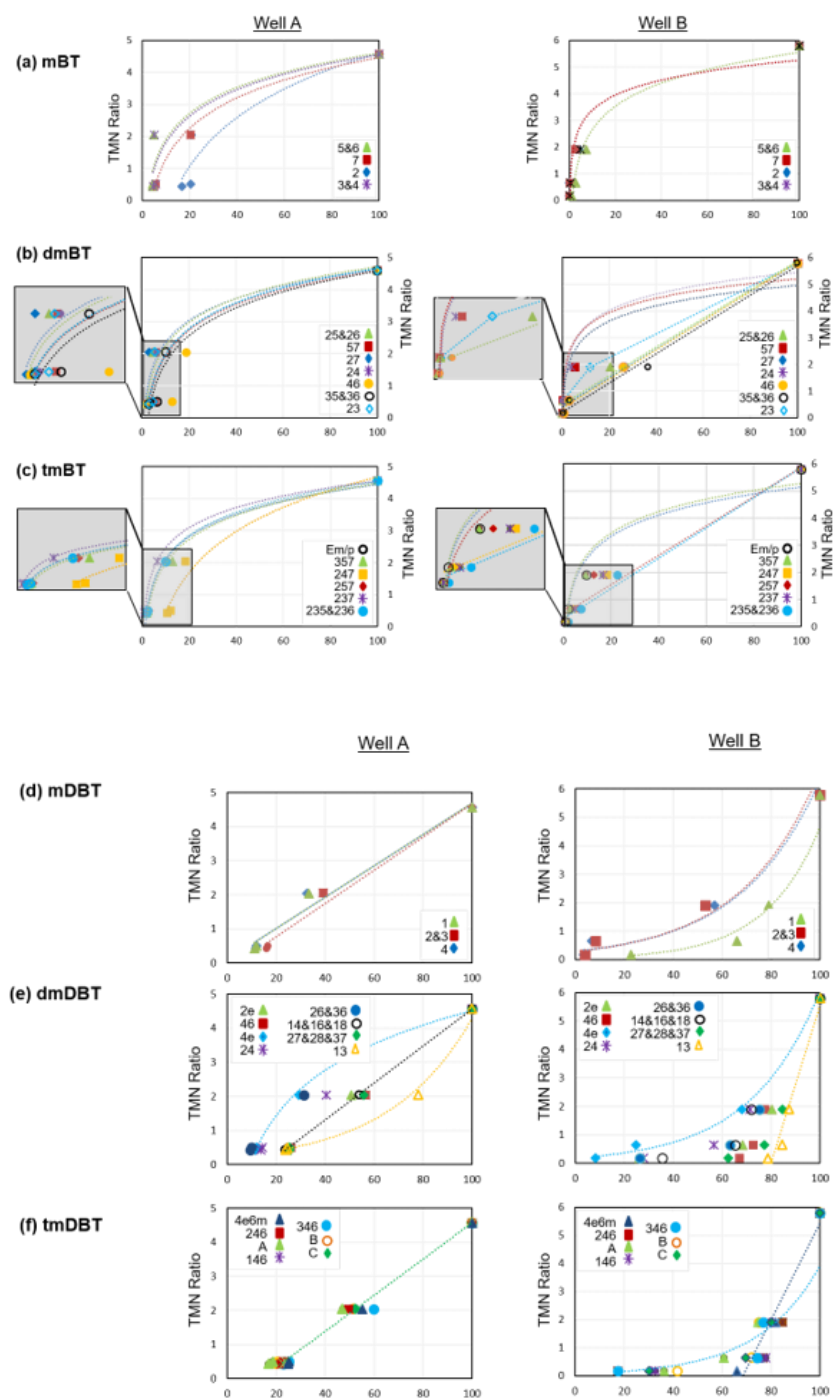
Figure 3.2 Isomer concentration profiles of: (a) mBTs; (b) dmBTs; (c) C$_3$-BTs in well A; and (d) mDBTs; (e) C$_2$-DBTs; (f) C$_3$-DBTs (A–C = unassigned C$_3$-DBT isomers) in well B. Product concentration values are plotted as % relative to the corresponding concentrations of the top (least biodegraded) samples (i.e. A1 and B1).

The down-well reduction rates of some isomers did not correlate so closely with relative abundances and may be more suggestive of a structural control. There was a notable distinction, for instance, in the well A abundance profiles of mBT isomers (**Figure 3.2a**, **Table 3.2**), although not well B oils (**Figure 3.2b**) probably because of their higher BLs. The concentrations of (co-eluting) 3- and 4-mBT and (co-eluting) 5- and 6-mBT were significantly more reduced in the deeper well A oils than 7-mBT and more so than 2-mBT. The 2-methyl substituent is next to the S-atom (β-position) which may provide greater steric hindrance to biodegradation. The ratio values of (co-eluting) 3- and 4-mBT/2-mBT (**Figure 3.3a**) measured from the well A oils show a generally linear ($R^2 = 0.82$) relationship with biodegradation as indicated by TMNr.

Distinct variations were also evident in the relative abundance profiles of several mDBT (**Figure 3.2d**), dmDBT (**Figure 3.2e**) and tmDBT (**Figure 3.2f**) isomers. 1-mDBT was clearly the most persistent of the mDBT isomers in the deeper well B oils with the down-well reduction of all mDBT isomers reflecting a logarithmic gradient (due to accentuated reduction in the deeper oils). A similar order (2- > 3- ~ 4- > 1) of mDBT isomer susceptibility to biodegradation was recently reported for several Linpan oils of the Bohai Bay Basin spanning BLs = 2–6 (Shi et al., 2017). A relatively high susceptibility of 2- and 3-mDBTs to aerobic biodegradation was also recognised in a light Arabian crude oil following exposure to cultured strains of Pseudomonas sp bacteria (Bayona et al., 1986) and was suggested to be due to the α-substitution of these products (i.e. methyl not adjacent to the S atom leaving adjacent unsubstituted α- and β- positions).

The 4-mDBT/1-mDBT ratio has been previously used to indicate thermal maturity (Radke, 1988; Punanova and Vinogradova, 2016), but the behaviour of these isomers in the well B oils reflects how biodegradation can also affect this ratio. There was little

variation in the approximately linear reduction rates of the mDBT isomers in the well A

oils possibly due to their lower BLs.
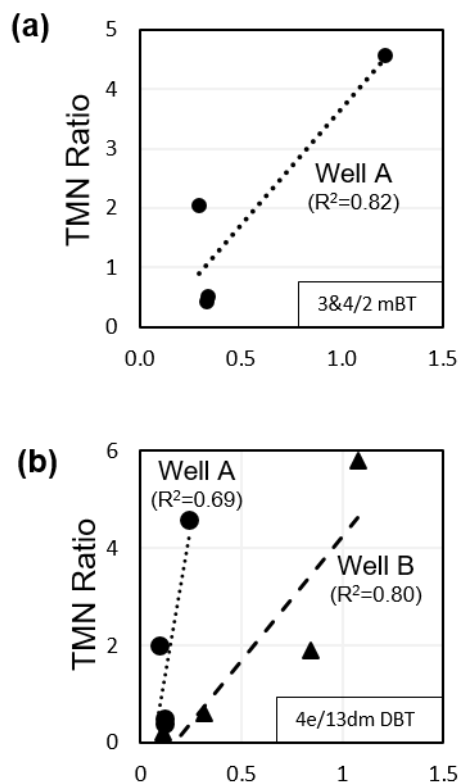
Figure 3.3 Well A profile of: (a) 3- and 4-mBT/2-mBT vs TMN Ratio; and well A
and B profiles of (b) 4-eDBT/1,3-dmDBT vs TMN Ratio.

The relative abundances of the C_2-DBT isomers in the highly biodegraded well B oils

reflected a very large variance in reduction rates (**Figure 3.2e**). 4E-DBTs seemed the most

susceptible to biodegradation, with its B3 compared to B2 concentration indicating a 64%

reduction between these two oils compared to a corresponding 3% reduction of the most

stable isomer 1,3-dmDBT (**Table 3.2**). The well B concentration profiles of the other

isomers further suggest 2,4-DBT and (co-eluting) 2,6- and 3,6-DBTs were biodegraded to

a greater extent than 4,6-DBT, (co-eluting) 1,4-, 1,6- and 1,8-DBTs, and (co-eluting) 2,7-

, 2,8- and 3,7-DBTs (**Figure 3.2e**, **Table 3.2**). Well A had generally similar C_2-DBT

biodegradation begaviour including very high and low biodegradation suceptibilies of 4-eDBT and 1,3-dmDBT, respectively.

A relatively high biodegrdation susceptibility for 4e-, 2,6- and 3,6-dm substituted isomers was also identified in biodegraded Linpan oils (Shi et al., 2017). The ratio of 4-eDBT/1,3-dmDBT in the well B oils reflected a general ($R^2 = 0.80$) relationship with TMNr (**Figure 3.3b**) although a potentially similar trend in the less biodgraded well A oils ($R^2 = 0.69$, **Figure 3.3b**) may be unrelated to biodegradation. Alkyl-DBT and alkyl-BT (e.g. 3- and 4-mBT/2-mBT, **Figure 3.3a**) isomers with different biodegradation susceptibilities may be helpful in monitoring the biodegradation progression of heavy S-rich oils, similar to the use of petroleum biodegradation parameters based on the relative abundance of alkyl-naphthalene isomers (TMNR, DNR, TeMNR; e.g. Greenwood et al., 2008). However, given the complexities of the PR petroleum reservoir and the fact biodegradation is one of just several major controls on the composition of these oils, the sensitivity of these OSC ratios to biodegradation should be confirmed by further study.

The reduction rates of C_3-DBT isomers down well B also showed some variation. For instance, several isomers (e.g. 1,4,6-tmDBT and 3,4,6-tmDBT) declined in a relatively slow linear fashion with biodegradation/TMNR compared to other isomers (e.g. 4e,6m-DBT and 2,4,6-tmDBT) whose accentuated reduction in the deeper oils produced a logarithmic type profile. Through well A there was an almost identical linear reduction of all C_3-DBTs. This similar isomer behaviour might be due a lack of biodegradative impact on these higher MW OSCs at the relatively low BLs of the well A oils, and their consistent reduction may be due to other alteration influences. Water washing can selectively remove hydrocarbons on the basis of their polarity or aqueous solubility (Palmer, 1993), with aromatic (and gasoline) hydrocarbons quite vulnerable to this alteration. Hydrocarbon alteration by water washing is often difficult to recognise due to the typically larger impact

of biodegradation, but like biodegradation becomes more significant through the oil-water transition zone (i.e. potentially greater impact on the deeper PR oils) and can have a more obvious effect in biologically hostile environments (Wang et al., 2016).

Table 3.2 Concentration (ng/mg) of alkyl-BTs and alkyl-DBTs measured by GC-MS analysis of Peace River oils. The extents (%) to which compound concentration is reduced in the next well sample is indicated in parentheses.

Compound(s)	Isomers	Well A				Well A			
		A1	A2	A3	A4	B1	B2	B3	B4
methylBT	2-mBT	38 (79)	8 (2)	7 (18)	6	23	tr	-	-
	7-mBT	18 (80)	4	tr	tr	119 (97)	3 (94)	tr	-
	5-&6-mBT	59 (95)	3 (7)	3 (4)	3	11	tr	tr	tr
	3-&4-mBT	46 (94)	3 (12)	3	tr	107 (96)	5 (88)	tr	tr
dimethylBT	2,7-dmBT	110 (97)	3 (1)	3	tr	175 (73)	47 (98)	tr	tr
	5,7-dmBT	49 (94)	3 (3)	3	tr	225 (95)	12 (93)	tr	tr
	2,5-&2,6-dmBT	114 (95)	6 (47)	3 (7)	3	303 (80)	62 (97))	tr	tr
	2,4-dmBT	76 (94)	5 (43)	3 (9)	3	385 (96)	15 (88)	tr	tr
	4,6-dmBT	27 (81)	5 (33)	3	tr	69 (74)	18 (90)	tr	tr
	3,5-&3,6-dmBT	52 (90)	5 (37)	3	tr	63 (64)	23 (92)	tr	tr
	2,3-dmBT	74 (94)	4 (15)	3	tr	363 (88)	43 (95)	tr	tr
C_3-BT	emBT/pBT	–	–	–	–	159 (91)	15 (80)	3	tr
	2,5,7-tmBT	36 (89)	4	tr	tr	149 (87)	19 (79)	4	tr
	2,4,7-tmBT	33 (82)	6 (33)	4 (13)	4	77 (17.7)	14 (3.6)	3	tr
	3,5,7-tmBT	93 (87)	12	tr	tr	333 (91)	31 (71)	9	tr
	2,3,7-tmBT	210 (93)	14 (81)	3	tr	548 (83)	92 (72)	26 (85)	4
	2,3,5-&2,3,6-tmBT	228 (90)	23 (76)	5 (26)	4	451 (77)	102 (68)	33 (74)	9

methylDBT	4-mDBT	348 (68)	113 (63)	42 (3)	41	1014 (43)	575 (88)	68 (48)	35
	2-&3-mDBT	262 (61)	103 (59)	43 (2)	42	744 (47)	394 (85)	60 (52)	29
	1-mDBT	395 (66)	132 (65)	47(6)	44	535 (21)	423 (16)	353 (65)	122
C$_2$-DBT	4-eDBT	94 (71)	28 (59)	11 (5)	11	164 (32)	112 (64)	41 (67)	14
	4,6-dmDBT	800 (43)	452 (54)	208 (5)	197	426 (23)	330 (6)	310 (8)	285
	2-eDBT	155 (49)	79 (51)	39 (3)	38	89 (20)	72 (15)	61 (62)	23
	2,4-dmDBT	255 (59)	103 (65)	36 (2)	35	224 (29)	160 (21)	127 (51)	63
	2,6-&3,6-dmDBT	521 (69)	162 (68)	52 (4)	49	694 (25)	523 (16)	438 (58)	183
	1,4-&1,6-&1,8-dmDBT	449 (46)	242 (54)	111 (5)	105	303 (28)	217 (9)	198 (46)	108
	2,7-&2,8-&3,7-dmDBT	1186 (44)	661 (54)	302 (0)	303	511 (15)	432 (9)	395 (9)	319
	1,3-dmDBT	390 (22)	304 (69)	95 (3)	92	153 (13)	133 (3)	129 (7)	120
C$_3$-DBT	4e6m-DBT	340 (45)	188 (55)	85 (1)	85	183 (18)	150 (8)	138 (12)	121
	2,4,6-tmDBT	512 (50)	254 (54)	117 (4)	112	331 (15)	280 (9)	254 (77)	58
	tmDBT A	597 (53)	281 (60)	111 (10)	100	339 (25)	254 (19)	206 (40)	123
	1,4,6-tmDBT	364 (48)	189 (54)	87 (4)	84	184 (21)	145 (2)	143 (58)	60
	3,4,6-tmDBT	679 (40)	407 (58)	171 (59)	155	339 (23)	260 (3)	252 (76)	59
	tmDBT B	261 (48)	135 (60)	53 (3)	52	121 (25)	91 (4)	87 (42)	51
	tmDBT C	300 (48)	157 (55)	71 (9)	65	135 (20)	108 (13)	94 (56)	41

δ³⁴S profiles

The $\delta^{34}S$ values of the highest abundance OSCs were measured by GC-ICPMS. This included alkyl-DBTs in the well A oils and both alky-BTs and alkyl-DBTs in well B oils (**Table 3.3**, **Figure 3.4**). The sensitivity limits for $\delta^{34}S$ analysis of petroleum OSCs has been estimated at about 50 pmol S per analyte peak (precision < 0.5‰; Amrani et al., 2009; Greenwood et al., 2014), although this can often be bettered with optimal analytical conditions (e.g. new or freshly conditioned analytical column and transfer capillary). Here, the standard limit of 50 pmol S equates to alkyl-BTs and alkyl-DBTs concentrations in the present PR aromatic fractions of ~ 50 ppm (**Table 3.2**; from LC of ~20 mg oil). In practice the $\delta^{34}S$ of OSCs in the ArF3 sub-fraction of PR oils (**Table 3.3**) were generally measured with good precision (most < 0.5‰ and just a few > 1.0‰) from OSCs with a corresponding aromatic fraction concentration > 40 ppm (**Table 3.2**).

Adequate ICPMS signal for a single $\delta^{34}S$ measurement was also obtained for a few OSCs at much lower concentrations by analysis of nearly all available sample following the reduction of ArF3 to very low solvent volumes (n.b. duplicate analysis of these trace concentrations typically was not possible). For example, the dmBT region of the m/z 32 chromatogram from GC-ICPMS analysis of the ArF3 of the B3 oil (**Figure 3.5a**) showed integrated peaks for 2,7-dmBT and (co-eluting) 2,5- and 2,6-dmBT, detected with comparable signal to noise as their *m/z* 162 peaks (< 2 ppm) by GC-MS analysis of the aromatic fraction (**Figure 3.5b**).
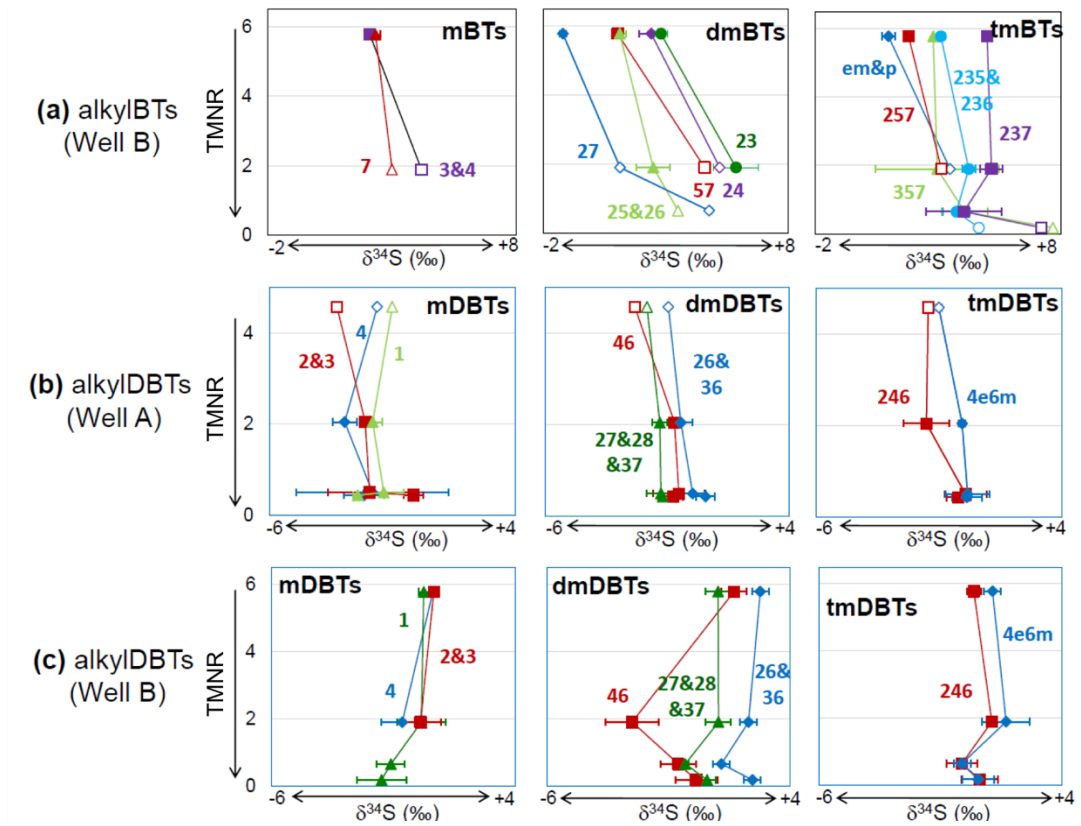
Figure 3.4 CSSIA data of oils showing: (a) $\delta^{34}S$ profiles of alkyl-BT isomers in well B oils; and (b) $\delta^{34}S$ profiles of alkyl-DBT isomers in well A and well B oils.
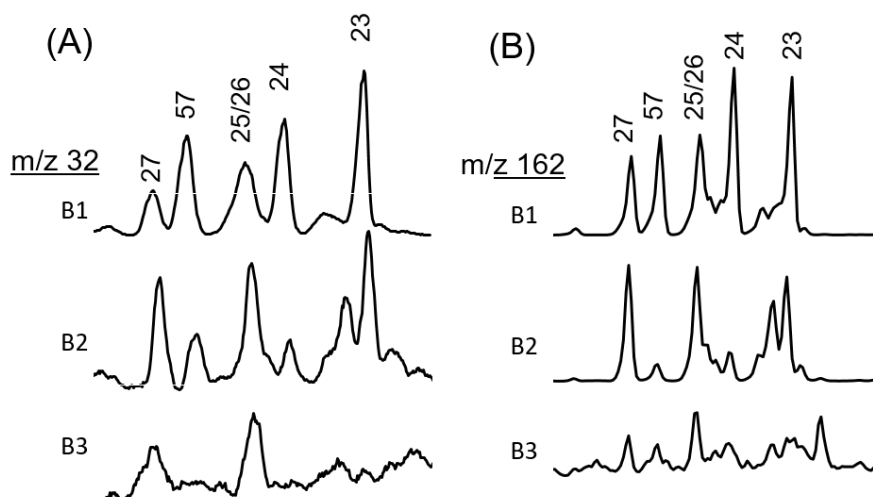
Figure 3.5 C$_2$-BT chromatogram regions of B1-B3 oils highlighted by (a) *m/z* 32 signal from GC-ICPMS analysis of their aromatic sub-fractions (ArF3); and (b) *m/z* 162 from GC-MS analysis of their aromatic fractions.

Table 3.3 $\delta^{34}S$ values (‰) of PR oils and their thioaromatic compounds. Standard variation of duplicate sample analysis indicated in parenthesis. Note that low ICPMS signals precluded duplicate analysis of some products.

Analyte	Compound	Well A				Well A			
		A1	**A2**	**A3**	**A4**	**B1**	**B2**	**B3**	**B4**
bulk oil $\delta^{34}S$*		1.4	1.6	0.3	0.2	2.1	1.7	1.5	1.7
Methyl-BT	7-mBT	-	-	-	-	2.3 (0.2)	3.0 (–)	-	-
	3-&4-mBT	-	-	-	-	2.1 (0.1)	4.2 (–)	-	-
Dimethyl-BTs	2,7-dmBT	-	-	-	-	–1.2 (0.1)	1.1 (–)	4.8 (–)	-
	5,7-dmBT	-	-	-	-	1.0 (0.1)	4.6 (–)	-	-
	2,5-&2,6-dmBT	-	-	-	-	1.1 (0.3)	2.5 (0.7)	3.5 (–)	-
	2,4-dmBT	-	-	-	-	2.4 (0.5)	5.2 (–)	-	-
	2,3-dmBT	-	-	-	-	2.8 (0.3)	5.9 (0.9)		-
Trimethyl-BTs	emBT/pBT	-	-	-	-	1.0 (0.3)	3.5 (–)	-	-
	2,5,7-tmBT	-	-	-	-	1.8 (0.0)	3.1 (–)	-	-
	3,5,7-tmBT	-	-	-	-	2.8 (0.0)	3.0 (2.5)	4.1 (0.9)	7.7 (–)
	2,3,7-tmBT	-	-	-	-	5.0 (0.1)	5.2 (0.5)	4.1 (1.5)	7.2 (–)
	2,3,5-&2,3,6-tmBT	-	-	-	-	3.0 (0.2)	4.3 (0.3)	3.8 (0.5)	4.7 (–)
Methyl-DBT	4-mDBT	–1.6 (–)[#]	–2.9 (0.5)	–1.8 (3.1)	–2.1 (0.8)	0.6 (0.1)	–0.6 (0.9)	-	-
	2-&3-mDBT	–3.2 (–)[#]	–2.1 (0.1)	–1.9 (1.7)	–0.1 (0.4)	0.7 (0.1)	0.1 (0.9)	-	-
	1-mDBT	–1.0 (–)[#]	–1.8 (0.4)	–1.3 (0.8)	–2.4 (0.2)	0.2 (0.2)	0.2 (1.0)	–1.1 (0.7)	–1.5 (0.9)
Dimethyl-DBT	4,6-dmDBT	–2.3 (–)[#]	–0.7 (0.1)	–0.5 (1.1)	–0.7 (0.4)	1.7 (0.5)	–2.5 (1.1)	–0.6 (0.7)	0.1 (0.9)

	2,6-&3,6-dmDBT	–0.9 (–)[#]	–0.4 (0.5)	0.0 (0.5)	0.6 (0.4)	2.8 (0.3)	2.3 (0.2)	1.2 (0.1)	2.5 (0.4)
	2,7-&2,8-&3,7-dmDBT	–1.8 (–)[#]	–1.3 (0.3)	–1.2 (0.6)	–1.2 (0.0)	1.0 (0.5)	1.1 (0.5)	–0.3 (0.1)	0.6 (0.3)
C$_3$-DBTs	4e6m-DBT	–1.0 (–)[#]	–0.1 (0.1)	0.2 (0.9)	0.1 (0.6)	1.2 (0.3)	1.7 (1.0)	–0.1 (0.3)	0.6 (0.7)
	2,4,6-tmDBT	–1.4 (–)[#]	–1.5 (0.9)	0.1 (0.9)	–0.2 (0.5)	0.4 (0.3)	1.1 (0.1)	–0.1 (0.6)	0.6 (0.8)

* Bulk δ^{34}S data provided by Thomas Oldenburg and Steve Larter (University of Calgary, Canada). EA-irMS δ^{34}S analysis of PR oils reported in Marcano et al. (2013).

[#] Electrical spike corrupted second acquisition of A1 oil.

The alkyl-BTs signals from GC-ICPMS analysis of ArF3 of all well A oils were too low for reliable $\delta^{34}S$ measurements. This was unexpected given the aromatic fraction concentrations of > 50 ppm for many of these products (particularly in A1 and A2). Furthermore, $\delta^{34}S$ values were generally measurable for co-occurring alkyl-DBTs (> 40 ppm) which suggests the lower MW alkyl-BTs may have been lost during the ArF3 workup from these oils. Relatively large (> 1‰) standard variations were evident from the duplicate $\delta^{34}S$ measurement of a few alkyl-DBTs in the deeper (and leaner) A3 and A4 oils, suggesting the DBT concentration of the ArF3 might also have been quite a bit lower than the measured aromatic fraction levels. Importantly, there is no S isotope fractionation of OSCs reduced in concentration by evaporation so any such losses will not have compromised the $\delta^{34}S$ values of alkyl-DBTs which were able to be measured from well A oils.

The $\delta^{34}S$ values for several of the alkyl-BTs measured in well B samples (**Figure 3.4a**) showed a consistent increase of up to several ‰ with increasing depth. The $\delta^{34}S$ value of 7-mBT and 3- and 4-mBT increased from B1 to B2 by +0.7‰ and +2.1‰, respectively. Their concentrations in the deeper oils were too low for $\delta^{34}S$ measurements. However, the higher concentrations and persistence of dmBTs and tmBTs allowed for $\delta^{34}S$ measurements of several isomers in B3 and B4. These products, particularly the dmBTs, were consistently enriched in ^{34}S with increasing well depth. The dmBTs showed increases in $\delta^{34}S$ values of between +2‰ to +6‰ (**Figure 3.4a**; **Table 3.3**). The $\delta^{34}S$ value of 3,5,7-tmBT increased by +5‰ whilst the other tmBTs increased between +1‰ to +2‰.

The increase in the $\delta^{34}S$ values of the alkyl-BTs would be consistent with preferential microbial utilisation or cleavage of ^{32}S bonds. Several studies have identified a similar kinetic control on the stable $\delta^{13}C$ and δD values of hydrocarbons in biodegraded

petroleum. The $\delta^{13}C$ values of residual hydrocarbon gases measured following aerobic biodegradation of marine sediment and anaerobic biodegradation of reservoir petroleum showed a significant enrichment in ^{13}C due to microbial utilisation of the smaller ^{12}C (Kinnaman et al., 2007; Wilkes et al., 2008). The large mass differential of H isotopes has contributed to major ^{2}H enrichment (e.g. 25–35‰) of n-alkanes in biodegraded petroleum (Pond et al., 2002; Sun et al., 2005; Asif et al., 2009).

Given the complexity of accumulation of the PR oil sands, however, it is possible that other factors besides biodegradation may have contributed to the down-well ^{34}S enrichment of alkyl-BTs. Thioaromatic compounds in petroleum can be ^{34}S enriched with increasing thermal maturity (Ellis et al., 2017), and the $\delta^{34}S$ values of BTs and DBTs homogenise at quite high maturities (Ellis et al., 2017; Rosenberg et al., 2017). However, the similar thermal maturity values of the PR oils [i.e. $C_{29}H/C_{30}H$ and TA/(TA+MA) values (**Error! Reference source not found.**) and others reported by (Marcano et al., 2013)] suggest thermal maturity is not a factor here.

The $\delta^{34}S$ values of several alkyl-DBTs measured in both well A and B oils (**Figure 3.4b,c**) remained relatively constant and did not reflect the same obvious enrichment in ^{34}S apparent in several of the alkyl-BTs measured in well B. This may be due to the greater biodegradation resistance of the higher MW DBTs. Kinetic ^{34}S enrichment may potentially be more effective at the very low analyte concentrations of the alkyl-BTs in the deeper well B oils. The reduced concentration of alkyl-DBTs down both oil wells might also be controlled by factors other than biodegradation (e.g. water washing) and which do not lead to S isotope fractionation.

The bulk $\delta^{34}S$ oil values showed a small (~1‰) decline down both wells, opposite the enrichment anticipated from the kinetic control of biodegradation. The bulk $\delta^{34}S$ values

of oils, inclusive of a typically abundant polar moiety, may lack the necessary resolution that specific OSCs (e.g. alkyl-BTs in the PR oils) can provide to distinguish the isotopic fractionations associated with secondary alteration processes such as biodegradation. Similarly, small variations in the bulk $\delta^{34}S$ values of other regionally proximal Canadian oil sands were previously attributed to differences in source charging, rather than biodegradation or thermal maturity controls (Méhay et al., 2009; Marcano et al., 2013). The Peace River hydrocarbon accumulations were produced by multiple source rock charges, with major contributions from Jurassic (i.e. Gordondale, Nordegg) and Devonian (Exshaw) source rocks (Larter et al., 2008; Adams et al., 2012). The bulk $\delta^{34}S$ and $\delta^{34}S_{OSC}$ values of the well B oils (**Table 3.3**) were generally a little enriched than the well A oils (**Table 3.3**). Marcano et al. (2013) reported the $\delta^{34}S$ values of unaltered (i.e. non-biodegraded) Exshaw oil sands were a few ‰ enriched compared to the Gordondale oil sands, which suggests the slightly enriched $\delta^{34}S$ values of the well B oils may reflect a greater contribution from Exshaw source rocks.

Conclusions

The reduced concentration of alkylated thioaromatics measured in biodegraded Peace River oils is typical of biodegradative loss. Seemingly varied biodegradation rates of different S compounds, including between different alkyl-BT and alkyl-DBT isomers, suggests the abundance ratio of selected products may contribute new molecular parameters to help characterise the biodegradation levels of S-rich petroleum. The $\delta^{34}S$ values of relatively low MW alkyl-BTs measured in well B showed a distinct ^{34}S enrichment in increasingly biodegraded oils consistent with a kinetic control on the preferential microbial utilisation of ^{32}S. In contrast, the $\delta^{34}S$ of alkyl-DBTs in the two wells studied showed no evidence of ^{34}S enrichment. This could relate to the increased isotopic

stability to biodegradation of the higher MW alkyl-DBTs, and possibly their persistence at concentrations above which any kinetic isotopic control becomes apparent. Alternatively, the decrease in the concentrations of alkyl-DBTs down the oil columns could be due to factors other than biodegradation (e.g. less OSC charging, water washing) and which have negligible influence on $\delta^{34}S$ values.

Bulk $\delta^{34}S$ values similarly showed no evidence of the biodegradation gradient in the wells, suggesting this traditonal S isotopic analyses lack the sensitivity to biodegradation that the $\delta^{34}S$ of certain compounds may have (e.g. alkyl-BTs). However, given the complex source and alteration history of the Peace River petroleum system, the OSC concentration and $\delta^{34}S$ trends presently observed in biodegraded PR oils should be considered cautiously until confirmed with further studies of other biodegraded S rich oils.

Acknowledgments

References

Adams, J.J. (2008) The Impact of Geological and Microbiological Processes on Oil Composition and Fluid Property Variations in Heavy Oil and Bitumen Reservoirs. PhD Thesis, University of Calgary, Canada.

Adams, J., Larter, S., Bennett, B., Huang, H., Westrich, J., van Kruisdijk, C. (2012) The dynamic interplay of oil mixing, charge timing, and biodegradation in forming the Alberta oil sands: Insights from geologic modeling and biogeochemistry. In: Hein, F.J., Leckie, D., Larter, S., Suter, J.R. (Eds.), Heavy-Oil and Oil-Sand Petroleum Systems in Alberta and Beyond. AAPG Studies in Geology 64, pp. 23–102

Adams, J.J., Riediger, C., Fowler, M., Larter, S.R. (2006) Thermal controls on biodegradation around the Peace River tar sands: Paleo-pasteurization to the west. Journal of Geochemical Exploration 89, 1–4.

Ahmed, M., Smith, J.W., George, S.C. (1999) Effects of biodegradation on Australian Permian coals. Organic Geochemistry 30, 1311–1322.

Alexander, R., Kagi, R.I., Woodhouse, G.W., Volkman, J.K. (1983) The geochemistry of some biodegraded Australian oils. The APEA Journal 23, 53–63.

Amrani, A., Lewan, M.D., Aizenshtat, Z. (2005) Stable sulfur isotope partitioning during simulated petroleum formation as determined by hydrous pyrolysis of Ghareb Limestone, Israel. Geochimica et Cosmochimica Acta 69, 5317–5331.

Amrani, A, Said-Ahmad, W., Shaked, Y., Kiene, R.P. (2013) Sulfur isotope homogeneity of oceanic DMSP and DMS. Proceedings of the National Academy of Sciences 110, 18413–18418.

Amrani, A., Sessions, A.L., Adkins, J.F. (2009) Compound-specific $\delta^{34}S$ analysis of volatile organics by coupled GC/multicollector-ICPMS. Analytical Chemistry 81, 9027–9034.

Asif, M., Grice, K., Fazeelat, T. (2009) Assessment of petroleum biodegradation using stable hydrogen isotopes of individual saturated hydrocarbon and polycyclic

aromatic hydrocarbon distributions in oils from the Upper Indus Basin, Pakistan. Organic Geochemistry 40, 301–311

Bayona, J.M., Albaiges, J., Solanas, A.M., Pares, R., Garrigues, P., Ewald, M. (1986) Selective aerobic degradation of methyl-substituted polycyclic aromatic hydrocarbons in petroleum by pure microbial cultures. International Journal of Environmental Analytical Chemistry 23, 289–303.

Bennett, B., Adams, J.J., Gray, N.D., Sherry, A., Oldenburg, T.B.P., Huang, H., Larter, S.R., Head, I.M. (2013) The controls on the compositoion of biodegraded oils in the deep subsurface – Part 3. The impact of microorganism distribution on petroleum geochemical gradients in biodegraded petroleum reservoirs. Organic Geochemistry 56, 94–105.

Bennett, B., Larter, S.R. (2008) Biodegradation scales: Applications and limitations. Organic Geochemistry 39, 1222–1228.

Berthou, F., Dreano, Y., Sandra, P. (1984) Liquid and gas chromatographic separation of isomeric methylated dibenzothiophenes. Journal of High Resolution Chromatography 7, 679–686.

Cai, C., Zhang, C., Cai, L., Wu, G., Jiang, L., Xu, Z., Li, K., Ma, A., Chen, L. (2009) Origins of Palaeozoic oils in the Tarim Basin: Evidence from sulfur isotopes and biomarkers. Chemical Geology 268, 197–210.

Creaney, S., Allan, J. (1990) Hydrocarbon generation and migration in the Western Canada Sedimentary Basin. In: Brooks, J. (Ed.), Classic Petroleum Provinces, Geological Society Special Publication. No 50 pp.189–202.

Deroo, G., Powell, T.G., Tissot, B., McCrossan, R.G. (1977) The origin and migration of petroleum in the Western Canadian Sedimentary Basin, Alberta – A geochemical and thermal maturation study. Geological Survey of Canada Bulletin 262, 1–136.

Depauw, G.A., Froment, G.F. (1997) Molecular analysis of the sulphur components in a light cycle oil of a catalytic cracking unit by gas chromatography with mass

spectrometric and atomic emission detection. Journal of Chromatography A 761, 231–247.

Ellis, G.S., Said-Ahmad, W., Lillis, P.G., Shawar, L., Amrani, A. (2017) Effects of thermal maturation and thermochemical sulfate reduction on compound-specific sulfur isotopic compositions of organosulfur compounds in Phosphoria oils from the Bighorn Basin, USA. Organic Geochemistry 103, 63–78.

Fedorak, P.M., Coy, D.L., Peakman, T.M. (1996) Microbial metabolism of some 2,5-substituted thiophenes. Biodegradation 7, 313–327.

Fedorak, P.M., Peakman, T.M. (1992) Aerobic microbial metabolism of some alkylthiophenes found in petroleum. Biodegradation 2, 223–236.

Fedorak, P.M., Westlake, D.W.S. (1984) Microbial degradation of organic sulfur compounds in Prudhoe Bay crude oil. Canadian Journal of Microbiology 29, 291–296.

Fisher, S.J., Alexander, R., Kagi, R.I. (1996) Biodegradation of alkylnaphthalenes in sediments adjacent to an off-shore petroleum production platform. Polycyclic Aromatic Compounds 11, 35–42.

Fisher, S.J., Alexander, R., Kagi, R.I., Oliver, G.A. (1998) Aromatic hydrocarbons as indicators of biodegradation in north Western Australian reservoirs. In: Purcell, P.G. and Purcell, R. (Eds), Sedimentary Basins of Western Australia. West Australian Basins Symposium. Petroleum Exploration Society of Australia, Perth, Australia, pp. 185–194.

George, S.C., Boreham, C.J., Minifie, S.A., Teerman, S.C. (2002) The effect of minor to moderate biodegradation on C_5 to C_9 hydrocarbons in crude oils. Organic Geochemistry 33, 1293–1317.

Greenwood, P.F., Amrani, A., Sessions, A., Raven, M.R., Holman, A.I., Dror, G., Grice, K., McCulloch, M.T., Adkins, J.F. (2014) Development and initial biogeochemical applications of compound specific $\delta^{34}S$ analysis. In: Grice, K.

(Ed.), RSC Detection Science Series No. 4: Principles and Practice of Analytical Techniques in Geosciences. Royal Society of Chemistry, Oxford

Greenwood, P.F., Mohammed, L.J, Schwark, L., McCulloch, M., Grice, K. (2018) The application of compound specific sulfur isotopes to the oil-source rock correlation of Kurdistan petroleum. Organic Geochemistry 117, 22–30.

Greenwood, P.F., Wibrow, S., George, S.J., Tibbett, M. (2008) Sequential hydrocarbon biodegradation in a soil from arid coastal Australia, treated with oil under laboratory controlled conditions. Organic Geochemistry 39, 1336–1346.

Grice, K., Alexander, R., Kagi, R.I. (2000) Diamondoid hydrocarbon ratios as indicators of biodegradation in Australian crude oils. Organic Geochemistry 31, 67–73.

Guthrie, J.M., Rooney, M.A., Chung, H.M. and Unomah, G. (2000) The effects of biodegradation versus recharging on the composition of oils, offshore Nigeria. Presented at the Annual Meeting of the American Association of Petroleum Geologists. 16–19 April 2000, New Orleans, LA, US.

He, N.N., Grice, K., Greenwood, P.F. (2019) The distribution and δ^{34}S values of organic sulfur compounds in biodegraded oils from Peace River (Alberta Basin, western Canada). Organic Geochemistry 128, 16–25.

Head, I.M., Jones, D.M., Larter, S.R. (2003) Biological activity in the deep subsurface and the origin of heavy oil. Nature 426, 344–352.

Izumi, Y., Ohshiro, T., Ogino, H., Hine, Y., Shimao, M. (1994) Selective Desulfurization of Dibenzothiophene by Rhodococcus erythropolisD-1. Physiology and Biotechnology 60, 223-226.

James, A.T., Burns, B.J. (1984) Microbial alteration of subsurface natural gas accumulations. American Association of Petroleum Geologists Bulletin 68, 957–960.

Kennicutt, M.C. (1988) The effect of biodegradation on crude oil bulk and molecular composition. Oil and Chemical Pollution 4, 89–112.

Kinnaman, F.S., Valentine, D.L., Tyler, S.C. (2007) Carbon and hydrogen isotope fractionation associated with the aerobic microbial oxidation of methane, ethane, propane and butane. Geochimica et Cosmochimica Acta 71, 271–283.

Kirimura, K., Furuya, T., Nishii, Y. (2001) Biodesulfurization of dibenzothiophene and its derivatives through the selective cleavage of carbon-sulfur bonds by a moderately thermophilic bacterim Bacillus subtilis WU-S2B. Journal of Bioscience and Bioengineering, 91, 262–266.

Kropp, K.G., Andersson, J.T., Fedorak, P.M. (1997) Bacterial transformations of naphthothiophenes. Applied and Environmental Microbiology 63, 3463–3473.

Kropp, K.G., Gonçalves, J.A., Andersson, J.T., Fedorak, P.M. (1994a) Bacterial transformations of benzothiophene and methylbenzothiophenes. Environmental Science and Technology 28, 1348–1356.

Kropp, K.G., Gonçalves, J.A., Andersson, J.T., Fedorak, P.M. (1994b) Microbially mediated formation of benzonaphthothiophenes from benzo[*b*]thiophenes. Applied and Environmental Microbiology 60, 3624–3631.

Kropp, K.G., Saftić, S., Andersson, J.T., Fedorak, P.M. (1996) Transformations of six isomers of dimethylbenzothiophene by three *Pseudomonas* strains. Biodegradation 7, 203–221.

Larter, S., Adams, J., Gates, I.D., Bennett, B., Huang, H. (2008) The origin, prediction and impact of oil viscosity heterogeneity on the production characteristics of tar sand and heavy oil reservoirs. Journal of Canadian Petroleum Technology 47, 52–61.

Larter, S., Huang, H., Adams, J., Bennett, B., Snowdon, L.R. (2012) A practical biodegradation scale for use in reservoir geochemical studies of biodegraded oils. Organic Geochemistry 45, 66–76.

Larter, S., Wilhelms, A., Head, I., Koopmans, M., Aplin, A., di Primio, R., Zwach, C., Erdmann, M., Telnaes, N. (2003) The controls on the composition of biodegraded oils in the deep subsurface – Part 1: Biodegradation rates in petroleum reservoirs. Organic Geochemistry 34, 601–613.

Leenheer, M.J. (1984) Mississippian Bakken and equivalent formations as source rocks in the Western Canadian Basin. Organic Geochemistry 6, 521–532.

López García, C., Becchi, M., Grenier-Loustalot, M.F., Païsse, O., Szymanski, R. (2002) Analysis of aromatic sulfur compounds in gas oils using GC with sulfur chemiluminescence detection and high-resolution MS. Analytical Chemistry 74, 3849–3857.

Marcano, N., Larter, S., Mayer, B. (2013) The impact of severe biodegradation on the molecular and stable (C, H, N, S) isotopic compositions of oils in the Alberta Basin, Canada. Organic Geochemistry 59, 114–132.

Mackenzie, A.S., Hoffmann, C.F., Maxwell, J.R. (1981) Molecular parameters of maturation in the Toarcian shales Paris Basin, France – III. Changes in aromatic steroid hydrocarbons. Geochimica et Cosmochimica Acta 45, 1345–1355.

Masterson, W.D., Dzou, L.I.P., Holba, A.G., Fincannon, A.L., Ellis, L. (2001) Evidence for biodegradation and evaporative fractionation in West Sak, Kuparuk and Prudhoe Bay field areas, North Slope, Alaska. Organic Geochemistry 32, 411–441.

Méhay, S., Adam, P., Kowalewski, I., Albrecht, P. (2009) Evaluating the sulfur isotopic composition of biodegraded petroleum: The case of the Western Canada Sedimentary Basin. Organic Geochemistry 40, 531–545.

Moldowan, J.M., Lee, C.Y., Sundararaman, P. (1992) Source correlation and maturity assessment of select oils and rocks from the Central Adriatic Basin (Italy and Yugoslavia). In: Moldowan, J.M., Albrecht, P., Philp, R.P. (Eds), Biological Markers in Sediments and Petroleum, Prentice Hall, Englewood Cliffs, New Jersey pp. 370–401.

Pallasser, R.J. (2000) Recognizing biodegradation in gas/oil accumulations through the δ^{13}C compositions of gas components. Organic Geochemistry 31, 1363–1373.

Palmer, S.E. (1993) Effect of biodegradation and water washing on crude oil composition. In: Engel, M.H., Macko, S.A. (Eds.), Organic Geochemistry: Principles and Applications. Plenum Press, New York, pp. 511–533.

Pond, K.L., Huang, Y., Wang, Y., Kulpa, C.F. (2002) Hydrogen isotopic composition of individual *n*-alkanes as an intrinsic tracer for bioremediation and source identification of petroleum contamination. Environmental Science and Technology 36, 724–728

Peters, K.E., Walters, C.C., Moldowan, J.M. (2005) The Biomarker Guide: Biomarkers and Isotopes in Petroleum Exploration and Earth History. Cambridge University Press, Cambridge, New York.

Punanova, S.A., Vinogradova, T.L. (2016) Geochemical features of mature hydrocarbon systems and indicators of their recognition. Geochemistry International 54, 817–823.

Radke, M. (1988) Application of aromatic compounds as maturity indicators in source rocks and crude oils. Marine and Petroleum Geology 5, 224–236.

Radke, M., Willsch, H., Leythaeuser, D., Teichmüller, M. (1982) Aromatic components of coal: Relation of distribution pattern to rank. Geochimica et Cosmochimica Acta 46, 1831–1848.

Rosenberg, Y.O., Meshoulam, A., Said-Ahmad, W., Shawar, L., Dror, G., Reznik, I.J., Feinstein, S., Amrani, A. (2017) Study of thermal maturation processes of sulfur-rich source rock using compound specific sulfur isotopes analysis. Organic Geochemistry 112, 59–74.

Rowland, S.J., Alexander, R., Kagi, R.I., Jones, D.M. (1986) Microbial degradation of aromatic components of crude oils: A comparison of laboratory and field observations. Organic Geochemistry 9, 153–161.

Shi, S., Chen, J., Zhu, L., Gao, L., Zhu, F. (2017) Biodegradation rates of dibenzothiophenes in oils: A case study from the Linpan oil field, Bohai Bay Basin, eastern China. Book of Abstracts, International Meeting of Organic Geochemistry 2017 (Florence, Italy, September 17–22).

Solanas, A.M., Pares, R. (1984) Degradation of aromatic petroleum hydrocarbons by pure microbial cultures. Chemosphere 13, 593–601.

Sun, Y., Chen, Z., Xu, S., Cai, P. (2005) Stable carbon and hydrogen isotopic fractionation of individual n-alkanes accompanying biodegradation: Evidence from a group of progressively biodegraded oils. Organic Geochemistry 36, 225–238.

Trolio, R., Grice, K., Fisher, S.J., Alexander, R., Kagi, R.I. (1999) Alkylbiphenyls and alkyldiphenylmethanes as indicators of petroleum biodegradation. Organic Geochemistry 30, 1241–1253.

Van Aarssen, B.G.K., Bastow, T.P., Alexander, R., Kagi, R.I. (1999) Distributions of methylated naphthalenes in crude oils: Indicators of maturity, biodegradation and mixing. Organic Geochemistry 30, 1213–1227.

Volkman, J.K., Alexander, R., Kagi, R.I., Rowland, S.J., Sheppard, P.N. (1984) Biodegradation of aromatic hydrocarbons in crude oils from the Barrow sub-basin of Western Australia. Organic Geochemistry 6, 619–632.

Wang, G., Xue, Y., Wang, D., Shi, S., Grice, K., Greenwood, P.F. (2016) Biodegradation and water washing within a series of petroleum reservoirs of the Panyu Oil Field. Organic Geochemistry 96, 65–76.

Wang, G.L., Wang, T.G., Simoneit, B.R.T., Zhang, L. (2013) Investigation of hydrocarbon biodegradation from a downhole profile in Bohai Bay Basin: implications for the origin of 25-norhopanes. Organic Geochemistry 55, 72–84.

Wenger, L.M., Davis, C.L., Isaksen, G.H. (2002) Multiple controls on petroleum biodegradation and impact on oil quality. SPE Reservoir Evaluation and Engineering 5, 375–383.

Wilkes, H., Vieth, A., Elias, R. (2008) Constraints on the quantitative assessment of in-reservoir biodegradation using compound-specific stable carbon isotopes. Organic Geochemistry 39, 1215–1221.

CHAPTER 4

Compound-specific δ^{34}S characterization of S-rich

lacustrine oils of the Bohai Bay Basin (NE China)

Statement of contribution (Nannan He): This chapter describes the δ^{34}S characterisation of S-rich lacustrine oils from two separate regions of the Bohai Bay Basin (Central East China). Following the general sections of **Introduction (4.1)** and **Analytical Methods (4.2)**, the two case studies are separately described and my and other contributions to these studies also separately given below:

S-rich oils and source rocks of Jinxain Sag (4.3):

I led this project with experimental and data interpretation contributions from my supervisors (P. Greenwood and K. Grice). Dr Hong Lu of the State Key Laboratory for Organic Geochemistry, China Academy of Sciences (Guanghzhou, China) provided all Jinxian Sag oil, rock and background samples plus regional information. The following manuscript on this work is presently being prepared for journal submission.

He, N., Grice, K., Lu, H., Greenwood, P.F. (In preparation) Compound specific sulfur isotope characterisation of Jinxian Sag petroleum. For submission to Organic Geochemistry.

S-rich oils of Dongpu Depression (4.4):

This project was conducted in collaboration with my supervisors (P. Greenwood and K. Grice) and Mr Changwei Ke and Professor Sumei Li from the Chinese Petroleum University (CUP) Beijing. The CUP colleagues provided the full set of 18 lacustrine oil samples from the Dongpu Depression (Bohai Bay Basin, China) and traditional hydrocarbon biomarker data from GC-MS analysis of these oils. I conducted the compound specific sulfur isotope analysis (CSSIA) and measured δ^{34}S values for a broad distribution of organic sulfur compounds (OSCs) in all but one oil which had only trace OSC concentrations. The δ^{34}S data and hydrocarbon biomarker data were jointly integrated and interpreted by all co-authors to evaluate the capacity of CSSIA data for distinguishing genetically different lacustrine oils (or of varied paleo-deposition) of the Dongpu Depression as well as a further investigation of the influence of thermal maturity and TSR on δ^{34}S data of petroleum OSCs. The collaborative study resulted in the following co-authored publication recently published.

Ke, C., Li, S., Zhang, H., He, N., Grice, K., Xu, T., & Greenwood, P. (2020) Compound specific sulfur isotopes of saline lacustrine oils from the Dongpu Depression, Bohai Bay Basin, NE China. Journal of Asian Earth Sciences, 104361.

A full copy of this paper is included in Appendix 2 at the end of this chapter. The description of this study in the body of this chapter relates to my specific contributions towards the S-isotope analysis and interpretations.

4.1 Introduction

Petroleum systems in the Bohai Bay Basin (BBB) provide nearly one-third of China's total oil production (Hao et al. 2010). The petroleum from this basin includes a number of S-rich oils and sour gas reservoirs. High concentrations of organic or inorganic S can reduce the quality and commercial viability of petroleum reserves and H_2S — a toxic, flammable and corrosive gas — poses a considerable safety risk throughout petroleum exploration and production activities (Dai et al., 2004). The petroleum exploration and research communities strive to better understand the mechanisms of organic sulfurisation and the genetic origins of reduced S (i.e. H_2S). The primary pathway and source of reduced S incorporated into organic or inorganic pools is the microbial sulfate reduction (MSR) of seawater SO_4^{2-}. Additional H_2S may also be sourced from the reduction of anhydrites at elevated geological temperatures (i.e. Thermochemical Sulfate Reduction, TSR). Diagenetic oxidation of reduced S (i.e. reaction of H_2S with organic compounds) can form Type I-S or II-S kerogens in suitable depositional environments (e.g. saline lacustrine systems). Alternatively, inorganic compounds such as pyrite can form on the interaction of H_2S with reactive Fe.

Molecular and stable isotopic characterisation of regional oils and source rocks can often help reveal the major reduced S sources and organic sulfurisation processes impacting petroleum samples. Here we use CSSIA to help characterise the organic sulfur in saline lacustrine oils from two complex petroleum regions of the BBB (**Figure 4.1**): (1) the Jinxian Depression, or Jinxian Sag as it is more commonly referred, where the source of the sour gas rich petroleum has attracted some controversy; and (2) the Dongpu Sag where biomarker characterisation has identified several separate petroleum families.

Petroleum formation history of Bohai Bay Basin (BBB)

The Bohai Bay Basin (BBB) is a rift basin developed in the late Jurassic through to the early Cenozoic on the basement of the North China Platform (Hu et al., 1986). Its tectonic evolutionary history consists of two periods: 1. A syn-rifting period (65–24.6 Ma) when sediments were deposited primarily under a lacustrine setting; 2. A post-rifting stage (24.6 Ma to recent) during which mainly fluvial facies where deposited (Hu et al., 2001; Gong et al., 2004; Wu et al., 2006). The strata in the BBB consists of the Kongdian Formation (Ek), the Shahejie Formation (Es$_4$–Es$_1$) and the Dongying Formation (Ed). Detailed stratigraphic information is given in **Error! Reference source not found.**.

Most of the reservoired petroleum in the BBB is thought to derive from three main Es lacustrine clastic sediment intervals: 1. Upper first interval (E$_{S1}$); 2. Middle third interval (E$_{S3}$); and 3. Lower fourth interval (E$_{S4}$; Zhang et al., 2005; 2009; 2012; Wang et al., 2010). Multiple charge events have contributed to a complex distribution of oils of varied hydrocarbon and organic sulfur compositions. However, general insights of several major charging events suggest low maturity E$_{S4}$ sourced oils were largely charged during the Paleogene (30−20 Ma) and high maturity Middle E$_{S3}$ oils from Neogene-Quaternary events (5 Ma−present; Hao et al., 2010; Guo et al., 2012).

Table 4.1 Paleogene stratigraphy of Bohai Bay Basin (modified from Chang et al., 1990).

Age (Ma)	System	Formation	Section	Thickness (m)	Lithological properties	Main sedimentary facies
25	Eogene	Dongying	Ed_1	200-600	Purplish red mudstone and sandstone intercalation	Fluvial
			Ed_2	500-1000	Grey and green mudstone and intercalated sandstone	Shallow and sub-deep lacustrine
30			Ed_3	300-700	Greenish-grey interbedding of sandstone and mudstone	Shallow lacustrine shore
35		Shahejie	Es_1	200-1000	Grey mudstone and intercalated oil shale, biological limestone and sandstone	Shallow and sub-deep lacustrine
40			Es_2	200-1000	Red sandstone and mudstone	Fluvial
			Es_3	1000-3000	Dark grey mudstone and intercalated oil shale	Deep lacustrine
45			Es_4	100-1000	Grey mudstone intercalated with oil shale, gypsum and saline rock. Lower part is red layers	Saline lacustrine
50		Kongdian	Ek_1	300-1000	Reddish-brown mudstone, intercalated with gypsum	Saline lacustrine
55			Ek_2	500-1500	Grey mudstone intercalated with sandstone	Sub-deep and deep lacustrine
60			Ek_3	400-1000	Red sandstone and conglomerate intercalated with mudstone	Fluvial
65						
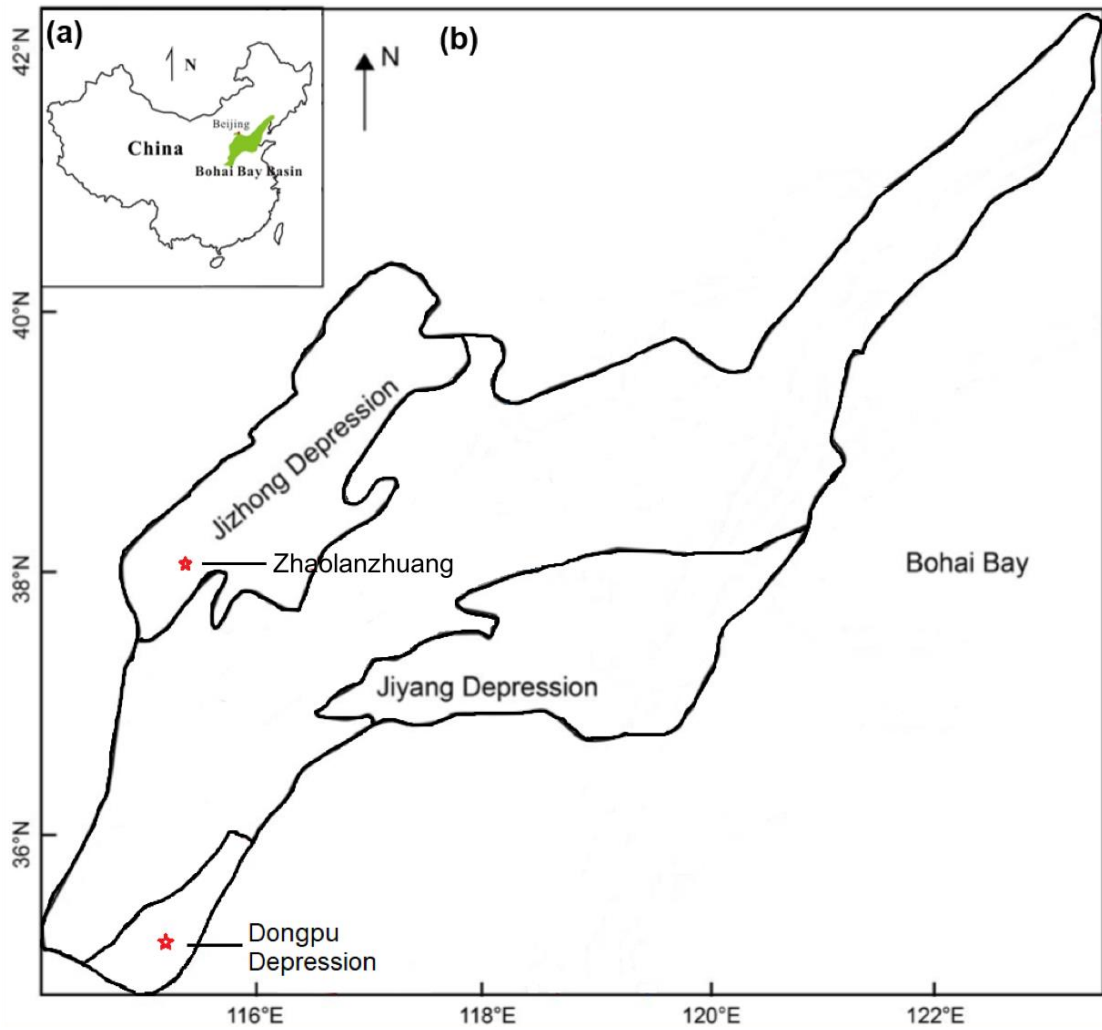
Figure 4.1 Regional map of Bohai Bay Basin showing location Dongpu Depression and Zhaolanzhuang well in Jinxian Depression.

4.2 Analytical Methods

4.2.1 Solvent extraction of bitumen

Rock samples from Zh2 well of Jinxian Sag were ground and solvent-extracted in DCM and methanol (9:1 v/v) using a Milestone Start E microwave extraction unit (Milestone Inc., Shelton, USA). The samples were heated from room temperature (~25 °C) to 80 °C over 10 minutes, then held at 80 °C for 15 minutes.

4.2.2 Colum chromatography

Saturated (SAT), aromatic (ARO) and polar fractions of the Jinxian Sag oils and Zh2 rock extracts (see Section 4.3.2) and Dongpu oils (Section 4.4.2) were separated by column chromatography on activated silica gel (160 °C). To further concentrate OSCs, aromatic fractions (AF0–AF5) were fractionated over aluminium oxide (Type 507C neutral; Fluka) using solutions of (1) AF0: n-hexane; (2) AF1: n-hexane:DCM (95:5 v/v); (3) AF2: n-hexane:DCM (90:10 v/v); (4) AF3: n-hexane:DCM (50:50 v/v); (5) AF4: DCM and (6) AF5: DCM:Methanol (50:50 v/v). The OSCs mostly eluted in the AF3 sub-fraction.

4.2.3 Hydropyrolysis (HyPy)

The kerogen fractions of the Jinxian Sag (Zh2) rocks were pyrolysed using a commercial hydropyrolysis (HyPy) apparatus (STRATA Technology Ltd) following traditional operating procedures (Snape et al., 1994, Love et al., 1995, Meredith et al., 2004, Aboglila et al., 2011, Lockhart et al., 2013; Grotheer et al., 2015). Briefly, the samples were pyrolysed without any catalyst – since the commonly used catalysts contain S - with resistive heating from 25 °C to 250 °C at 300 °C/min, and then from 250 °C to the final temperature of 550 °C at 8 °C/min with the final temperature held for 2 min. A constant pressure (150 bar) and flow rate (5 L/min) of ultra-high purity hydrogen (BOC Group)

was maintained throughout thermal treatment. The released compounds were cold trapped on a silica-filled trap, chilled with dry ice. HyPy released products adsorbed on the silica trap were eluted with DCM (40 mL) on a large chromatographic column (40cm × i.d. 0.8cm). Elemental sulfur was removed from the HyPy fraction with HCl-activated copper turnings.

4.2.4 Molecular and isotopic analysis

The molecular and isotopic analysis of the ARO fractions of the crude oil and rock extracts and the HyPy released fraction of the kerogens was conducted by GC-MS and GC-ICPMS, respectively. The instrumentation and analytical procedures were largely the same as described for the analysis of the Peace River sand oils in Chapter 3 and the related He et al. (2019) publication.

4.3 Compound specific δ^{34}S isotope analysis of oils and source rocks from the Jinxian Sag

4.3.1 Petroleum Geology of Jinxian Sag

Jinxian Sag is located in the southwest of Jizhong Depression, which is one of many faulted Eocene depressions in Bohai Bay Basin. This sag is filled with 2–4 km of palaeogene sediments. Nanguzhuang Anticline divides Jinxian Sag into two parts in Es_4–Ek deposition: (i) a northern half-graben area, where evaporitic saline-hypersaline lacustrine sediments are dominant in Es_4–Ek_1, producing high H_2S petroleum, and (ii) a southern full-graben area, where brackish freshwater and freshwater lacustrine deposits are common in Es_4–Ek_1 and Ek_{2+3}, responsible for oils with low to zero H_2S contents are found in oil (Zhang et al., 2005).

Petroleum from the Zhaolanzhuang field of the Jizhong Depression in the northern graben are well known for their sour gas nature, containing some of the highest

concentrations of H_2S (40–92%) of all the petroleums of China (Zhang et al., 2015). Several high-S oils in shallow anhydrite-rich reservoirs were associated with the sour gas. There has been much conjecture about the major sources of these petroleums, with different groups separately proposing that MSR (Cai et al., 2005, Worden and Cai, 2006) and TSR (Zhang et al., 2005; 2006) were the main source of reduced S in the system and implied origin of the OSCs incorporated into the petroleum. The contrasting views escalated to an earnest debate which included consideration of bulk $\delta^{34}S$ values (0, 11 and 16‰) of three high S oils (S $\geq$ 3.5%) and a purported $\delta^{34}S_{H2S}$ value of 0‰ (Cai et al.,2005), however the reliability of the $\delta^{34}S_{H2S}$ data — originally reported in an unpublished master thesis by Mr. Guangfeng Fan — was subsequently questioned by Zhang et al. (2006).

4.3.2 Oil and Source Rock Samples of Zhaolanzhuang (Zh) oil field

Two crude oil samples from Well 7 and Well 39 of the Zhaolanzhuang (Zh) oil field and seven rock samples collected from the Zh2 well (

Table 4.2) were analyzed for their OSC composition and compound-specific $\delta^{34}S$ values. All three wells are from the northern region of the Jinxian sag, where the S and H_2S contents of the petroleum are typically high. The oils represent two of the three production oils from the organic geochemistry study of Cai et al. (2005) — the third oil (Zh41-3) was not available. The Zh7 oil had the highest S content with S and H_2S compositions of 15% and 40%, respectively (

Table 4.2). Well Zh2 is in the same oil reservoir as the Zh7 and Zh39 wells, and the selected rock-core samples (2490–3211m) span the primary E_{S4} source strata.

Table 4.2 List of samples from Jinxian Sag.

	Sample	Reservoir	Depth (m)	Sulfur (%) [a]	H$_2$S content (%) [b]
Oil	Zh7	Es$_4$	2232	14.69	40.2
	Zh39	Es$_4$	2794	3.49	
Rock	Zh2-32	Es$_4$	2411		
	Zh2-37	Es$_4$	2430		
	Zh2-66	Es$_4$	2545		
	Zh2-70	Es$_4$	2560		
	Zh2-77	Es$_4$	2588		
	Zh2-93	Es$_4$	2651		
	Zh2-106	Es$_4$	2702		

[a] from Cai et al. (2005).
[b] from Zhang et al. (2005).

4.3.3 Molecular and Isotopic Compositions of Jinxian Sag oil and rocks

Selected ion chromatographs of C$_0$−C$_3$-BT and C$_0$−C$_3$-DBT products from the GC-MS analysis of the aromatic fractions of Zh7 oil, and the bitumen and kerogen fractions of Zh2-70 rock are shown in **Figure 4.2**. Generally similar distributions of thioaromatic products were detected from all of the oil and rock samples. Within the bitumen, abundances of the alkyl-BTs were more variable than the alkyl-DBTs and no BT products were detected from the kerogen (HyPy treated) fractions of the rocks. The greater detection variability of the BTs was likely due to their relatively high volatility (cf. higher MW DBTs) and susceptibility to loss during solvent based laboratory procedures.
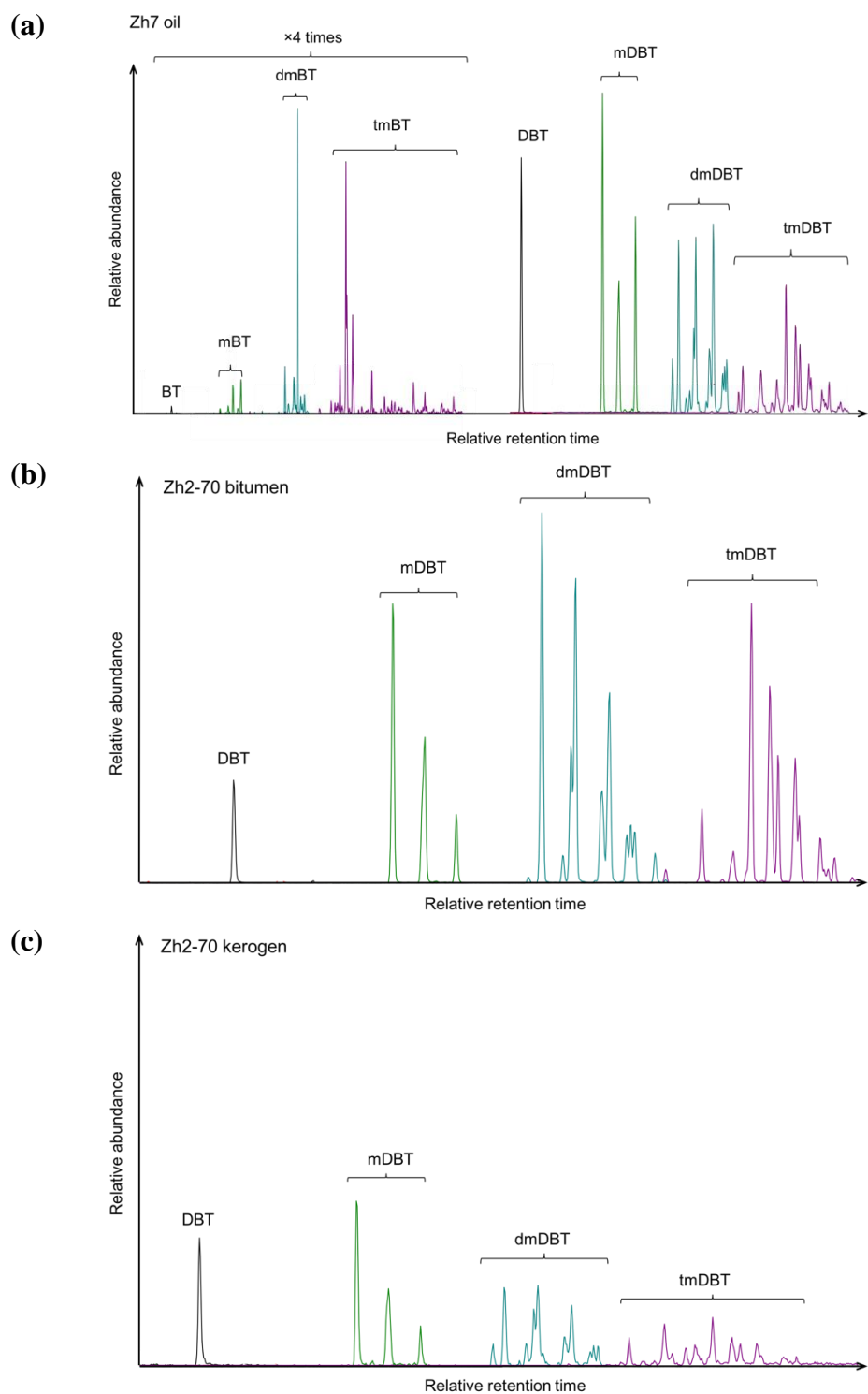
Figure 4.2 Selected ion chromatograms of OSCs (*m/z* 134, 148, 162, 176, 184, 198, 212, 226) in Jinxian Sag samples. (a) BTs and DBTs in Zh7 oil; (b) DBTs in bitumen fraction of Zh2-70 rock; (c) DBTs in kerogen fraction of Zh2-70 rock.

Table 4.3 δ^{34}S values of OSCs in crude oils, bitumen and kerogen fractions of rocks from Jinxian Sag.

OSCs	Crude oil				Bitumen fraction of rocks														Kerogen fraction of rocks					
	Zh7 oil		Zh39 oil		Zh2-32		Zh2-37		Zh2-66		Zh2-70		Zh2-77		Zh2-93		Zh2-106		Zh2-70		Zh2-93		Zh2-106	
	δ^{34}S	S.V.	δ^{34}S	S.V.	δ^{34}S	S.V.	δ^{34}S	S.V.	δ^{34}S	S.V.	δ^{34}S	S.V.	δ^{34}S	S.V.	δ^{34}S	S.V.	δ^{34}S	S.V.	δ^{34}S	S.V.	δ^{34}S	S.V.	δ^{34}S	S.V.
BT																			17.4	–				
mBTi																			21.4	3				
mBTii																			21.4	–				
mBTii																								
mBTiv																								
dmBTi	2.6	–																	20.5	–			5.6	1.6
dmBTii	4.8	–																	20	2			9.9	–
dmBTiii	1.8	–																	19	1.6			10.6	–
dmBTiv																			17.7	0.8			7.9	–
dmBTv																			17.7	0.8			7.9	–
dmBTvi																								
tmBTi	3.1	–																	22.3	–	48.5	–	1.5	–
tmBTii	2.1	–																	19.8	–	78.2	–	6.3	–
tmBTiii	1.6	–																	20.3	–	36.6	–	4.8	–
tmBTiv																			18.5	0.5			5.7	–
tmBTv																			14.5	–				
tmBTvi																								
TemBTi																								
TemBTii																								
DBT	-3.1	0.8	12.9	0.2	4	–	17.4	–	15.7	1.5	15.2	–	11.5	–	10.1	0.4	1.4	0.5	16.3	0.2	11.6	0.5	3.6	0.2
4-mDBT	-4.8	1.8	10.6	0.8	9	–	16.3	–	17.8	0.8	15.3	–	11.7	–	10	0.4	2.1	0.3	15.7	1.2	9.4	0.6	3.4	1
2&3-mDBT	-5.4	1.8	10.5	1.7	4.7	–	18.9	–	18.2	0.8	15.8	–	12.1	–	10.3	0.5	2.1	0.9	16.2	–	10	1.8	3.8	1.4
1-mDBT	-1.1	1.3	11	0.9	3.1	–	19.7	–	20	0.2	16.1	–	10.9	–	10.8	0.6	3.3	1.1	16.4	3	11.1	–	2.7	0.9
dmDBTi	-6.4	1.2	11.1	1.2	11.5	–	14	–	18.5	0.7	15.2	–	12.9	–	10.7	0.6	1.1	0.3	16.6	–	7.3	1.6	4.4	0.3
dmDBTii	-1.9	2.4	10.9	0.9	8.5	–	16.1	–	18.5	0.2	15.8	–	14	–	9.7	0.5	2.4	0.5	16.5	0.4	6.2	2.8	5.6	1.6
dmDBTiii	-1.5	1.7	11.4	0.9	12.1	–	17.4	–	19.7	0.1	16.5	–	14	–	10.3	0.4	3.6	0.8	15.4	0.2	8.3	1.3	4.1	1.2
tmDBTi	-4.1	1.8	11.3	1.8	17	–	15.7	–	20.6	0.3	16.3	–	12.5	–	9.9	0.7	2.2	1.1	15	–	11.1	1.1	3.3	0.2
tmDBTii			10.9	1.3			16.7	–	18.9	1	15.8	–	14.9	–	10	0.6	2	0.9	13.8	1.1	7.5	1.4	3.3	1.9

The $\delta^{34}S$ values of OSCs in the Zh7 and Zh39 oils are given in **Table 4.3**. The $\delta^{34}S$ values of alkyl-DBTs were measured in both oils, but $\delta^{34}S$ values of alkyl-BTs were only measured in Zh7. The unsuccessful $\delta^{34}S_{BT}$ measurements from Zh39 was likely due to the low concentrations of the BTs in this oil. The $\delta^{34}S_{OSC}$ profile of the Zh7 and Zh39 oils are displayed in **Figure 4.3**. The bulk $\delta^{34}S$ values of these oils and also of the Zh41-3 previously reported by Cai et al. (2005) are also shown (dotted lines in Figure 4.3) for comparison. The average $\delta^{34}S$ values of OSCs from Zh7 (–0.4‰) and Zh39 (+11.2‰) were generally consistent with the bulk $\delta^{34}S$ values reported by Cai et al. (2005).
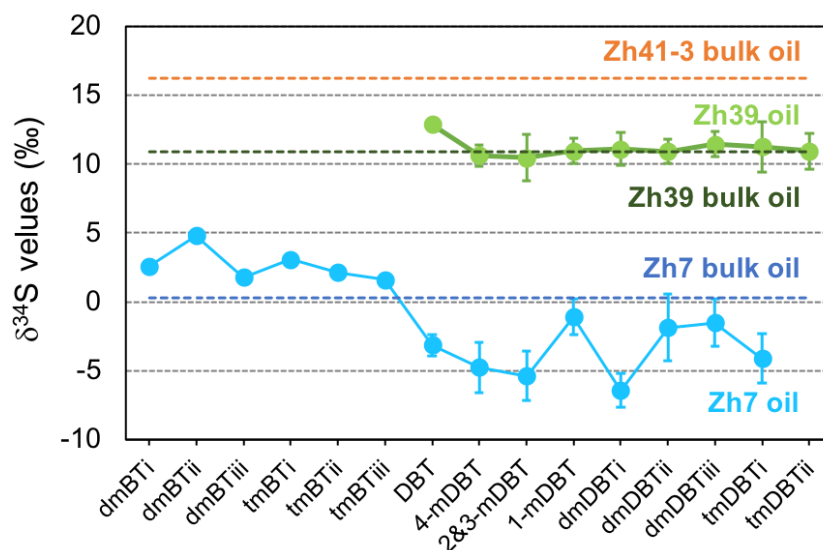
Figure 4.3 The $\delta^{34}S$ profile of BTs and DBTs measured in the Zh7 oil and the DBTs measured in the Zh39 oils. Ave $\delta^{34}S_{OSC}$ Zh7 = −0.4‰; Ave $\delta^{34}S_{OSC}$ Zh39 = +11.2‰. The dotted lines correspond to bulk $\delta^{34}S$ value of Zh7, Zh39 and Zh41-3 reported by Cai et al. (2005).

The $\delta^{34}S_{DBTs}$ values of the rocks (**Table 4.3**) are depicted in **Figure 4.4**. The bitumen fraction of the rock samples varied between 1‰ to 17‰ (**Figure 4.4a**), reflecting a similar range of $\delta^{34}S_{DBTs}$ values to the oils. The kerogen fraction of three rocks (Zh2-70, 93 and 106), selected to cover the full range of bitumen $\delta^{34}S_{DBT}$ values were analysed to allow S-

isotopic comparison of free and kerogen bound compounds (**Figure 4.4b**). The $\delta^{34}S_{DBTs}$ of the kerogen and bitumen of these three rocks were very similar (Ave $\delta^{34}S_{DBTs}$ of bitumen/kerogen of the rock were Zh2-70 = 15.8‰/15.8‰; Zh2-93 = 10.2‰/9.2‰; and Zh2-106 = 2.2‰/3.8‰).
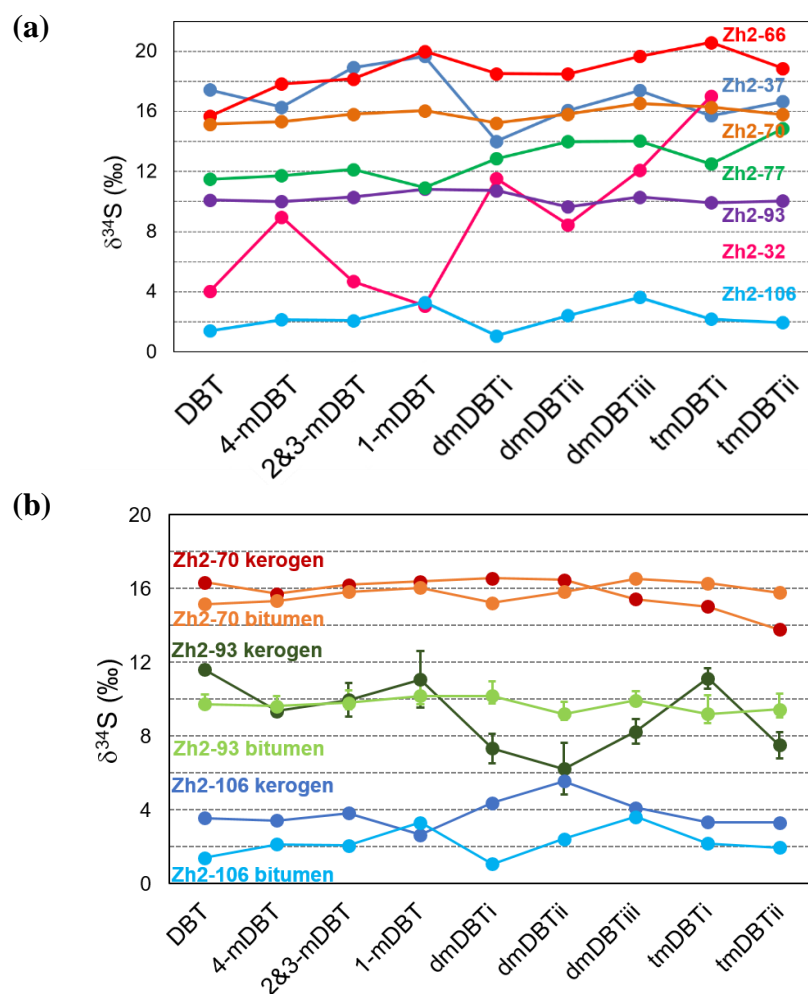
Figure 4.4 $\delta^{34}S$ of DBTs in (a) bitumen of all Zh2 rocks analysed (b) bitumen and kerogen fractions of three selected Zh2 rocks. Error bars shown for Zh2-93 bitumen and kerogen (Figure 4.4b) is standard variance from duplicate analysis of this sample (analyses of other samples had similar standard variances).

4.3.4 Origin and History of BBB Petroleum

The two major formation mechanisms of subsurface H_2S are MSR and TSR (Peters et al., 2005).

The **MSR** reaction in low-temperature reservoirs (<80 °C) can be simplified as follows:

$$CH_4 + SO_4^{2-} = CO_3^{2-} + H_2S + H_2O.$$

TSR in geological environments such as carbonate reservoirs at high temperature (>110 °C) can be described as:

$$SO_4^{2-} + Hydrocarbons + H_2O = carbonate + CO_2 + H_2S + S^0 + OSCs + H_2O$$

Common mineral sulfates include anhydrite ($CaSO_4$) and gypsum ($CaSO_4 2H_2O$), with others such epsomite ($MgSO_4$) sometimes geologically present in relatively low abundance. OSCs often detected in petroleum samples include alkyl sulfides, thioaromatics (BTs, DBTs) and thiadiamondoids (Amrani, 2014).

The S origin of the sour gas rich petroleum ($\leq$ 92% H_2S) of the Jinxian Sag was previously contended by two groups separately proposing a predominant MSR source (Cai et al., 2005; Worden and Cai, 2006) or a predominant TSR source (Zhang et al., 2005; Zhang et al., 2006). Evidence supporting an MSR source included the relatively low bulk $\delta^{34}S$ values measured for some Zh oils, e.g. 0‰ in the high S content (15%) Zh7 oil (Cai et al., 2005). A similar value (~0‰ H_2S) was given in a previous report (Fan et al., 1992). Significantly, these $\delta^{34}S$ values were much lower than the $\delta^{34}S$ values (+34 to +40‰) given for anhydrites of the Jinxian Sag. It was acknowledged, however, that the location of the proposed MSR process must have been external to the reservoir, since H_2S concentrations in excess of 40% and the high temperatures of petroleum reservoirs in Jinxian Sag (75–100 °C) would be too

hostile to support microbial activity. Most microbes cease to metabolise at geological temperatures > 80 °C (Postgate, 1984; Ehrlich, 1990).

In contrast to the MSR origin, Zhang et al. (2005) independently favoured a TSR source of the S in Jinxian Sag petroleum. They proposed that TSR was the most likely production mechanism for the very high H_2S concentrations (up to 90%) of the sour gas reservoirs. MSR typically does not contribute to petroleum H_2S concentrations much above 3% (Zhu et al. 2003, 2013). They did report $\delta^{34}S$ values of elemental sulfur over a wide range (1–22‰), with the upper values approaching the $\delta^{34}S$ values given for some anhydrites (30–35‰) potentially due to the occurrence of TSR. They too favoured formation of H_2S remote from the reservoir (representing one similarity to the MSR model), but because reservoir temperatures were too low to directly initiate TSR. They suggested TSR would have been more likely supported by the elevated geothermal environment of Ek–Es4 source strata extending to depths of 5,000 m and furthermore that faults extending upwards and penetrating the shallower sour gas reservoirs were ideal conduits for vertical migration.

The debate over the competing proposed mechanisms initially advocated for MSR (Cai et al., 2005) and TSR (Zhang et al., 2005) was subsequently developed (Cai and Warden, 2006; Zhang et al., 2006). Zhang et al. (2006) specifically questioned the validity of unverified $\delta^{34}S_{H2S}$ data cited by Cai et al. (2005) — originally reported by Fan et al. (1992) as part on an incomplete MSc. Zhang et al. (2006) concluded that "we cannot yet convincingly explain, completely, the origin of these sour gases with the available, incomplete dataset". Hence, additional research was required to further explore the mechanisms.

Given the ongoing uncertainty about the sources of the gas and oil reservoirs in the Jinxian Sag, the currently measured $\delta^{34}S_{OSC}$ data was scrutinized for evidence of the origin of the

organic S in oils and rocks from the Zhaolanzhuang oil field. The $\delta^{34}S_{OSC}$ values across the two oils spanned a wide range of values (~-6.4 to +12.9‰), but of each oil (Zh7 Ave = −0.4‰; Zh39 Ave = 11.2‰) was very close to their previously measured bulk $\delta^{34}S$ values (Zh7 = +0.3‰, Zh39 = +10.9‰; Cai et al., 2005). The bulk $\delta^{34}S$ value of oil from the Zh41-3 well was also previously reported to be +16.2‰ (Cai et al., 2005). These values showed no consistent relationship with the S content of the oils (S content of Zh7=14.7%; Zh39=3.5%; Zh41-3=10.9%).

The $\delta^{34}S$ of BTs (Ave = 2.7‰) were only measured here for the Zh7 oil, where they were slightly more enriched in ^{34}S than the DBTs (Ave = −3.5‰). An enrichment of BTs compared to DBTs can arise during the early to moderate stages of TSR (Amrani et al., 2012), however the relatively modest difference observed here is not sufficiently diagnostic of a TSR event (the low $\delta^{34}S$ values of these compounds are also quite far from the high $\delta^{34}S$ values of the regional anhydrite available for TSR).

The $\delta^{34}S_{OSC}$ values of the Zh2 rocks (1.1 to 20.6 ‰; **Table 4.3**) spanned a similar range to the oils. The bitumen fraction of the rocks may have been influenced by secondary events such as migrating petroleum which could introduce allochthonous hydrocarbons and OSCs. To evaluate this possibility the $\delta^{34}S$ values of OSC in the kerogen fractions of three selected rocks were separately measured. The kerogen fraction of rocks are less susceptible to secondary alteration than the free hydrocarbon phase (i.e. bitumen) or the maltenes of oils.

The $\delta^{34}S_{DBTs}$ of the kerogen and bitumen fraction of the three rocks analysed were similar (Ave $\delta^{34}S_{DBTs}$ of bitumen/kerogen of the rock were Zh2-70 ~ 15.8‰/15.8‰, Zh2-93 ~ 10.2‰/9.2‰ and Zh2-106 ~ 2.2‰/3.8‰). This consistency implies that the $\delta^{34}S$ composition of the bitumen had not been impacted by any secondary events. The $\delta^{34}S_{OSC}$

values of both the bitumen and kerogen rocks therefore can confidently be considered indicative of the $\delta^{34}S$ value of diagenetically incorporated petroleum S.

The petroleum content of the Zh2 rocks was essentially sourced from the same source strata across a relatively narrow geological time where seawater SO_4^{2-} values can be considered constant — Engel and Zumberge (2007) reported the $\delta^{34}S$ values of Eocene seawater sulfate in the narrow range of +18 to +24‰. One possible explanation for the large variation in the $\delta^{34}S_{OSCs}$ values observed between different Zhaolanzhuang oils and rocks is that organic sulfurization occurred in a S limited or closed system environment. The ES_4–Ek_1 strata in the northern Jinxian Sag were previously proposed to be deposited in a closed hydrological system (e.g. eutrophic lake), on the basis of hydrocarbon characteristics indicative of primary algal input (e.g. high C_{27} steranes; high steranes/hopanes; Cai et al., 2005; Kuo, 1994; Horsfield et al., 1994).

In a S-restricted system the preferential reduction of ^{34}S depleted SO_4^{2-} would result in a slight enrichment in the residual SO_4^{2-} pool over time. Temporal variations in the $\delta^{34}S$ of the reduced S pool (i.e. H_2S), and in turn produced inorganic (i.e. pyrite) and organic sulfur (i.e. petroleum; via reduced S intermediates, S^0, S_x^{2-}), would subsequently mirror the $\delta^{34}S$ dynamics of the source sulfate. This $\delta^{34}S$ behaviour of a restricted system S-cycle (**Figure 4.5**) is representative of a Rayleigh distillation process (Broecker and Oversby, 1971; Hale and Drew, 2010).
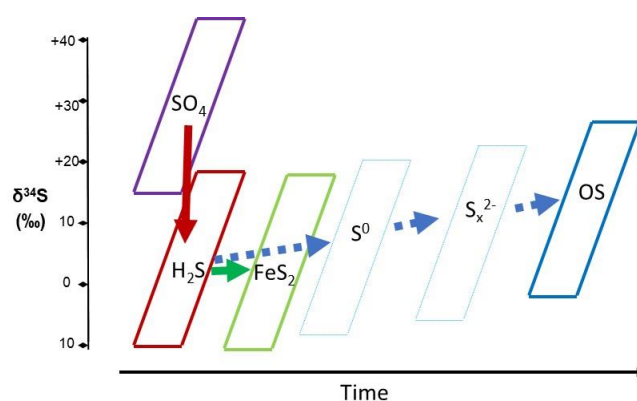
Figure 4.5 S-cycle and $\delta^{34}S$ dynamics of SO_4^{2-} restricted system proposed for Jinxian Sag. Nb., Time axis is dimensionless.

A restricted SO_4^{2-}-$\delta^{34}S$ model (**Figure 4.5**) would be consistent with rocks (and the petroleum subsequently generated from them) with relatively ^{34}S depleted OSCs being formed by early organic sulfurization processes, and the rocks with more ^{34}S enriched OSCs formed by latter sulfurization processes when the reduced S pool was heavier. Differences evident in the $\delta^{34}S$ of OSCs co-occurring in the same oils was similarly proposed to be due to differences in the timing of formation of these OSCs in a restricted and isotopically dynamic SO_4^{2-} system (Shawar et al., 2020). The Zh2 rock data does suggest a general trend of lower values for deeper rocks. This would seem consistent with the organic S of the deeper, older rocks having utilized early formed pool of relatively ^{34}S depleted reduced S. The generally ^{34}S enriched organic S of younger, shallower rocks was produced later from ^{34}S enriched H_2S – reduced from ^{34}S enriched SO_4^{2-} pool in a restricted system. Correlation of the $\delta^{34}S_{OSC}$ profiles of the bitumen fractions from the full set of Zh2 rocks (**Figure 4.4a**) showed a couple of breaks in the increasing $\delta^{34}S$ value— shallower/younger sample trend, most notably the relatively depleted values of Zh37 (2430 m) and to a lesser extend Zh32 (2411 m). This might arise from occasional relaxation of

the SO_4^{2-} limitation, such as by periodical flushing where fresh SO_4^{2-} is added to the residual pool.

The dissimilatory reduction of sulfate (i.e. MSR) is central to the mechanism proposed here for the formation of organic sulfur in Zhaolanzhuang oils and rocks. Whilst this implies a MSR contribution of H_2S to the petroleum of this region, it does not resolve whether just MSR is responsible for the high sour gas concentrations of some reservoirs. A contribution of externally migrated TSR to some gas and oil accumulations cannot be ruled out, and indeed would still seem plausible given the very high H_2S levels (i.e. ~90%) reported in some wells. Further direct correlation (e.g. $\delta^{34}S$) of reservoir H_2S with the organic S of co-occurring oils and also to relevant minerals (pyrite, anhydrites) of the sedimentary system is needed to fully resolve this issue – and may be difficult to conduct given current restrictions to field sampling.

4.4 Compound Specific $\delta^{34}S$ analysis of oils from the Dongpu Sag.

4.4.1 Geology and petroleum characteristics of Dongpu Depression

The geological setting of the Dongpu Depression is described in detail in the co-authored paper from this collaborative study (Ke et al., 2020; Appendix 2). In brief, the Dongpu Depression is located in the southwestern part of the Bohai Bay Basin and has four defined tectonic units: the eastern sub-depression; the western sub-depression; the central uplift and the western slope (Qi and Yang, 2010). Different tertiary aged lacustrine facies occur in the northern (saline) and southern (freshwater) sectors of the depression (Wang et al., 2015). Lacustrine oils typically derive from non-marine algal and bacterial organic matter and have low content of sulfur (Peters, et al., 2005). The high sulfur content of the Dongpu sediments is due to microbial sulfate reduction (MSR, Cai et al., 2005, Worden and Cai, 2006). Type II kerogens and Types II–III kerogens of Es_3–Es_4 intervals were responsible

for the northern and southern oils, respectively (Peng et al., 2003; Change et al., 2007; Chen et al., 2018). A number of S-rich oils have been discovered in both regions.

Dongpu oils also span a wide range of thermal maturities providing the opportunity for further investigation of thermal influences (i.e. thermal maturity and TSR) on the $\delta^{34}S$ character of petroleum sulfur. Geological conditions (i.e. high reservoir temperature, free sulfur and authigenic pyrite) and reagents (reduced S and hydrocarbons) can also be favorable to TSR (Orr, 1974; Zhang et al., 2008), the occurrence of which has been confirmed by the detection of thiadiamondoids (TDs) in some drill cores. CSSIA measurements conducted as part of an initial detailed characterization of a selected few Dongpu oils (Ji et al., 2018) showed evidence of [34]S enriched BTs and TDs (cf. DBTs) indicative of TSR. Whilst the impacts of TSR on the $\delta^{34}S$ character of oils have been well studied, the impacts of other controlling factors, such as oil window thermal maturities (Ellis et al., 2017) and paleo-environment are only beginning to be understood.

4.4.2 Dongpu Sag oil samples

The oil samples used in this study comprised sixteen crude oils distributed in the northern part of the Dongpu Depression (**Table 4.4**). Two additional freshwater lacustrine facies oils from Shanchunji (SCJ) and Macheng (MC) oilfields in southern Dongpu areas were analysed for comparison (**Table 4.4**). The northern oils were selected from Weicheng (WC, 2 oils), Pucheng (PC, 4 oils), Lintun (LT, 2 oils) and Wenliu (WL, 8 oils) oilfields (**Table 4.4**). Colleagues from the Chinese Petroleum University provided all the oil samples along with traditional hydrocarbon biomarker data which showed they spanned five separate lacustrine oil families. The $\delta^{34}S$ values of thioaromatic compounds measured in all the oils were primarily evaluated for their capacity to distinguish the genetically different Dongpu Depression oils (or varied paleo-depositional environments). The hydrocarbon data also

showed thermal maturity variations amongst this suite of oil samples, presenting the opportunity to further investigate the influence of thermal maturity and TSR on $\delta^{34}S$ data.

Table 4.4 Dongpu Sag oil samples.

Tectonic Belt	Sample No	Well	Strata	Depth (m)
WC	1	Ming85	Es_2	1612.2−1630
	2	Wei77-10	Es_4	2734−2799
PC	3	Pu7-18	Es_3	3233.5−3517
	4	Pu7-111	Es_3	3608.9−3712.5
	5	Wei42-21	Es_3	3660−3716.8
	6	Wei42-26	Es_3	3451−3466.6
LT	7	PS18	Es_3	3886.4−4237.1
	8	PS18-2	Es_3	4167−4207.3
WL	9	Wen92-60	Es_3	2673−2824
	10	Wen13-281	Es_3	3377.3−3453.3
	11	Wen13-319	Es_3	3417.4−3689.5
	12	Wen13-429	Es_3	3282.1−3288.1
	13	Wen203-58	Es_3	3770.6−4081.9
	14	Wen203-63	Es_3	4360.6−4414.4
	15	Wen72-53	Es_3	3273.4−3527
	16	Wen88-59	Es_3	3515.1−3877.5
SCJ	17	Chun24-1	Es_3	2714.8−2727.9
MC	18	Ma19-30	Es_3	2848.4−2900.6

4.4.3 Molecular and Isotopic Composition of OSCs in Dongpu Sag oils

Most of the Dongpu oils showed similarly high abundances and similar distributions of alkyl-DBTs. Additional series of alkylated (C_2–C_4) benzothiophenes (BTs) were detected in three samples (Wen203-63, Ming85, Wei77-10) and 1−3 caged thiadiamondoids (TDs) were detected in two oils (Pu7-111, Pu7-18).

The OSC $\delta^{34}S$ data measured across the suite of 17 Dongpu oils spanned a wide range of +11‰ to +48‰ (**Table 4.5**). $\delta^{34}S$ measurements were generally achievable for the three methyl-DBT resolved peaks (4-m; coeluting 3&2-m; 1-m), three isomerically unassigned dimethyl-DBTs (dmDBT$_{i-iii}$) and two isomerically unassigned trimethyl-DBTs (tmDBT$_{i-ii}$). The $\delta^{34}S$ analyses of BTs in the three oils in which they occurred extended to four C_2-

BT isomers (C_2BT_i, C_2BT_{ii}, C_2BT_{iii}, C_2BT_{iv}), four C_3-BT isomers (C_3BT_i, C_3BT_{ii}, C_3BT_{iii}, C_3BT_{iv}) and two C_4-BT isomers (C_4BT_i, C_4BT_{ii}). The C_2–C_4-BTs present in the Ming 85, Wei77-10 and Wen203-63 oils were all ^{34}S enriched compared with their co-occurring DBTs (**Table 4.5**), resulting in $\Delta^{34}S_{(BTs–DBTs)}$ values of 11.7‰, 6.3‰ and 11.8‰, respectively. The Ma19-30 oil has a low sulfur content and all OSCs were too low in concentration for GC-ICPMS measurement. δ^{34}S measured TDs in the PC oils included one thiaadamantane compound (A_i), two thiadiamantane compounds (D_{i-ii}), and five thiatriamantane compounds (T_{i-v}). The thiadiamondoid δ^{34}S values were also more ^{34}S enriched than the DBTs in these oils (e.g. $\delta^{34}S_{TA-DBT}$ ~10‰; **Table 4.5**).

Table 4.5 $\delta^{34}S$ values of OSCs measured in Dongpu oils.

| OSCs	Ming85		Wei77-10		Pu7-18		Pu7-111		Wei42-21		Wei42-26		PS18		PS18-2		Wen92-60		Wen13-281		Wen13-319		Wen13-429		Wen203-58		Wen203-63		Wen72-53		Wen88-59		Chun24-1		Ma19-30	
	$\delta^{34}S$	S.V.	$\delta^{34}S$	S.V.	$\delta^{34}S$	S.V.	$\delta^{34}S$	S.V.	$\delta^{34}S$	S.V.	$\delta^{34}S$	S.V.	$\delta^{34}S$	S.V.	$\delta^{34}S$	S.V.	$\delta^{34}S$	S.V.	$\delta^{34}S$	S.V.	$\delta^{34}S$	S.V.	$\delta^{34}S$	S.V.	$\delta^{34}S$	S.V.	$\delta^{34}S$	S.V.	$\delta^{34}S$	S.V.	$\delta^{34}S$	S.V.	$\delta^{34}S$	S.V.	$\delta^{34}S$	S.V.
C3BTi	34.5	–	20.9	–																					30.7	–								
C3BTii	39.6	–																																
C3BTiii	35.8	–	28.9	–																					39.7	–								
C3BTiv	29.6	0.1	39.9	–																					47.8	–								
C4BTi	27.6	0.3	24	–																					31.9	–								
C4BTii	26	1.1	36.6	–																					40.7	–								
C4BTiii	32.2	–																																
C4BTiv	28.8	–	25.5	–																					32	–								
C5BTi	30.8	0.7	30.4	–																					33.3	–								
C5BTii	33	–																																
average of BTs	31.3		29.4																						36.6									
DBT	19	0.7	21.6	0.1	31.4	1.2	33.6	0.7	34.8	0.3	28.7	0.3	24.9	0.4	24.6	0.4	17.3	0.2	18.9	0.6	20.5	0.8	15.2	0.2	15.8	0.1	20.4	1.7	19.2	–	22.4	0.4	18.4	1.1		
4-mDBT	17.6	0.2	19.6	0.4	26	0.3	28.6	0.2	29.8	0.5	24.4	–	22.8	0.6	22.4	0.4	16.4	0.1	24.4	0.1	25.2	0.4	12.8	0.1	25.8	1.5	21.2	2.6	18.9	–	26.7	–	17.9	–		
2&3-mDBT	20.1	0.6	21.3	0.1	27.6	–	30.5	0.7	34.2	0.1	27	0.7	24.8	0.6	23.9	0.2	18.2	1	24.5	0.8	23.9	0.3	15.1	–	25.7	0.3	22.4	1.4	20.6	–	25.9	–	19.2	–		
1-mDBT	23.5	0.1	26	0.8	28.9	–	32.1	–	37.5	–	28.2	–	25.5	0.6	25.2	0.1	19.3	0.5	26.9	0.4	26.6	0.7	16.6	–	28.1	1.6	24.4	0.8	22.4	–	29.2	–				
dmDBTi	18.6	–	22.5	–	24.8	1.1	25.1	0.5	24	0.6	18.1	–	22.2	1	21.2	0.8	14.2	0.3	24	0.7	25.2	0.2	11.1	–	30.8	1.7	19.2	–	25.1	–	25.9	0.7	19.6	–		
dmDBTii	17.7	–	21.5	0.1	25.1	0.2	26	0.9	26.3	0.9	22.1	0.2	24.1	0.1	22.9	0.1	15.4	1	24.6	0.7	25.2	0.7	10.9	0.2	28.6	2	20.1	–	21.2	–	27.1	–	18.7	0.9		
dmDBTiii	22.4	0.7	25.3	0.7	27.4	0.6	30.2	–	27.4	–	22.5	–	24.4	0.2	23.1	0.1	16.9	0.7	26.2	0.4	26.4	0.5	12.1	–	29.5	1	24.3	–	22.7	–	27.7	–	17.6	1.1		
tmDBTi	20.6	–	25	–	26.5	1	29.3	–	25.9	0.8	20.5	0.2	24.2	0.5	22.5	0.2	15.7	0	25.5	1.5	26.7	1.1	14.3	–			33.9	–			25.3	–	18.9	–		
tmDBTii	21.7	0.1	25.8	–	27	0.6	26.5	–	27.8	1	20.9	0.7	24.3	0.1	22.4	0	16.6	0.1	27.6	1	27.3	0.3	12.3	–			37.3	–			26.5	–	17.1	–		
average of DBTs	19.9		23.2		27.2		29.1		29.7		23.6		24.1		23.1		17.0		24.8		25.2		13.4		26.3		24.8		21.4		26.3		18.4			
1TD					40.8	–	45.6	–																										
2TDi					35.5	0.9	37.7	–																										
2TDii					34.5	0.3	36.4	–																										
3TDi					34.9	0.6	36.9	–																										
3TDii					34.2	1.6	34.4	–																										
3TDiii					33.1	1	30.7	–																										
3TDiv					27.7	1.9	21	–																										
3TDv					35	0.7	33.1	–																										
average of TDs					34.4		34.5																											
$Dd^{34}S_{(BTs-DBTs)}$	11.4		6.3																						11.8									
$Dd^{34}S_{(1-mDBT-4-mDBT)}$	5.9		6.4		2.9		3.4		7.7		3.9		2.7		2.8		3		2.5		1.4		3.8		2.4		3.2		3.5		2.6					

4.4.4 Genetic, Depositional and thermal influences on the $\delta^{34}S$ composition of Dongpu oils

The source and thermal history of the oils has been constrained by their GC-MS analysed molecular composition — data provided by collaborators at China University of Petroleum (Beijing, China). This data along with detailed source correlation commentary is given in the co-authored paper Ke et al. (2020; Appendix 2). On the basis of source diagnostic hydrocarbon biomarkers most of the northern saline lacustrine oils — i.e. all but Wei 42-26 and Wei42-21 which are situated in a transitional zone between the PC and WC oilfields — could be subdivided into four tectonically aligned oil families: OF1 = WC oils; OF2 = two PC oils (i.e. Pu7-111 and Pu7-18); OF3 = LT oils; OF4 = WL oils. The southern oil (Chun24-1) is potentially indicative of a separate freshwater lacustrine distinct oil family (OF5).

The $\delta^{34}S$ profiles of these five oil families, as well as the two unassigned oils (Wei 42-26 and Wei42-21), are separately shown in Error! Reference source not found..

(a)

(b)

OF-2 (PC oils)

(c)

OF-3 (LT oils)

(d)

OF-4 (WL oils)

(e)

(f)
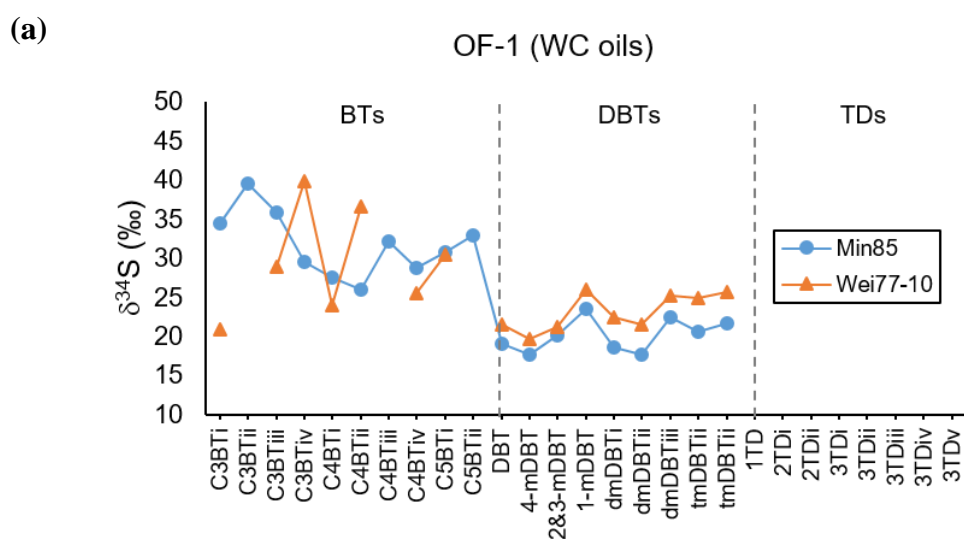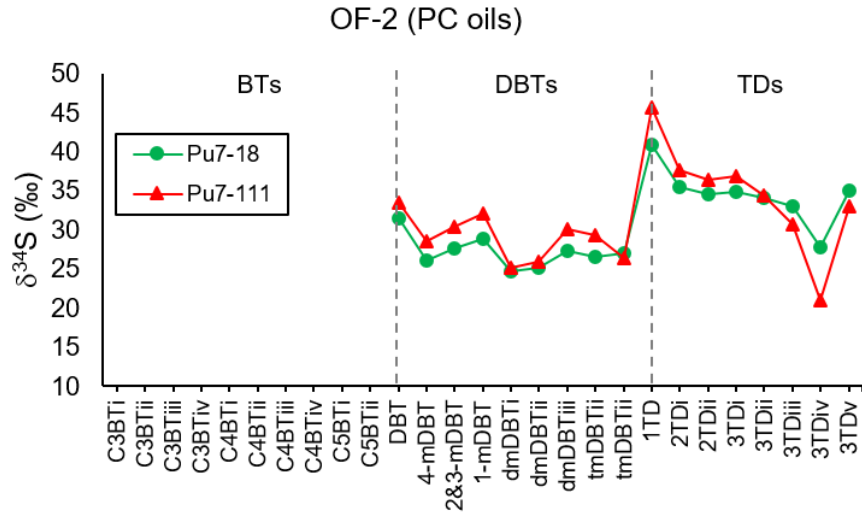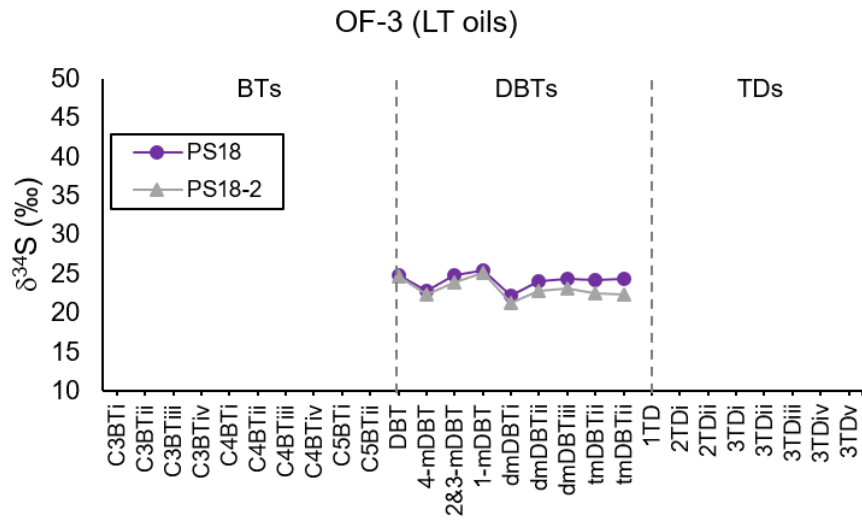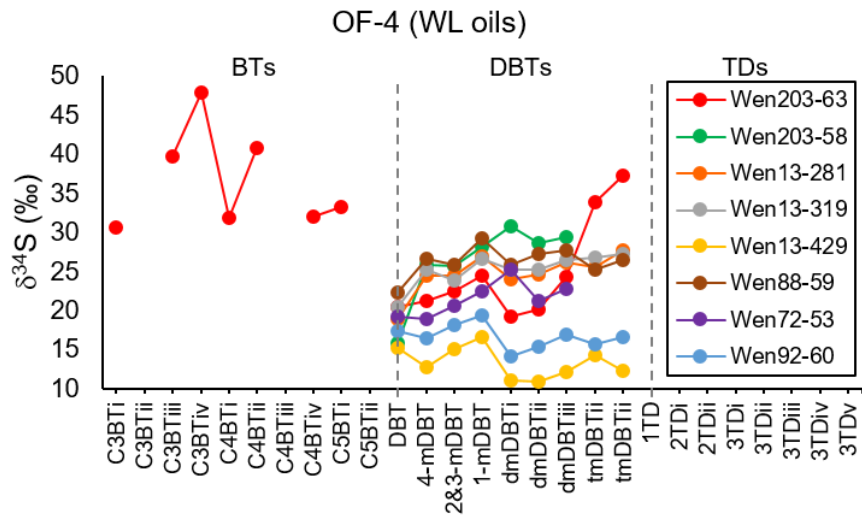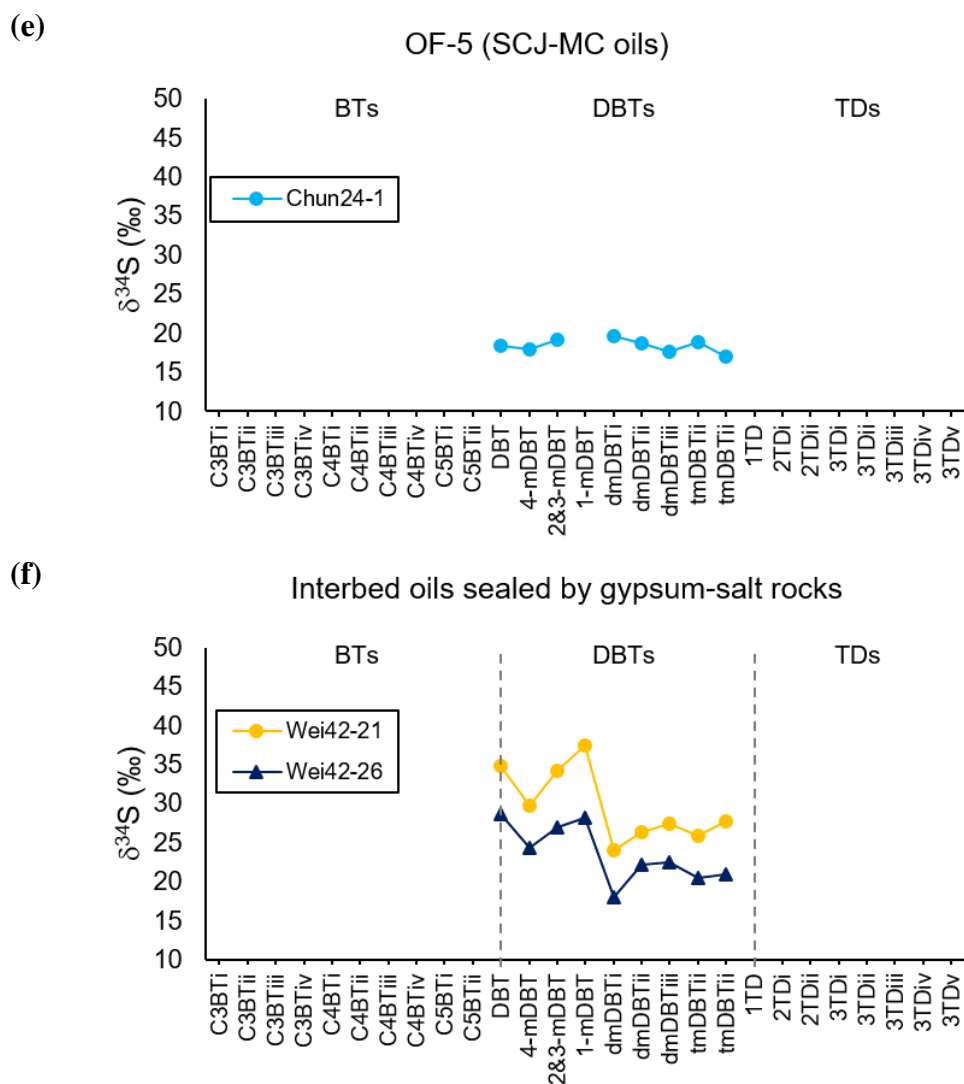
Figure 4.6 δ^{34}S of OSCs in oils from Dongpu Depression (a) OF1 = WC oils; (b) OF2 = Pu7-111 and Pu7-18; (c) OF3 = LT oils; (d) OF4 = WL oils; (e) OF5 = freshwater lacustrine oils; and (f) Wei 42-21 and Wei42-26.

The alkyl-DBTs of most oils showed small variance in their δ^{34}S values, although the two LT oils (OF3) and the southern Chun24-1 (OF1) had a more linear δ^{34}S$_{DBT}$ profile (**Figure 4.6c**). The δ^{34}S$_{OSC}$ data of the five biomarker defined oil families showed several consistent differences, suggesting good potential for the use of compound specific sulfur isotopes in genetic or paleo-depositional distinction of these saline and freshwater

lacustrine oils. The $\delta^{34}S$ character of the five biomarker defined oil families can be summarized as follows:

OF1 - The DBTs in the WC oils (**Figure 4.6a**) had relatively depleted $\delta^{34}S$ values (+18 to +25‰). The BTs were notably more enriched in ^{34}S ($\delta^{34}S$ ~+25 to +40‰). The difference between the average values of alkyl-BTs and alkyl-DBTs (i.e. $\Delta\delta^{34}S_{BTs-DBTs}$) of Ming85 and Wei77-10 in the WC oilfield was 11.7‰ and 6.3‰, respectively.

OF2 - The OSCs measured in the PC oils (**Figure 4.6b**) generally had the heaviest $\delta^{34}S$ values (average +30‰) and included particularly ^{34}S enriched TDs with $\delta^{34}S$ approaching 40‰. There was a large sulfur isotope gap between TDs and DBTs, with the $\Delta\delta^{34}S_{TDs-DBTs}$ of Pu7-18 and Pu7-111 being 7.3‰ and 5.4‰, respectively (typical of TSR altered oils, discussed *infra*).

Nb. The two interbedded oils (Wei42-21 and Wei42-26, **Figure 4.6f**) situated between the WC and PC oilfields showed a distinctive decline in $\delta^{34}S$ values with increasing alkylation $\delta^{34}S_{DBT} \sim \delta^{34}S_{mDBT} > \delta^{34}S_{C2-DBT}$ distinguished them from the other two PC oils grouped as OF2.

OF3 - The LT oils (**Figure 4.6c**) had relatively depleted $\delta^{34}S$ values (+21 to +25‰) which showed little variance with alkylation.

OF4 - The WL oils (**Figure 4.6d**) showed a relatively broad range of $\delta^{34}S$ values (+11 to +25‰). The methyl-DBTs in the higher (oil window) maturity WL oils had relatively constant $\delta^{34}S$ values markedly more

enriched than DBT. Alkyl-BTs detected in Wen203-63 were also ^{34}S enriched compared to the alkyl-DBTs ($\Delta\delta^{34}S_{BTs-DBTs}$= 11.8‰). The alkyl-DBTs in two of the lower maturity WL oils (Wen13-429; Wen92-60) had depleted δ^{34}S values (Ave = 13.4−16.7‰), slightly more depleted than the WC oils (OF1; Ave =20.1−23.1‰). One contrast to the WC oils was the slight depletion in δ^{34}S with increasing alkylation observed for Wen13-429 and Wen92-60 i.e. $\delta^{34}S_{1\text{-mDBT}}> \delta^{34}S_{\text{dmDBTiii}}> \delta^{34}S_{\text{tmDBTii}}$ (**Figure 4.6d**). The low maturity Wen72-53 oil showed the opposite trend of enrichment in δ^{34}S with increasing DBT alkylation which could reflect a mixed oil source (Zhang et al., 2017).

OF5   - The DBTs in the southern Sanchunji oil (Chun24-1; **Figure 4.6e**) had quite depleted δ^{34}S values (Ave 18.4‰), which remained relatively constant with increasing alkylation. Similar δ^{34}S distributions of OSCs were previously reported from two freshwater lacustrine oils from the Tabei (TB) Uplift of the Tarim Basin (i.e. Y33 and Y41; Li et al., 2010).

The $\delta^{34}S_{OSC}$ data also hinted at several potential trends with hydrocarbon parameters indicative of paleodepositional conditions or secondary thermal processes (thermal maturity and TSR). There was a general trend of decreasing δ^{34}S values for oils along a north to south gradient (consistent with the decrease in salinity or gypsum development) with the PC oils most enriched in ^{34}S, followed by the LT and high maturity WL oils. The low maturity WC and WL oils had similar δ^{34}S values, and the southern Chun24-1 oils

was most depleted in ^{34}S (**Figure 4.6a**). These potential relationships are separately discussed in more detail below.

Paleo-deposition

The hydrocarbon ratio C_{35}-H/C_{34}-H is sensitive to the salinity and redox conditions of depositional environments (Peters et al., 2005). A potential linear relationship was observed between C_{35}-H/C_{34}-H and $\delta^{34}S_{DBT}$ values (r^2=0.56; **Figure 4.7** Linear regression of C35-/C34-hopane and (a) δ^{34SDBT} and (b) $\Delta\delta^{34S}$$_{(1-mDBT – 4-mDBT)}$, respectively.

a) and an inverse relationship between C_{35}-H/C_{34}-H and $\Delta\delta^{34}S$ $_{1-mDBT – 4-mDBT}$ values of most oils (r^2=0.62; **Figure 4.7** Linear regression of C35-/C34-hopane and (a) δ^{34SDBT} and (b) $\Delta\delta^{34S}$$_{(1-mDBT – 4-mDBT)}$, respectively.

b) — exceptions being the WC and PC oils which had been significantly impacted by TSR (discussed below). No obvious relationship was evident between $\delta^{34}S$ $_{DBT}$ values and Pr/Ph ratios (Ke et al., 2020; Appendix 2). The Pr/Ph isoprenoid ratio is often responsive to salinity levels but can be additionally influenced by other redox changes.

The apparent $\delta^{34}S$ relationship with C_{35}-H/C_{34}-H values suggests $\delta^{34}S_{OSC}$ values are influenced by the salinity levels of sedimentary environments, with more enriched $\delta^{34}S$ values supported by brackish/saline paleo-environments. This might also account for the depleted $\delta^{34}S_{DBT}$ values of the freshwater lacustrine Chun24-1 oil. The bulk $\delta^{34}S$ values of saline lacustrine crude oils have generally been found to be heavier than those of marine

mudstone and freshwater lacustrine oils (Amrani et al., 2005; Zhang et al., 2005; Xue et al., 2014).

The decrease in $\Delta\delta^{34}S_{1m-4mDBTs}$ from ~2‰ to 4‰ with increasing C_{35}-H/C_{34}-H values (**Figure 4.7** Linear regression of C35-/C34-hopane and (a) δ^{34SDBT} and (b) $\Delta\delta^{34}S_{(1\text{-}mDBT - 4\text{-}mDBT)}$, respectively.

b), evident for all but the two TSR impacted WC oils, suggests that the 4-mDBTs were ^{34}S enriched at a quicker rate than 1-mDBT, likely due to the lower thermal stability of 1-mDBT (Ellis et al., 2017). $\Delta^{34}S_{1m-4mDBTs}$ values (**Table 4.5**) did show an increase with the 'resin and asphaltene' content (Table 1 of Ke et al., 2020) of the oils (**Figure 4.8** Linear regression of content of resin and asphaltene (%) and $\Delta\delta^{34S1m}_{-4mDBTs.}$

). This may reflect a lesser effect of thermal stability on the polar fraction of oils which have a relatively high content of S, much of it constrained by strong covalently bonds.

(a)

(b)
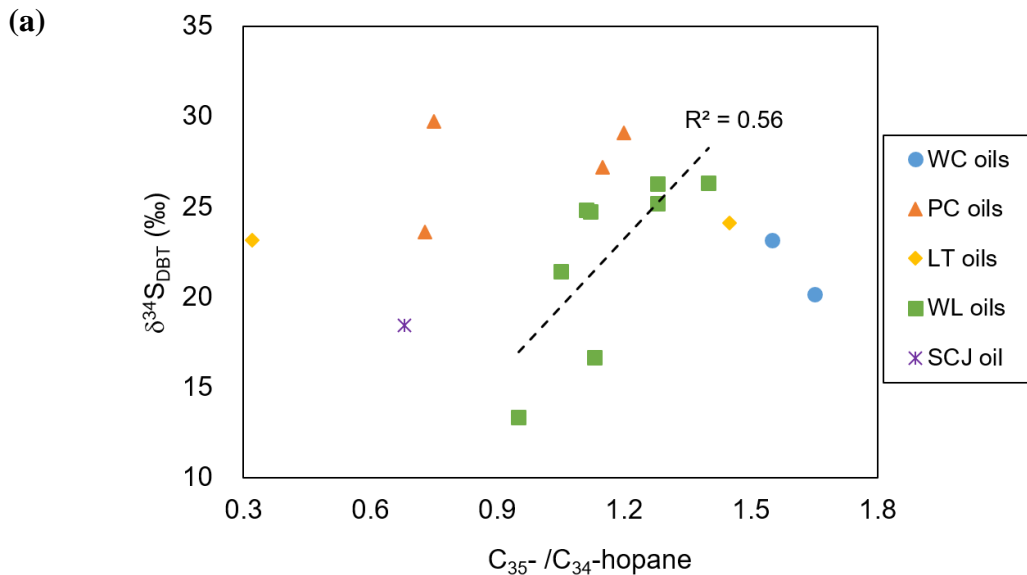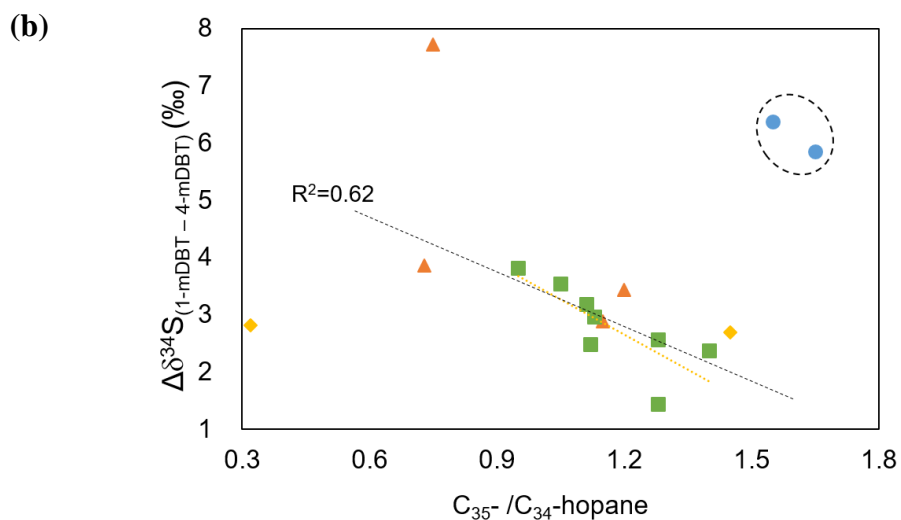
Figure 4.7 Linear regression of C_{35}-/C_{34}-hopane and (a) $\delta^{34}S_{DBT}$ and (b) $\Delta\delta^{34}S_{(1\text{-mDBT} - 4\text{-mDBT})}$, respectively.
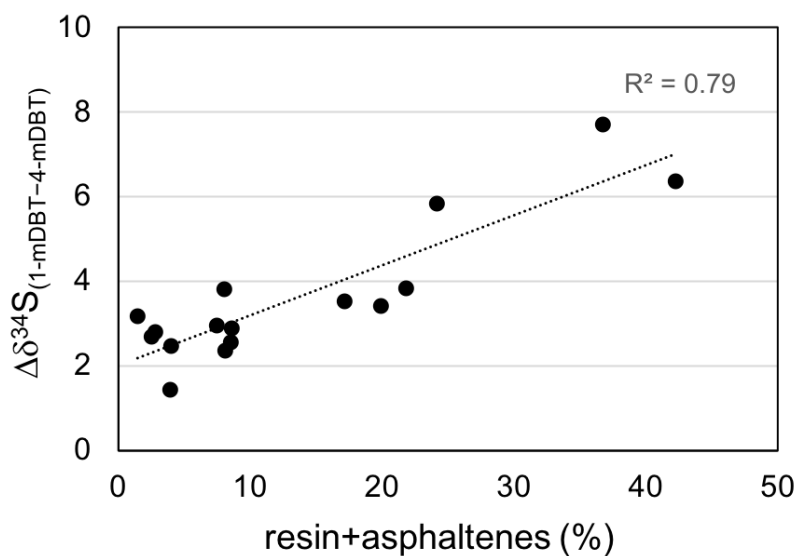
Figure 4.8 Linear regression of content of resin and asphaltene (%) and $\Delta\delta^{34}S_{1m-4mDBTs}$.

Thermal Maturity

The $\delta^{34}S_{DBT}$ values of the Dongpu oils, particularly the WL oils (OF4) also showed an increasing trend with several established hydrocarbon maturity parameters, i.e. C_{29} sterane

αββ/(ααα+αββ) and 4-/1-mDBT (**Figure 4.9a and b**). The $\delta^{34}S_{DBT}$ values of the WC (OF1) and PC (OF2) oils however showed a strong deviation from most of the thermal maturity parameters (**Figure 4.9**) likely due to the effects of TSR on the $\delta^{34}S_{DBT}$ value of these oil (discussed below).

(a)

(b)

(c)

(d)

(e)
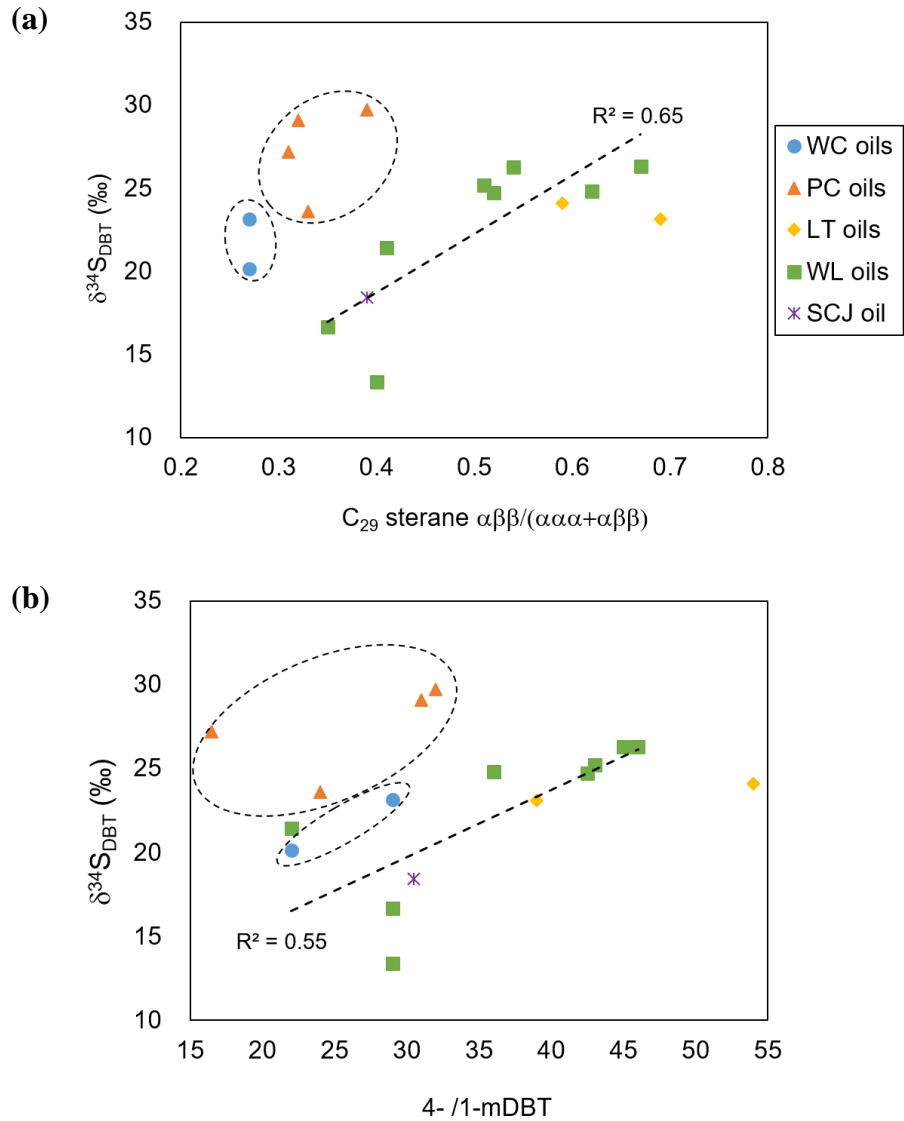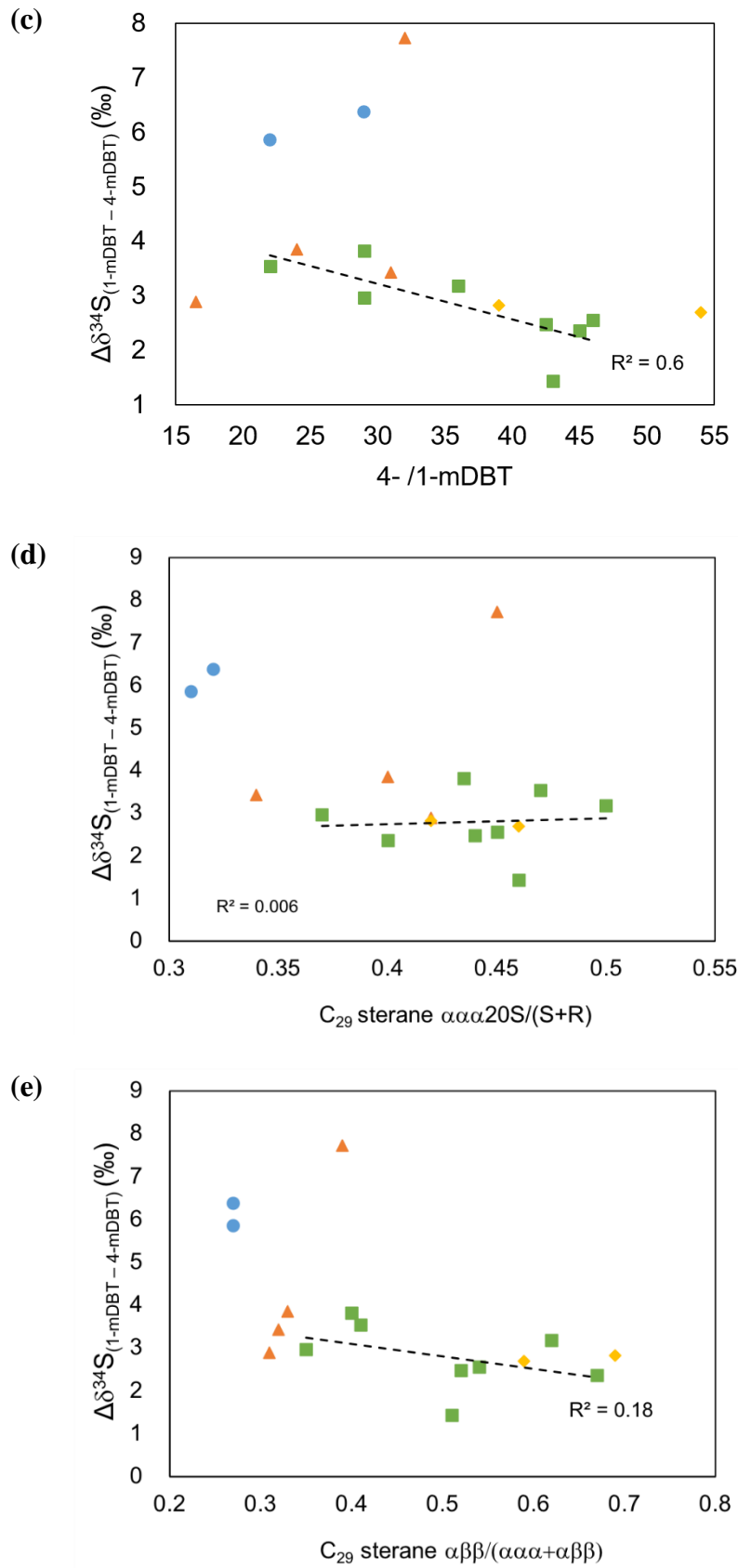
Figure 4.9 Plots of established molecular thermal maturity parameter's versus $\delta^{34}S_{DBT}$ values and parameters measured from Dongpu oils.

The difference in the δ^{34}S values of the 1-mDBT and 4-mDBT isomers of several oils also suggested a potential relationship with the molecular based thermal maturity parameter 4-/1-mDBT (**Figure 4.9c**). The $\Delta\delta^{34}$S$_{1m-4mDBTs}$ values showed a reasonable inverse relationship with the maturity parameter 4-mDBT/1-mDBT (r^2=0.6) suggesting a certain thermal impact on the δ^{34}S values of the mDBTs. A decrease in the magnitude of $\Delta\delta^{34}$S$_{1m-4mDBTs}$ with increasing maturity is probably related to the different thermal stabilities of mDBT isomers (4-mDBT > 1-mDBT) and the general homogenization of OSCs with increasing maturity (Amrani, 2014; Ellis et al., 2017). Deviation from this general trend by several samples (e.g. Wei42-21, Wen203-63 and Pu7-18) is likely due to TSR impacts (discussed below).

However, there was no obvious relationship between $\Delta\delta^{34}$S$_{1m-4mDBTs}$ and C$_{29}$ sterane $\alpha\alpha\alpha$ 20S/(S+R) or C$_{29}$ sterane $\alpha\beta\beta/(\alpha\alpha\alpha+\alpha\beta\beta)$ (**Figure 4.9d and e**), two parameters often sensitive to thermal maturity, reflecting the complexity of S-isotope fractionation in sedimentary systems.

Thermochemical Sulfate Reduction

Much of the low maturity saline lacustrine oils in the northern Dongpu Depression were sourced from Es$_3$~Es$_4$ source rocks with a burial depth greater than 3000m (Zhang et al., 2017). According to burial history and well-testing data these depths imply an original reservoir temperature >110 °C which is more than sufficient to support TSR. Fluid inclusion data indicated temperatures of 125–140 °C for the Wei42-21 and Wei42-26 oil reservoirs (Jiang et al., 2016). Furthermore, free sulfur and authigenic pyrites, both

reagents and products of TSR, have been commonly observed in drill cores from the clastic reservoirs of the Dongpu Depression (Orr, 1974; Zhang et al., 2008).

The $\delta^{34}S_{OSC}$ data of several oils were consistent with TSR impacts. The $\delta^{34}S$ values of the C_2–C_4-BT detected in two OF1 oils (Ming 85, Wei77-10; **Figure 4.6a**) and one OF4 oil (Wen203-63; **Figure 4.6d**) were significantly heavier than the alkyl-DBTs in these oils. The $\Delta\delta^{34}S_{BTs–DBTs}$ for Ming85, Wei77-10 and Wen203-63 were 11.7‰, 6.3‰ and 11.8‰ (**Table 4.5**), respectively. Similarly, the $\delta^{34}S$ values of thiadiamondoids (TDs) detected in the two PC (OF2) oils were distinctly heavier than the co-occurring DBTs (**Figure 4.6b**) — with $\Delta\delta^{34}S_{TDs–DBTs}$ of 7.3‰ (Pu7-18) and 5.4‰ (Pu7-111; **Table 4.5**), respectively. TSR can also lead to large $\Delta\delta^{34}S_{1mDBT–4mDBT}$ values (Ellis et al., 2017) such as observed for several oils across most of the four northern oil families (Ming85, Wei77-10, Wei42-21, Wei42-26, PS18-2, and Wen203-63). The $\delta^{34}S$ difference between mDBT isomers and different OSC classes is due to their respective thermal and TSR stabilities to the high temperature abiotic reaction. For instance, BTs and TDs inherit ^{34}S enriched reduced S from the mineral sulfate source utilized during TSR at a faster rate than DBTs (Amrani et al., 2012; Gvirtzman et al., 2015).

The TDs are themselves diagnostic products of TSR (Wei et al., 2012). The occurrence of TDs (Pu7-111, Pu7-18 and Wen203-63) in several oils has been confirmed by Electrospray ionization Fourier transform ion cyclotron resonance mass spectrometry conducted by researchers at the Chinese Petroleum University (Unpublished results).

4.5 Conclusions

The CSSIA of petroleum samples from the Jinxian and Dongpu Sags of BBB have demonstrated the potential of $\delta^{34}S$ values of their OSCs for helping identify the origin of the organic sulfur content of oils and source rocks, correlate genetically connected

lacustrine oils and better understand the S-cycle of these petroleum systems. Whilst these early results are particularly encouraging, the $\delta^{34}S_{OSC}$ data should be used cautiously in petroleum correlation studies due to the varied interactions of several potentially significant geochemical controls on petroleum $\delta^{34}S_{OSC}$ values. Where possible the $\delta^{34}S_{OSC}$ data should be integrated with other complimentary analytical information including from established methods.

The wide range in $\delta^{34}S$ values of DBTs in oil and rock samples (~0 to +20‰) from the Zhaolanzhuang oil field of the Jinxian Sag was interpreted as being due to different timing of generation in a S-restricted petroleum system. The premise of this model is the initially incorporated petroleum S (i.e. of the deeper, older rocks) was from a pool of relatively ^{34}S depleted reduced S, with later formed petroleum S (i.e. younger shallower rocks) being more ^{34}S enriched due to the Rayliegh Distillation isotopic phenomenon of a closed system. Periodical flushing of the system with fresh SO_4^{2-} may account for the relatively depleted $\delta^{34}S_{OSC}$ values of the two shallowest rocks analysed. The potential influence of secondary fluids on the $\delta^{34}S_{OSC}$ values of the rocks and oils was ruled out by CSSIA of the hydropyrolysates released from the kerogen fraction of the rocks.

The $\delta^{34}S_{OSC}$ distributions of the Dongpu oils showed several distinguishing features for each of five hydrocarbon biomarker defined oil families, although the $\delta^{34}S_{OSC}$ resolution of the different oil families was not nearly as defining as the traditional biomarker appraisal. This could have been due to the superimposed impact of paleo-environmental conditions, thermal maturity and TSR on $\delta^{34}S_{OSC}$ values. Changes in these conditions as indicated by established hydrocarbon parameters (e.g. C_{35}-H/C_{34}-H for depositional environment; sterane and mDBT parameters for thermal maturity) was reflected by measurable shifts in the $\delta^{34}S$ values of alkyl-DBT compounds, with the magnitude of the

shift varying between different compounds and isomers (e.g. few ‰ change in $\Delta\delta^{34}S_{1m-4mDBTs}$).

References

Aboglila, S., Grice, K., Trinajstic, K., Snape, C., Williford, K.H. (2011) The significance of 24-norcholestanes, 4-methylsteranes and dinosteranes in oils and source-rocks from East Sirte Basin (Libya). Applied Geochemistry, 26, 1694–1705.

Amrani, A., Aizenshtat, Z. (2004) Mechanisms of sulfur introduction chemically controlled: $\delta^{34}S$ imprint. Organic Geochemistry 35, 1319–1336.

Amrani, A., Deev, A., Sessions, A.L., Tang, Y.C., Adkins, J.F., Hill, R.J., Moldowan, J.M., Wei, Z.B. (2012) The sulfur-isotopic compositions of benzothiophenes and dibenzothiophenes as a proxy for thermochemical sulfate reduction. Geochimica et Cosmochimica Acta 84, 152–164.

Amrani, A., Dror, G., Said-Ahmad, W., Feinstein, S. and Reznik, I. J. (2013) The distribution and sulfur isotope ratios of specific organic sulfur compounds during pyrolysis of thermally immature kerogen. 26th International Meeting of Organic Geochemistry, Tenerife, Spain. Book of Abstracts, vol. 2, pp. 561–562.

Amrani, A. (2014) Organosulfur compounds: molecular and isotopic evolution from biota to oil and gas. Annual Review of Earth and Planetary Sciences, 42, 733–768.

Broecker, W.S. and Oversby, V.M. (1971) Rayleigh distillation. Chemical Equilibria in the Earth, pp.165–167.

Cai, C.F., Worden, R.H., Wolff, G.A., Bottrell, S., Wang, D.L., Li, X. (2005) Origin of sulfur rich oils and H_2S in Tertiary lacustrine sections of the Jinxian Sag, Bohai Bay Basin, China. Applied Geochemistry 20, 1427–1444.

Cai C., Li K., Anlai M., Zhang C., Xu Z., Worden R.H., Wu G., Zhang B., Chen L. (2009) Distinguishing Cambrian from Upper Ordovician source rocks: Evidence from sulfur isotopes and biomarkers in the Tarim Basin. Organic Geochemistry 40, 755–768.

Canfield, D., Boudreau, B.P., Mucci, A., Gundersen, J.K. (1998) The early diagenetic formation of organic sulfur in the sediments of Mangrove Lake, Bermuda. Geochimica et Cosmochimica Acta 62, 767–781.

Chambers, L.A., Trudinger, P.A., Smith, J.W., Burns, M.S. (1975) Sulfur isotope fractionation during sulfate reduction by dissimilatory sulfate reducing bacteria. Canadian Journal of Microbiology 21, 1602–1607.

Chang, Z., Chen, Z., Zhang, Y., Peng, J., Jin, Z. (2007) Investigation on geochemistry characterisitics of crude oil from weicheng-wenmingzhai area in Dongpu depression. Fault-Block Oil Gas Field 14, 1–3 (in Chinese).

Chen, X., Li, S., Zhang, H., Xu, T., Zhang, Y., Wan, Z., Ji, H., Guo, Z. (2018) Controlling Effects of Gypsum-salt on Hydrocarbon Generation of Source Rocks in Dongpu Sag and Its Significance on Petroleum Geology. Geoscience 32, 1125–1136 (in Chinese).

Dai, J.X., Hu, J.Y., Jia, C.Z., Fang, Y.S., Sun, Z.D., Wei, L.H., Yuan, J.P., Yang, W. (2004) Suggestions for scientifically and safely exploring and developing high H_2S gas fields. Petroleue Exploration and Development 31 (2), 1−5 (in Chinese).

Ehrlich, H. L., Brierley, C. L. (1990) Microbial mineral recovery. McGraw-Hill, Inc.

Ellis, G.S., Said-Ahmad, W., Lillis, P.G., Shawar, L., Amrani, A. (2017) Effects of thermal maturation and thermochemical sulfate reduction on compound-specific sulfur isotopic compositions of organosulfur compounds in Phosphoria oils from the Bighorn Basin, USA. Organic Geochemistry 103, 63–78.

Engel, M.H., Zumberge, J.E. (2007) Secular change in the stable sulfur isotope composition of crude oils relative to marine sulfates and sulfides. Book of Abstracts, International Meeting of Organic Geochemistry 2007 (Torquay, UK, September 19–24,). pp. 523–524.

Fan, H.G., Dai, J.X., Qi, H.F. (1992) Controls on bacterially originated H_2S. Petroleum Exploration and Development 19 (Supplement), 71–75 (in Chinese).

Gong, Z.S. (2004) Neotectonics and petroleum accumulation in offshore Chinese basins. Earth Science-Journal of China University of Geosciences 29, 513–517 (in Chinese with English abstract).

Guo, X., Liu, K., He, S., Song, G., Wang, Y., Hao, X., Wang, B. (2012) Petroleum generation and charge history of the northern Dongying Depression, Bohai Bay Basin, China: Insight from integrated fluid inclusion analysis and basin modelling. Marine and Petroleum Geology 32, 21–35.

Grotheer, H., Robert, A.M., Greenwood, P.F., Grice, K. (2015) Stability and hydrogenation of polycyclic aromatic hydrocarbons during hydropyrolysis (HyPy) — Relevance for high maturity organic matter. Organic Geochemistry 86, 45–54.

Gvirtzman, Z, Said-Ahmad, W., Ellis, G.S., Hill, R. J., Moldowan, J.M., Wei, Z., Amrani, A. (2015) Compound-specific sulfur isotope analysis of

thiadiamondoids of oils from the Smackover Formation, USA. Geochimica Cosmochimica Acta 167, 144–161.

Hao, F., Zhou, X.H., Zhu, Y.M., Zou, H.Y., Yang, Y.Y. (2010) Charging of oil fields surrounding the Shaleitian uplift from multiple source rock intervals and generative kitchens, Bohai Bay basin, China. Marine and Petroleum Geology 27, 1910–1926.

He, N., Grice, K., Greenwood, P.F. (2019) The distribution and $\delta^{34}S$ values of organic sulfur compounds in biodegraded oils from Peace River (Alberta Basin, western Canada). Organic Geochemistry 128, 16–25.

Horsfield, B., Curry, D.J., Bohacs, K., Littke, R., Rullkötter, J., Schenk, H.J., Radke, M., Schaefer, R.G., Carroll, A.R., Isaksen, G. and Witte, E.G. (1994) Organic geochemistry of freshwater and alkaline lacustrine sediments in the Green River Formation of the Washakie Basin, Wyoming, USA. Organic Geochemistry 22(3-5), pp.415–440.

Hu, J., Xu, S., Tong, X., Wu, H. (1986) The Bohai bay basin. In: Zhu, X. (Ed.), Chinese Sedimentary Basins. Elsevier, Amsterdam, pp. 89–105.

Hu, S.B., O'Sullivan, P.B., Raza, A., Kohn, B.P. (2001) Thermal history and tectonic subsidence of the Bohai basin, northern China: a Cenozoic rifted and local pullapart basin. Physics of the Earth and Planetary Interiors 126, 221–235.

Ji, H., Li, S., Greenwood, P., Zhang, H., Pang, X., Xu, T., Shi, Q. (2018) Geochemical characteristics and significance of heteroatom compounds in lacustrine oils of the Dongpu Depression (Bohai Bay Basin, China) by negative-ion Fourier transform ion cyclotron resonance mass spectrometry. Marine and Petroleum Geology 97, 568–591.

Ke, C.W., Li, S.M., He, N.N., Grice, K., Zhang, H.A., Xu, T.W., Zhang, Y.X., Greenwood, P. (2020) Compound specific sulfur isotopes of saline lacustrine oils from the Dongpu Depression, Bohai Bay Basin, NE China. Journal of Asian Earth Sciences, 104361.

Kuo, L. C. (1994) Lower Cretaceous lacustrine source rocks in northern Gabon: Effect of organic facies and thermal maturity on crude oil quality. Organic Geochemistry 22(2), 257–273.

Li, Q.Q., Liu, P. (2017) The formation and distribution of heavy oil in the area of Luojia Kenxi, Bonan Sag. Journal of Xi'an Petroleum University (Natural Science Edition) 32, doi: 10.3969 /j.issn.1673-064X.2017.04.006 (in Chinese).

Lockhart, R.S., Berwick,L.J., Greenwood, P.F., Grice, K., Kraal, P., Bush, R. (2013) Analytical pyrolysis for determining the molecular composition of contemporary monosulfidic black ooze. Journal of Analytical and Applied Pyrolysis 104, 640–652.

Love, G.D., Snape, C.E., Carr, A.D., Houghton, R.C. (1995) Release of covalently-bound alkane biomarkers in high yields from kerogen via catalytic hydropyrolysis. Organic Geochemistry 23, 981–986.

Meredith, W., Russell, C.A., Cooper, M., Snape, C.E., Love, G.D., Fabbri, D., Vane, C.H. (2004) Trapping hydropyrolysates on silica and their subsequent thermal desorption to facilitate rapid fingerprinting by GC-MS. Organic Geochemistry 35, 73–89.

Orr, W.L. (1974) Changes in the sulfur content and isotopic ratios of sulfur during petroleum Maturation-study of Big Horn Basin Paleozoic oil. AAPG Bulletin 58, 2295–2318.

Peng, J., Wu, X., He, X., Liu, Y. (2003) Oil and gas accumulating law in Machang area Dongpu Depression. Journal of Shandong University of Science and Technology (Natural Science) 22, 100–112 (in Chinese).

Peters, K.E., Walters, C.C., Moldowan, J.M. (2005) The Biomarker Guide. Biomarkers and Isotopes in Petroleum Systems and Earth History, vols. 1 and 2, Cambridge University Press, USA.

Postgate, J. (1984) Microbes, microbiology and the future of man. The Microbe II. Prokaryotes and Eukaryotes, 319–333.

Qi, J., Yang, Q. (2010) Cenozoic structural deformation and dynamic processes of the Bohai Bay basin province, China. Marine and Petroleum Geology 27, 757–771.

Radke M., Welte D.H. and Willsch H. (1986) Maturity parameters based on aromatic hydrocarbons: Influence of the organic matter type. Organic Geochemistry 10(1), 51–63.

Radke M. (1988) Application of aromatic compounds as maturity indicators in source rocks and crude oils. Marine and Petroleum Geology 5(3), 224–236.

Shawar, L., Said-Ahmad, W., Ellis, G. S., Amrani, A. (2020) Sulfur isotope composition of individual compounds in immature organic-rich rocks and possible geochemical implications. Geochimica et Cosmochimica Acta 274, 20–44.

Sim, M.S., Ono, S., Donovan, K., Templer, S.P., Bosak, T. (2011) Effect of electron donors on the fractionation of sulfur isotopes by a marine Desulfovibrio sp., Geochimica et Cosmochimica Acta 75, 4244–4259.

Snape,C.E., Lafferty, C.J., Eglinton, G., Robinson, N., Collier, R. (1994) The potential of hydropyrolysis as a route for coal liquefaction. International Journal of Energy Research 18, 233–242.

Sun, J., Zhang, S.Q., Wei, C.G., Sun, Y.T., Liu, J.H. (2006) Study on the formation, migration and accumulation of hydrogen sulfide in Luojia Oilfield. West-China Exploration Engineering, 123, 81–83.

van Hale, R. and Frew, R.D. (2010) Rayleigh distillation equations applied to isotopic evolution of organic nitrogen across a continental shelf. Marine and Freshwater Research, 61(3), pp.369–378.

Waldo, G.S., Carlson, R.M., Moldowan, J.M., Peters, K.E., Penner-Hahn, J.E. (1991) Sulfur speciation in heavy petroleums: Information from X-ray absorption near-edge structure. Geochimica et Cosmochimica Acta 55, 801–814.

Wang, G.L., Wang, T.G., Simoneit, B.R.T., Zhang, L.Y., Zhang, X.J. (2010) Sulfur rich petroleum derived from lacustrine carbonate source rocks in Bohai Bay Basin, East China. Organic Geochemistry 41, 340–354.

Wang, M., Sherwood, N., Li, Z.S., Lu, S.F., Wang, W.G., Huang, A.L., Peng, J., Lu, K. (2015) Shale oil occurring between salt intervals in the Dongpu Depression, Bohai Bay Basin, China. International Journal of Coal Geology 152, 100–112.

Wei, Z.B., Moldowan, J.M., Fago, F., Dahl, J.E., Cai, C.F., Peters, K.E. (2007) Origins of Thiadiamondoids and Diamondoidthiols in Petroleum. Energy and Fuels 21, 3431–3436.

Werne, J.P., Lyons, T., Hollander, D.J., Formolo, M.J., Sinninghe-Damsté, J.S. (2003) Reduced sulfur in euxinic sediments of the Cariaco Basin: sulfur isotope constraints on organic sulfur formation. Chemical Geology 195, 159–179.

Werne, J.P., Hollander, D.J., Lyons, T., Sinninghe-Damsté, J.S. (2004) Organic sulfur biogeochemistry: recent advances and future research directions. In: Amend, J.P., Edwards, K.J., Lyons, T. (Eds.), Sulfur Biogeochemistry: Past and Present. The Geological Society of America Special Papers, Boulder, CO. Vol. 379, pp. 135–150.

Worden, R.H., Cai, C.F. (2006) Geochemical characteristics of the Zhaolanzhuang sour gas accumulation and thermochemical sulfate reduction in the Jinxian Sag of Bohai Bay Basin by Zhang et al. Organic Geochemistry 36, 1717−1730.

Wu, L., Xu, H.M., Cheng, J.H. (2006) Evolution of sedimentary system and analysis of sedimentary source in Paleogene of the Bozhong Sag, Bohai bay. Marine Geology and Quaternary Geology 26, 81–88 (in Chinese with English abstract).

Zhang, S.C., Zhu, G.Y., Liang, Y.B., Dai, J.X., Liang, H.B., Li, M.W. (2005) Geochemical characteristics of the Zhaolanzhuang sour gas accumulation and thermochemical sulfate reduction in the Jixian Sag of Bohai Bay Basin. Organic Geochemistry 36, 1717−1730.

Zhang, S.C., Zhu, G.Y., Dai, J.X., Liang, Y.B., Li, M.W., Liang, H.B. (2006) Comments by Worden and Cai (2006) on Zhang et al. (2005) [Organic Geochemistry 36, 1717−1730]. Organi Geochemistry 37, 515–518.

Zhang, T., Amrani, A., Ellis, G.S., Ma, Q., Tang, Y. (2008) Experimental investigation on thermochemical sulfate reduction by H_2S initiation. Geochimica et Cosmochimica Acta 72, 3518–3530.

Zhang, L., Liu, Q., Zhu, R., Li, Z., Lu, X. (2009) Source rocks in Mesozoic−Cenozoic continental rift basins, east China: A case from Dongying Depression, Bohai Bay Basin. Organic Geochemistry 40, 229–242.

Zhang, S., Zhang, L., Bao, Y., Li, X., Liu, Q., Li, J., Yin, Y., Zhu, R., Zhang, S. (2012) Formation fluid characteristics and hydrocarbon accumulation in the Dongying sag, Shengli Oilfield. Petroleum Exploration and Development 39, 423–435.

Zheng, Y.F., Chen, J.F. (2000) Stable Isotope Geochemistry. Science Press, Beijing (in Chinese).

Zhu, G.Y., Zhang, S.C., Li, J., Jin, Q. (2004) Formation and distribution of natural gas with high content of hydrogen sulfide in China. Petroleum exploration and development 31, 18–21 (in Chinese).

CHAPTER 5

$\delta^{34}S$ characteristics of Tarim Basin oils (NW China): Implication on the sources of oils and extent of TSR alteration

5.1 Introduction

The Tarim Basin, the largest hydrocarbon-bearing basin in China (area 5.6×10^5 km^2), is a superimposed structure comprised of Paleozoic-aged rocks buried to depths between 6,000 m and 12,000 m (Wang et al., 2013). High maturity petroleum within this basin has been discovered in deep reservoirs extending to depths of 7,000 m. Petroleum from deeply-buried Cambrian gas condensate reservoirs often have a very high S content due to type II-S kerogen sources or occurrences of TSR.

The major sources of the very deep oils in the Tazhong area remains controversial (Cai et al., 2015a; Cai et al., 2015b; Li et al., 2010; Li et al., 2015). The long held consensus was that Tazhong oils were predominantly sourced from Middle–Upper Ordovician source rocks, supporting evidence including distinctive biomarkers (e.g. regular steranes, dinosteranes, triaromatic dinosteranes, 24-isopropylcholestane and 24-norcholestane) and the relatively low $\delta^{13}C$ values of normal alkanes (Hanson et al., 2000; Zhang et al., 2000a,b, 2002, 2005). It has alternatively been suggested that Cambrian to Lower Ordovician rock strata make the most significant contribution to the Tazhong oils, based on the detection of aryl isoprenoids and related biomarkers (Sun et al., 2003). Cambrian–Lower Ordovician source rocks sulfur isotope data and high concentrations of H$_2$S in several regional condensate gases have also been attributed to TSR of mineral sulfates that

are widely and exclusively developed in Middle Cambrian strata (Chen et al., 2008). The outcomes of two separate biomarker studies of crude oils and fluid inclusion samples (Pan and Liu, 2009; Li et al., 2010), integrated with $\delta^{13}C$ data of individual n-alkanes, was that most crude oils from Tazhong Uplift were a mixture of hydrocarbon inputs from an initial oil charge from Cambrian–Lower Ordovician strata ($\in$–O_1) and a later oil charge from Middle–Upper Ordovician source rocks (O_{2+3}). It was further suggested that two different organic facies may exist in Cambrian strata, generating oils with different biomarker and $\delta^{13}C$ character. One facies of the Cambrian strata was thought responsible for a distinctive V shaped distribution of C_{27}–C_{29} steranes similar to those in Upper Ordovician source rocks, whilst a more linear sterane distribution ($C_{27} \leq C_{28} < C_{29}$) typical of a Cambrian–Lower Ordovician origin was indicative of another facies (Cai et al., 2015).

In the Tazhong (southern) and Tabei (northern) areas of the Tarim Basin (**Figure 5.1**), hydrocarbon charging occurred in three main periods—late Caledonian stage (ca. 450–430 Ma), late Hercynian stage (ca. 293–255 Ma) and late Himalayan stage (ca. 12–2 Ma). Oils were mainly produced by the first and the third charges, while gas was largely associated with the second charge (Yu et al., 2011). Tazhong and Tabei oils may share a similar origin since both uplift areas occur within the same cratonic region which actually covers most of the Tarim Basin (Zhang and Huang, 2005). There have been several biomarker-based source appraisals of Tabei oils (Sun et al., 2003; Li et al., 2010; Yu et al., 2011; Zhu et al., 2013). Biodegradation was reported to have impacted most of the hydrocarbons in the Tabei area during the early Hercynian (ca. 386–372 Ma), with additional unaltered oil introduced in the late Hercynian (Zhu et al., 2013). Oil migration and mixing was also supported by tectonic activity (Cai et al., 2015).

The Maigaiti Slope is the most prospective petroleum exploration area in the Southwest Depression of the Tarim Basin, with multiple source layers and oil shows (Cui et al.,

158

2012). Compound-specific sulfur isotope analysis (CSSIA) has not yet been applied to oil-source correlation studies of petroleum from the Southwest Depression (or Tabei oils). Tectonic activity and evolution of the paleo-uplift are thought to control hydrocarbon migration and accumulation in the Maigaiti Slope (Wu et al., 2012). The hydrocarbon generation history in this part of the Tarim Basin involved accumulation from two separate charging events – one during the late Hercynian (ca. 290–285 Ma) contributing to the accumulation of oil and the other during the late Himalayan period (ca. 10–4 Ma) mostly contributing oil cracked gas; Wu et al., 2012; Cui et al., 2013).

In the present study, CSSIA was conducted on a selection of oils from three active petroleum exploration regions of the Tarim Basin: Tazhong Uplift (south), Tabei Uplift (north) and Southwest Depression. These analyses, complimented by a brief hydrocarbon biomarker assessment, were undertaken to further investigate the oil sources of the Tarim Basin and potentially help predict the spatial distribution and quality of hydrocarbons throughout the basin. This represents the first dedicated CSSIA study of Tabei and Southwest oils, though others have applied CSSIA to oil suites from the Tazhong Uplift (Cai et al., 2016; Li et al., 2015). These previous studies showed the δ^{34}S character of alkyl-DBTs can help to resolve different oil families, e.g. the relatively depleted δ^{34}S values (4–9‰) of Lower Ordovician derived oils (i.e. TZ62) were distinguished from the more widely distributed carboniferous oils which have more enriched δ^{34}S values (20–30‰); and occurrences of TSR were identified by very enriched δ^{34}S$_{OSC}$ values (e.g. δ^{34}S$_{BTs}$ ~40‰ in the ZS1C oil).

Oil from the extremely deep ZS1C well of the Tazhong Uplift has also been studied here. This oil has attracted significant previous interest as petroleum geochemists investigate the potential of an active Cambrian petroleum source in the Tarim Basin (e.g. Zhu et al.,

2015, 2016). It has been characterized as having been severely impacted by TSR (Zhu et al., 2016). The very high $\delta^{34}S$ values of thioaromatic and thiadiamondoid compounds in this oil (some >40‰) — measured in the present study and previously by others (Li et al., 2015; Cai et al., 2016) are amongst the most enriched OSCs recorded in crude oils— can be attributed to extensive TSR. Here, the impacts of TSR on the $\delta^{34}S$ character of OSCs thermally released from the asphaltene fractions of the ZS1C oil were also investigated. The asphaltene fraction of oils represents a pseudo-kerogen fraction of relatively high molecular weight. Hydrocarbons constrained within, or occluded by, this covalent network have shown to be more resistant to secondary alteration events such as biodegradation (e.g. Russell et al., 2004; Silva et al 2008) and may offer similar protection from the effects of TSR. Hydrocarbon and OSCs can be thermally released from the asphaltene fraction by various pyrolysis procedures (e.g. hydropyrolysis, microscale sealed vessel pyrolysis).

5.2 Samples and experiments

5.2.1 Samples

A total of 24 crude oils from the three Tarim Basin sub-structures were provided for this study by Prof. Guangyou Zhu of Petrochina's Research Institute of Petroleum Exploration and Development (RIPED). These comprised 12 oils from the Tabei Uplift (north Tarim Basin), 7 oils from the Tazhong Uplift (central Tarim Basin) and 5 oils from the Maigaiti Slope of the Southwest Depression (**Figure 5.1**; **Table 5.1**). These oils were sourced from a range of Carboniferous (C), Devonian (D), lower (O_1) and middle (O_2) Ordovician and Cambrian ($\in$) reservoirs.
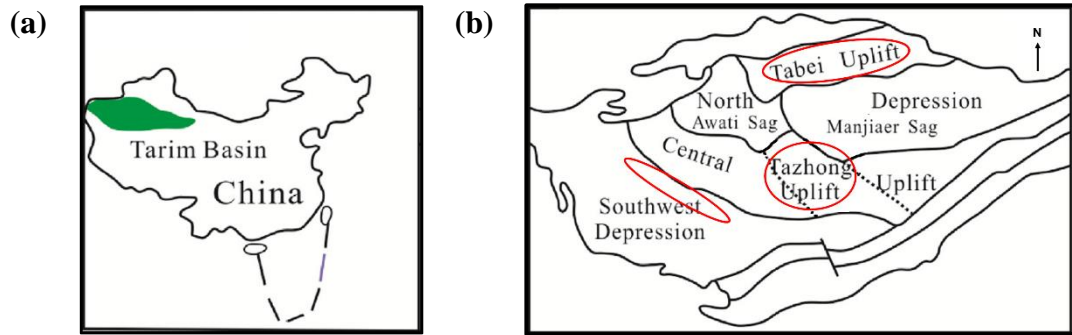
Figure 5.1 Location of (a) Tarim Basin (NW China); and sub-basin structures of (b) Tabei Uplift, Tazhong Uplift and Southwest Depression. Modified from Cai et al. (2015).

Table 5.1 Tarim Basin oils used in this study.

Locations	Wells	Strata	Depth
Tabei Uplift	FY202	O_2	7346-7465
	FY205		
	YM2	O_3	5940-5953
	YM5		
	YM6		
	RP2-1	O_2	6859-6910
	XK4	O	6834-6850
	XK7		6880-6980
	Ha7	O_2	6578-6632
	Ha701		
	Ha9		
	Ha901		
Tazhong Uplift	ZG2	O	5866-5893
	ZG5		6412
	ZG17		6438-6448
	GL2	O	--
	TZ83	O_1	5661-5681
	ZS1C	$\in$	6520
	ZS5		--
Southwest Depression	LS2	O	5741-5830
	Ma3	C	1414-1424
	Ma4	O	2018-2022
	Qun6	D	5383-5595
	Qun7	D	5383-5595

5.2.2 Experimental

Asphaltene precipitation

The asphaltene fraction of TSR impacted ZS1C oil was precipitated in excess cold n-pentane overnight under cool conditions (0~4 °C) and isolated by filtration of the residual maltene fraction. The asphaltenes were re-dissolved in DCM and transferred at room-temperature onto pre-activated silica gel for hydropyrolysis.

Column chromatography

All oils (except ZS1C oil) were separated into saturated, aromatic and polar fractions by silica gel column chromatography by sequential elution of n-hexane; 30% DCM in n-hexane; and DCM, respectively. The de-asphaltened maltene fraction of ZS1C oil was separated into saturated, aromatic and sulfidic fractions on a silver nitrate-silica gel filled column by sequential elution of hexane; DCM; and acetone, respectively, as described in Gvirtzman et al. (2015). Thiadiamondoid products were isolated in the sulfidic fraction which elutes with the acetone. Nb. thiadiamondoids and DBTs which are typically both concentrated in the aromatic fraction of silica gel columns can co-elute during GC analyses. Thioaromatic products in the respective aromatic fractions were further purified over an aluminum oxide (Type 507C neutral; Fluka, St. Louis, United States) column by successive elutions with different concentrations of DCM in *n*-hexane (as described in Section 2.2.2 of Chapter 2).

Hydropyrolysis (HyPy)

The asphaltene fraction (~30 mg, adsorbed on silica gel) was pyrolysed using a commercial HyPy apparatus (STRATA Technology Ltd) and following traditional operating procedures (Snape et al., 1994, Love et al., 1995, Meredith et al., 2004, Aboglila

et al., 2011, Lockhart et al., 2013; Grotheer et al., 2015). Briefly, the samples were pyrolysed with resistive heating from 25 °C to 250 °C at 300 °C/min, and then from 250 °C to a final temperature of 550 °C at 8 °C/min with the final temperature held for 2 min. A constant pressure (150 bar) and flow rate (5 L/min) of ultra-high purity hydrogen (BOC Group) was maintained throughout thermal treatment. The released compounds were isolated on a silica-filled cold trap (i.e. dry ice chilled). The silica was loaded on a column and adsorbed products were eluted with DCM (40 mL). The HyPy released bitumen fraction of the asphaltenes was stripped of elemental sulfur by the addition of HCl-activated copper turnings.

Molecular and isotopic analysis

CSSIA and molecular analysis of the oil and HyPy released asphaltene fractions was conducted by GC-ICPMS and GC-MS, respectively. The instrumentation and operation procedures used for these analyses were as described in Chapter 3 (and in He et al., 2019).

Additional GC×GC-MS analysis was conducted on several oil fractions to scrutinise the presence of thiadiamondoids. These analyses were conducted on a Leco Pegasus IV GC×GC-TOFMS system comprising an Agilent 6890 GC using a splitless auto-injector (7683B series) and a dual stage (cold and hot jet) cryogenic modulator (Leco, Saint Joseph, MI, USA). The primary column was a 60 m × 0.25 mm × 0.25 μm Rxi 5Sil MS (Restek, Bellefonte, PA, USA), coupled to a secondary 1.4 m × 0.25 mm × 0.25 μm DB-17 ms (Agilent) column. The carrier gas was ultra-high purity helium used at a constant flow of 2 mL min^{-1}. The inlet temperature was 310 °C with 1 μL injection. The samples were heated from 40 °C (1 min isothermal) to 320 °C at 3 °C min^{-1} (isothermal 30 min). A modulation period of 3 s was used, with a secondary oven offset of 10 °C and a modulator offset of 15 °C. Mass spectrometer parameters included an electron ionisation energy of

70 eV; an ion source temperature of 250 °C and a transfer line temperature of 320 °C. The scan speed was 100 Hz with a mass range of 45–580 Daltons (Da). A ChromaTOF (LECO) software package was used for instrument control and data analysis.

5.3 Result and discussion

5.3.1 Molecular characterization and biomarker appraisal of oils

The TICs from GC-MS analysis of the saturated fraction of Tabei (e.g. **Figure 5.2a-c**), Tazhong (e.g. **Figure 5.2d-f**) and Southwest oils (e.g. **Figure 5.2g-i**) consistently showed a prominent unresolved complex mixture (UCM) indicative of biodegradation. The biodegradation derived terpenoid 25-norhopane was also detected in a few oils (e.g. Ha7, Ha9). All oils also showed a homologous series of n-alkanes, including relatively low MW compounds ($\geq C_{11}$) which are vulnerable to early stages of biodegradation. The co-occurrence of these compounds in oils showing other features indicative of biodegradation (i.e. UCM, 25-norhopane) suggest they are mixed oils, consistent with previous reports of multiple hydrocarbon charge events from each of the Tarim Basin formations investigated (Wu et al., 2012; Cui et al., 2013; Zhu et al., 2013; Cai et al., 2015). Biodegradation was reported to have impacted most of the hydrocarbons in the Tabei area. An early Hercynian (late Devonian) oil charge was associated with secondary biodegradation, whereas subsequently introduced hydrocarbons during a late Hercynian event may have been unaltered (Zhu et al., 2013).
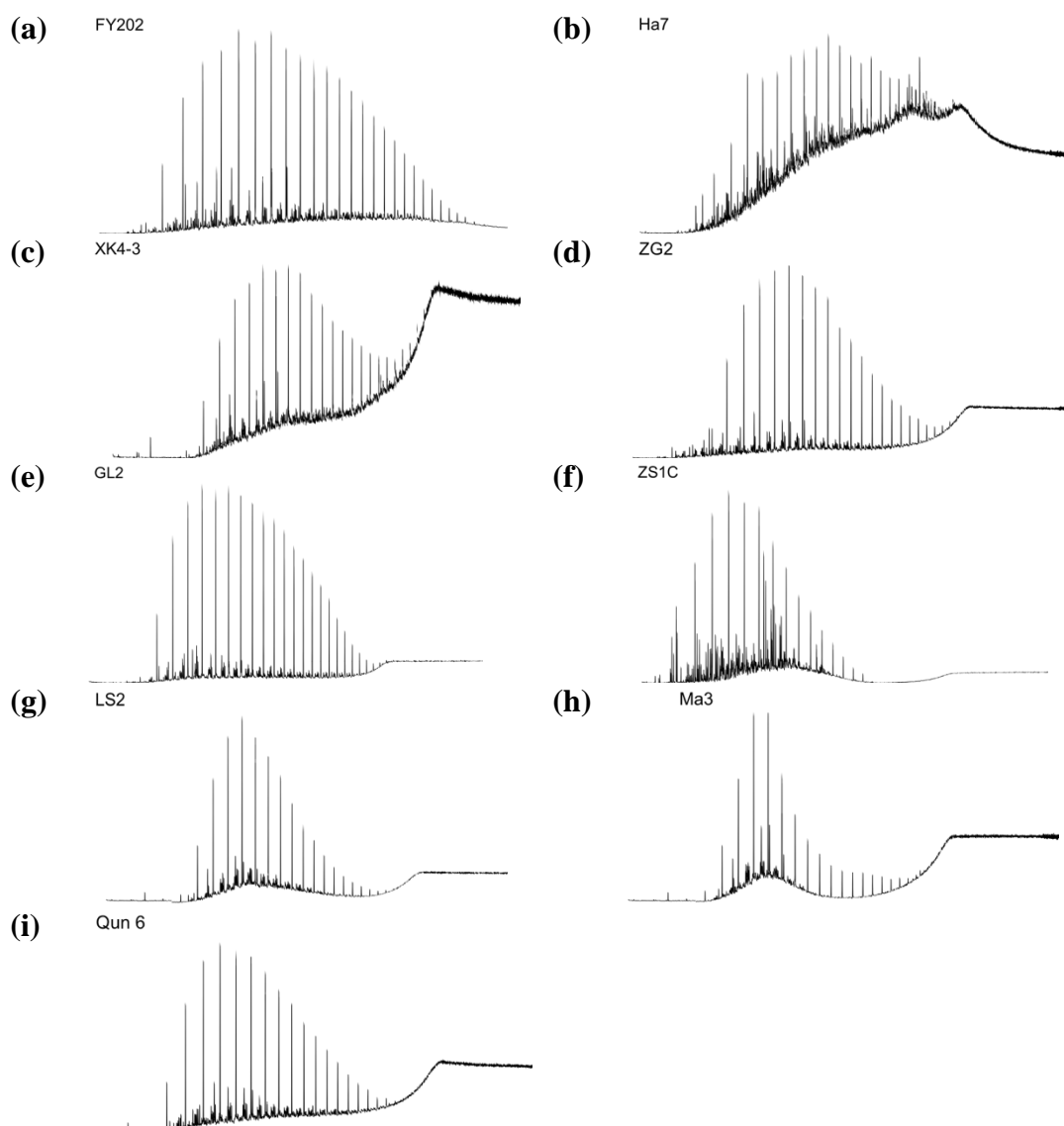
Figure 5.2 TICs from GC-MS analysis of the saturated hydrocarbon fraction of representative oils from Tabei Uplift (a–c); Tazhong Uplift (d–f); and Southwest Depression (g–i).

The C_{27}–C_{29} regular sterane distribution of oils has often been used in organic geochemistry studies to help resolve different hydrocarbon sources. Tarim Basin oils from different source rock strata have been reported to have quite different sterane distributions. The relative abundances of C_{27}–C_{29} steranes in Cambrian and Lower-Ordovician sourced petroleum typically show a linear ($C_{27} < C_{28} < C_{29}$) or "anti-L" profile ($C_{27} < C_{28} = C_{29}$),

whereas Middle–Upper Ordovician source rocks generally show a distinct "V" shape distributions ($C_{28} < C_{27}$ and C_{29}; Cai et al., 2009; Li et al., 2010, 2015). Exceptions to these trends do occur, such as the "V" shape C_{27}–C_{29} sterane distribution reported for the Cambrian sourced XK2 rock (Cai et al., 2015).

A "V" shaped C_{27}–C_{29} sterane distribution was observed for most of the current oil suite (e.g. **Figure 5.3**), although only trace concentrations of steranes were detected in several oils (e.g. ZG5, TZ83, ZS5 and LS2 oils) which could be due to TSR (Cai et al., 2015; Zhu et al., 2018). The distinctive V-shaped sterane profile is indicative of input from Middle-Upper Ordovician sources.

Li et al. (2010) previously reported different values for the C_{27}-/C_{29}-sterane $\alpha\beta\beta$ 20 (R+S) ratios of Ordovician (O_3: 1.25–1.37) and Cambrian ($\in$: 0.24–0.51) oils of the Tarim Basin. The values of the C_{27}-/C_{29}-sterane ratio presently measured in the Tabei oils was 0.8–1.1; in the Tazhong oils it was 1.1–3.1; and in the Southwest oils it was 0.9–1.4. These values suggest all the oils represent a mixture of Ordovician and Cambrian inputs.

(e)

GL2

(f) ZG17

(g) Ma4

(h)

Qun6

(i) Qun7
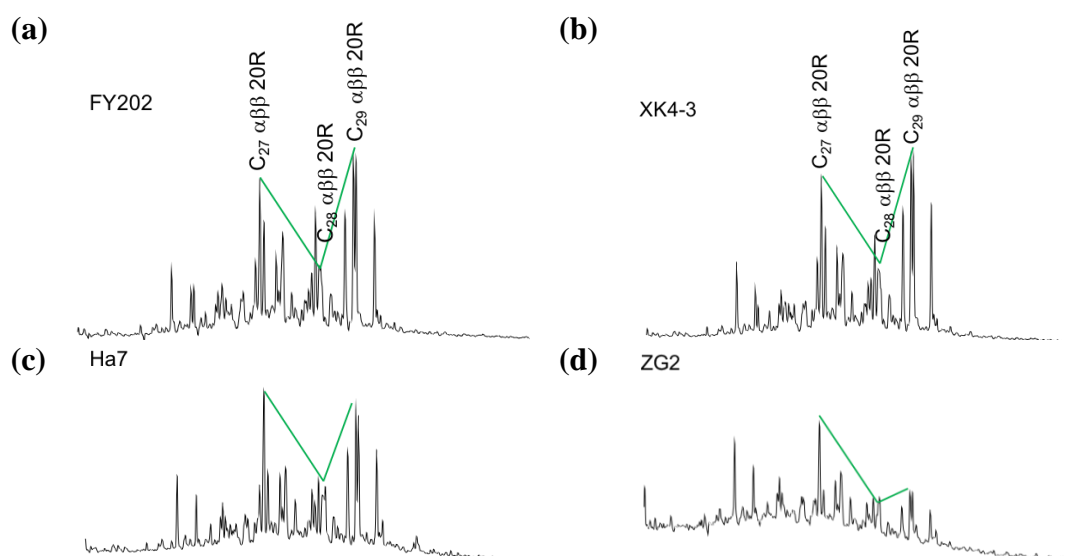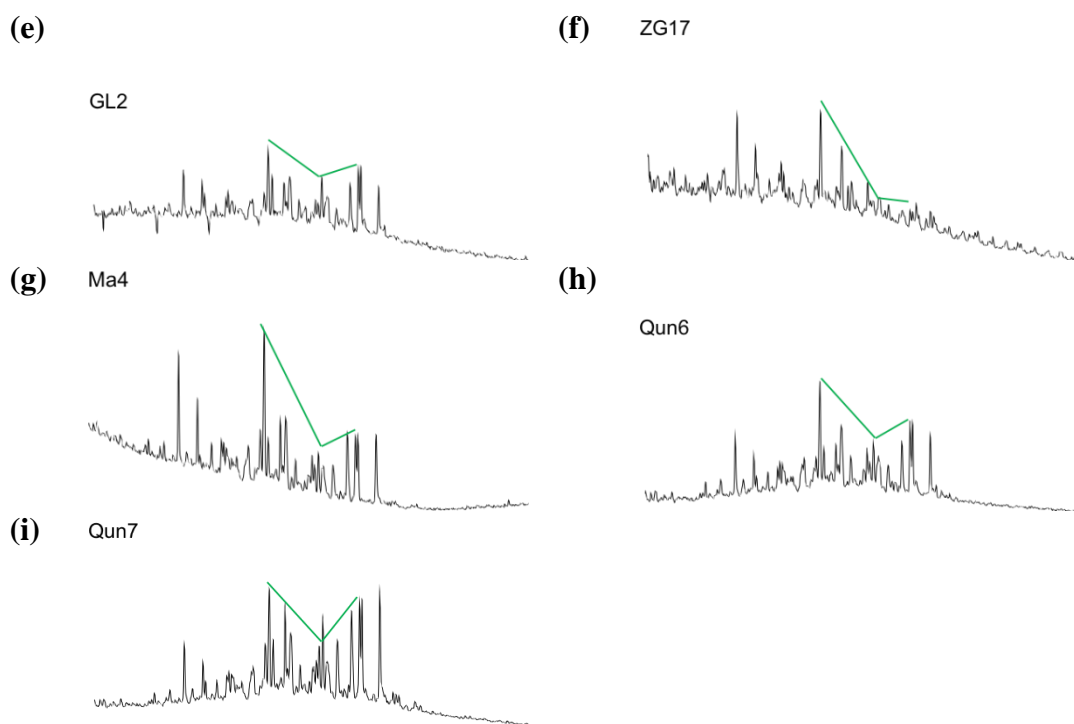
Figure 5.3 Partial *m/z* 217 chromatograms from GC-MS of saturated hydrocarbon fractions highlighting C_{27}-C_{29} sterane region of selected Tabei oils (a–c); Tazhong oils (d–f); and Southwest oils (g–i).

Gammacerane is a terpenoid biomarker indicative of highly reducing or hypersaline depositional conditions (Poole and Claypool, 1984; Palmer, 1984; Moldowan et al., 1985). The ratio of gammacerane to C_{30}-hopane has been reported to be higher in Cambrian source rocks than Upper-Ordovician source rocks of Tazhong Uplift (O_3: 0.1–0.11, $\in$: 0.18–0.26, Li et al., 2010). The values of the gammacerane/C_{30}-hopane ratio measured in the Tabei and Tazhong oils were between 0.1–0.6 and 0.1–0.5, respectively. Most of the oils showed higher values than reported for the Upper-Ordovician source rocks, indicative of a reducing or hypersaline depositional environment. In the Tazhong Uplift, the Ordovician carbonate rocks include inbioclastic grainstone, packstone and mudstone to sandstone, and the Cambrian strata is composed of tidal platforms, platform-marginal carbonates and evaporite rocks. Anhydrite and salt beds are well developed in Middle Cambrian (Li et al., 2010). The high gammacerane/C_{30}-hopane ratios of the Tabei and

Tazhong oils also points to a Cambrian source influence. The ratios of gammacerane/C_{30}-hopane in Southwest oils (from C, D and O strata) ranged from 0.1 to 0.3, closer to the values of Ordovician strata implying more significant hydrocarbon input from Ordovician source rocks.

The overall hydrocarbon biomarker assessment of the oils from these three locations suggests they have mixed $\in$ and O_3 strata origins, with mostly Cambrian source input to the Tabei and Tazhong oils (e.g. high gammacerane).

The thermal maturity of petroleum samples has often been inferred from various molecular parameters (Peters et al., 2005). Two such indices include the ratio of diasteranes (rearranged steranes) to regular steranes (i.e. the diasterane parameter) and the ratio of 4-mDBT to 1-mDBT (mDBT parameter). Li et al. (2010) reported the C_{29}-dia/C_{29}-reg values in Upper Ordovician source rocks (0.36–0.51) were a little higher than in Cambrian source rocks (0.23–0.29) of the Tazhong Uplift, suggesting a slight maturity difference. A wide range of generally higher diasterane parameter values were measured in the presently analysed oils (0.3–2.2; **Figure 5.4, Table 5.2**). The C_{29}-dia/C_{29}-reg ratio of the Tabei oils were in a quite narrow range (0.5–0.7; except YM5 = 1) suggesting a generally constant maturity. Larger ranges of these values were observed for the Southwest (0.3–0.9) oils and moreso the Tazhong oils (0.5–2.2) indicating these oil groups may reflect a broader range of thermal maturities extending to very high maturities in the case of the Tazhong oils. The mDBT parameter values of the oils similarly showed generally high values/maturity in Tazhong oils and relatively low values/maturity in Tabei and Southwest oils. However, the maturities indicated by these parameters were inconsistent for some oils. For instance, the ZS1C oil showed a relatively low C_{29}-dia/C_{29}-

reg value (0.5) but a high mDBT value (16.1). The latter ratio was clearly affected by the OSCs produced by TSR (Amrani, 2014).
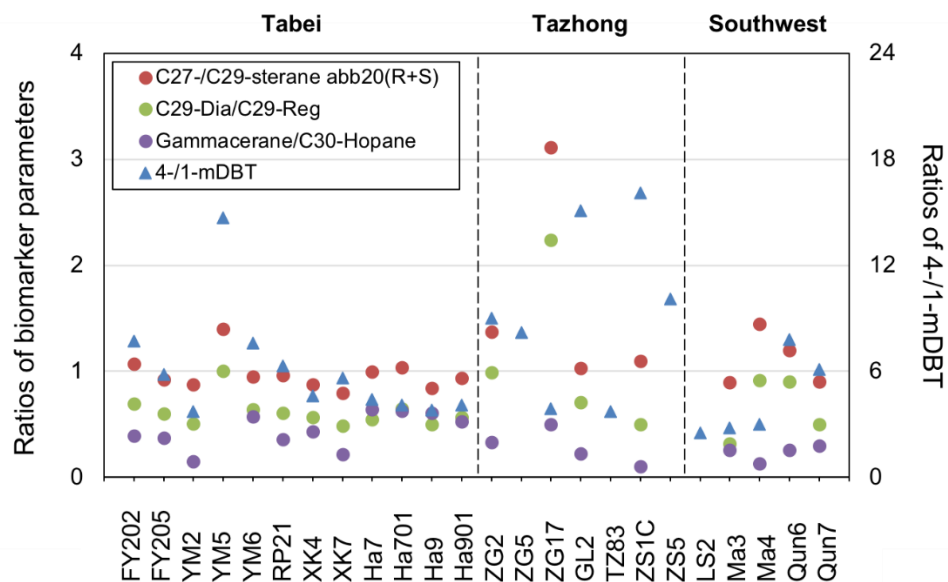
Figure 5.4 Molecular thermal maturity and paleo-environment parameter values of the Tarim Basin oils.

C_0–C_3 dibenzothiophenes (DBTs) are present in all oils, but benzothiophenes (BTs) are absent in most of the samples. Biodegradation, associated with early Hercynian petroleum (Zhu et al., 2013), may have removed the more susceptible BTs although these relatively volatile low MW products might also have been lost during sample treatment or storage. Thiaadamantanes, caged-S compounds formed by TSR, have previously been reported in some Tazhong and Southwest oils (i.e. ZG5, TZ83, ZS1C, ZS5 and LS2, Cai et al., 2015; Zhu et al., 2018). The occurrence of TSR implies high geological temperatures (>100°C) and this process can distort the behavior of other thermally controlled molecular trends. For instance, DBT-based thermal maturity parameters will be directly impacted by

introduction of TSR produced DBTs (as highlighted above for mDBT parameter value of

ZS1C).

Table 5.2 Geochemical parameters of the Tarim Basin oils.

	Wells	C_{29}-Dia/C_{29}-Reg	C_{27}-/C_{29}-sterane abb20(R+S)	Gammacerane/C_{30}-Hopane	4-/1-mDBT	TAs
Tabei oils	FY202	0.7	1.1	0.4	7.7	
	FY205	0.6	0.9	0.4	5.8	
	YM2	0.5	0.9	0.1	3.7	
	YM5	1	1.4	—	14.7	
	YM6	0.6	1	0.6	7.6	
	RP21	0.6	1	0.4	6.3	
	XK4	0.6	0.9	0.4	4.6	
	XK7	0.5	0.8	0.2	5.6	
	Ha7	0.5	1	0.6	4.4	
	Ha701	0.6	1	0.6	4.1	
	Ha9	0.5	0.8	0.6	3.8	
	Ha901	0.6	0.9	0.5	4.1	
Tazhong oils	ZG2	1	1.4	0.3	9	
	ZG5	–	–	–	8.2	Y[a]
	ZG17	2.2	3.1	0.5	3.9	
	GL2	0.7	1	0.2	15.1	
	TZ83	–	–	–	3.7	Y[a]
	ZS1C	0.5	1.1	0.1	16.1	Y[a]
	ZS5	–	–	–	10.1	Y[a]
Southwest oils	LS2	–	–	–	2.5	Y[b]
	Ma3	0.3	0.9	0.3	2.8	
	Ma4	0.9	1.4	0.1	3	
	Qun6	0.9	1.2	0.3	7.8	
	Qun7	0.5	0.9	0.3	6.1	

C_{29}-Dia/C_{29}-Reg: C_{29}-Diasterane/C_{29}-Regular sterane

TAs: alkyl thia-admantanes

Y = Yes, detected.

a: reported by Cai et al. (2015)

b: reported by Zhu et al. (2018)

5.3.2 $\delta^{34}S$ of OSCs

$\delta^{34}S$ values were generally measured for C_0–C_3 DBTs in all oils, and occasionally also the thiadiamondoids detected in some of the oils. $\delta^{34}S$ of BTs was not achievable due to their low concentrations in the oils in which they were detected. The values and standard variations (SV) of all the C_0–C_3 DBTs in each oil sample are listed in **Table 5.3**, and the $\delta^{34}S_{DBTs}$ profile of oils from the three Tarim Basin locations (distinguished by 3 different colors) are shown in Error! Reference source not found.**a.** The averaged $\delta^{34}S_{DBT}$ values of each oil is depicted in **Error! Reference source not found.b**. Generally, the $\delta^{34}S$ value of the DBTs in oils from each of the three sub-basin locations were in a similar range of 14–32‰, and the averaged $\delta^{34}S_{DBT}$ values of the oils were mostly within 17–27‰. These values are closer to the bulk $\delta^{34}S$ values measured for Cambrian kerogens (10–22‰) of the Tarim Basin, than the more depleted bulk $\delta^{34}S$ values of Lower Ordovician (7–9‰) and Middle–Upper Ordovician (4–7‰) kerogens (Cai et al., 2005, 2009, 2015a).

Exceptions in the present data set include the Tazhong ZS1C oil which showed much enriched values (Ave $\delta^{34}S_{DBT}$ ~37‰), which can be attributed to TSR, and three of the SW oils with notably more depleted values (Ave $\delta^{34}S$ = 5–10‰) possibly reflecting a distinct source of organic S. The full range of $\delta^{34}S$ values from each of the three oil regions investigated are separately presented in more detail below.

(a)

(b)
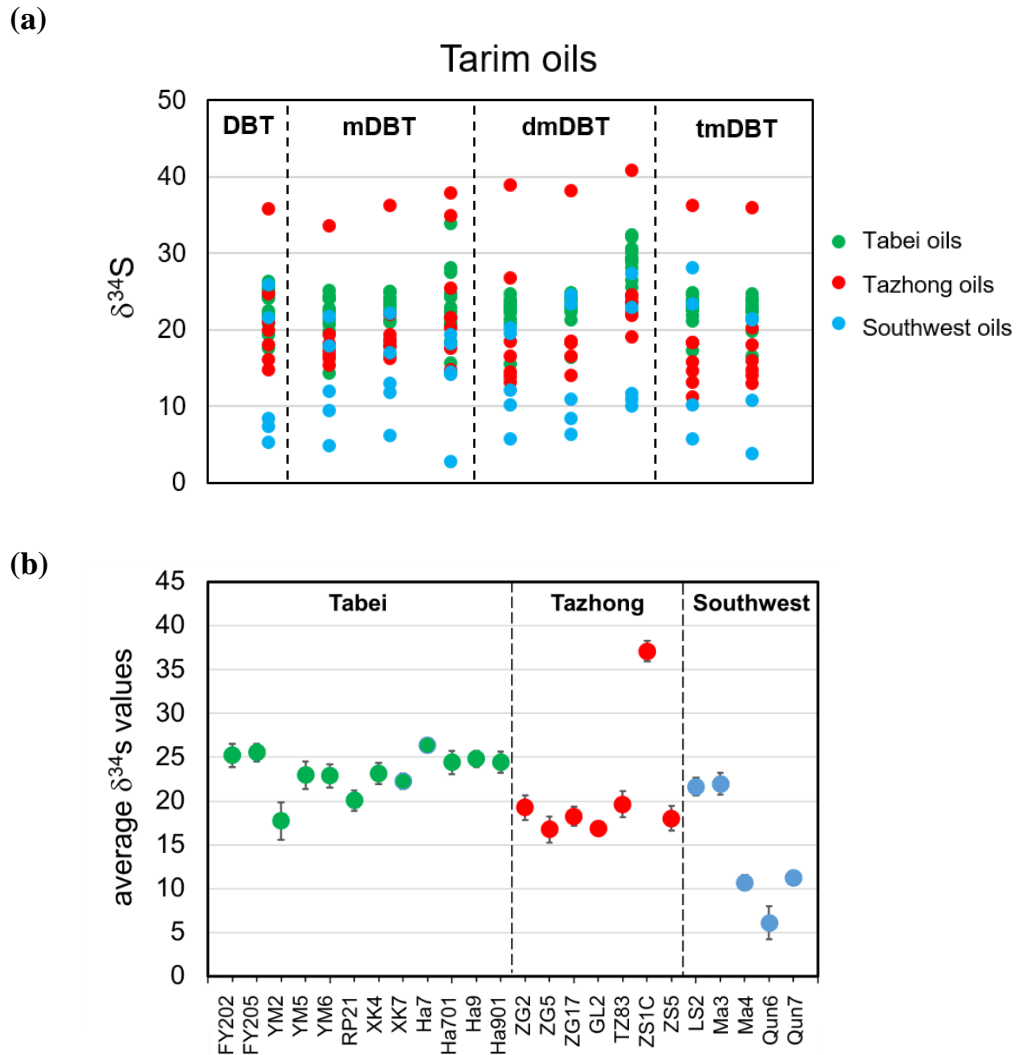
Figure 5.5 δ^{34}S values measured from Tarim Basin oils (a) δ^{34}S of individual DBT compound; and (b) average δ^{34}S of all DBT compounds in oil.

The δ^{34}S$_{DBTs}$ profiles for each of the Tazhong oils are presented in **Error! Reference source not found.**. Averaged δ^{34}S values in the Tazhong oils range from 17‰ to 37‰ (Error! Reference source not found.**b**), with ZS1C having notably more enriched δ^{34}S values than the other oils (due to TSR, as described in Chapter 2). The δ^{34}S values of Tazhong oils (except ZS1C) are generally consistent with the δ^{34}S values of kerogen in

Cambrian source rocks — a similar geochemical assignment (including correlation of δ^{34}S

data) was previously made by Cai et al. (2015a).
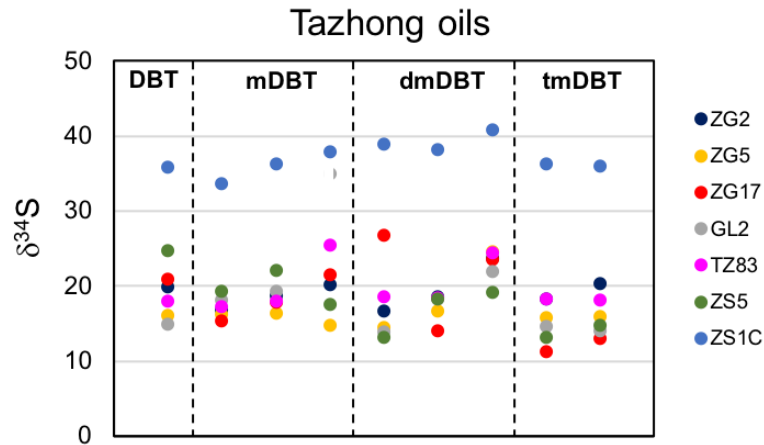
Figure 5.6 δ^{34}S values of individual DBT compounds measured in Tazhong oils.

δ^{34}S$_{DBTs}$ values of all Tabei oils are presented in **Error! Reference source not found.**.

Averaged δ^{34}S values in Tabei oils span a narrow range from 18‰ to 26‰ (**Error!**

Reference source not found.b). The oil with most depleted values was YM2 (Ave δ^{34}S

= 17.7‰), whilst the highest values were measured in Ha7 (Ave δ^{34}S = 26.3‰). Similar

to the Tazhong oils, the δ^{34}S$_{DBTs}$ values of Tabei oils would seem consistent with a

Cambrian source (δ^{34}S Cambrian kerogens = 10–22‰, Cai et al., 2015a).
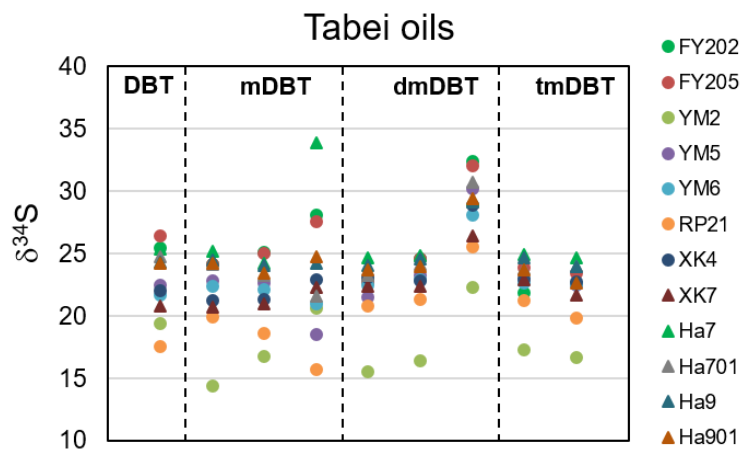
Figure 5.7 $\delta^{34}S$ values of individual DBT compounds measured in Tabei oils.

The $\delta^{34}S_{DBT}$ profiles of the SW oils are given in **Error! Reference source not found.**. These profiles can be divided into 2 groups. The first group (Ma4, Qun6, Qun7) have generally low $\delta^{34}S$ values (mostly < 11‰). Their depleted $\delta^{34}S$ values suggests the organic sulfur in these oils derived from a different source than the Cambrian source believed responsible for the Tabei and Tazhong oils. A likely origin of these oils are Ordovician source rocks for which the $\delta^{34}S$ of their kerogen fraction were reported to range from 4–9‰ (lower than the kerogen of Cambrian rocks >10‰, Cai et al., 2015a). An Ordovician origin would also be consistent with the low gammacerane abundances of these oils (gammacerane/C_{30}-hopane < 0.3). The Qun6 and Qun7 oils are from Devonian reservoirs, which may have been charged by petroleum migrated from Ordovician sources. The second group of SW oils (LS2 and Ma3) had more enriched $\delta^{34}S$ values (Ave ~22‰). These might derive from a different source (i.e. Cambrian), or alternatively may reflect thermal influences. Molecular maturity indicators (**Table 5.2**) did suggest the SW oils spanned a broad range of thermal maturities, but the ~10‰ difference in the $\delta^{34}S_{DBT}$ values of the two SW oil groups is more likely due to TSR than more traditional thermal

maturity which typically contributes modest $\delta^{34}S$ variances (Ellis et al., 2017; Rosenberg et al., 2017).
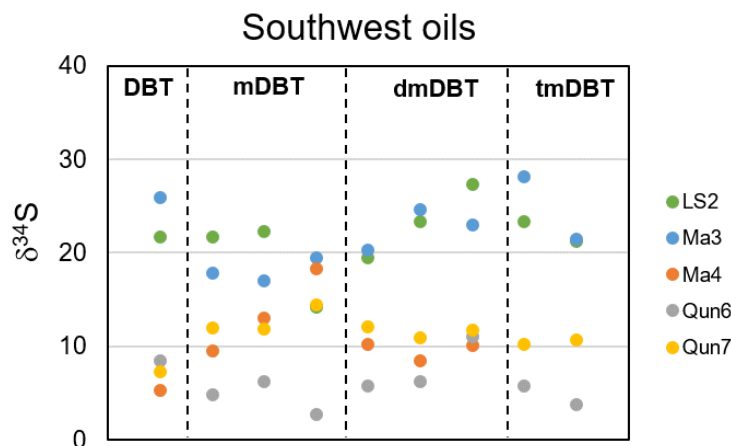
Figure 5.8 $\delta^{34}S$ values of individual DBT compounds measured in SW oils.

Analytical evidence of TSR is sometimes difficult to detect. Generally, high H_2S concentrations, the presence of diagnostic thiadiamondoids compounds (Seewald, 2003; Wei et al., 2007, 2012) and occasionally also enriched $\delta^{34}S$ values of H_2S or OSC can indicate the occurrence of TSR. Very enriched $\delta^{34}S_{OSC}$ values (>30‰, e.g. ZS1C) can be firm indicators of TSR, but many TSR impacted oils have lighter values which are thus not particularly definitive. For instance, Zhu et al. (2018) previously measured and compared the ~25‰ $\delta^{34}S_{OSC}$ values of the LS2 oil as similar to $\delta^{34}S_{OSC}$ reported for other Tarim Basin oils (mostly Tazhong oils) and much less than the $\delta^{34}S_{OSC}$ values of the TSR enriched ZS1C oil. As such, the $\delta^{34}S$ values of this oil were not definitively inferring of TSR, however, the use of GC×GC-MS to detect large distributions of alkyl-thiadiamondoids compounds in LS2 provided supporting evidence of TSR (Zhu et al., 2018). Zhu et al. (2018) further reported the LS2 reservoir has no sulfate evaporites and was at a temperature of 144 °C which they considered relatively low for TSR, proposing it to be a secondary reservoir for migrated TSR-derived petroleum sourced from deeper

and hotter (>200°C) Cambrian strata. Thus the ~10‰ difference between the $\delta^{34}S$ values of LS2 and the group one SW oils would seem due to a combination of source and TSR controls.

There have been no previous reports of TSR impacting the Ma3 oil, and no TSR diagnostic thiadiamondoid products were not detected here by GC-MS analysis. Thus, there was no direct evidence of TSR impacting these oils which might then account for its enriched $\delta^{34}S_{OSC}$ values (cf. group 1 SW oils). To further scrutinize for the potential trace level presence of thiadiamondoids in Ma3 this oil was analysed by GC×GC-MS. For comparison, GC×GC-MS analysis was also performed here on the ZS1C and LS2 oils in which thiadiamondoids are known to occur (i.e. for product correlation purposes) as well as a selected oil from each of the Tabei (FY202) and Tazhong (ZG2) sample suites displaying upper range $\delta^{34}S$ values that potentially reflect the influence of TSR.

Table 5.3 δ^{34}S of alkyl-DBTs in Tarim oils.

|	Wells	DBT		4-mDBT		2&3-mDBT		1-mDBT		dmDBTi		dmDBTii		dmDBTiii		tmDBTi		tmDBTii		Average	
		d^{34}S	S.V.	d^{34}S	S.V.	d^{34}S	S.V.	d^{34}S	S.V.	d^{34}S	S.V.	d^{34}S	S.V.	d^{34}S	S.V.	d^{34}S	S.V.	d^{34}S	S.V.	d^{34}S	S.V.
Tabei oils	FY202	25.4	1	24.2	1	25.1	0.9	28.1	2.7	22.7	2.1	24.6	0.9	32.4	–	21.9	1.4	22.5	0.9	25.2	1.4
	FY205	26.4	2.2	24.1	1.2	25	1.4	27.6	–	22.7	1.3	24.6	0.3	32	–	23.8	0.4	23.4	0.1	25.5	1
	YM2	19.4	–	14.4	–	16.8	2	20.7	–	15.5	2.8	16.4	1.5	22.3	–	17.3	–	16.6	–	17.7	2.1
	YM5	22.5	–	22.8	0.7	22.7	1.7	18.6	–	21.5	2.8	23.3	0.5	30.2	–	22.8	2.2	22.5	–	23	1.6
	YM6	21.7	–	22.4	1.8	22.1	0.7	20.9	–	22.4	–	22.9	1.4	28.1	–	22.7	1.3	22.6	–	22.9	1.3
	RP21	17.6	0.7	19.9	0.4	18.6	0.7	15.7	–	20.8	–	21.4	2.6	25.6	–	21.2	2.1	19.8	0.6	20.1	1.2
	XK4	22	0.6	21.3	1.2	21.3	2.1	22.9	–	23.1	0.3	22.8	2.5	28.9	–	23	0.1	22.8	1.6	23.1	1.2
	XK7	20.8	1.3	20.7	0.1	21	–	22.3	–	22.4	0.5	22.4	1.4	26.4	–	22.9	1.1	21.6	–	22.3	0.9
	Ha7	25.4	0.3	25.1	0.5	24.2	0.4	33.9	–	24.7	1	24.8	0.3	29.3	–	24.9	0.3	24.7	–	26.3	0.5
	Ha701	24.7	0.4	24.1	–	23.3	3	21.6	–	23.3	–	24.1	0.5	30.7	–	23.8	–	24	–	24.4	1.3
	Ha9	24.3	0.4	24.5	0.1	24	0.6	24.2	–	24	1.4	24.5	0.1	29.2	–	24.6	1.4	24	2.5	24.8	0.9
	Ha901	24.2	1.1	24.2	0.4	23.4	1.7	24.7	0.8	23.7	0.3	23.9	0.2	29.4	2.9	23.7	2.7	22.7	0.6	24.4	1.2
Tazhong oils	ZG2	19.9	–	16.8	0.9	18.7	0.7	20.2	–	16.6	2.5	18.6	1.5	23.7	–	18.3	–	20.3	–	19.2	1.4
	ZG5	16.2	1.9	16.2	0.4	16.3	0.5	14.7	–	14.5	3.3	16.6	0.6	24.6	–	15.9	1.6	15.9	2.1	16.8	1
	ZG17	20.9	1.1	15.4	0.6	17.8	2.3	21.6	–	26.8	–	14.1	–	23.6	–	11.2	0.4	13	–	18.3	1.1
	GL2	14.9	–	18.1	–	19.3	–			13.9	–	18.3	–	21.9	–	14.6	–	14.1	–	16.9	–
	TZ83	18	0.7	17.3	0	18	1.4	25.4	–	18.5	3.3	18.5	2.9	24.4	–	18.3	0.6	18.1	–	19.6	1.5
	ZS1C	35.9	0.4	33.6	2.4	36.3	0.2	37.9	–	38.9	2.5	38.3	1.8	40.8	–	36.3	0.2	36	0.5	37.1	1.1
	ZS5	24.7	–	19.3	0.9	22.1	1	17.6	–	13.2	2.8	18.3	0.4	19.1	–	13.1	1.9	14.8	–	18	1.4
Southwest oils	LS2	21.7	0.8	21.7	1.2	22.3	1.2	14.2	–	19.5	0.2	23.3	2.3	27.4	–	23.4	1.1	21.3	0.3	21.6	1.0
	Ma3	25.9	–	17.9	2.1	17	–	19.4	–	20.2	1.1	24.6	–	22.9	0.5	28.2	–	21.4	–	22	1.2
	Ma4	5.3	0.4	9.5	0.1	13	0.9	18.3	1.6	10.2	1.8	8.5	0.8	10.1	0.5	–	–	–	–	10.7	0.9
	Qun6	8.5	2.4	4.9	2.6	6.2	–	2.7	–	5.8	1.1	6.3	1.6	11	–	5.8	–	3.8	–	6.1	1.9
	Qun7	7.3	0.1	11.9	0.1	11.9	–	14.5	0.1	12.1	0.2	10.9	0.1	11.7	–	10.2	–	10.7	0.2	11.2	0.1

Note: S.V. = standard variation of duplicate sample analysis, where dash given the data derives from just one analysis (due to low analyte concentrations).

2D chromatograms for *m/z* 154 + 168 + 182 from GC×GC-MS analysis of LS2 (Error! Reference source not found.**a)** and ZS1C (Error! Reference source not found.**b)** oils show the occurrence of C_1-C_2 thiaadamantanes in both oils. However, no C_1–C_2 (or any other) thiaadamantanes were detected in the corresponding analysis of Ma3, or FY202 and ZG2 (**Figure 5.9c-e**). The consistent presence of the relatively volatile low MW product 1,1-biphenyl (*m/z* 154) in the analysis of all oils (**Figure 5.9a-e**) indicated none of the oils has been topped prior to GC×GC-MS analysis (i.e. absence of thiaadmantanes was not due to evaporation).

(c)

(d)

(e)
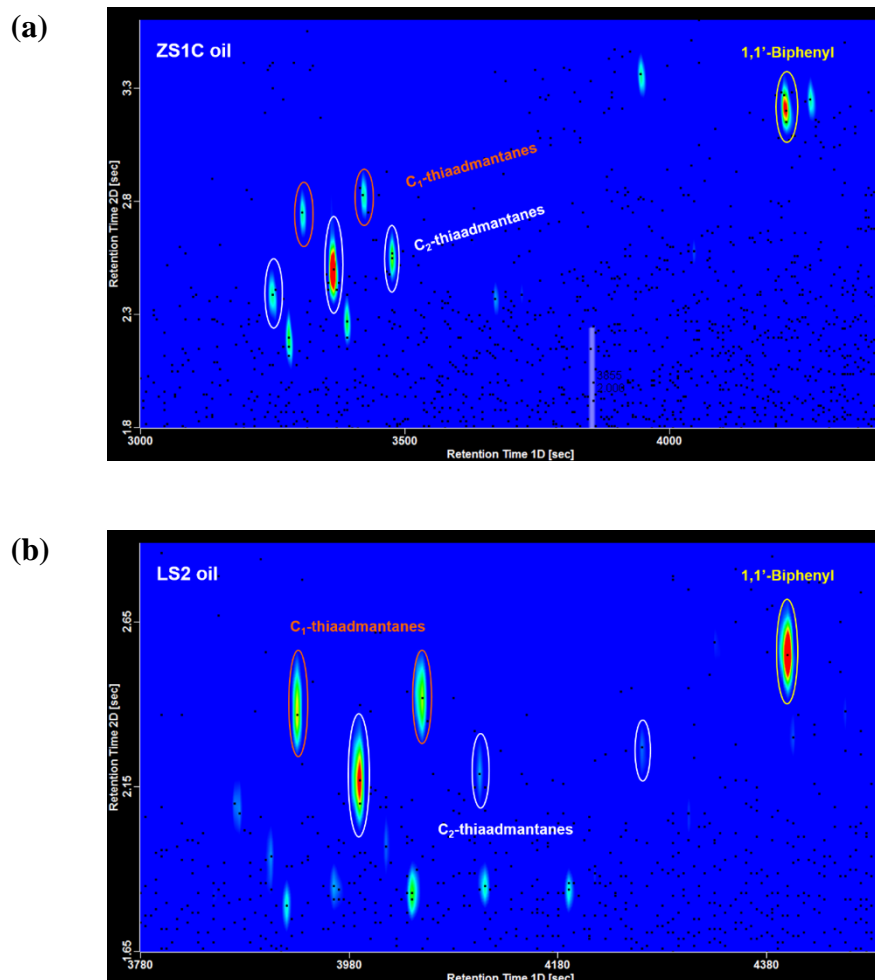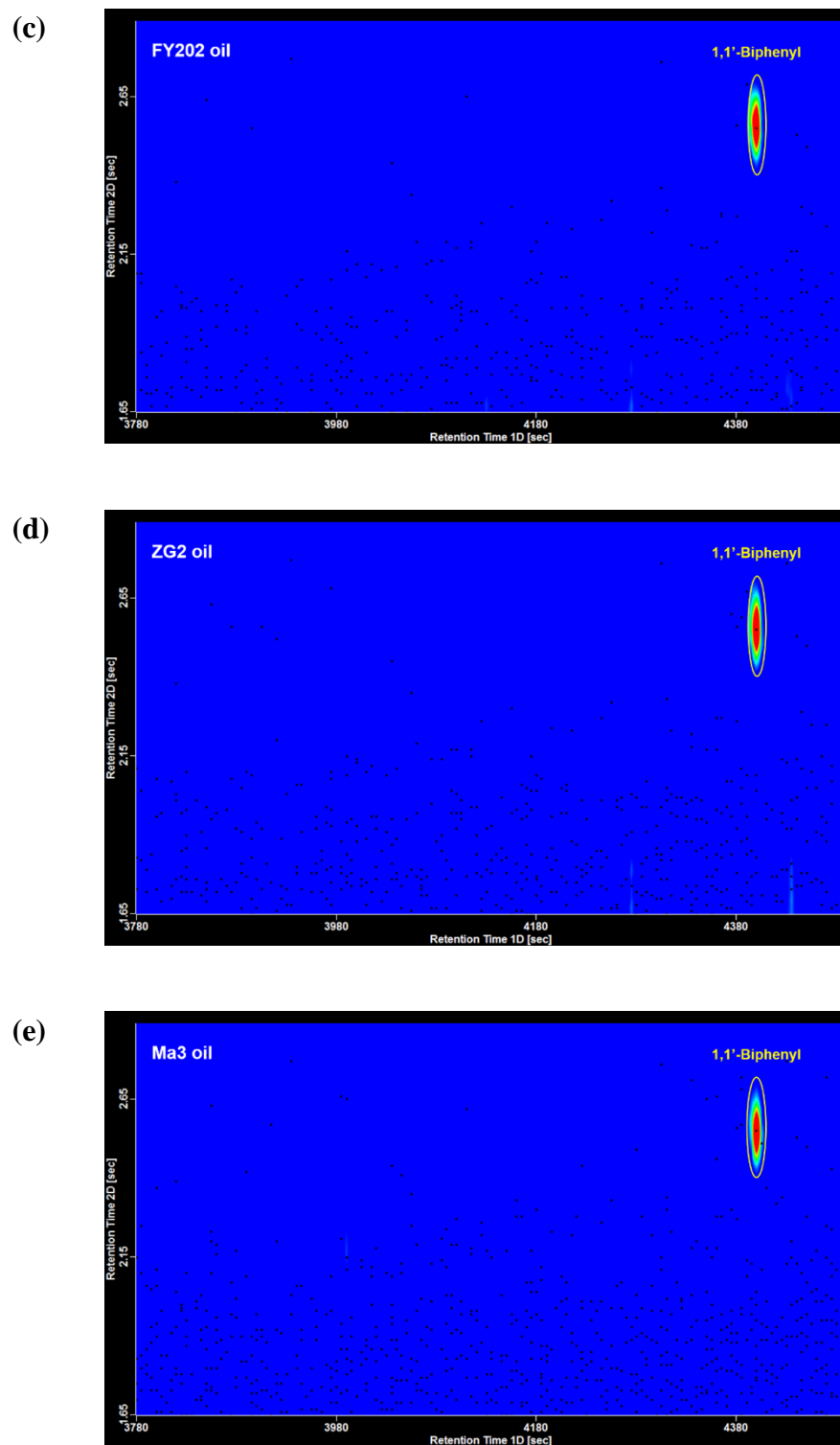
Figure 5.9 Ectracted ion chromatographs of GC×GC-MS for C_1–C_2 thiaadamantanes (*m/z* 168 and 182) and 1,1'-biphenyl (*m/z* 154) in selected Tarim Basin oils.

In the absence of any evidence indicating TSR had impacted the Ma3 oil, the relatively enriched $\delta^{34}S_{OSC}$ values of this oil (cf. group 1 SW oils) might also reflect the $\delta^{34}S$ signature of a different source – quite possibly (like LS2) from Cambrian sources which (unlike LS2) had not been impacted by TSR.

5.3.3 $\delta^{34}S$ of OSCs thermally released from asphaltene fraction of the TSR impacted ZS1C oil

The HyPy treatment of the asphaltene fraction of the ZS1C oil released a broad distribution of thioaromatic compounds (i.e. BTs and DBTs), but few thiadiamondoids. The distribution of thioaromatic compounds within the asphaltene hydropyrolysates, analysed by GC-MS, is shown in **Figure 5.10**. The $\delta^{34}S$ of the HyPy released BTs and DBT$_S$ measured by GC-ICPMS are shown in **Figure 5.11.** For comparison, the corresponding $\delta^{34}S$ values of these compounds measured in the PdCl$_2$ treated fraction of the ZS1C oil (Chapter 2) and also from previously reported data from CSSIA of the aromatic fraction of this oil (Li et al., 2015; Cai et al., 2016) are also shown in **Figure 5.11**. CSSIA of the ZS1C oil has consistently displayed a significant differential between the $\delta^{34}S$ values of BTs (more enriched) and DBTs due to the severe TSR impacts on this oil.

Interestingly, the $\delta^{34}S$ of values of BTs and DBTs released from the asphaltene fraction of ZS1C showed little difference. The average values of $\delta^{34}S_{BTs}$ (35.9‰) and $\delta^{34}S_{DBTs}$ (36.4‰) values in the asphaltene hydropyrolysates fraction were similar to the average $\delta^{34}S_{DBTs}$ (34.4‰) values of the PdCl$_2$ fraction. This result suggests the BTs released from the HyPy fraction had not been impacted by TSR (at least not to the same enriched extent), unlike the free (maltene phase) BTs in the oil which had become more enriched in ^{34}S due to incorporation of the heavier $\delta^{34}S$ signature of H$_2$S reduced from anhydrites. The

seeming imperviousness of TSR on the δ^{34}S character of asphaltene BTs suggests covalent constraints within the asphaltene network, or occluded sequestration, protects them from TSR alteration, potentially maintaining (fully or partially) the isotopic integrity of the pre-altered oil. The sulfur isotopic preservation of OSCs is similar to the isotopic (δ^{13}C and δD) and molecular protection afforded to the hydrocarbon constituents of the asphaltene fraction (Pan et al., 2002; Russell et al., 2004; Silva et al 2008).
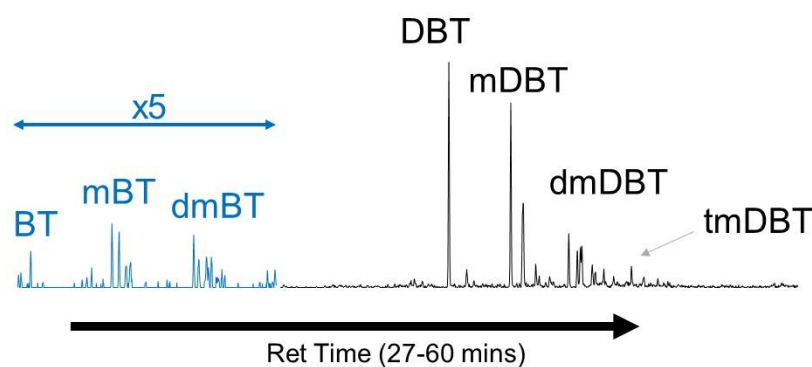
Figure 5.10 Summed chromatogram (*m/z* 134+148+162+176+184+190+198+212 +226) highlighting OSCs detected by GC-MS analysis of asphaltene hydropyrolysates fraction of ZS1C oil.
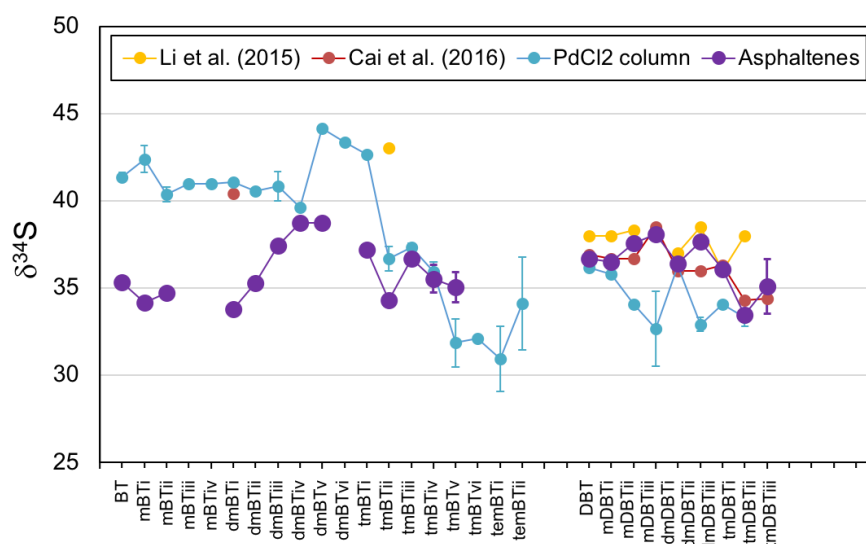
Figure 5.11 δ^{34}S of OSCs in maltene and asphaltene hydropyrolysates fraction of ZS1C oil.

5.4 Conclusions

The application of CSSIA to Tarim Basin oils can help to define the source inputs of these typically mixed and complex oils. Traditional biomarker appraisal of a suite of oils from the Tabei Uplift, Tazhong Uplift and Southwest Depression regions of the Tarim Basin showed evidence for major Cambrian (high gammacerane) and to a lesser extent Ordovician (V-shaped C_{27}–C_{29} sterane profile) inputs. The aliphatic composition of the oils also indicated biodegradation (UCM) — suggesting additional late Devonian input which has been previously associated with biodegradation (Zhu et al., 2013), and non-alteration (low MW n-alkanes) of separate petroleum charges.

The $\delta^{34}S_{DBTs}$ values (~17–25‰) of most Tabei and Tazhong oils pointed to their organic S being largely sourced from Cambrian strata. Three SW oils had distinctively lower $\delta^{34}S_{DBTs}$ values (<11‰) which suggested more significant input of petroleum from Ordovician source rocks. The higher values of two other SW oils (LS2 and Ma3) could be due to either TSR (confirmed in LS2 by occurrence of thiadiamondoids) or input from Cambrian sources (also proposed occurrence on LS2, Zhu et al., 2018).

High $\delta^{34}S_{OSCs}$ values of oils such as the >30‰ values of DBTs in ZS1C oil are an indicator of TSR. TSR can lead to an enrichment in the $\delta^{34}S$ value of the OSCs in oils as they incorporate the heavy isotopic signature of anhydrites. Here, for the first time, we show that OSCs (i.e. BTs) constrained within the asphaltene fraction of oils — and analytically released by HyPy — are isotopically protected from secondary alteration by TSR. The $\delta^{34}S$ values of biodegraded oils had previously been considered unreliable for source correlation studies, but the present result suggests the $\delta^{34}S$ values of OSCs constrained within the asphaltene fraction of TSR impacted oils may be useful for source appraisals.

References

Aboglila, S., Grice, K., Trinajstic, K., Snape, C., Williford, K.H. (2011) The significance of 24-norcholestanes, 4-methylsteranes and dinosteranes in oils and source-rocks from East Sirte Basin (Libya). Applied Geochemistry 26, 1694–1705.

Amrani, A. (2014) Organosulfur Compounds: Molecular and Isotopic Evolution from Biota to Oil and Gas. Annual Review of Earth and Planetary Sciences 42, 733–768.

Cai, C.F., Zhang, C.M., Cai, L.L., Wu, G.H., Liang, J., Xu, Z.M., Li, K.K., Ma, A.L., Chen, L.X. (2009) Origins of palaeozoic oils in the Tarim Basin: Evidence from sulfur isotopes and biomarkers. Chemical Geology 268, 197–210.

Cai, C.F., Zhang, C.M., Worden, R.H., Wang, T.K., Li, H.X., Jiang, L., Huang, S.Y., Zhang, B.S. (2015a) Application of sulfur and carbon isotopes to oil-source rock correlation: A case study from the Tazhong area, Tarim Basin, China. Organic Geochemistry 83-84, 140–152.

Cai, C.F., Hu, G.Y., Li, H.X., Jiang, L., He, W.X., Zhang, B.S., Jia, L.Q., Wang, T.K. (2015b) Origins and fates of H_2S in the Cambrian and Ordovician in Tazhong area: Evidence from sulfur isotopes, fluid inclusions and production data. Marine and Petroleum Geology 67, 408–418.

Cai, C., Amrani, A., Worden, R. H., Xiao, Q., Wang, T., Gvirtzman, Z., Jia, L. (2016) Sulfur isotopic compositions of individual organosulfur compounds and their genetic links in the Lower Paleozoic petroleum pools of the Tarim Basin, NW China. Geochimica et Cosmochimica Acta 182, 88–108.

Chen, L., Yang, H., Wu, G., Han, J., Cai, C., Zhai, S. (2008) Characteristics of the Ordovician reef–shoal reservoir in Tazhong No. 1 Slope-break Zone, Tarim Basin. Xinjiang Petroleum Geology 29, 327–330 (in Chinese).

Cui, J., Wang, T., Zou, C., Li, M., Li, N., Hu, J. (2012) Geochemical characteristics and oil-source correlation of oil-sand extracts of Kelatuo Anticline in the northern Kashi Sag, NW Tarim Basin, China. Energy Exploration & Exploitation 30(4), 609–621.

Cui, J., Wang, T., Li, M., Ou, G., Geng, F., Hu, J. (2013) Oil filling history of the Bashituo Oilfield in the Markit Slope, SW Tarim Basin, China. Petroleum Science 10(1), 58–64.

Ellis, G.S., Said-Ahmad, W., Lillis, P.G., Shawar, L., Amrani, A. (2017) Effects of thermal maturation and thermochemical sulfate reduction on compound-specific sulfur isotopic compositions of organosulfur compounds in Phosphoria oils from the Bighorn Basin, USA. Organic Geochemistry 103, 63–78.

Grotheer, H., Robert, A.M., Greenwood, P.F., Grice, K. (2015) Stability and hydrogenation of polycyclic aromatic hydrocarbons during hydropyrolysis (HyPy) — Relevance for high maturity organic matter. Organic Geochemistry 86, 45–54.

Hanson, A.D., Zhang, S., Moldowan, J.M. (2000) Molecular organic geochemistry of the Tarim Basin, Northwest China. American Association of Petroleum Geologists Bulletin 84, 1109–1128.

He, N., Grice, K., Greenwood, P.F. (2019). The distribution and δ^{34}S values of organic sulfur compounds in biodegraded oils from Peace River (Alberta Basin, western Canada). Organic Geochemistry 128, 16–25.

Li, S.M., Pang, X.Q., Jin, Z.J., Yang, H.J., Xiao, Z.Y., Gu, Q.Y., Zhang, B.S. (2010) Petroleum source in the Tazhong Uplift, Tarim Basin: New insights from geochemical and fluid inclusion data. Organic Geochemistry 41, 531–553.

Li, S.M., Amrani, A., Pang, X.Q., Yang, H.J., Said-Ahmed, W., Zhang, B.S., Pang, Q.J. (2015) Origin and quantitative source assessment of deep oils in the Tazhong Uplift, Tarim Basin. Organic Geochemistry 78, 1–22.

Lockhart, R.S., Berwick,L.J., Greenwood, P.F., Grice, K., Kraal, P., Bush, R. (2013) Analytical pyrolysis for determining the molecular composition of contemporary monosulfidic black ooze. Journal of Analytical and Applied Pyrolysis 104, 640–652.

Love, G.D., Snape, C.E., Carr, A.D., Houghton, R.C. (1995) Release of covalently-bound alkane biomarkers in high yields from kerogen via catalytic hydropyrolysis. Organic Geochemistry 23, 981–986.

Meredith, W., Russell, C.A., Cooper, M., Snape, C.E., Love, G.D., Fabbri, D., Vane, C.H. (2004) Trapping hydropyrolysates on silica and their subsequent thermal desorption to facilitate rapid fingerprinting by GC-MS. Organic Geochemistry 35, 73–89.

Moldowan, J.M., Seifert, W.K., Gallegos, E.J. (1985) Relationship between petroleum composition and depositional environment of petroleum source rocks. American Association of Petroleum Geologists Bulletin 69, 1255–1268.

Palmer, S.E. (1984) Hydrocarbon source potential of organic facies of the lacustrine Elko Formation (Eocene/Oligocene), Northeast Nevada. In: Hydrocarbon Source Rocks of the Greater Rocky Mountain Region (J.Woodward, F. F. Meissner and J. L. Clayton, eds.), Rocky Mountain Association of Geologists, Denver, CO.

Pan, C., Geng, A., Liao, Z., Xiong, Y., Fu, J., Sheng, G. (2002) Geochemical characterization of free versus asphaltene-sorbed hydrocarbons in crude oils: implications for migration-related compositional fractionations. Marine and Petroleum Geology 19(5), 619–632.

Pan, C., Liu, D. (2009) Molecular correlation of free oil, adsorbed oil and inclusion oil of reservoir rocks in the Tazhong uplift of the Tarim basin, China. Organic Geochemistry 40(3), 387–399.

Poole, F. G. and Claypool, G. E. (1984) Petroleum source-rock potential and crude-oil correlation in the Great Basin. In: Hydrocarbon Source Rocks of the Greater Rocky Mountain Region (J. Woodward, F. F. Meissner and J. L. Clayton, eds.), Rocky Mountain Association of Geologists, Denver, CO.

Rosenberg, Y.O., Meshoulam, A., Said-Ahmad, W., Shawar, L., Dror, G., Reznik, I.J., Feinstein, S., Amrani, A. (2017) Study of thermal maturation processes of sulfur-rich source rock using compound specific sulfur isotope analysis. Organic Geochemistry 112, 59–74.

Russell, C. A., Snape, C. E., Meredith, W., Love, G. D., Clarke, E., Moffatt, B. (2004) The potential of bound biomarker profiles released via catalytic hydropyrolysis to reconstruct basin charging history for oils. Organic Geochemistry 35, 1441–1459.

Seewald, J.S. (2003) Organic-inorganic interactions in petroleum-producing sedimentary basins. Nature, 426, 327–333.

Silva, T. F., Azevedo, D. A., Rangel, M. D., Fontes, R. A., Neto, F. R. A. (2008) Effect of biodegradation on biomarkers released from asphaltenes. Organic geochemistry 39(8), 1249–1257.

Snape,C.E., Lafferty, C.J., Eglinton, G., Robinson, N., Collier, R. (1994) The potential of hydropyrolysis as a route for coal liquefaction. International Journal of Energy Research 18, 233–242.

Sun, Y., Xu, S., Lu, H., Cai, P. (2003) Source facies of the Paleozoic petroleum systems in the Tabei uplift, Tarim Basin, NW China: Implications from aryl isoprenoids in crude oils. Organic Geochemistry 34, 629–634.

Wei, Z., Moldowan, J.M., Fago, F., Dahl, J.E., Cai, C., Peters, K.E. (2007) Origins of thiadiamondoids and diamondoidthiols in petroleum. Energy Fuels 21, 3431–3436.

Wei, Z., Walters, C.C., Moldowan, J.M., Mankiewicz, P.J., Pottorf, R.J., et al. (2012) Thiadiamondoids as proxies for the extent of thermochemical sulfate reduction. Organic Geochemistry 44, 53–70.

Wu, G.H., Li. H.H., Zhang, L., Wang, C.L., Bo, Z. (2012) Reservoir-forming conditions of Ordovician weathering crust in the Maigaiti slope, Tarim Basin, NW China. Petroleum Exploration and Development 39(2), 155–164.

Yu, S., Pan, C., Wang, J., Jin, X., Jiang, L., Liu, D., Lv, X.X., Qin, J.Z., Qian, Y.X., Ding, Y., Chen, H. (2011) Molecular correlation of crude oils and oil components from reservoir rocks in the Tazhong and Tabei uplifts of the Tarim Basin, China. Organic Geochemistry 42(10), 1241–1262.

Zhang, S., Hanson, A.D., Moldowan, J.M., Graham, S.A., Liang, D.G., Chang, E., Fago, F. (2000a) Paleozoic oil-source rock correlations in the Tarim Basin, NW China. Organic Geochemistry 31, 273–286.

Zhang, S., Zhang, B., Wang, F., Liang, D., He, Z. (2000b) Middle–Upper Ordovician: The main source of the oils in the Tarim Basin. Marine Oil and Gas Geology 5, 16–22 (in Chinese).

Zhang, S., Liang, D., Li, M., Xiao, Z., He, Z. (2002) (Molecular fossils and oil-source rock correlations in Tarim Basin, NW China). Chinese Science Bulletin 47 (Suppl.), 16–23 (in Chinese).

Zhang, S. and Huang, H. (2005) Geochemistry of Palaeozoic marine petroleum from the Tarim Basin, NW China: Part 1. Oil family classification. Organic Geochemistry 36, 1204–1214.

Zhang, S., Huang, H., Xiao, Z., Liang, D. (2005) Geochemistry of Palaeozoic marine petroleum from the Tarim Basin, NW China. Part 2: Maturity assessment. Organic Geochemistry 36, 1215–1225.

Zhang, S.C., Huang, H.P., Su, J., Liu, M., Wang, X.M., Hua J. (2015) Geochemistry of Paleozoic marine petroleum from the Tarim Basin, NW China: Part 5. Effect of maturation, TSR and mixing on the occurrence and distribution of alkyldibenzothiophenes. Organic Geochemistry 86, 5–18.

Zhu, G., Zhang, S., Su, J., Zhang, B., Yang, H., Zhu, Y., Gu, L. (2013) Alteration and multi-stage accumulation of oil and gas in the Ordovician of the Tabei Uplift, Tarim Basin, NW China: Implications for genetic origin of the diverse hydrocarbons. Marine and Petroleum Geology 46, 234–250.

Zhu, G.Y., Huang, H.P., Wang, H.T. (2015) Geochemical significance of discovery in Cambrian reservoirs at well ZS1 of the Tarim Basin, NW China. Energy Fuel 29, 1332–1344.

Zhu, G.Y., Wang, H.T., Weng, N. (2016) TSR-altered oil with high-abundance thiaadamantanes of a deep-buried cambrian gas condensate reservoir in Tarim Basin. Marine & Petroleum Geology 69, 1–12.

Zhu, G., Zhang, Y., Zhang, Z., Li, T., He, N., Grice, K., .Neng, Y., Greenwood, P. (2018) High abundance of alkylated diamondoids, thiadiamondoids and

thioaromatics in recently discovered sulfur-rich LS2 condensate in the Tarim Basin. Organic geochemistry 123, 136–143.

CHAPTER 6

Conclusions and Recommendations

6.1 Conclusions

This PhD involved the CSSIA of carefully selected standard compounds and a large range of high S content petroleum samples. Several of the key outcomes from this study will extend the application of this still relatively novel analytical approach to future petroleum exploration and research studies.

Laboratory experiments with authentic organic sulfur compounds and representative oil samples confirmed the S-isotopic integrity of all but the most volatile petroleum OSCs through common sample preparation procedures involving large scale solvent loss/evaporation or separation of major oil fractions by traditional and newly applied methods. The positive evaluation of laboratory procedures enhances the analytical basis and confidence of GC-ICPMS measurement and the subsequent interpretation of $\delta^{34}S_{OSC}$ data from petroleum (and other) samples. Specifically, these experiments showed:

- There was no measurable change in the $\delta^{34}S$ value of two DCM dissolved OSCs (DBT and $C_{18}SH$) on their partial evaporation following removal of dissolving solvent. $C_{12}SH$, a higher vapor pressure compound, did show a small enrichment (+3‰) after ~66% of the compound was lost to evaporation. A separate evaporation-$\delta^{34}S$ study (Rosenberg et al., 2017) of standard compounds reported similarly small or negligible $\delta^{34}S$ fractionation of OSCs common to petroleum — this study reported a very small ^{34}S enrichment (<2‰) in very low molecular

weight products (i.e. butyl-thiol, dimethyl-thiophene) of high volatility but no shift in the δ^{34}S values of BT and DBT.

- The δ^{34}S values of OSCs in the aromatic fractions of two oils were essentially the same when isolated by Al_2O_3 or $PdCl_2$ stationary phase columns. The $PdCl_2$ column provided higher concentrations of OSCs than the more traditionally applied alumina column. Higher analyte concentrations help to maximise the numbers of OSCs which can be analysed and the δ^{34}S precision of the GC-ICPMS measurement.

- The δ^{34}S values of thioaromatics (BTs, DBT$_S$) and caged-S compounds (TDs) of one oil (ZS1C) separated using a novel methylation/demethylation fractionation method were also largely similar to the values of the same compounds in the aromatic fraction from an Al_2O_3 column. The δ^{34}S integrity of this quite intrusive separation procedure, however, should be further assessed with other samples and experiments before it should be considered compatible with CSSIA.

Application of CSSIA to the selected fractions of oils exposed to regular secondary petroleum reservoir processes (i.e. biodegradation, TSR) has also provided new information about the associated δ^{34}S fractionation of OSCs: The first insight of the influence of biodegradation on δ^{34}S values of petroleum OSCs was revealed by CSSIA of a series of biodegraded oil sands (Athabasca, Canada). A study of oils from Peace River wells spanning biodegradation levels of ~3-6 showed:

- The δ^{34}S values of several alkyl-BTs (particularly dimethyl-BTs) in increasingly biodegraded oils showed a distinct enrichment ($\leq$6‰) consistent with preferential utilisation of the smaller isotope (^{32}S). The higher MW alkyl-DBTs

are more resistant to biodegradation and the $\delta^{34}S_{DBT}$ values of the oils showed no change, indicating a stability at biodegradation levels of 3–6. The varied $\delta^{34}S$ sensitivity of different OSCs to biodegradation will assist the high resolution characterisation of oil biodegradation levels.

A number of previous studies (e.g. Amrani et al., 2012; Gvirtman et al., 2015) have demonstrated that TSR can lead to the large and varied $\delta^{34}S$ fractionations of OSCs in the free maltene fraction of impacted oils. The present research has established that the covalently constrained or sequestered products in the more polar and higher molecular weight asphaltene fraction provides some protection to the $\delta^{34}S_{OSC}$ effects of this alteration:

- The $\delta^{34}S$ values of BTs and DBTs in the asphaltene hydropyrolysates fraction of a severely TSR impacted oil (ZS1C) had similar values of ~35‰. This contrasts the substantial isotopic differential (>5‰) these product types show in the maltene fraction of this oil. This result confirms OSCs in the asphaltene fraction are protected from at least the full isotopic impacts of TSR incident on the free fractions and may even maintain the $\delta^{34}S$ values of diagenetically incorporated OSCs in heavily TSR impacted oils. The asphaltene fraction maintenance of $\delta^{34}S_{OSC}$ signatures may be beneficial to oil-source correlation studies.

The analytical development and improved understanding of $\delta^{34}S$-petroleum alteration relationships from these controlled experiments were complimented with several applied studies of high S-oils from three active petroleum regions of China — The Jinxian and Dongpu Sags of Bohai Bay Basin (East Central China) and the Tarim Basin (NE China). These field studies demonstrate the practical utility of the current CSSIA technology.

Specific aims included a greater understanding of the origin and formation pathway of the organic S of petroleum reservoirs and occurrences of TSR throughout these oil provinces.

The source of the sour gas rich petroleum of the Jinxian Sag has been the focus of previous attention, up until the closure of these oil wells several years ago on the grounds of safety concerns about the high H_2S levels. Earlier organic (and inorganic) geochemical appraisal of Jinxian Sag petroleum samples, including consideration of bulk $\delta^{34}S$ values, had led to the contrasting assertions by different groups that MSR and TSR were separately responsibly for the high S content of the petroleum. The presently conducted CSSIA research of two archived oils and several source rock samples from the Zhaolanzhuang oil field has led to the proposal of the following sophisticated model of S-cycling in the Jinxian Sag:

- The broad range of $\delta^{34}S_{OSC}$ values (~0‰ to +20‰) observed amongst the different oil and rock samples analysed was attributed to a temporal variation in the $\delta^{34}S$ of reduced S available for organic sulfurization. This implies the petroleum system was sulfate restricted, inducing a kinetic control such that initially reduced S was ^{34}S depleted and the residual sulfate ^{34}S enriched. Such a closed S-system model could account for the general trend of more depleted $\delta^{34}S_{OSC}$ values in the deeper Zh rocks (i.e. utilising early generated ^{32}S depleted H_2S).

An integrated hydrocarbon composition and CSSIA study of saline and freshwater lacustrine oils from Dongpu Sag was able to separate the samples into 5 separate oil

families. These results (briefly detailed below) highlight the oil correlation capacity, but also potential limitations, of the $\delta^{34}S$ signatures of S-rich saline lacustrine oils:

- Differences in the $\delta^{34}S_{OSC}$ magnitude and profiles of the oils were consistent with the hydrocarbon biomarker classification of the five oil families. However, the $\delta^{34}S_{OSC}$ data of the Dongpu oils was also influenced by paleo-environmental conditions (reflected by C_{35}-/C_{34}-hopanes), thermal maturity (C_{29} sterane and mDBT parameters) and TSR ($\Delta\delta^{34}S_{BTs-DBTs} = 6–12‰$) factors. These multiple variables warn that the $\delta^{34}S$ correlation of oils from complex petroleum systems should be conducted with caution and where possible integrated with other complimentary analytical information.

The huge petroleum reserves of the Tarim Basin continue to be the target of intensive exploration. The consensus is that most of the regional oil is of Cambrian origin, but some petroleum might also include a major input from Ordovician sources. Clarification of the relative contribution of Cambrian and Ordovician sources to Tarim basin petroleum remains an active research question for petroleum and organic geochemists. This issue was explored further here by CSSIA (and complimentary hydrocarbon characterization) of a selection of oils from each of the Tazhong, Tabei and SW oil fields. Key outcomes of this study included:

- The $\delta^{34}S$ of OSCs in the oils from Tazhong Uplift and Tabei Uplift demonstrated a mixed origin of Cambrian (mostly) and Upper Ordovician source rocks. A group of three Southwest oils showed much more depleted $\delta^{34}S$ values than all other oils studied and was attributed to a primary Ordovician source rock origin. The relatively enriched $\delta^{34}S_{OSC}$ values of some oils (> +40‰ in ZS1C) reflected

the impacts of TSR which can be supported by the deep depths/high temperatures of many Tarim Basin oils.

The research conducted in this PhD project (highlights above) has revealed new insights to the S-cycles of petroleum systems. Several practical benefits achievable from the $\delta^{34}S$ measurement of individual petroleum compounds have been demonstrated. However, a higher maturity petroleum (and broader biogeoscience) application of CSSIA will require continued development of the analytical technology and application to a wide range of high S petroleum (and other organic S) samples from a variety of geological settings. Continuous flow CSIA applications of carbon (C) and hydrogen (H) — both developed decades earlier than CSSIA — took many years of concerted research to evolve into the widely accepted hydrocarbon characterization methods of today. These established CSIA approaches are now widely practiced by the international petroleum research and exploration communities. A similar trend for CSSIA would see it have a constructive future in petroleum characterization endeavors.

6.2 Recommendations from this Research

In addition to the holistic advice of continued analytical development of the CSSIA technology and broader application to a wide range of petroleum samples, several specific recommendations are offered to verify some of the newly discovered petroleum-$\delta^{34}S_{OSC}$ relationships as well as to address a few stumbling blocks or issues encountered though this project.

- The effect of biodegradation evident from the $\delta^{34}S$ of OSCs in a set of biodegraded oils from the Athabasca oil sands included an anticipated $\delta^{34}S$ enrichment of some compounds (e.g. dmBTs), whereas other compounds (e.g. DBTs) showed no $\delta^{34}S$ variance. The Athabasca oil sands is an extremely

complex system due to varied biodegradation, source and thermal maturity dynamics. The $\delta^{34}S_{OSC}$ enrichment observed with biodegradation should be verified with further CSSIA studies of appropriate biodegraded samples. Whist the initial microcosm experiment did not lead to sufficient biodegradation of OSCs in the ZS1C oil, this approach warrants further attention given the capacity to control biodegradation as the sole variable. Several modifications to the present approach may help to increase the rate of OSC biodegradation. Firstly, sulfur-reducing bacteria (SRB) isolates or bacterial consortia enriched in SRB could be used instead of the total microfloral population of a common soil. Secondly, a S-rich aromatic fraction could be used as the biodegrading fuel, rather than a whole oil which contains many preferentially degradable hydrocarbons.

- The relatively low $\delta^{34}S$ values of BTs in the asphaltene hydropyrolysates fraction of the TSR impacted ZS1C oil indicated they had not been enriched like the same free compounds in the maltene fraction of the oil. This result indicated covalently bound OSCs of the asphaltene fraction are protected from TSR alteration. The extent of this protection, however, still needs to be established. Are asphaltene OSCs fully protected and thus representative of diagenetically incorporated S, or just partially protected such that they are not as enriched to the same extent as the free compounds of the maltene fraction? The former outcome would obviously be more beneficial to oil correlation studies. Whether all OSCs in the asphaltene fraction receive the same level of protection is another query. These issues could be investigated by further study and comparison of the asphaltene and maltene fractions of TSR impacted oils. Laboratory based TSR simulations with selected oils where the $\delta^{34}S_{OSC}$ composition of respective fractions are known might also

help to establish the S-isotopic stability of the asphaltene fraction to increasing levels of TSR.

- Petroleum applications of CSSIA would benefit from an extension of the numbers and types of OSCs which are measured by GC-ICPMS. A larger range of $\delta^{34}S_{OSC}$ data would increase the resolution with which source and other organic sulfur process controls could be defined. The petroleum OSCs analyzed in this PhD project were largely restricted to alkylated thioaromatics (e.g. BTs, DBTs) and alkylated thiadiamondoids (TD$_S$). These compounds are typically the major products of the easily prepared ARO fraction of petroleum samples. A much larger variety of GC resolvable OSCs can occur in petroleum samples (e.g. alkylated sulfides, thiols, thiophenes, thianes, thioalanes, etc., Sinninghe-Damste et al., 1990), and many other OSCs occur in the polar fraction of oils (typically not subjected to GC analysis without derivatization). An historic technical challenge for ICPMS measurement of GC resolved compounds has been the effective transfer of higher molecular weight compounds. High flows of argon and other cooling gases into the ICP torch can impede the transfer of low volatility compounds. The development of further technical strategies to support the $\delta^{34}S$ measurement of high molecular weight OSCs related to terpenoid biomarkers (e.g. steroid thiophenes, hopanoid sulfides) would provide valuable new source relevant information.

- Improved product assignment of different isomers is another more general recommendation for studies concerned with characterization of the organic sulfur composition of petroleum samples. The isomer identification of GC resolved alkyl-BT and alkyl-DBT isomers in the present study proved challenging and

was largely limited to correlation of major isomers present in well studied petroleum samples; or previously reported elution orders (Berthou et al., 1984; Depauw and Froment, 1997; López García et al., 2002). More extensive product assignments could be overcome by a greater availability of standard compounds, some of which could be sourced from commercial suppliers whilst others could be prepared by synthetic chemistry.

References

Berthou, F., Dreano, Y., Sandra, P. (1984) Liquid and gas chromatographic separation of isomeric methylated dibenzothiophenes. Journal of High Resolution Chromatography 7, 679–686.

Depauw, G.A., Froment, G.F. (1997) Molecular analysis of the sulphur components in a light cycle oil of a catalytic cracking unit by gas chromatography with mass spectrometric and atomic emission detection. Journal of Chromatography A 761, 231–247.

López García, C., Becchi, M., Grenier-Loustalot, M.F., Païsse, O., Szymanski, R. (2002) Analysis of aromatic sulfur compounds in gas oils using GC with sulfur chemiluminescence detection and high-resolution MS. Analytical Chemistry 74, 3849–3857.

Rosenberg, Y.O., Meshoulam, A., Said-Ahmad, W., Shawar, L., Dror, G., Reznik, I. J., Amrani, A. (2017) Study of thermal maturation processes of sulfur-rich source rock using compound specific sulfur isotope analysis. Organic Geochemistry 112, 59–74.

Sinninghe Damste, J.S., De Leeuw, J.W. (1990) Analysis, structure and geochemical significance of organically-bound sulphur in the geosphere: State of the art and future research. Organic Geochemistry 16, 1077–1101.

Bibliography

A

Aboglila, S., Grice, K., Trinajstic, K., Snape, C., Williford, K.H. (2011) The significance of 24-norcholestanes, 4-methylsteranes and dinosteranes in oils and source-rocks from East Sirte Basin (Libya). Applied Geochemistry, 26, 1694–1705.

Adams, J.J., Riediger, C., Fowler, M., Larter, S.R. (2006) Thermal controls on biodegradation around the Peace River tar sands: Paleo-pasteurization to the west. Journal of Geochemical Exploration 89, 1–4.

Adams, J.J. (2008) The Impact of Geological and Microbiological Processes on Oil Composition and Fluid Property Variations in Heavy Oil and Bitumen Reservoirs. PhD Thesis, University of Calgary, Canada.

Adams, J., Larter, S., Bennett, B., Huang, H., Westrich, J., van Kruisdijk, C. (2012) The dynamic interplay of oil mixing, charge timing, and biodegradation in forming the Alberta oil sands: Insights from geologic modeling and biogeochemistry. In: Hein, F.J., Leckie, D., Larter, S., Suter, J.R. (Eds.), Heavy-Oil and Oil-Sand Petroleum Systems in Alberta and Beyond. AAPG Studies in Geology 64, pp. 23–102.

Ahmed, M., Smith, J.W., George, S.C. (1999) Effects of biodegradation on Australian Permian coals. Organic Geochemistry 30, 1311–1322.

Alexander, R., Kagi, R.I., Woodhouse, G.W., Volkman, J.K. (1983) The geochemistry of some biodegraded Australian oils. The APEA Journal 23, 53–63.

Amrani, A., Aizenshtat, Z. (2004) Mechanisms of sulfur introduction chemically controlled: $\delta^{34}S$ imprint. Organic Geochemistry 35, 1319–1336.

Amrani, A., Lewan, M. D., & Aizenshtat, Z. (2005) Stable sulfur isotope partitioning during simulated petroleum formation as determined by hydrous pyrolysis of Ghareb Limestone, Israel. Geochimica et Cosmochimica Acta 69, 5317–5331.

Amrani, A., Sessions, A.L., Adkins, J.F. (2009) Compound-specific $\delta^{34}S$ analysis of volatile organics by coupled GC/multicollector-ICPMS. Analytical Chemistry 81, 9027–9034.

Amrani, A., Deev, A., Sessions, A. L., Tang, Y., Adkins, J. F., Hill, R. J., Wei, Z. (2012) The sulfur-isotopic compositions of benzothiophenes and dibenzothiophenes as a proxy for thermochemical sulfate reduction. Geochimica et Cosmochimica Acta 84, 152–164.

Amrani, A., Deev, A., Sessions, A.L., Tang, Y.C., Adkins, J.F., Hill, R.J., Moldowan, L.M., Wei, Z.B. (2012) The sulfur-isotopic compositions of benzothiophenes and dibenzothiophenes as a proxy for thermochemical sulfate reduction. Geochimica et Cosmochimica Acta 84, 152–164.

Amrani, A., Dror, G., Said-Ahmad, W., Feinstein, S. and Reznik, I. J. (2013) The distribution and sulfur isotope ratios of specific organic sulfur compounds during pyrolysis of thermally immature kerogen. 26th International Meeting of Organic Geochemistry, Tenerife, Spain. Book of Abstracts, vol. 2, pp. 561–562.

Amrani, A, Said-Ahmad, W., Shaked, Y., Kiene, R.P. (2013) Sulfur isotope homogeneity of oceanic DMSP and DMS. Proceedings of the National Academy of Sciences 110, 18413–18418.

Amrani, A. (2014) Organosulfur compounds: Molecular and isotopic evolution from biota to oil and gas. Annual review earth planetary science 42, 733–768.

Anderson, T.F. and Pratt, L.M. (1995) Isotopic evidence for the origin of organic sulfur and elemental sulfur in marine sediments. ACS Symposium Series 612, 378–396.

Asif, M., Grice, K., Fazeelat, T. (2009) Assessment of petroleum biodegradation using stable hydrogen isotopes of individual saturated hydrocarbon and polycyclic aromatic hydrocarbon distributions in oils from the Upper Indus Basin, Pakistan. Organic Geochemistry 40, 301–311.

B

Bayona, J.M., Albaiges, J., Solanas, A.M., Pares, R., Garrigues, P., Ewald, M. (1986) Selective aerobic degradation of methyl-substituted polycyclic aromatic hydrocarbons in petroleum by pure microbial cultures. International Journal of Environmental Analytical Chemistry 23, 289–303.

Bennett, B., Adams, J.J., Gray, N.D., Sherry, A., Oldenburg, T.B.P., Huang, H., Larter, S.R., Head, I.M. (2013) The controls on the compositoion of biodegraded oils in the deep subsurface – Part 3. The impact of microorganism distribution on petroleum geochemical gradients in biodegraded petroleum reservoirs. Organic Geochemistry 56, 94–105.

Bennett, B., Larter, S.R. (2008) Biodegradation scales: Applications and limitations. Organic Geochemistry 39, 1222–1228.

Berthou, F., Dreano, Y., Sandra, P. (1984) Liquid and gas chromatographic separation of isomeric methylated dibenzothiophenes. Journal of High Resolution Chromatography 7, 679–686.

Bolshakov, G.F. (1986) Organic sulfur compounds of petroleum. Journal of Sulfur Chemistry 5, 103–393.

Bottcher, M.E., Thamdrup, B., Vennemann, T.W. (2001) Oxygen and sulfur isotope fractionation during anaerobic bacterial disproportionation of elemental sulphur. Geochimica et Cosmochimica 65, 1601–1609.

Broecker, W.S. and Oversby, V.M. (1971) Rayleigh distillation. Chemical Equilibria in the Earth, pp.165–167.

Brunner, B. and Bernasconi, S.M. (2005) A revised isotope fractionation model for dissimilatory sulfate reduction in sulfate reducing bacteria. Geochimica et Cosmochimica Acta 69, 4759–4771.

Butler, I.B., Bottcher, M.E., Rickard, D., Oldroyd, A. (2004) Sulfur isotope partitioning during experimental formation of pyrite via the polysulfide and hydrogen sulfide pathways: Implications for the interpretation of sedimentary and hydrothermal pyrite isotope records. Earth and Planetary Science Letters 228, 495–509.

C

Cai, C.F., Worden, R.H., Wolff, G.A., Bottrell, S., Wang, D.L., Li, X. (2005) Origin of sulfur rich oils and H_2S in Tertiary lacustrine sections of the Jinxian Sag, Bohai Bay Basin, China. Applied Geochemistry 20, 1427–1444.

Cai C., Li K., Anlai M., Zhang C., Xu Z., Worden R.H., Wu G., Zhang B., Chen L. (2009a) Distinguishing Cambrian from Upper Ordovician source rocks: Evidence from sulfur isotopes and biomarkers in the Tarim Basin. Organic Geochemistry 40, 755–776.

Cai, C.F., Zhang, C.M., Cai, L.L., Wu, G.H., Jiang, L., et al. (2009b) Origins of Palaeozoic oils in the Tarim Basin: Evidence from sulfur isotopes and biomarkers. Chemical Geology 268, 197–210.

Cai, C., Zhang, C., He, H., Tang, Y. (2013) Carbon isotope fractionation during methane-dominated TSR in East Sichuan Basin gasfields, China: A review. Marine and Petroleum Geology 48, 100–110.

Cai, C.F., Zhang, C.M., Worden, R., Wang, H., Li, H.X., Jiang, L., Huang, S.Y., Zhang, B.S. (2015a) Application of sulfur and carbon isotopes to oil-source rock correlation: A case study from the Tazhong area, Tarim Basin, China. Organic Geochemistry, 83–84, 140–152.

Cai, C.F., Hu, G.Y., Li, H.X., Jiang, L., He, W.X., Zhang, B.S., Jia, L.Q., Wang, T.K. (2015b) Origins and fates of H_2S in the Cambrian and Ordovician in Tazhong area: Evidence from sulfur isotopes, fluid inclusions and production data. Marine and Petroleum Geology 67, 408–418.

Cai, C., Amrani, A., Worden, R.H., Xiao, Q., Wang, T., Gvirtzman, Z., Li, H., Said-Ahmad, W. and Jia, L. (2016) Sulfur isotopic compositions of individual organosulfur compounds and their genetic links in the Lower Paleozoic petroleum pools of the Tarim Basin, NW China. Geochimica et Cosmochimica Acta 182, 88–108.

Cai, C., Xu, C., He, W., Zhang, C., Li, H. (2017a) Biomarkers and C and S isotopes of the Permian to Triassic solid bitumen and its potential source rocks in NE Sichuan Basin. Geofluids, 2017.

Cai, C., Xiang, L., Yuan, Y., Xu, C., He, W., Tang, Y., Borjigin, T. (2017b) Sulfur and carbon isotopic compositions of the Permian to Triassic TSR and non-TSR altered solid bitumen and its parent source rock in NE Sichuan Basin. Organic Geochemistry 105, 1–12.

Canfield, D.E., Thamdrup, B. (1994) The production of ^{34}S-depleted sulfide during bacterial disproportionation of elemental sulphur. Science 266, 1973–1975.

Canfield, D., Boudreau, B.P., Mucci, A., Gundersen, J.K. (1998) The early diagenetic formation of organic sulfur in the sediments of Mangrove Lake, Bermuda. Geochimica et Cosmochimica Acta 62, 767–781.

Canfield, D.E., Habicht, K.S., Thamdrup, B. (2000) The Archean sulfur cycle and the early history of atmospheric oxygen. Science 288, 658–661.

Canfield, D.E. (2001) Biogeochemistry of sulfur isotopes. Mineralogy and Geochemistry, 43, 607–636.

Canfield, D.E., Farquhar, J., Zerkle, A.L. (2010) High isotope fractionations during sulfate reduction in a low-sulfate euxinic ocean analog. Geology 38, 415–418.

Chambers, L.A., Trudinger, P.A., Smith, J.W., Burns, M.S. (1975) Sulfur isotope fractionation during sulfate reduction by dissimilatory sulfate reducing bacteria. Canadian Journal of Microbiology 21, 1602–1607.

Chang, Z., Chen, Z., Zhang, Y., Peng, J., Jin, Z. (2007) Investigation on geochemistry characterisitics of crude oil from weicheng-wenmingzhai area in Dongpu depression. Fault-Block Oil Gas Field 14, 1–3 (in Chinese).

Chen, L., Yang, H., Wu, G., Han, J., Cai, C., Zhai, S. (2008) Characteristics of the Ordovician reef–shoal reservoir in Tazhong No. 1 Slope-break Zone, Tarim Basin. Xinjiang Petroleum Geology 29, 327–330 (in Chinese).

Chen, X. (2017) Hydrocarbon Generation and Accumulation Effect of saline Lacustrine Strata Bearing gypsum-salt Rock in Dongpu Sag, Bohai Bay Basin. PhD dissertation. China University of Petroleum (Beijing), pp. 48–51 (in Chinese).

Chen, X., Li, S., Zhang, H., Xu, T., Zhang, Y., Wan, Z., Ji, H., Guo, Z. (2018) Controlling Effects of Gypsum-salt on Hydrocarbon Generation of Source Rocks in Dongpu Sag and Its Significance on Petroleum Geology. Geoscience 32, 1125–1136 (in Chinese).

Chen, Y., Tian, C., Li, K., Cui, X., Wu, Y., Xia, Y. (2016). Influence of thermal maturity on carbon isotopic composition of individual aromatic hydrocarbons during anhydrous closed-system pyrolysis. Fuel 186, 466–475.

Clayton, C.J., Bjorøy, M. (1994) Effect of maturity on $^{13}C/^{12}C$ ratios of individual compounds in North Sea oils. Organic Geochemistry 21, 737–750.

Connan, J., Cassou, A.M. (1980) Properties of gases and petroleum liquids derived from terrestrial kerogen at various maturation levels. Geochimica et Cosmochimica Acta 4, 1–23.

Creaney, S., Allan, J. (1990) Hydrocarbon generation and migration in the Western Canada Sedimentary Basin. In: Brooks, J. (Ed.), Classic Petroleum Provinces, Geological Society Special Publication. No 50 pp.189–202.

Cristadoro, A., Kulkarni, S.U., Burgess, W.A., Cervo, E.G., Räder, H.J., Müllen, K., Thies, M.C. (2009) Structural characterization of the oligomeric constituents of petroleum pitches. Carbon 47, 2358–2370.

Cui, J., Wang, T., Zou, C., Li, M., Li, N., Hu, J. (2012) Geochemical characteristics and oil-source correlation of oil-sand extracts of Kelatuo Anticline in the northern Kashi Sag, NW Tarim Basin, China. Energy Exploration & Exploitation 30(4), 609–621.

Cui, J., Wang, T., Li, M., Ou, G., Geng, F., Hu, J. (2013) Oil filling history of the Bashituo Oilfield in the Markit Slope, SW Tarim Basin, China. Petroleum Science 10(1), 58–64.

D

Dai, J.X., Hu, J.Y., Jia, C.Z., Fang, Y.S., Sun, Z.D., Wei, L.H., Yuan, J.P., Yang, W. (2004) Suggestions for scientifically and safely exploring and developing high H_2S gas fields. Petroleue Exploration and Development 31 (2), 1–5 (in Chinese).

Dawson, D., Grice, K., Alexander, R., Edwards, D. (2007) The effect of source and maturity on the stable isotopic compositions of individual hydrocarbons in sediments and crude oils from the Vulcan Sub-basin, Timor Sea, Northern Australia. Organic Geochemistry 38, 1015–1038.

Demirbas, A., Alidrisi, H., Balubaid, M.A. (2015) API gravity, sulfur content, and desulfurization of crude oil. Petroleum Science and Technology 33, 93–101.

Depauw, G.A., Froment, G.F. (1997) Molecular analysis of the sulphur components in a light cycle oil of a catalytic cracking unit by gas chromatography with mass spectrometric and atomic emission detection. Journal of Chromatography A 761, 231–247.

Detmers, J., Brüchert, V., Habicht, K. S., Kuever, J. (2001) Diversity of sulfur isotope fractionations by sulfate-reducing prokaryotes. Applied and Environmental Microbiology 67, 888–894.

Deroo, G., Powell, T.G., Tissot, B., McCrossan, R.G. (1977) The origin and migration of petroleum in the Western Canadian Sedimentary Basin, Alberta – A geochemical and thermal maturation study. Geological Survey of Canada Bulletin 262, 1–136.

Dijkmans, T., Djokic, M.R., van Geem, K.M., Marin, G.B. (2015) Comprehensive compositional analysis of sulfur and nitrogen containing compounds in shale oil using GC× GC-FID/SCD/NCD/TOF-MS. Fuel 140, 398–406.

Ding, T., Valkiers, S., Kipphardt, H., De Bi`ever, P., Taylor, P.D.P., et al. (2001) Calibrated sulfur isotope abundance ratios of three IAEA sulfur isotope reference materials and V-CDT with a reassessment of the atomic weight of sulfur. Geochimica et Cosmochimica Acta 65, 2433–2437.

Durand, B. and Monin, J.C. (1980) Elemental analysis of kerogens (C, H, O, N, S, Fe). In: Kerogen. Insoluble Organic Matter from Sedimentary Rocks (B. Durand, ed.), Editions Technip, Paris, pp. 113–142.

E

Eckelmann, W.R., Broecker, W.S., Whitlock, D.W., Allsup, J.R. (1962) Implications of carbon isotopic composition of total organic carbon of some recent sediments and ancient oils. AAPG bulletin 46, 699–704.

Eglinton, G. and Calvin, M. (1967) Chemical fossils. Scientific American 216, 32–43.

Ehrlich, H. L., Brierley, C. L. (1990) Microbial mineral recovery. McGraw-Hill, Inc.

Ellis, G.S., Said-Ahmad, W., Lillis, P.G., Shawar, L., Amrani, A. (2017) Effects of thermal maturation and thermochemical sulfate reduction on compound-specific sulfur isotopic compositions of organosulfur compounds in Phosphoria oils from the Bighorn Basin, USA. Organic Geochemistry 103, 63–78.

Engel, M.H., Zumberge, J.E. (2007) Secular change in the stable sulfur isotope composition of crude oils relative to marine sulfates and sulfides. Book of Abstracts, International Meeting of Organic Geochemistry 2007 (Torquay, UK, September 19–24,). pp. 523–524.

F

Fan, H.G., Dai, J.X., Qi, H.F. (1992) Controls on bacterially originated H_2S. Petroleum Exploration and Development 19 (Supplement), 71–75 (in Chinese).

Faure, G. and Mensing, T.M. (2005) Isotopes, Principles and Applications, John Wiley & Sons, Hoboken, NJ, 3rd Ed.

Fedorak, P.M., Coy, D.L., Peakman, T.M. (1996) Microbial metabolism of some 2,5-substituted thiophenes. Biodegradation 7, 313–327.

Fedorak, P.M., Peakman, T.M. (1992) Aerobic microbial metabolism of some alkylthiophenes found in petroleum. Biodegradation 2, 223–236.

Fedorak, P.M., Westlake, D.W.S. (1984) Microbial degradation of organic sulfur compounds in Prudhoe Bay crude oil. Canadian Journal of Microbiology 29, 291–296.

Fike, D.A., Grotzinger, J.P. (2008) A paired sulfate-pyrite δ^{34}S approach to understanding the evolution of the Ediacaran-Cambrian sulfur cycle. Geochimica et Cosmochimica Acta 72, 2636–2648.

Fisher, S.J., Alexander, R., Kagi, R.I. (1996) Biodegradation of alkylnaphthalenes in sediments adjacent to an off-shore petroleum production platform. Polycyclic Aromatic Compounds 11, 35–42.

Fisher, S.J., Alexander, R., Kagi, R.I., Oliver, G.A. (1998) Aromatic hydrocarbons as indicators of biodegradation in north Western Australian reservoirs. In: Purcell, P.G. and Purcell, R. (Eds), Sedimentary Basins of Western Australia. West Australian Basins Symposium. Petroleum Exploration Society of Australia, Perth, Australia, pp. 185–194.

Fontanive, F.C., Souza-Silva, É.A., da Silva, J.M., Caramão, E.B., Zini, C.A. (2016) Characterization of sulfur and nitrogen compounds in Brazilian petroleum derivatives using ionic liquid capillary columns in comprehensive two-dimensional gas chromatography with time-of-flight mass spectrometric detection. Journal of Chromatography A 1461, 131–143.

Freeman, K.H., Hayes, J.M., Trendel, J.M., Albrecht, P. (1990) Evidence from carbon isotope measurements for diverse origins of sedimentary hydrocarbons. Nature 343, 254–256.

G

Gaffney, J.S., Premuzic, E.T., Manowitz, B. (1980) On the usefulness of sulfur isotope ratios in crude oil correlations. Geochimica et Cosmochimica Acta 44, 135–139.

Gao, H., Chen, F., Liu, G., Liu, Z. (2009) Advances, problems and prospect in studies of origin of salt rocks of the Paleogene Shahejie Formation in Dongpu Sag. Journal of Palaeogeography 11, 251–264 (in Chinese).

Gao, H., Zheng, R., Xiao, Y., Meng, F., Chen, F., Bai, G., Luan, Y., Tan, X., Shi, Y. (2015) Origin of the slat rock of Paleogene Shahejie formation in Dongpu sag, Bohai Bay Basin: evidences from sedimentology and geochemistry. Acta Petroleum Sinica 36, 19–32 (in Chinese).

George, S.C., Boreham, C.J., Minifie, S.A., Teerman, S.C. (2002) The effect of minor to moderate biodegradation on C_5 to C_9 hydrocarbons in crude oils. Organic Geochemistry 33, 1293–1317.

Gillaizeau, B. and Tang, Y. (2001) Reaction mechanistic studies for the thermochemical sulfate reduction. In Abstract for 20th International Meeting on Organic Geochemistry, Nancy, France (p. 81).

Gong, Z.S. (2004) Neotectonics and petroleum accumulation in offshore Chinese basins. Earth Science-Journal of China University of Geosciences 29, 513–517 (in Chinese with English abstract).

Greenwood, P.F., Wibrow, S., George, S.J., Tibbett, M. (2008) Sequential hydrocarbon biodegradation in a soil from arid coastal Australia, treated with oil under laboratory-controlled conditions. Organic Geochemistry 39, 1336–1346.

Greenwood, P.F., Amrani, A., Sessions, A., Raven, M.R., Holman, A.I., Dror, G., Grice, K., McCulloch, M.T., Adkins, J.F. (2014) Development and initial biogeochemical applications of compound specific $\delta^{34}S$ analysis. In: Grice, K. (Ed.), RSC Detection Science Series No. 4: Principles and Practice of Analytical Techniques in Geosciences. Royal Society of Chemistry, Oxford.

Greenwood, P.F., Amrani, A., Sessions, A., Raven, M.R., Holman, A., Dror, G., Grice, K., McCulloch, M.T., Adkins, J.F. (2015) Development and Initial Biogeochemical Applications of Compound-Specific Sulfur Isotope Analysis. In: Principles and Practice of Analytical Techniques in Geosciences. The Royal Society of Chemistry, UK.

Greenwood, P.F., Mohammed, L., Grice, K., McCulloch, M., Schwark, L. (2018) The application of compound-specific sulfur isotopes to the oil-source rock correlation of Kurdistan petroleum. Organic geochemistry 117, 22–30.

Grice, K., Alexander, R., Kagi, R.I. (2000) Diamondoid hydrocarbon ratios as indicators of biodegradation in Australian crude oils. Organic Geochemistry 31, 67–73.

Grice, K., Audino, M., Boreham, C.J., Alexander, R., Kagi, R. (2001) Distributions and stable carbon isotopic compositions of biomarkers in torbanites from different palaeogeographical locations. Organic Geochemistry 32, 1195–1210.

Griebler, C., Safinowski, M., Vieth, A., Richnow, H.H., Meckenstock, R.U. (2004). Combined application of stable carbon isotope analysis and specific metabolites determination for assessing in situ degradation of aromatic hydrocarbons in a tar oil-contaminated aquifer. Environmental science and technology 38(2), 617–631.

Grotheer, H., Robert, A.M., Greenwood, P.F., Grice, K. (2015) Stability and hydrogenation of polycyclic aromatic hydrocarbons during hydropyrolysis (HyPy) — Relevance for high maturity organic matter. Organic Geochemistry 86, 45–54.

Guo, X., Liu, K., He, S., Song, G., Wang, Y., Hao, X., Wang, B. (2012) Petroleum generation and charge history of the northern Dongying Depression, Bohai Bay Basin, China: Insight from integrated fluid inclusion analysis and basin modelling. Marine and Petroleum Geology 32, 21–35.

Guthrie, J.M., Rooney, M.A., Chung, H.M. and Unomah, G. (2000) The effects of biodegradation versus recharging on the composition of oils, offshore Nigeria.

Presented at the Annual Meeting of the American Association of Petroleum Geologists. 16–19 April 2000, New Orleans, LA, US.

Gvirtzman, Z., Said-Ahmed, W., Ellis, G.S., Hill, R.J., Moldowan, J.M., Wei, Z.B., Amrani, A. (2015) Compound-specific sulfur isotope analysis of thiadiamondoids of oils from the Smackover Formation, USA. Geochimica et Cosmochimica Acta 167, 144–161.

H

Hao, F., Zhou, X.H., Zhu, Y.M., Zou, H.Y., Yang, Y.Y. (2010) Charging of oil fields surrounding the Shaleitian uplift from multiple source rock intervals and generative kitchens, Bohai Bay basin, China. Marine and Petroleum Geology 27, 1910–1926.

Hanson, A.D., Zhang, S., Moldowan, J.M. (2000) Molecular organic geochemistry of the Tarim Basin, Northwest China. American Association of Petroleum Geologists Bulletin 84, 1109–1128.

He, N.N., Grice, K., Greenwood, P.F. (2019) The distribution and δ^{34}S values of organic sulfur compounds in biodegraded oils from Peace River (Alberta Basin, western Canada). Organic Geochemistry 128, 16–25.

Head, I.M., Jones, D.M., Larter, S.R. (2003) Biological activity in the deep subsurface and the origin of heavy oil. Nature 426, 344–352.

Ho, T.Y., Rogers, M.A., Drushel, H.V., Koons, C.B. (1974) Evolution of sulfur compounds in crude oils. AAPG Bulletin 58, 2338–2348.

Hoefs, J. (1997) Stable Isotope Geochemistry. Springer-Verlag, New York.

Horsfield, B., Curry, D.J., Bohacs, K., Littke, R., Rullkötter, J., Schenk, H.J., Radke, M., Schaefer, R.G., Carroll, A.R., Isaksen, G. and Witte, E.G. (1994) Organic geochemistry of freshwater and alkaline lacustrine sediments in the Green River Formation of the Washakie Basin, Wyoming, USA. Organic Geochemistry 22(3-5), pp.415–440.

Hu, J., Xu, S., Tong, X., Wu, H. (1986) The Bohai bay basin. In: Zhu, X. (Ed.), Chinese Sedimentary Basins. Elsevier, Amsterdam, pp. 89–105.

Hu, S.B., O'Sullivan, P.B., Raza, A., Kohn, B.P. (2001) Thermal history and tectonic subsidence of the Bohai basin, northern China: a Cenozoic rifted and local pullapart basin. Physics of the Earth and Planetary Interiors 126, 221–235.

Huang, L., Sturchio, N.C., Abrajano, T., Heraty, L.J., Holt, B.D. (1999) Carbon and chlorine isotope fractionation of chlorinated aliphatic hydrocarbons by evaporation. Organic Geochemistry 30, 777–785.

Hunt T. S. (1863) Report on the Geology of Canada. Canadian Geological Survey report: Progress to 1863.

Hurtgen, M.T. (2012) The Marine Sulfur Cycle, Revisited. Science 337, 305–306.

Hwang, I.H., Youn, J.M., Doe, J.W., Park, T.S., Kang, H.K., Ha, J.H., Na, B.G. (2017) Study on the applicability analysis of HPLC for fuel marker (Unimark 1494DB) in petroleum products. Journal of the Korean Applied Science and Technology 34(4), 1076–1084.

I

Idiz, E.F., Tannenbaum, E., Kaplan, I.R. (1990) Pyrolysis of high-sulfur Monterey kerogens: Stable isotopes of sulfur, carbon, and hydrogen.

Izumi, Y., Ohshiro, T., Ogino, H., Hine, Y., Shimao, M. (1994) Selective Desulfurization of Dibenzothiophene by Rhodococcus erythropolisD-1. Physiology and Biotechnology 60, 223–226.

J

Jain, P.S., Bari, S.B. (2010) Isolation of lupeol, stigmasterol and campesterol from petroleum ether extract of woody stem of Wrightia tinctoria. Asian Journal of Plant Sciences 9(3), 163.

James, A.T., Burns, B.J. (1984) Microbial alteration of subsurface natural gas accumulations. American Association of Petroleum Geologists Bulletin 68, 957–960.

Javadli, R., de Klerk, A. (2012) Desulfurization of heavy oil. Applied Petrochemical Research 1, 3–19.

Jehlička, J., Urban, O., Pokorný, J. (2003) Raman spectroscopy of carbon and solid bitumens in sedimentary and metamorphic rocks. Spectrochimica Acta Part A 59, 2341–2352.

Ji, H., Li, S., Greenwood, P., Zhang, H., Pang, X., Xu, T., Shi, Q. (2018) Geochemical characteristics and significance of heteroatom compounds in lacustrine oils of the Dongpu Depression (Bohai Bay Basin, China) by negative-ion Fourier transform ion cyclotron resonance mass spectrometry. Marine and Petroleum Geology 97, 568–591.

Ji, Y., Zhou, S., Cheng, T. (2015) Application of sequence stratigraphy to subtle oil–gas reservoir exploration: take example of the third member Shahejie formation Dongpu Depression. Acta Geologica Sinica 89, 395–395.

Jia, W.L., Chen, S.S., Zhu, X.X., Peng, P.A., Xiao, Z.Y. (2017) D/H ratio analysis of pyrolysis-released *n*-alkanes from asphaltenes for correlating oils from different sources. Journal of Analytical and Applied Pyrolysis 126, 99–104.

Jiang, Y., Fang, L., Liu, J., Hu, H., Xu, T. (2016) Hydrocarbon charge history of the Paleocene reservoir in the northern Dongpu depression, Bohai Bay Basin, China. Petroleum Science 13, 625–641.

Johansen, N.G., Ettre, L.S., Miller, R.L. (1983) Quantitative analysis of hydrocarbons by structural group type in gasolines and distillates: I. Gas chromatography. Journal of Chromatography A 256, 393–417.

K

Kaplan, I. R. (1975) Stable isotopes as a guide to biogeochemical processes. Proceedings of the Royal Society of London, 189, 183–211.

Kaplan, I.R. and Rittenberg, S.C. (1964) Microbiological fractionation of sulphur isotopes. Microbiology 34, 195–212.

Ke, C.W., Li, S.M., He, N.N., Grice, K., Zhang, H.A., Xu, T.W., Zhang, Y.X., Greenwood, P. (2020) Compound specific sulfur isotopes of saline lacustrine oils from the Dongpu Depression, Bohai Bay Basin, NE China. Journal of Asian Earth Sciences, 104361.

Kennicutt, M.C. (1988) The effect of biodegradation on crude oil bulk and molecular composition. Oil and Chemical Pollution 4, 89–112.

Kim, D., Jin, J.M., Cho, Y., Kim, E.H., Cheong, H.K., Kim, Y.H., Kim, S. (2015) Combination of ring type HPLC separation, ultrahigh-resolution mass spectrometry, and high field NMR for comprehensive characterization of crude oil compositions. Fuel 157, 48–55.

Kinnaman, F.S., Valentine, D.L., Tyler, S.C. (2007) Carbon and hydrogen isotope fractionation associated with the aerobic microbial oxidation of methane, ethane, propane and butane. Geochimica et Cosmochimica Acta 71, 271–283.

Kirimura, K., Furuya, T., Nishii, Y. (2001) Biodesulfurization of dibenzothiophene and its derivatives through the selective cleavage of carbon-sulfur bonds by a moderately thermophilic bacterim Bacillus subtilis WU-S2B. Journal of Bioscience and Bioengineering, 91, 262–266.

Kohnen, M.E.L., Damste, J.S.S., van Dalen, A.C.K., Haven, H.L.T., Rullkotter, J., De Leeuw, J.W. (1990) Origin and diagenetic transformations of C_{25} and C_{30} highly branched isoprenoid sulphur compounds: Further evidence for the formation of organically bound sulphur during early diagenesis. Geochimica et Cosmochimica Acta 54, 3053–3063.

Kok, M.D., Schouten, S., Sinninghe Damste, J.S. (2000) Formation of insoluble, nonhydrolyzable, sulfur-rich macromolecules via incorporation of inorganic sulfur species into algal carbohydrates. Geochimica et Cosmochimica Acta 64, 2689–2699.

Kouketsu, Y., Mizukami, T., Mori, H., Endo, S., Aoya, M., Hara, H., Nakamura, D., Wallis, S. (2014) A new approach to develop the Raman carbonaceous material geothermometer for low-grade metamorphism using peak width. Island Arc 23, 33–50.

Krein, E.B. (1993) Organic sulfur in the geosphere: analysis, structure and chemical processes. See Patai & Rappoport 1993, pp. 975–1032.

Kropp, K.G., Gonçalves, J.A., Andersson, J.T., Fedorak, P.M. (1994a) Bacterial transformations of benzothiophene and methylbenzothiophenes. Environmental Science and Technology 28, 1348–1356.

Kropp, K.G., Gonçalves, J.A., Andersson, J.T., Fedorak, P.M. (1994b) Microbially mediated formation of benzonaphthothiophenes from benzo[*b*]thiophenes. Applied and Environmental Microbiology 60, 3624–3631.

Kropp, K.G., Saftić, S., Andersson, J.T., Fedorak, P.M. (1996) Transformations of six isomers of dimethylbenzothiophene by three *Pseudomonas* strains. Biodegradation 7, 203–221.

Kropp, K.G., Andersson, J.T., Fedorak, P.M. (1997) Bacterial transformations of naphthothiophenes. Applied and Environmental Microbiology 63, 3463–3473.

Krouse, H.R., Viau, C.A., Eliuk, L.S., Ueda, A., Halas, S. (1988) Chemical and isotopic evidence of thermochemical sulphate reduction by light hydrocarbon gases in deep carbonate reservoirs. Nature 333, 415–419.

Kuo, L. C. (1994) Lower Cretaceous lacustrine source rocks in northern Gabon: Effect of organic facies and thermal maturity on crude oil quality. Organic Geochemistry 22(2), 257–273.

Kvalheim, O.M., Christy, A.A., Telnaes, N., Bjørseth, A. (1987) Maturity determination of organic matter in coals using the methylphenanthrene distribution. Geochimica et cosmochimica Acta 51, 1883–1888.

L

Lafargue, E., Marquis, F. and Pillot, D. (1998) Rock-Eval 6 applications in hydrocarbon exploration, production, and soil contamination studies. Revue de l'Insitut Francais du Petrole 53, 421–437.

Larter, S. R. and Horsreld, B. (1993) Determination of structural components of kerogens by the use of analytical pyrolysis methods. In Organic Geochemistry, eds. M. H. Engel and S. A. Macko, pp. 271–288. Plenum Press, NY.

Larter, S., Wilhelms, A., Head, I., Koopmans, M., Aplin, A., di Primio, R., Zwach, C., Erdmann, M., Telnaes, N. (2003) The controls on the composition of biodegraded oils in the deep subsurface – Part 1: Biodegradation rates in petroleum reservoirs. Organic Geochemistry 34, 601–613.

Larter, S., Adams, J., Gates, I.D., Bennett, B., Huang, H. (2008) The origin, prediction and impact of oil viscosity heterogeneity on the production characteristics of tar sand and heavy oil reservoirs. Journal of Canadian Petroleum Technology 47, 52–61.

Larter, S., Huang, H., Adams, J., Bennett, B., Snowdon, L.R. (2012) A practical biodegradation scale for use in reservoir geochemical studies of biodegraded oils. Organic Geochemistry 45, 66–76.

Lawrence, B.M. (1968) The use of silver nitrate impregnated silica gel layers in the separation of monoterpene hydrocarbons. Journal of Chromatography 38, 535–537.

Leenheer, M.J. (1984) Mississippian Bakken and equivalent formations as source rocks in the Western Canadian Basin. Organic Geochemistry 6, 521–532.

Li, J., Zhang, J., Liu, S., Fan, Z., Xue, H., Sun, Z., Yu, T. (2016) Sedimentology and sequence stratigraphy of the Paleogene lower second member of the Shahejie Formation, W79 Block, Wenliu Oilfield, Bohai Bay Basin, China. Russian Geology and Geophysics 57, 944-957.

Li, Q.Q., Liu, P. (2017) The formation and distribution of heavy oil in the area of Luojia Kenxi, Bonan Sag. Journal of Xi'an Petroleum University (Natural Science Edition) 32, doi: 10.3969 /j.issn.1673-064X.2017.04.006 (in Chinese).

Li, S.M., Pang, X.Q., Jin, Z.J., Yang, H.J., Xiao, Z.Y., Gu, Q.Y., Zhang, B.S. (2010) Petroleum source in the Tazhong Uplift, Tarim Basin: New insights from geochemical and fluid inclusion data. Organic Geochemistry 41, 531–553.

Li, S., Pang, X., Yang, H., Xiao, Z., Gu, Q., Zhang, W. (2010) Geochemical characteristics and families of the crude oils in the Yingmaili Oilfield, Tarim Basin. Geoscience 24(4), 643–653 (In Chinese).

Li, S., Amrani, A., Pang, X., Yang, H., Said-Ahmad, W., Zhang, B. and Pang, Q. (2015) Origin and quantitative source assessment of deep oils in the Tazhong Uplift, Tarim Basin. Organic Geochemistry 78, pp.1–22.

Li, X., Zhang, J., Xie, J., Li, C., Dai, Y., Li, W., Li, S. (2015) Sedimentary and sequence-stratigraphic characteristics of the lower second submember, Shahejie formation, M1 block, Wenmingzhai oilfield, Dongpu depression, China. Arabian Journal of Geosciences 8, 5397–5406.

Liberti, A., Cartoni, G.P. and Bruner, F. (1965) Isotope effect in gas chromatography. In: Gas Chromatography 1964 (A. Goldup, et.), Elsevier, Amsterdam, pp. 301–312.

Liu, L., Ren, Z. (2007) Thermal evolution of Dongpu sag. Petroleum Exploration and Development 4, 419-423 (in Chinese).

Lockhart, R.S., Berwick,L.J., Greenwood, P.F., Grice, K., Kraal, P., Bush, R. (2013) Analytical pyrolysis for determining the molecular composition of contemporary monosulfidic black ooze. Journal of Analytical and Applied Pyrolysis 104, 640–652.

López García, C., Becchi, M., Grenier-Loustalot, M.F., Païsse, O., Szymanski, R. (2002) Analysis of aromatic sulfur compounds in gas oils using GC with sulfur chemiluminescence detection and high-resolution MS. Analytical Chemistry 74, 3849–3857.

Love, G.D., Snape, C.E., Carr, A.D., Houghton, R.C. (1995) Release of covalently-bound alkane biomarkers in high yields from kerogen via catalytic hydropyrolysis. Organic Geochemistry 23, 981–986.

Love, G.D., Stalvies, C., Grosjean, E., Meredith, W. (2008) Analysis of molecular biomarkers covalently bound within Neoproterozoic sedimentary kerogen. The paleontological Society Papers 14, 67–83.

Lu, H., Greenwood, P., Chen, T., Liu, J., Peng, P.A. (2011) The role of metal sulfates in thermochemical sulfate reduction (TSR) of hydrocarbons: Insight from the yields and stable carbon isotopes of gas products. Organic geochemistry, 42(6), 700–706.

M

Maher, T.P. (1966) Semi-quantitative analysis of hydrocarbon mixtures by gas chromatography without complete separation of components. Journal of Chromatographic Science 4, 355–362.

Marcano, N., Larter, S., Mayer, B. (2013) The impact of severe biodegradation on the molecular and stable (C, H, N, S) isotopic compositions of oils in the Alberta Basin, Canada. Organic Geochemistry 59, 114–132.

Mackenzie, A.S., Hoffmann, C.F., Maxwell, J.R. (1981) Molecular parameters of maturation in the Toarcian shales Paris Basin, France – III. Changes in aromatic steroid hydrocarbons. Geochimica et Cosmochimica Acta 45, 1345–1355.

Marshak, S. (2015) Earth: Portrait of a Planet, 3rd Ed. New York, NY, U.S.A, W.W. Norton & Company.

Maslen, E., Grice, K., Le Metayer, P., Dawson, D., Edwards, D. (2011) Stable carbon isotopic compositions of individual aromatic hydrocarbons as source and age indicators in oils from western Australian basins. Organic Geochemistry 42, 387–398.

Masterson, W.D., Dzou, L.I.P., Holba, A.G., Fincannon, A.L., Ellis, L. (2001) Evidence for biodegradation and evaporative fractionation in West Sak, Kuparuk and Prudhoe Bay field areas, North Slope, Alaska. Organic Geochemistry 32, 411–441.

Méhay, S., Adam, P., Kowalewski, I., Albrecht, P. (2009) Evaluating the sulfur isotopic composition of biodegraded petroleum: The case of the Western Canada Sedimentary Basin. Organic Geochemistry 40, 531–545.

Meredith, W., Russell, C.A., Cooper, M., Snape, C.E., Love, G.D., Fabbri, D., Vane, C.H. (2004) Trapping hydropyrolysates on silica and their subsequent thermal desorption to facilitate rapid fingerprinting by GC-MS. Organic Geochemistry 35, 73–89.

McNamara, J., Thode, H.G. (1950) Comparison of the isotope constitution of terrestrial and meteoritic sulfur. Physical Review Journals 78, 307–308.

Meyers, P. A. (1994) Preservation of elemental and isotopic source identification of sedimentary organic matter. Chemical Geology 144, 289–302.

Michaelis, W., Seifert, R., Nauhaus, K., et al. (2002) Microbial reefs in the Black Sea fueled by anaerobic oxidation of methane. Science 297, 1013–1015.

Mirasol-Robert, A., Grotheer, H., Bourdet, J., Suvorova, A., Grice, K., McCuaig, T.C., Greenwood, P.F. (2017) Evidence and origin of the different types of sedimentary organic matter and its implications on Paleoproterozoic orogenic gold mineralisation Precambrian Research) 299, 319–338.

Moldowan, J.M., Seifert, W.K., Gallegos, E.J. (1983) Identification of an extended series of tricyclic terpanes in petroleum. Geochimica et Cosmochimica Acta 47, 1531–1534.

Moldowan, J.M., Seifert, W.K., Gallegos, E.J. (1985) Relationship between petroleum composition and depositional environment of petroleum source rocks. American Association of Petroleum Geologists Bulletin 69, 1255–1268.

Moldowan, J.M., Lee, C.Y., Sundararaman, P. (1992) Source correlation and maturity assessment of select oils and rocks from the Central Adriatic Basin (Italy and Yugoslavia). In: Moldowan, J.M., Albrecht, P., Philp, R.P. (Eds), Biological Markers in Sediments and Petroleum, Prentice Hall, Englewood Cliffs, New Jersey pp. 370–401.

Moustafa, N.E., Anderson, J.T. (2011) Analysis of polycyclic aromatic sulfur heterocycles in Egyptian petroleum condensate and volatile oils by gas chromatography with atomic emission detection. Fuel Processing Technology 92, 547–555.

Murray, A.P., Summons, R.E., Boreham, C.J., Dowling, L.M. (1944) Biomarker and n-alkane isotope profiles for Tertiary oils: Relationship to source rock depositional setting. Organic Geochemistry 22, 521–542.

N

Nelson, B.C., Eglinton, T.I., Seewald, J.S., Vairavamurthy, M.A., Miknis, F.P. (1995) Transformations in organic sulfur speciation duringmaturation ofmonetary shale: Constraints from laboratory experiments. ACS Symposium Series 612, 138–166.

O

Orr, W.L. (1974) Changes in sulfur content and isotopic ratios of sulfur during petroleum maturation: Study of Big Horn Basin Paleozoic oils. AAPG Bulletin 58, 2295–2318.

Orr, W.L. (1977) Geologic and geochemical controls on the distribution of hydrogen sulfide in natural gas. In Advances in Organic Geochemistry 1975, ed. R Campos and J Goni, Oxford, UK, pp. 571–597.

Orr, W.L. (1986) Kerogen/asphaltene/sulfur relationships in sulfur-rich Monterey oils. Organic Geochemistry 10, 499–516.

Orr, W.L. and Sinninghe Damste, J.S.S. (1990) Geochemistry of Sulfur in Petroleum Systems. ACS Symposium Series 429, 2–29.

O'Sullivan, G. and Kalin, R.M. (2008) Investigation of the range of carbon and hydrogen isotopes within a global set of gasolines. Environmental Forensics 9, pp. 166–176.

P

Pallasser, R.J. (2000) Recognizing biodegradation in gas/oil accumulations through the $\delta^{13}C$ compositions of gas components. Organic Geochemistry 31, 1363–1373.

Palmer, S.E. (1984) Effect of water washing on $C_{15}+$ hydrocarbon fraction of crude oils from northwest Palawan, Phillipines. American Association of Petroleum Geologists Bulletin 68, 137–149.

Palmer, S.E. (1984) Hydrocarbon source potential of organic facies of the lacustrine Elko Formation (Eocene/Oligocene), Northeast Nevada. In: Hydrocarbon Source Rocks of the Greater Rocky Mountain Region (J.Woodward, F. F. Meissner and J. L. Clayton, eds.), Rocky Mountain Association of Geologists, Denver, CO.

Palmer, S.E. (1993) Effect of biodegradation and water washing on crude oil composition. In: Engel, M.H., Macko, S.A. (Eds.), Organic Geochemistry: Principles and Applications. Plenum Press, New York, pp. 511–533.

Pan, C., Geng, A., Liao, Z., Xiong, Y., Fu, J., Sheng, G. (2002) Geochemical characterization of free versus asphaltene-sorbed hydrocarbons in crude oils: implications for migration-related compositional fractionations. Marine and Petroleum Geology 19(5), 619–632.

Pan, C., Liu, D. (2009) Molecular correlation of free oil, adsorbed oil and inclusion oil of reservoir rocks in the Tazhong uplift of the Tarim basin, China. Organic Geochemistry 40(3), 387–399.

Parker, P. L. (1964) The biogeochemistry of the stable isotopes of carbon in a marine bay. Geochimica et Cosmochimica Acta 28, 1155–1164.

Peng, J., Wu, X., He, X., Liu, Y. (2003) Oil and gas accumulating law in Machang area Dongpu Depression. Journal of Shandong University of Science and Technology (Natural Science) 22, 100–112 (in Chinese).

Peters, K.E. and Cassa, M.R. (1994) Applied source rock geochemistry. In: The Petroleum System—From Source to Trap (L. B. Magoon and W. G. Dow, eds.), American Association of Petroleum Geologists, Tulsa, OK, pp. 93–117.

Peters, K.E., Moldowan, J.M. (1991) Effects of source, thermal maturity, and biodegradation on the distribution and isomerization of homohopanes in petroleum. Organic Geochemistry 17, 47–61.

Peters, K.E., Walters, C.C., Moldowan, J.M. (2005) The Biomarker Guide. Biomarkers and Isotopes in Petroleum Systems and Earth History, vols. 1 and 2, Cambridge University Press, USA.

Pompeckj, J.F. (1901) Die Jura-Ablagerungen zwischen Regensburg und Regenstauf. Geologisches Jahrbuch 14, 139–220 (in German).

Pond, K.L., Huang, Y., Wang, Y., Kulpa, C.F. (2002) Hydrogen isotopic composition of individual *n*-alkanes as an intrinsic tracer for bioremediation and source identification of petroleum contamination. Environmental Science and Technology 36, 724–728.

Poole, F. G. and Claypool, G. E. (1984) Petroleum source-rock potential and crude-oil correlation in the Great Basin. In: Hydrocarbon Source Rocks of the Greater Rocky Mountain Region (J. Woodward, F. F. Meissner and J. L. Clayton, eds.), Rocky Mountain Association of Geologists, Denver, CO.

Postgate, J. (1984) Microbes, microbiology and the future of man. The Microbe II. Prokaryotes and Eukaryotes, 319–333.

Poulson, S.R., Drever, J.I. (1999) Stable isotope (C, Cl, and H) fractionation during vaporization of trichloroethelene. Environmental Science and Technology 33, 3689–3694.

Punanova, S.A., Vinogradova, T.L. (2016) Geochemical features of mature hydrocarbon systems and indicators of their recognition. Geochemistry International 54, 817–823.

Q

Qi, J., Yang, Q. (2010) Cenozoic structural deformation and dynamic processes of the Bohai Bay basin province, China. Marine and Petroleum Geology 27, 757–771.

R

Radke, M. and Welte, D.H. (1981) Advances in Organic Geochemistry. Wiley, Chichester, 1983, pp. 504–512.

Radke, M., Willsch, H., Leythaeuser, D., Teichmüller, M. (1982) Aromatic components of coal: Relation of distribution pattern to rank. Geochimica et Cosmochimica Acta 46, 1831–1848.

Radke M., Welte D.H. and Willsch H. (1986) Maturity parameters based on aromatic hydrocarbons: Influence of the organic matter type. Organic Geochemistry 10(1), 51–63.

Radke M. (1988) Application of aromatic compounds as maturity indicators in source rocks and crude oils. Marine and Petroleum Geology 5(3), 224–236.

Radke, M., Willsch, H. (1993) Generation of alkylbenzenes and benzo [*b*] thiophenes by artificial thermal maturation of sulfur-rich coal. Fuel 72, 1103–1108.

Radke, M., Vriend, S.P., Ramanampisoa, L.R. (2000) Alkyldibenzofurans in terrestrial rocks: influence of organic facies and maturation. Geochimica et Cosmochimica Acta 64, 275–286.

Raiswell, R. and Berner, R.A. (1985) Pyrite formation in euxinic and semi-euxinic sediments. American Journal of Science 285, 710–724.

Riboulleau, A., Derenne, S., Sarret, G., Largeau, C., Baudin, F., Connan, J. (2000) Pyrolytic and spectroscopic study of a sulphur-rich kerogen from the "Kashpir

oil shales" (Upper Jurassic, Russian platform). Organic Geochemistry 31, 1641–1661.

Rickard, D. and Luther, G.W. (2007) Chemistry of Iron Sulfides. Chemical Reviews 107, 514–562.

Robson, W.J., Sutton, P.A., McCormack, P., Chilcott, N.P., Rowland, S.J. (2017) Class type separation of the polar and apolar components of petroleum. Analytical chemistry 89(5), 2919–2927.

Rontani, J. F., Bosser-Joulak, F., Rambeloarisoa, E., Bertrand, J. C., Giusti, G., Faure, R. (1985) Analytical study of Asthart crude oil asphaltenes biodegradation. Chemosphere 14(9), 1413–1422.

Rosenberg, Y.O., Meshoulam, A., Said-Ahmad, W., Shawar, L., Dror, G., Reznik, I. J., Amrani, A. (2017) Study of thermal maturation processes of sulfur-rich source rock using compound specific sulfur isotope analysis. Organic Geochemistry 112, 59–74.

Rowland, S.J., Alexander, R., Kagi, R.I., Jones, D.M. (1986) Microbial degradation of aromatic components of crude oils: A comparison of laboratory and field observations. Organic Geochemistry 9, 153–161.

Russell, C. A., Snape, C. E., Meredith, W., Love, G. D., Clarke, E., Moffatt, B. (2004) The potential of bound biomarker profiles released via catalytic hydropyrolysis to reconstruct basin charging history for oils. Organic Geochemistry 35, 1441–1459.

S

Said-Ahmad, W. and Amrani, A. (2013) A sensitive method for the sulfur isotope analysis of dimethyl sulfide and dimethylsulfoniopropionate in seawater. Rapid Communications in Mass Spectrometry 27(24), 2789–2796.

Scalan, E. S., Smith, J. E. (1970) An improved measure of the odd-even predominance in the normal alkanes of sediment extracts and petroleum. Geochimica et Cosmochimica Acta 34, 611-620.

Schimmelmann, A., Lewan, M.D., Wintsch, R.P. (1999) D/H isotope ratios of kerogen, bitumen, oil, and water in hydrous pyrolysis of source rocks containing kerogen types I, II, IIS, and III. Geochimica et Cosmochimica Acta 63(22), 3751–3766.

Schimmelmann, A., Sessions, A.L., Boreham, C.J., Edwards, D.S., Logan, G.A., Summons, R.E. (2004) D/H ratios in terrestrially sourced petroleum systems. Organic Geochemistry 35(10), 1169–1195.

Schimmelmann, A., Sessions, A.L., Mastalerz, M. (2006) Hydrogen isotopic (D/H) composition of organic matter during diagenesis and thermal maturation. Annual review earth planetary science 34, 501–533.

Schoell, M. (1983) Genetic characteristics of natural gases. American Association of Petroleum Geologists Bulletin 67, 2225–2238.

Seewald, J.S. (2003) Organic-inorganic interactions in petroleum-producing sedimentary basins. Nature 426, 327–333.

Seifert, W.K. and Moldowan, J.M. (1981) Paleoreconstruction by biological markers. Geochimica et Cosmochimica Acta 45, 783–794.

Sessions, A.L., Sylva, S.P., Summons, R.E., Hayes, J.M. (2004) Isotopic exchange of carbon-bound hydrogen over geologic timescales. Geochimica et Cosmochimica Acta 68(7), 1545–1559.

Shawar, L., Said-Ahmad, W., Ellis, G. S., Amrani, A. (2020) Sulfur isotope composition of individual compounds in immature organic-rich rocks and

possible geochemical implications. Geochimica et Cosmochimica Acta 274, 20–44.

Shao X., Pang X., Li H., Hu T., Xu T., Xu Y., Li B. (2018) Pore network characteristics of lacustrine shales in the Dongpu Depression, Bohai Bay Basin, China, with implications for oil retention. Marine and Petroleum Geology 96, 457–473.

Shi, S., Chen, J., Zhu, L., Gao, L., Zhu, F. (2017) Biodegradation rates of dibenzothiophenes in oils: A case study from the Linpan oil field, Bohai Bay Basin, eastern China. Book of Abstracts, International Meeting of Organic Geochemistry 2017 (Florence, Italy, September 17–22).

Shin, W.J., Lee, K.S. (2010) Carbon isotope fractionation of benzene and toluene by progressive evaporation. Rapid Communications in Mass Spectrometry 24, 1636–1640.

Silliman, J.E., Meyers, P.A. and Bourbonniere, R.A. (1996) Record of postglacial organic matter delivery and burial in sediments of Lake Ontario. Organic Geochemistry 24, 463–472.

Silva, T. F., Azevedo, D. A., Rangel, M. D., Fontes, R. A., Neto, F. R. A. (2008) Effect of biodegradation on biomarkers released from asphaltenes. Organic geochemistry 39(8), 1249–1257.

Sim, M.S., Ono, S., Donovan, K., Templer, S.P., Bosak, T. (2011) Effect of electron donors on the fractionation of sulfur isotopes by a marine Desulfovibrio sp., Geochimica et Cosmochimica Acta 75, 4244–4259.

Sinninghe Damste, J.S., De Leeuw, J.W. (1990) Analysis, structure and geochemical significance of organically-bound sulphur in the geosphere: State of the art and future research. Organic Geochemistry 16, 1077–1101.

Snape, C.E., Lafferty, C.J., Eglinton, G., Robinson, N., Collier, R. (1994) The potential of hydropyrolysis as a route for coal liquefaction. International Journal of Energy Research 18, 233–242.

Solanas, A.M., Pares, R. (1984) Degradation of aromatic petroleum hydrocarbons by pure microbial cultures. Chemosphere 13, 593–601.

Sripada, K., Andersson, J.T. (2005) Liquid chromatographic properties of aromatic sulfur heterocycles on a Pd(II)-containing stationary phase for petroleum analysis. Analytical and Bioanalytical Chemistry 382, 735–741.

Stach, E., Mackowsky, M.T., Teichmuller, M., et al. (1982) Coal Petrology. Gebruder Borntraeger, Berlin.

Stadnitskaia, A., Ivanov, M.K., Blinova, V., Kreulen, R., van Weering, T.C.E. (2006) Molecular and carbon isotopic variability of hydrocarbon gases from mud volcanoes in the Gulf of Cadiz, NE Atlantic. Marine and Petroleum Geology 23, 281–296.

Stinnett, J. W. (1982) The deep earth gas hypothesis: Big on promises, but evidence looks thin. Synergy 2, 12–20.

Sun, J., Zhang, S.Q., Wei, C.G., Sun, Y.T., Liu, J.H. (2006) Study on the formation, migration and accumulation of hydrogen sulfide in Luojia Oilfield. West-China Exploration Engineering, 123, 81–83.

Sun, Y., Xu, S., Lu, H., Cai, P. (2003) Source facies of the Paleozoic petroleum systems in the Tabei uplift, Tarim Basin, NW China: Implications from aryl isoprenoids in crude oils. Organic Geochemistry 34, 629–634.

Sun, Y.G., Chen, Z.Y., Xu, S.P., Cai, P.X. (2005) Stable carbon and hydrogen isotopic fractionation of individual *n*-alkanes accompanying biodegradation: Evidence from a group of progressively biodegraded oils. Organic Geochemistry 36, 225–238.

T

Taylor, G.H., Teichm¨uller, M., Davis, A., et al. (1998) Organic Petrology. Gebruder Borntraeger, Berlin.

Thode, H.G., Munster, J. (1970) Sulfur isotope abundances and genetic relations of oil accumulations in Middle East Basin. The American Association of Petroleum Geologists Bulletin 54, 627–637.

Thode, H.G. (1981) Sulfur isotope ratios in petroleum research and exploration: Walliston Basin. The American Association of Petroleum Geologists Bulletin 65, 1527–1537.

Tissot, B.P. and Welte, D.H. (1984) Petroleum Formation and Occurrence. Springer-Verlag, New York.

Tissot, B.P., Durand, B., Espitali´e, J. and Combaz, A. (1974) Influence of the nature and diagenesis of organic matter in formation of petroleum. American Association of Petroleum Geologists Bulletin 58, 499–506.

Treibs, A. (1936) Chlorophyll and hemin derivatives in organic mineral substances. Angewandte Chemie 49, 682–686.

Trolio, R., Grice, K., Fisher, S.J., Alexander, R., Kagi, R.I. (1999) Alkyl-biphenyls and alkyl-diphenylmethanes as indicators of petroleum biodegradation. Organic Geochemistry 30, 1241–1253.

V

van Aarssen, B.G.K., Bastow, T.P., Alexander, R., Kagi, R.I. (1999) Distributions of methylated naphthalenes in crude oils: Indicators of maturity, biodegradation and mixing. Organic Geochemistry 30, 1213–1227.

van Hale, R. and Frew, R.D. (2010) Rayleigh distillation equations applied to isotopic evolution of organic nitrogen across a continental shelf. Marine and Freshwater Research, 61(3), pp.369–378.

van Krevelen, D.W. (1961) Coal. Elsevier, New York.

Volkman, J.K., Alexander, R., Kagi, R.I., Rowland, S.J., Sheppard, P.N. (1984) Biodegradation of aromatic hydrocarbons in crude oils from the Barrow sub-basin of Western Australia. Organic Geochemistry 6, 619–632.

W

Waldo, G.S., Carlson, R.M., Moldowan, J.M., Peters, K.E., Penner-Hahn, J.E. (1991) Sulfur speciation in heavy petroleums: Information from X-ray absorption near-edge structure. Geochimica et Cosmochimica Acta 55, 801–814.

Walters, C.C., Qian, K., Wu, C., Mennito, A.S., Wei, Z. (2011) Proto-solid bitumen in petroleum altered by thermochemical sulfate reduction. Organic Geochemistry, 42, 999–1006.

Wang, G.L., Wang, T.G., Simoneit, B.R.T., Zhang, L.Y., Zhang, X.J. (2010) Sulfur rich petroleum derived from lacustrine carbonate source rocks in Bohai Bay Basin, East China. Organic Geochemistry 41, 340–354.

Wang, G.L., Wang, T.G., Simoneit, B.R.T., Zhang, L. (2013) Investigation of hydrocarbon biodegradation from a downhole profile in Bohai Bay Basin: Implications for the origin of 25-norhopanes. Organic Geochemistry 55, 72–84.

Wang, G., Xue, Y., Wang, D., Shi, S., Grice, K. and Greenwood, P.F. (2016) Biodegradation and water washing within a series of petroleum reservoirs of the Panyu Oil Field. Organic geochemistry 96, 65–76.

Wang, L., Huang, Y.S. (2001) Hydrogen isotope fractionation of low molecular weight n-alkanes during progressive vaporization. Organic Geochemistry 32, 991–998.

Wang, M., Zhao, S.Q., Chung, K.H., Xu, C.M., Shi, Q. (2014) Approach for selective separation of thiophenic and sulfidic sulfur compounds from petroleum by methylation/demethylation. Analytical Chemistry 87, 1083–1088.

Wang, M., Sherwood, N., Li, Z.S., Lu, S.F., Wang, W.G., Huang, A.L., Peng, J., Lu, K. (2015) Shale oil occurring between salt intervals in the Dongpu Depression, Bohai Bay Basin, China. International Journal of Coal Geology 152, 100–112.

Waseda, A. and Iwano, H. (2008) Characterization of natural gases in Japan based on molecular and carbon isotope compositions. Geofluids 8, 286–292.

Wei, Z., Moldowan, J.M., Fago, F., Dahl, J.E., Cai, C., Peters, K.E. (2007) Origins of thiadiamondoids and diamondoidthiols in petroleum. Energy Fuels 21, 3431–3436.

Wei, Z., Walters, C.C., Moldowan, J.M., Mankiewicz, P.J., Pottorf, R.J., et al. (2012) Thiadiamondoids as proxies for the extent of thermochemical sulfate reduction. Organic Geochemistry 44, 53–70.

Wenger, L.M., Davis, C.L., Isaksen, G.H. (2002) Multiple controls on petroleum biodegradation and impact on oil quality. SPE Reservoir Evaluation and Engineering 5, 375–383.

Werne, J.P., Lyons, T., Hollander, D.J., Formolo, M.J., Sinninghe-Damsté, J.S. (2003) Reduced sulfur in euxinic sediments of the Cariaco Basin: sulfur isotope constraints on organic sulfur formation. Chemical Geology 195, 159–179.

Werne, J.P., Hollander, D.J., Lyons, T., Sinninghe-Damsté, J.S. (2004) Organic sulfur biogeochemistry: recent advances and future research directions. In: Amend, J.P., Edwards, K.J., Lyons, T. (Eds.), Sulfur Biogeochemistry: Past and Present. The Geological Society of America Special Papers, Boulder, CO. Vol. 379, pp. 135–150.

Werne, J.P., Lyons, T.W., Hollander, D.J., Schouten, S., Hopmans, E.C., Sinninghe Damste, J.S. (2008) Investigating pathways of diagenetic organic matter sulfurization using compound-specific sulfur isotope analysis. Geochimica et Cosmochimica Acta 72, 3489–3502.

Werner, R.A., Brand, W.A. (2001) Referencing strategies and techniques in stable isotope ratio analysis. Rapid Communications in Mass Spectrometry 15, 501–519.

Whiteman, J.P., Smith, E.A.E., Besser, A.C., Newsome, S.D. (2019) Diversity, 11, 8.

Wilkes, H., Vieth, A., Elias, R. (2008) Constraints on the quantitative assessment of in-reservoir biodegradation using compound-specific stable carbon isotopes. Organic Geochemistry 39, 1215–1221.

Woese, C.R., Magrum, L.J. and Fox, G.E. (1978) Archaebacteria. Journal of Molecular Evolution, 11, 245–252.

Worden, R.H., Smalley, P.C. (1996) H2S-producing reactions in deep carbonate gas reservoirs: Khuff Formation, Abu Dhabi. Chemical Geology 133, 157–171.

Worden, R.H., Cai, C.F. (2006) Geochemical characteristics of the Zhaolanzhuang sour gas accumulation and thermochemical sulfate reduction in the Jinxian Sag of Bohai Bay Basin by Zhang et al. Organic Geochemistry 36, 1717−1730.

Wu, L., Xu, H.M., Cheng, J.H. (2006) Evolution of sedimentary system and analysis of sedimentary source in Paleogene of the Bozhong Sag, Bohai bay. Marine Geology and Quaternary Geology 26, 81–88 (in Chinese with English abstract).

Wu, G.H., Li. H.H., Zhang, L., Wang, C.L., Bo, Z. (2012) Reservoir-forming conditions of Ordovician weathering crust in the Maigaiti slope, Tarim Basin, NW China. Petroleum Exploration and Development 39(2), 155–164.

X

Xiao, Q., Sun, Y.G., Zhang, Y.D., Chai, P.X. (2012) Stable carbon isotope fractionation of individual light hydrocarbons in the C_6–C_8 range in crude oil as induced by natural evaporation: Experimental results and geological implications. Organic Geochemistry 50, 44–56.

Xue, C., Chi, G., Li, Z., Dong, X. (2014) Geology, geochemistry and genesis of the Cretaceous and Paleocene sandstone-and conglomerate-hosted Uragen Zn-Pb deposit, Xinjiang, China: A review. Ore Geology Reviews 63, 328–342.

Y

Yeh, H.W., Epstein, S. (1981) Hydrogen and carbon isotopes of petroleum and related organic matter. Geochimica et Cosmochimica Acta 45, 753–762.

Yu, S., Pan, C., Wang, J., Jin, X., Jiang, L., Liu, D., Lv, X.X., Qin, J.Z., Qian, Y.X., Ding, Y., Chen, H. (2011) Molecular correlation of crude oils and oil

components from reservoir rocks in the Tazhong and Tabei uplifts of the Tarim Basin, China. Organic Geochemistry 42(10), 1241–1262.

Z

Zhang, H., Li, S., Xu, T., Pang, X., Zhang, Y., Wan, Z., Ji, H. (2017) Characteristics and formation mechanism for the saline lacustrine oil from the north Dongpu sag. Geoscience 31, 768–778 (in Chinese).

Zhang, K., Qi, J., Zhao, Y., Chen, S. (2007) Structure and evolution of cenozoic in Dongpu sag. Xinjiang Petroleum Geology 28, 714–717 (in Chinese).

Zhang, S., Hanson, A.D., Moldowan, J.M., Graham, S.A., Liang, D.G., Chang, E., Fago, F. (2000a) Paleozoic oil-source rock correlations in the Tarim Basin, NW China. Organic Geochemistry 31, 273–286.

Zhang, S., Zhang, B., Wang, F., Liang, D., He, Z. (2000b) Middle–Upper Ordovician: The main source of the oils in the Tarim Basin. Marine Oil and Gas Geology 5, 16–22 (in Chinese).

Zhang, S., Liang, D., Li, M., Xiao, Z., He, Z. (2002) (Molecular fossils and oil-source rock correlations in Tarim Basin, NW China). Chinese Science Bulletin 47 (Suppl.), 16–23 (in Chinese).

Zhang, S. and Huang, H. (2005) Geochemistry of Palaeozoic marine petroleum from the Tarim Basin, NW China: Part 1. Oil family classification. Organic Geochemistry 36, 1204–1214.

Zhang, S., Huang, H., Xiao, Z., Liang, D. (2005) Geochemistry of Palaeozoic marine petroleum from the Tarim Basin, NW China. Part 2: Maturity assessment. Organic Geochemistry 36, 1215–1225.

Zhang, S.C., Zhu, G.Y., Liang, Y.B., Dai, J.X., Liang, H.B., Li, M.W. (2005) Geochemical characteristics of the Zhaolanzhuang sour gas accumulation and thermochemical sulfate reduction in the Jixian Sag of Bohai Bay Basin. Organic Geochemistry 36, 1717–1730.

Zhang, S.C., Zhu, G.Y., Dai, J.X., Liang, Y.B., Li, M.W., Liang, H.B. (2006) Comments by Worden and Cai (2006) on Zhang et al. (2005) [Organic Geochemistry 36, 1717−1730]. Organi Geochemistry 37, 515–518.

Zhang, T., Amrani, A., Ellis, G.S., Ma, Q., Tang, Y. (2008) Experimental investigation on thermochemical sulfate reduction by H_2S initiation. Geochimica et Cosmochimica Acta 72, 3518–3530.

Zhang, L., Liu, Q., Zhu, R., Li, Z., Lu, X. (2009) Source rocks in Mesozoic−Cenozoic continental rift basins, east China: A case from Dongying Depression, Bohai Bay Basin. Organic Geochemistry 40, 229–242.

Zhang, S., Zhang, L., Bao, Y., Li, X., Liu, Q., Li, J., Yin, Y., Zhu, R., Zhang, S. (2012) Formation fluid characteristics and hydrocarbon accumulation in the Dongying sag, Shengli Oilfield. Petroleum Exploration and Development 39, 423–435.

Zhang, S.C., Huang, H.P., Su, J., Liu, M., Wang, X.M., Hua J. (2015) Geochemistry of Paleozoic marine petroleum from the Tarim Basin, NW China: Part 5. Effect of maturation, TSR and mixing on the occurrence and distribution of alkyldibenzothiophenes. Organic Geochemistry 86, 5–18.

Zheng, Y.F., Chen, J.F. (2000) Stable Isotope Geochemistry. Science Press, Beijing (in Chinese).

Zhu, G.Y., Zhang, S.C., Li, J., Jin, Q. (2004) Formation and distribution of natural gas with high content of hydrogen sulfide in China. Petroleum exploration and development 31, 18–21 (in Chinese).

Zhu, G.Y., Zhang, S.C., Liang, Y.B., Dai, J.X., Li, J. (2005) Isotopic evidence of TSR origin for natural gas bearing high H_2S contents within the Feixianguan Formation of the northeastern Sichuan Basin, southwestern China. Science in China Series D: Earth Sciences 48, 1960–1971.

Zhu, G., Zhang, S., Su, J., Zhang, B., Yang, H., Zhu, Y., Gu, L. (2013) Alteration and multi-stage accumulation of oil and gas in the Ordovician of the Tabei Uplift,

Tarim Basin, NW China: Implications for genetic origin of the diverse hydrocarbons. Marine and Petroleum Geology 46, 234–250.

Zhu, G.Y., Huang, H.P., Wang, H.T. (2015) Geochemical significance of discovery in Cambrian reservoirs at well ZS1 of the Tarim Basin, NW China. Energy Fuel 29, 1332–1344.

Zhu, G.Y., Wang, H.T., Weng, N. (2016) TSR-altered oil with high-abundance thiaadamantanes of a deep-buried cambrian gas condensate reservoir in Tarim Basin. Marine & Petroleum Geology 69, 1–12.

Zhu, G., Zhang, Y., Zhang, Z., Li, T., He, N., Grice, K., Greenwood, P. (2018) High abundance of alkylated diamondoids, thiadiamondoids and thioaromatics in recently discovered sulfur-rich LS2 condensate in the Tarim Basin. Organic Geochemistry 123, 136–143.

Appendix 1

Laboratory simulated biodegradation of a S-rich oil

Experimental

Soil and Oil Samples

The soil used in this study was provided by the soil science group at the University of Western Australia (UWA). The soil was originally collected from 0 to 10 cm depth at Mount Misery (South Australia). It had no known spill history and was characterized by low carbon (4.8%) and macronutrient values (0.007 g total N/kg soil; 0.014g P/kg soil; 0.21g K/kg soil). It was stored at 4 °C and sieved to 2 mm prior to microcosm incubation.

The S-rich ZS1C oil from the Tarim Basin (NW China) was used to treat the soils in these experiments. This oil was selected because of its rich distribution and high concentrations of organic sulfur compounds (OSCs). Previous characterisation of this oil (detailed in Chapters 2 and 5 of this thesis) showed it contained high concentrations of thioaromatic and thiadiamondoid compounds indicative of severe thermochemical sulfate reduction (TSR; Li et al., 2015). Prior to soil application the oil was stored in a glass container at 4 °C to minimize volatilization and microbial activity.

Microcosms and Incubation

Soil samples (90 g dry weight) were treated with ZS1C oil (50 mL/kg soil) in glass jars (385 mL). Control samples were also prepared without addition of oil. All samples were mixed with 100 mg/kg P (as $NaH_2PO_4 \cdot 2H_2O$), 100 mg/kg N (NH_4NO_3) and water (60% soil water holding capacity) to promote microbial activity. Samples were incubated in the

dark at 25 °C, and watered on a weekly basis to help maintain water holding capacity near 60% (Carter and Tibbett, 2008). Sub-samples of the treated soils (10 g) were collected for gas chromatography-mass spectrometry (GC-MS) analysis on days 30, 60 and 90. Duplicated treatments and analyses were conducted. This laboratory-approach has previously proved successful for hydrocarbon biodegradation studies of oils (e.g. Greenwood et al. 2008).

GC-MS Analyses

Extracts of the sub-samples were obtained with a mixture of DCM and methanol (v:v, 9:1) using a Milestone Start E microwave extraction unit (Milestone Inc., USA). The samples were heated from room temperature (~25 °C) to 80 °C over 10 minutes, then held at 80 °C for 15 minutes. Separate saturated and aromatic hydrocarbon fractions were isolated by column chromatography of the extracts on silica gel (pre-activated at 160 °C) with hexane and a mixture of hexane and DCM (v:v, 7:3), respectively. GC-MS analysis of the saturated and aromatic fractions was conducted with a HP 6890 GC coupled to a HP 5973 mass selective detector. The compounds were chromatographically separated on a DB-5 fused silica capillary column (60 m × 0.25 mm i.d. × 0.25 µm film thickness) with 1 mL/min helium carrier gas. The GC oven was temperature programmed from 40 °C to 325 °C at 3 °C/min then held isothermally at the final temperature for 45 min. Electron impact (70 eV) full scan (*m/z* 50–550) mass spectral data was acquired.

Results and Discussion

The alkyl-naphthalene and alkyl-DBT distributions of the fresh ZS1C oil (i.e. at commencement of microcosm experiment) and the recovered oil following 90 days of microcosm treatment are highlighted by the selected ion chromatograms shown in Error! Reference source not found.**-1**. The alkyl-naphthalenes were only marginally different

after 90 days of treatment to the original oil (**Error! Reference source not found.-1a**).

There was a very slight reduction in the methyl- and dimethyl-naphthalene abundances

relative to the higher molecular-weight (and more resistant) dimethyl-naphthalenes. This

indicates a very low degree of biodegradation, reflected by only minor decreases in alkyl-

naphthalene parameter values sensitive to biodegradation (Fisher et al., 1998; Greenwood

et al., 2008; Error! Reference source not found.**-1** and **Figure A1-2**).

(a)

(b)

(c)

(d)
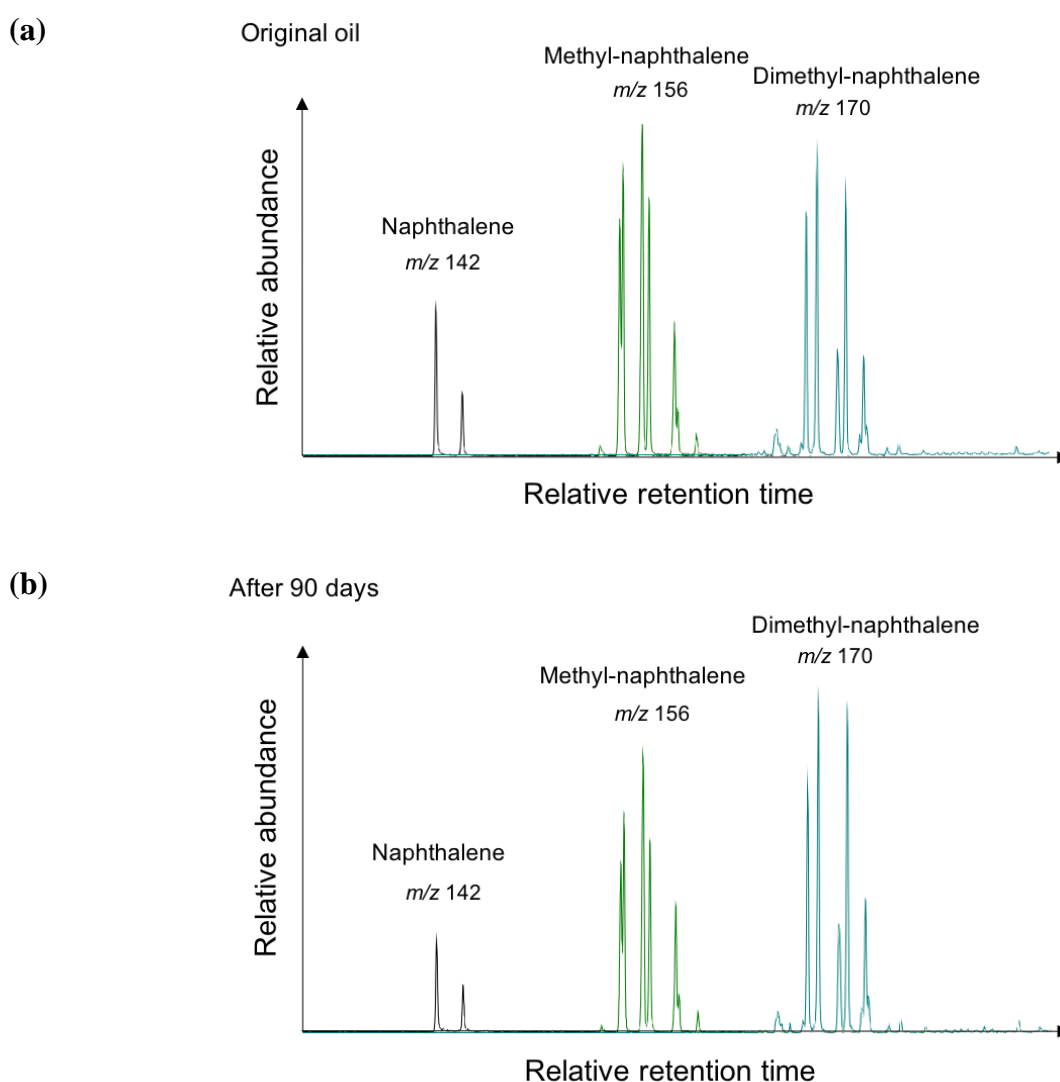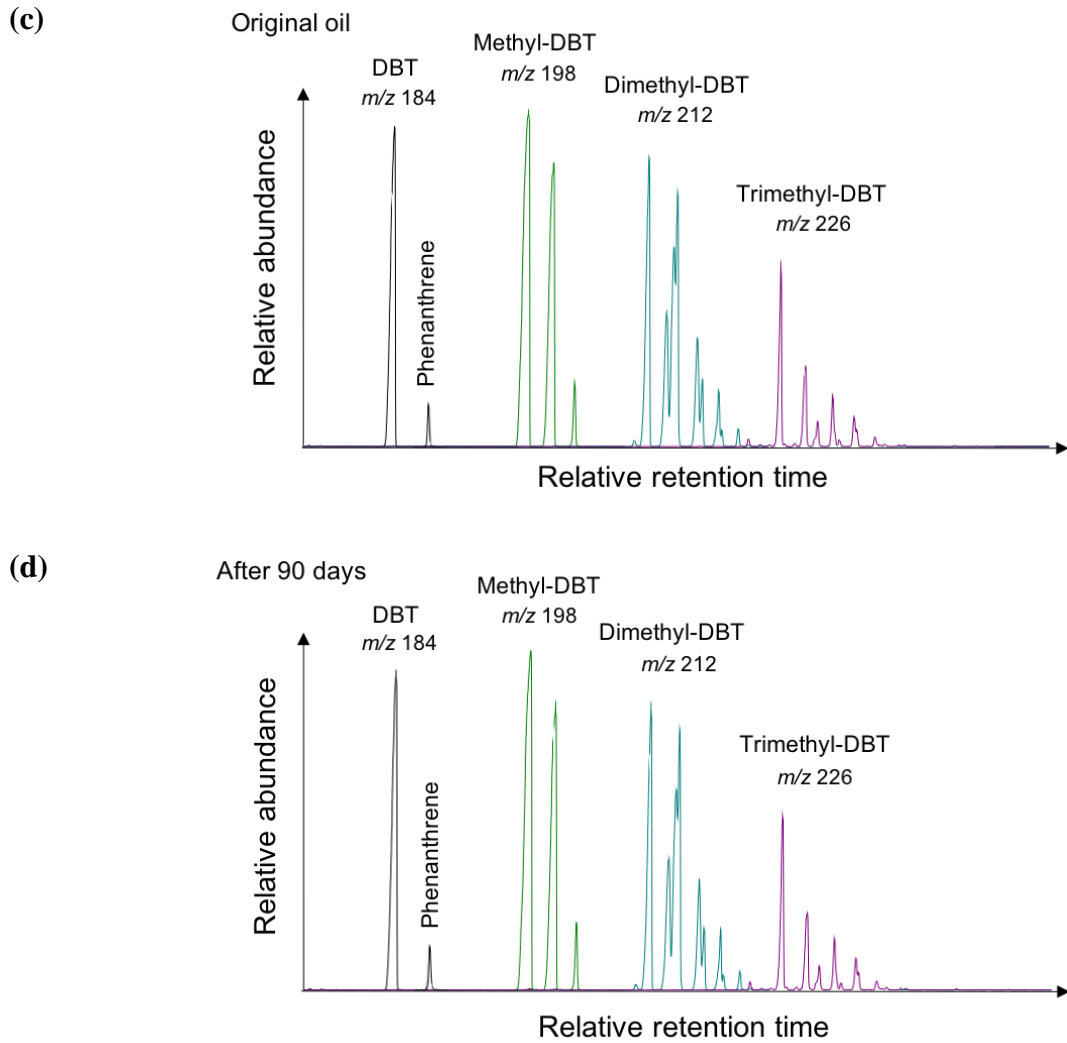
Figure A1-1. Partial selected ion chromatograms showing alkyl-naphthalene and alkyl-dibenzothiophene (DBT) distributions of original ZS1C oil (a and c) and soil extracted oil following 90 days treatment (b and d).
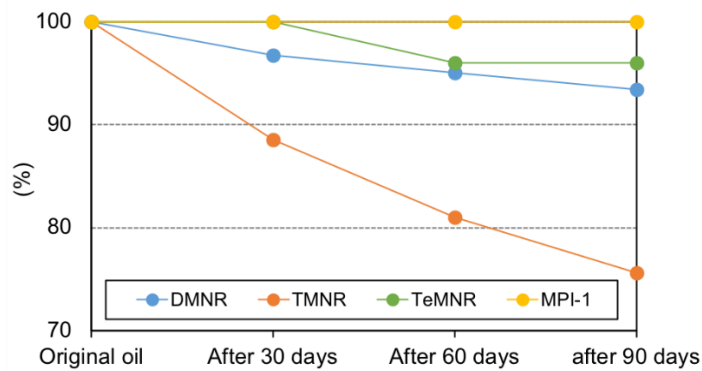
Figure A1-2. Temporal variations of biodegradation parameters. The parameters are plotted as % relative to their values in the original oil .

Table A1-1. Biodegradation sensitive parameters measured for the original oil and the soil recovered oils following 30, 60 and 90 days treatment.

Biodegradation parameters	Original oil	After 30 days	After 60 days	after 90 days
Dimethylnaphthalene ratio (DMNR) = 1,6-DMN/1,5-DMN	6.1	5.9	5.8	5.7
Trimethylnaphthalene ratio (TMNR) = 1,3,6-TMN/1,2,4-TMN	46.3	41	37.5	35
Tetramethylnaphthalene ratio (TeMNR) = 1,3,6,7-TeMN/1,3,5,7-TeMN	2.5	2.5	2.4	2.4
MPI-1 (Methylphenanthrene Index) = 1.5*(2-MP+3-MP)/(Phenan+1-MP+9-MP)	1.26	1.26	1.26	1.26

The alkyl-DBT distributions of the fresh oil (**Figure A1-1c**) and 90 day treated oil (**Figure A1-1**d) were essentially identical, reflecting no biodegradation of these OSCs over the duration of the microcosm experiments. Similarly, there was no change in the distribution of alkyl-phenanthrenes (similar sized/3-ringed hydrocarbons) indicated by consistent MPI-1 values (**Table A1-1**, **Figure A1-2**). The lack of any change in the 3 ringed DBTs (and alkyl-phenanthrenes) is not surprising given only a slight change was evident in the more vulnerable 2-ringed naphthalenes. The ZS1C oil contains low concentrations of alkyl-BTs, but none were detected from any of the soil treatments, probably due to their relatively high volatility.

References

Carter, D.O., Tibbett, M. (2008) Does repeated burial of skeletal muscle tissue (Ovis aries) in soil affect subsequent decomposition? Applied Soil Ecology 40, 529–535.

Fisher, S.J., Alexander, R., Kagi, R.I., Oliver, G.A. (1998) Aromatic hydrocarbons as indicators of biodegradation in north Western Australian reservoirs. In: Purcell, P.G. and Purcell, R. (Eds), Sedimentary Basins of Western Australia. West Australian Basins Symposium. Petroleum Exploration Society of Australia, Perth, Australia, pp. 185–194.

Greenwood, P.F., Wibrow, S., George, S.J., Tibbett, M. (2008) Sequential hydrocarbon biodegradation in a soil from arid coastal Australia, treated with oil under laboratory controlled conditions. Organic Geochemistry 39, 1336–1346.

Li, S.M., Amrani, A., Pang, X.Q., Yang, H.J., Said-Ahmad, W., Zhang, B.S., Pang, Q.J. (2015) Origin and quantitative source assessment of deep oils in the Tazhong Uplift, Tarim Basin. Organic Geochemistry 78, 1-22.
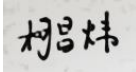
Appendix 2

PERMISSION TO USE COPYRIGHT MATERIAL AS SPECIFIED BELOW:

Changwei Ke, Sumei Li, Hongan Zhang, Nannan He, Kliti Grice, Tianwu Xu, Paul Greenwood. (2020) Compound specific sulfur isotopes of saline lacustrine oils from the Dongpu Depression, Bohai Bay Basin, NE China. Journal of Asian Earth Sciences, 104361.

I hereby give permission for **Nannan He** to include the abovementioned material(s) in her higher degree thesis for Curtin University, and to communicate this material via the institutional repository. This permission is granted on a non-exclusive basis and for an indefinite period.

I confirm that I am the copyright owner of the specified material.

Signed: 柯昌炜

Name: Changwei Ke

Position: PhD Student of China University of Petroleum-Beijing

Date: 1st March 2020

Compound specific sulfur isotopes of saline lacustrine oils from the Dongpu Depression, Bohai Bay Basin, China

Changwei Ke[a], Sumei Li[a,*], Hongan Zhang[b], Nannan He[c], Kliti Grice[c], Tianwu Xu[b], Paul Greenwood[c, d]

[a] State Key Laboratory of Petroleum Resources and Prospecting, China University of Petroleum (Beijing), Beijing, China

[b] SINOPEC Zhongyuan Oilfield Company, Puyang, He'nan, China

[c] Department of Earth and Planetary Sciences, Curtin University, Perth, Australia

[d] School of Earth Sciences, University of Western Australia, Perth, Australia

Abstract: Lacustrine oils from type I-II kerogen from the Dongpu Depression of Bohai Bay Basin have been characterised by compound specific sulfur isotope and hydrocarbon biomarker analyses. The sample suite included sixteen saline lacustrine oils from the northern part of the Dongpu Depression, most of which (i.e., all but two interbedded samples) could be separated into four tectonically aligned oil families (OF1-4) on the basis of differences in their hydrocarbon composition (e.g. high MW n-alkanes, isoprenoids, polycyclic terpenoids). The other two oils studied were freshwater lacustrine oils from the south of the Dongpu Depression, the hydrocarbon composition of which indicated a fifth oil family (OF5). The $\delta^{34}S$ values of organic sulfur compounds ($\delta^{34}S_{OSCs}$) in the oils showed several general differences consistent with the five hydrocarbon biomarker defined oil families, including the relative magnitude of their $\delta^{34}S$ values: Ave $\delta^{34}S_{OSCs}$ values: OF1 = 19‰ (relatively depleted

δ^{34}S); OF2= 28‰ (enriched δ^{34}S); OF3 = 24‰ (intermediate δ^{34}S); OF4 = 25‰ (intermediate δ^{34}S); and OF5 = 18‰ (depleted δ^{34}S); and the respective δ^{34}S$_{OSCs}$ profiles of the oils, e.g., the intermediate δ^{34}S values of the LT oils (OF3) showed little variance with alkylation (< 4‰ **Table 4.5**), whereas the intermediate δ^{34}S values of the higher maturity Wenliu oils (OF4) showed ^{34}S enriched alkylated DBTs compared to base DBT ($\Delta\delta^{34}$S$_{alkylDBT\text{-}DBT}$ = +7‰). This demonstrates the potential of δ^{34}S$_{OSC}$ data assisting the genetic correlation of S-rich saline lacustrine oils. However, separate correlations between some of the δ^{34}S$_{OSCs}$ data and hydrocarbon indicators of paleo-environmental (C$_{35}$-/C$_{34}$-hopanes), thermal maturity (C$_{29}$ sterane and MDBT parameters) and TSR ($\Delta\delta^{34}$S$_{BTs\text{–}DBTs}$ = 6–12‰) impacts suggest each of these factors also influenced the δ^{34}S character of the Dongpu oils. Therefore, δ^{34}S$_{OSCs}$ data should be used cautiously in correlation of oils from complex petroleum systems and where possible integrated with other complimentary analytical information.

Keywords: Stable sulfur isotopes; organic sulfur compounds, hydrocarbon biomarkers, oil correlation

1. Introduction

This study explores the potential of continuous flow compound specific S isotope analysis (CSSIA) to help characterise the origin and geochemical history of lacustrine oils in the Dongpu Depression of the Bohai Bay Basin. CSSIA was first demonstrated a decade ago (Amrani et al., 2009) and has since helped establish the sources and genetic types of crude oils and petroleum source rocks, e.g., $\delta^{34}S$ correlation of dibenzothiophenes ($\delta^{34}S_{DBTs}$) in Lower Paleozoic crude oils of the Tarim Basin with regional Lower Cambrian source rocks (Cai et al., 2015, 2016); $\delta^{34}S_{DBTs}$ correlation of oils and source rocks of Kurdistan (Arabian Platform; Greenwood et al. 2018); the $\delta^{34}S$ values of sour gas petroleum from Sichuan Basin were attributed to Upper Permian mudstones from local (P_3l and P_3w) formations (Cai et al., 2017a, b). The S-isotopic character of saline lacustrine oils, however, have not previously been studied in detail.

The petroleum system in the Dongpu Depression is highly complex due to mixed input from several major sources and varied paleo-depositional and thermal conditions. Lacustrine oils typically derive from non-marine algal and bacterial organic matter and have low content of sulfur (Peters, et al., 2005). The high sulfur content of the Dongpu sediments and oils can be attributed to bacterial sulfate reduction. Types II–III kerogens of the third and fourth members of the Tertiary Shahejie Formation (Es_3–Es_4,) are responsible for S-rich oils discovered mostly in the northern (saline lacustrine oils) but some also in the southern (freshwater lacustrine oils) regions of the Depression (Peng et al., 2003; Change et al., 2007; Chen et al., 2018), although the full identity of the active source rocks and their respective quantitative significance has not been fully established.

Geochemical studies have shown the northern saline lacustrine oils have widely varied chemical properties and also span low to relatively high maturities (Zhang et al., 2017; Ji et al., 2018) attributed to source rock heterogeneity across several isolated sags. The present oil suite may therefore allow further investigation of the effects of depositional and thermal dynamics on the $\delta^{34}S$ character of oils. The $\delta^{34}S$ of organic sulfur compounds ($\delta^{34}S_{OSCs}$) have previously been shown to be sensitive to secondary petroleum alterations by thermochemical sulfate reduction (TSR; Amrani et al., 2012; Gvirtzman et al., 2015), increasing oil window maturity (Ellis et al., 2017; Rosenberg et al., 2017); as well also as microbial degradation (He et al., 2019). Differences in $\delta^{34}S$ values between alkylated dibenzothiophenes (DBTs) and benzothiophenes (BTs) or thiadiamondoids (TDs) are very sensitive to early stage TSR (Amrani et al., 2012; Gvirtzman et al., 2015) although a higher degree of TSR is still best evaluated though traditional indicators such as diagnostic hydrocarbons (e.g., TDs), high H_2S levels or ^{34}S enriched oils or H_2S (Zhang et al., 2008; Wei et al., 2012). Ellis et al (2017) also showed differences between the $\delta^{34}S$ values of methyl DBT isomers (i.e., $\Delta^{34}S$ =1-mDBT–4-mDBT) were sensitive to thermal maturity and even more so to TSR.

2. Geological setting

The Dongpu Depression, located in the southwestern part of the Bohai Bay Basin, is a typical saline lacustrine basin (Wang et al., 2015). The depression covers an area of 5,300 km^2 with a north-north-east (NNE) topography contour narrowing from northeast to southwest (Figure A2-1a), such that the depression is wide in the south but narrow in the north (Figure A2-1). The eastern areas and the Luxi Uplift are bounded by the Lanliao Fault; the western areas overlie the Neihuang uplift; the southern areas are bordered by the Lankao Uplift and the northern areas are connected

to the Shenxian Depression. Four separate tectonic units of the depression have been defined as: the eastern sub-depression; the western sub-depression; the central uplift and the western slope (Figure A2-1; Qi and Yang, 2010). Since the beginning of the Cenozoic (Es_4–Ed and Ng–Q) there have been two major tectonic cycles which have been subdivided into five evolutionary stages (Figure A2-2): initial rifting (depositional episode of the Es_4 strata); advanced rifting (Es_3); post-rifting (Es_2–Es_1); rifting termination (Ed); and subsidence (Ng, Nm, and Q) (Zhang et al., 2007; Gao et al., 2009).

The Dongpu Depression is founded on a Mesozoic and Paleozoic basement, with significant Cenozoic formations including the Paleogene Shahejie (Es) and Dongying (Ed) formations; and the Neogene Guantao (Ng) and Minghuazhen (Nm) formations - comprising a total thickness of about 8,000 m (Figure A2-2). The Shahejie Formation, with a total thickness of about 1500 m, has been divided into four members (Es_1 to Es_4; Shao et al, 2018). The Es_1 and Es_3–Es_4 strata derive from two separate source rocks and the Es_3 and Es_4 have been further divided into three (Es_3^1 to Es_3^3) and two (Es_4^1 and Es_4^2) sub-members, respectively (Wang et al., 2015; Li et al., 2016; Shao et al, 2018). The Es_3–Es_4 intervals comprise the main source rocks for the regional petroleum with the Es_1 stratum containing immature source rocks.

The Dongpu Depression can also be divided into two distinct sedimentary facies regions separated by the Yellow River: with saline lacustrine facies north of the river and freshwater lacustrine facies south of the river (Figure A2-1a; Gao et al., 2015; Chen et al., 2018). Furthermore, Type II and Types II–III kerogens of Es_3-Es_4 intervals were responsible for the northern and southern oils, respectively (Figure A2-6a; Peng et al., 2003, Chang et al., 2007).

Gypsum-salt rocks, distributed in the center of the depression and on slope areas, have significantly impacted oil and gas generation in the north of the depression (Figure A2-1b; Ji et al., 2015; Jiang et al., 2016). Generally, the gypsum-salt rocks, mud shales, and sandstones are mutually intermingled, and form a favorable combination of reservoir and seal (Figure A2-1b and Figure A2-2). These rocks do not occur in southern areas of the depression where less petroleum has been discovered (Liu and Ren, 2007; Gao et al., 2009; Li et al., 2015).

Figure A2-1 (a) Regional structural map showing the location of the Dongpu Depression; (b) cross section of the North Depression. See (a) for map location of the cross section.
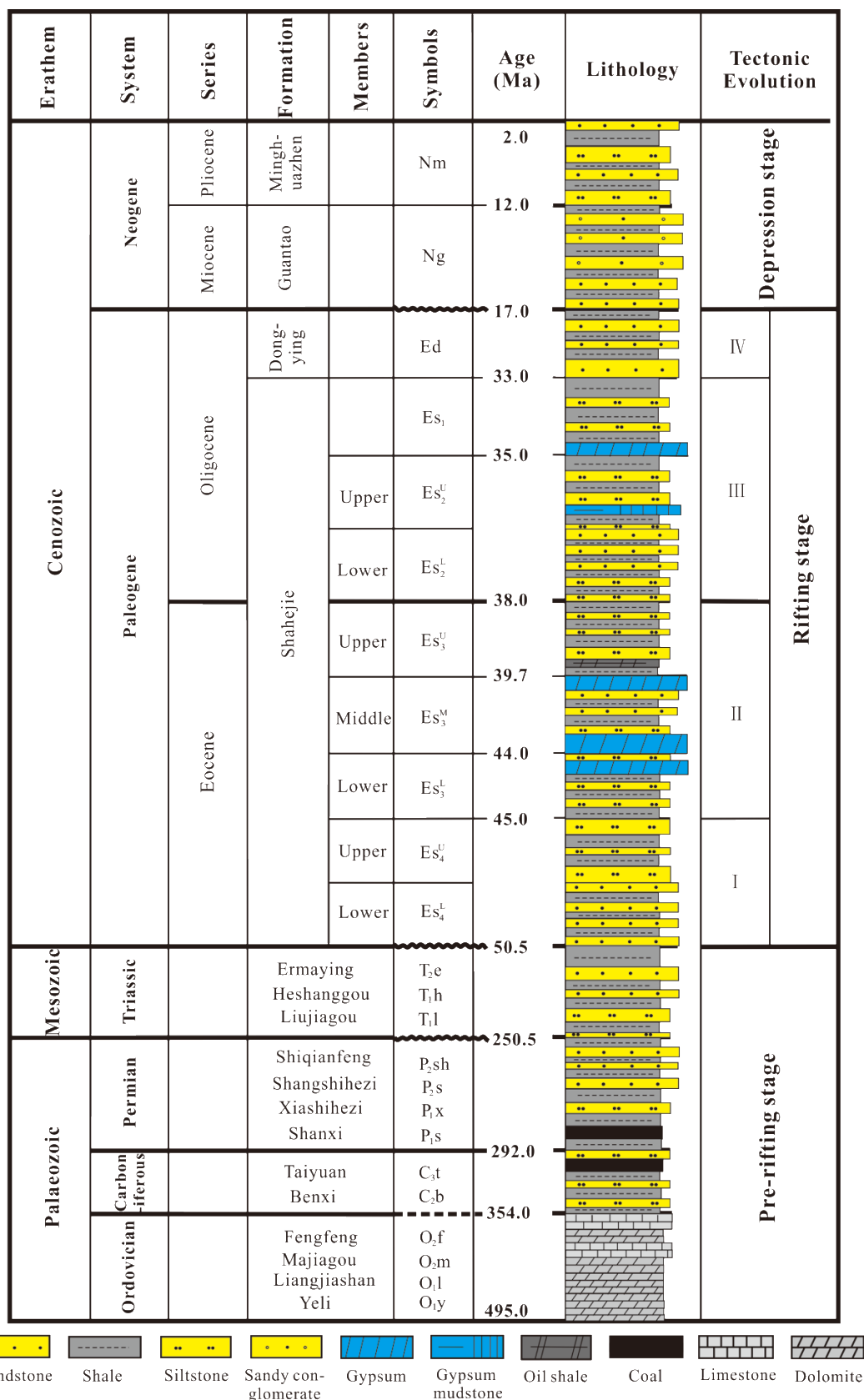
Figure A2-2 General stratigraphic column of the Dongpu Depression.

3. Samples and methods

A total of 18 S-rich lacustrine oils were used in this study. These come from the northern Weicheng (WC; 2 oils), Pucheng (PC; 4), Liutun (LT; 2) and Wenliu (WL; 8) oilfields; and southern Sanchunji (SCJ, 1) and Machang (MC, 1) oilfields (Figure A2-1a). GC-MS analysis of the hydrocarbon and organic sulfur composition of all oils was first performed to support product identification and traditional molecular constraint of the source, depositional environment and thermal history of the oils. The $\delta^{34}S_{OSCs}$ values of the oils were measured by gas chromatography (GC) inductively coupled plasma (ICP) mass spectrometry (MS). All oils gave $\delta^{34}S_{OSCs}$ data except the MC oil in which the OSCs abundances proved too low for viable $\delta^{34}S$ measurements.

3.1. GC-MS analysis

GC-MS analysis of the saturated (SAT) and aromatic (ARO) hydrocarbon fractions of the oils isolated by column chromatography was performed using an Agilent 6890 gas chromatograph interfaced to an Agilent 5975I mass selective detector (MSD). Internal standards were added to the SAT (5α-androstane) and ARO (D50-anthracene) fractions to assist quantification. Helium with a purity of 99.999% was used as the carrier gas at a flow rate of 1 mL/min; the GC columns used were HP-5MS (30 m × 0.25 mm × 0.25 μm) and HP-5MS (60 m × 0.25 mm × 0.25 μm) for the SAT and ARO analysis, respectively. For the SAT fractions analysis, the GC oven was heated from 50 °C (held for initial 2 min) at 2 °C/min to 100 °C and then at 3 °C/min to 310 °C (held for final 30 min). For ARO fraction analysis, the GC oven was heated from 60 °C at 8 °C/min to 150 °C and then 4 °C/min to 320 °C (held for a final 10 min). 70 eV electron impact mass spectra were acquired by full scan (FS) and selective ion

monitoring (SIM) including *m/z* 85, 123, 217, 218, 231, 191, 177, 397, 412 for SAT and *m/z* 128, 142, 156, 170, 184, 198, 178, 192, 206, 220, 184, 198, 212, 226, 154, 168, 182, 196, 234, 228, 242, 256, 252, 166, 180, 194, 202, 216, 231, 245, 121, 135, 149 for ARO.

3.2 Compound-specific stable sulfur isotope analyses

CSSIA of the ARO fraction of the oils was conducted with an Agilent 6890 GC coupled to a Thermo Neptune Plus multicollector ICP MS (Greenwood et al., 2018). The OSCs were separated with a DB-5MS GC column (30 m × 0.25 mm × 0.1 μm) with He carrier gas at a constant flow rate of 3ml/min. The GC oven was heated from 100 °C (held for 0.5 min) at a rate of 8 °C/min to 300 °C (held for 15 min). Argon gas (purity of 99.999%) for the plasma torch was pre-heated and introduced co-axially with the analytes from the GC. The ICP MS measured $\delta^{34}S$ values were converted to true $\delta^{34}S$ values using standard compound measured correction factors and reported as permil (‰) relative to the international sulfur isotope standard Vienna Canyon Diablo Troilite (VCDT). Two pulses of a SF_6 gas standard were included at both the start and end of all sample analyses to internally calibrate $\delta^{34}S$ measurements.

4. Geochemical characteristics and classification of the crude oils

4.1. Physical properties and group compositions of the crude oils

The physical properties of Dongpu Depression oils vary considerably (Chen, 2017; Ji et al., 2018). Crude oils range in density from 0.80–0.99 g·cm^{-3} and viscosities from 4–815 mPa. Their pour points range from 0–40 °C and wax contents vary widely within the light-medium oil range (0.2 % to 13.9%). There are large differences between the saline lacustrine northern oils and the freshwater lacustrine southern oils (Ji et al., 2018). For instance, the northern oils have relatively high densities (Ave 0.87

$g \cdot cm^{-3}$ Cf. 0.83 $g \cdot cm^{-3}$ in south oils), high viscosity (96 mPa·s north; 17 mPa·s south), low pour points (26 °C north; 30–37 °C south) and generally high sulfur contents (mostly 0.5-2% north; < 0.2% south). All oils showed regular wax contents (average 10.3% and 14.5% for the north and south, respectively).

The relative abundances of the polarity-based fractions of the oils isolated by column chromatography (Table A2-1) were largely consistent with their physical properties. The SAT (40–95% north; 82–84% south) and ARO (4–46% north; 12–13% south) fraction contents of the northern and southern oils spanned slightly different ranges. The SAT/ARO ratio also seemed related to thermal maturity, i.e, deep and high thermal maturity (R_0=1%) LT oils had the highest SAT/ARO ratio (> 10), and relatively low resin and asphaltene contents (Table A2-1).

4.2. Molecular composition and oil families of the crude oils

4.2.1. Hydrocarbon biomarkers

The SAT fraction composition of all the northern oils were generally similar with a dominant bimodal distribution of n-alkanes extending to beyond nC_{40} (Figure A2-3). The nC_{21}-/nC_{22}+ and $(nC_{28}+nC_{29})/(nC_{21}+nC_{22})$ ratios were within the ranges 0.5–3.4 (Ave 1.0) and 0.5–1.4 (Ave 0.6; Table A2-1), respectively, and are typical values of aquatic organism and higher plant sources (Peters et al., 2005). Most of the LT, WL and southern (SCJ-MC) oils showed no obvious odd or even carbon preference (CPI and OEP both ~ 1; Table A2-1). However, a small even carbon preference was observed for the two WC oils and three of the four PC oils (OEP=0.88–0.92; Table A2-1), suggesting a relatively lower maturity than the other oils. The relative high abundances of phytane (Pr/Ph= 0.4–0.7; Table A2-1, Figure A2-1) and the high MW n-alkanes nC_{37} and nC_{38} reflect the strong reductive environment (Peters et al., 2005)

of the saline lacustrine facies of the northern oils. The aliphatic hydrocarbon composition of the two southern oils were also generally similar to the northern oils, but notable distinctions such as relatively high abundance of pristane (Pr/Ph > 1) and lack of nC_{37}–nC_{38} predominance are consistent with a weakly reduced depositional environment (Connan and Cassou, 1980; Peters et al., 2005).

The terpenoid composition of the northern oils showed several characteristics typical of saline lacustrine sources, including relatively high abundances of gammacerane (G) and C_{35}-hopanes. The G/C_{31}-hopane ratio of the oils ranged from 0.8 - 1.6 (Table A2-2). Gammacerane typically derives from photosynthetic bacteria and is conspicuous in saline lacustrine facies sourced oils and rocks. High abundances of gammacerane are also often associated with water stratification and the deposition of organic matter in reduced primitive sedimentary environments (e.g. brine). The C_{35}-hopane/C_{34}-hopane (C_{35}-H/C_{34}-H) ratios of the oils span a wide range of values (0.2–4.1; Table A2-2) with most of the lower maturity ($R_o < 0.7$) oils having C_{35}-H/C_{34}-H values > 1. The southern crude oils generally had a lower abundance of gammacerane (G/C_{31} hopane = 0.32–0.39) and no predominance of C_{35} hopanes (Figure A2-4, Table A2-2) typical of freshwater lacustrine oils. Most of the oils showed relatively low abundances of tricyclic terpanes (Figure A2-4), consistent with their low thermal maturity (Moldowan et al., 1983; Peters et al., 2005).

Sterane distributions of all northern and southern oils were generally similar. The C_{27}, C_{28}, and C_{29} regular sterane profiles were asymmetric for shallow depth oils; but symmetric (V–shaped distribution) for deeper oils (Figure A2-4; Table A2-2). C_{27} steroids are indicative of marine algal input, whereas C_{29} steroids may have originated from terrigenous inputs such as higher plants (Peters et al., 2005). Diasteranes and pregnanes were both detected in relatively low abundance (diasteranes/regular

steranes < 0.25; $C_{21\text{-}22}$-pregnane/$C_{27\text{-}29}$-regular sterane = 0.01–0.11; Table A2-2) which is also typical of a low thermal maturity (Peters et al., 2005). Higher levels of maturity might have been implied from the upper ranges of C_{29} $\alpha\alpha\alpha20S/(R + S)$ and C_{29} $\alpha\beta\beta/(\alpha\alpha\alpha + \alpha\beta\beta)$ sterane maturity indices (0.3–0.5 and 0.3–0.7, respectively, Table A2-2; Peters et al., 2005). However, normal–peak oil window maturities were further supported by methylphenanthrene (MPI$_1$) calculated vitrinite equivalent reflectance values R_c or R_o = 0.6–2.0% (Table A2-2; Kvalheim, 1987; Radke and Willsch, 1993; Radke et al., 2000; Peters et al., 2005).

A:saline lacustrine oil
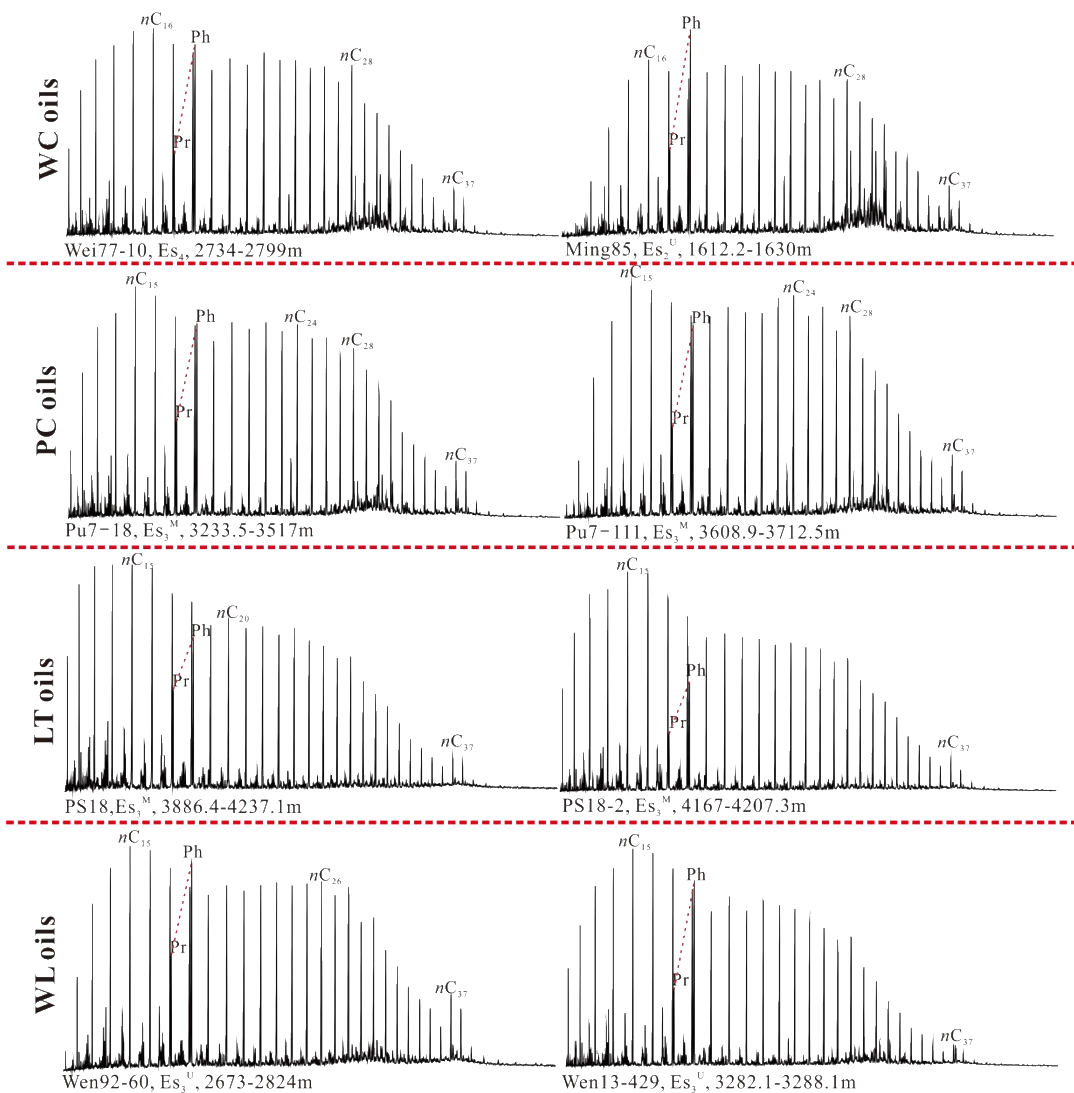
B:freshwater lacustrine oil
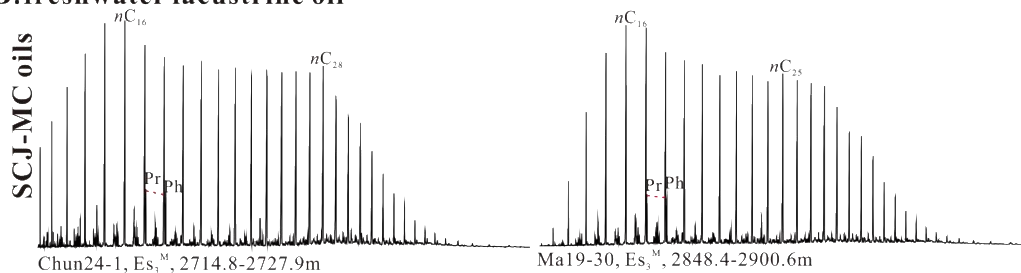
Figure A2-3 Total ion chromatogram (TIC) from the GC-MS analysis of the saturate fraction of Dongpu Depression oils.
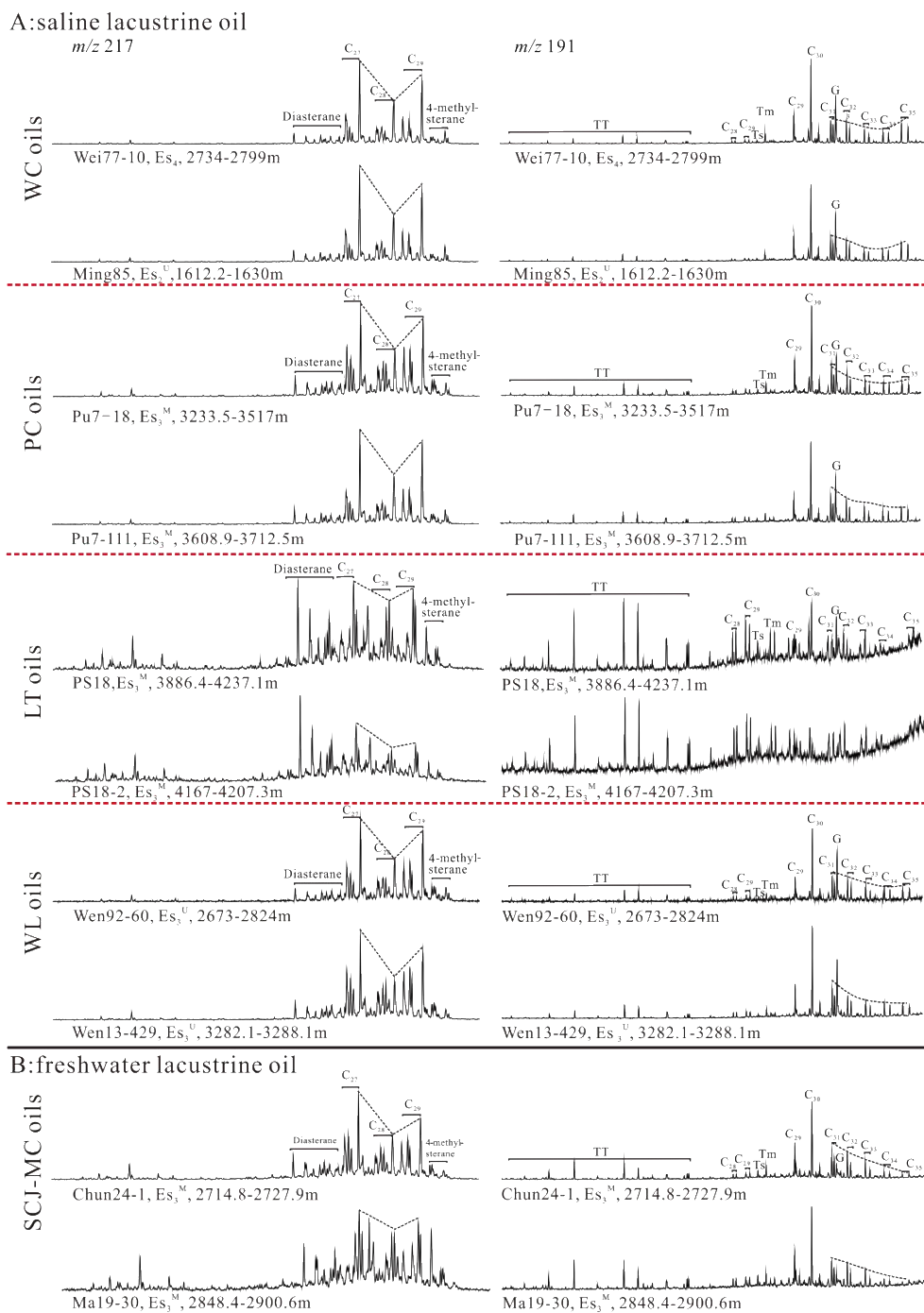
Figure A2-4 Mass chromatograms of *m/z* 217 and *m/z* 191 of saturates from the Dongpu Depression crude oils (A: saline lacustrine oil; B: freshwater lacustrine oil).

Table A2-1 Group composition and paraffin parameters for the oils from the Dongpu Depression.

Tectonic Belt	Sample No	Well	Depth (m)	Strata	Density (g/cm³)	Viscosity (mPa·s)	Pour point (°C)	Wax content (%)	Sulfur content (%)	Sat (%)	Aro (%)	Resin+Asp (%)	Sat/Aro	CPI	OEP	Pr/Ph	Pr/ nC_{17}	Ph/ nC_{18}	nC_{21}-/ nC_{22}+	$(nC_{28}+nC_{29})/(nC_{21}+nC_{22})$
WC	1	Ming85	1612.2-1630	Es_2^U	0.92	36.21	33.00	12.73	1.52	51.72	24.14	24.14	2.14	0.92	0.91	0.39	0.84	2.06	0.64	1.01
	2	Wei77-10	2734-2799	Es_4	0.87	9.25	21.00	12.42	1.46	40.63	17.14	42.22	2.37	0.90	0.92	0.42	0.64	1.59	0.82	0.93
PC	3	Pu7-18	3233.5-3517	Es_3^M	0.91	21.57	34.00	11.83	0.32	45.36	46.05	8.59	0.99	0.96	0.88	0.50	0.72	1.52	0.83	0.87
	4	Pu7-111	3608.9-3712.5	Es_3^M	0.86	11.36	29.00	10.57	0.58	64.24	15.89	19.87	4.04	0.99	1.08	0.48	0.63	1.37	0.71	0.95
	5*	Wei42-21	3660-3716.8	Es_3^M	0.87	18,44	19.00	11.10	0.05	52.80	10.49	36.71	5.03	0.98	0.90	0.62	0.41	0.74	0.63	1.21
	6*	Wei42-26	3451-3466.6	Es_3^M	0.90	28.47	22.00	11.25	0.05	56.39	21.80	21.80	2.59	0.98	0.90	0.62	0.53	0.94	0.45	1.41
LT	7	PS18	3886.4-4237.1	Es_3^M	0.83	5.35	23.00	/	0.06	90.94	6.52	2.54	13.94	0.96	0.94	0.52	0.42	0.88	1.29	0.67
	8	PS18-2	4167-4207.3	Es_3^M	0.82	5.13	23.50	/	0.06	90.68	6.50	2.82	13.96	0.96	1.00	0.54	0.44	0.89	1.02	0.87
WL	9	Wen92-60	2673-2824	Es_3^U	0.83	6.79	33.00	8.30	1.09	72.43	20.09	7.48	3.60	0.93	1.01	0.43	0.52	1.32	0.81	0.89
	10	Wen13-281	3377.3-3453.3	Es_3^M	0.85	6.49	32.00	19.08	0.21	84.00	12.00	4.00	7.00	0.97	1.01	0.53	0.51	1.04	1.11	0.70
	11	Wen13-319	3417.4-3689.5	Es_3^M	0.82	5.68	31.00	16.72	0.33	74.70	21.34	3.95	3.50	1.01	1.01	0.49	0.52	1.16	0.97	0.77
	12	Wen13-429	3282.1-3288.1	Es_3^U	0.86	6.62	34.00	10.71	0.34	76.72	15.27	8.02	5.03	0.95	1.03	0.41	0.65	1.76	1.08	0.69
	13	Wen203-58	3770.6-4081.9	Es_3^M	0.81	4.35	28.00	4.78	0.19	85.53	6.38	8.09	13.40	0.96	1.02	0.53	0.74	1.51	1.19	0.62
	14	Wen203-63	4360.6-4414.4	Es_3^M	0.80	2.93	27.00	5.23	0.11	94.97	3.55	1.48	26.75	0.99	1.07	0.61	0.80	1.46	1.69	0.54
	15	Wen72-53	3273.4-3527	Es_3^M	0.83	5.91	31.00	10.09	0.14	65.79	17.11	17.11	3.85	0.94	0.99	0.37	0.60	1.64	0.65	0.88
	16	Wen88-59	3515.1-3877.5	Es_3^M	0.83	4.82	29.00	13.35	0.08	77.58	13.92	8.51	5.57	0.97	1.09	0.72	0.49	0.93	3.35	0.48
SCJ	17	Chun24-1	2714.8-2727.9	Es_3^M	0.83	17.36	30.00	16.40	0.11	81.59	11.72	6.69	6.96	1.01	1.19	1.21	0.32	0.30	0.82	1.02
MC	18	Ma19-30	2848.4-2900.6	Es_3^M	0.83	5.62	37.00	6.87	0.05	84.26	12.77	2.98	6.60	1.04	1.03	1.19	0.29	0.27	0.74	0.97

Note: Sat: saturates; Aro: aromatics; Asp: asphaltenes; Sat/Aro: saturates/aromatics; CPI: $[(C_{25}+C_{27}+C_{29}+C_{31}+C_{33})/(C_{26}+C_{28}+C_{30}+C_{32}+C_{34})+(C_{25}+C_{27}+C_{29}+C_{31}+C_{33})/(C_{24}+C_{26}+C_{28}+C_{30}+C_{32})]/2$; OEP: $(C_i+6C_{i+2}+C_{i+4})/(4C_{i+1}+4C_{i+3})$ or $(4C_{i+1}+4C_{i+3})/(C_i+6C_{i+2}+C_{i+4})$, among which i + 2 is the maximum peak of n-alkanes with i corresponding to odd and even member respectively (Scalan and Smith, 1970); Pr/Ph: pristane/phytane; Pr/ nC_{17}: pristane/ nC_{17}; Ph/ nC_{18}: phytane/ nC_{18}; nC_{21}-/ nC_{22}+: $\sum nC_{21}$-/$\sum C_{22}$+; *: The oils are situated between the Weicheng and Pucheng oilfields, which were sealed by salt-gypsum rocks. These two oils were not classified as PC oils from views of both their tectonic situations and different geochemical features from the others.

4.2.2. Hydrocarbon classification of oil families

Molecular hydrocarbon parameters reflective of genetic differences between the northern saline lacustrine oils and the southern freshwater lacustrine oils included the values of Pr/Ph, C_{35}-H/C_{34}-H, and G/C_{31}-hopane ratios (Figures A2-4–6, Table A2-2). The northern oils could be further subdivided into four oil families (OFs), with the southern oils a separate fifth OF.

OF-1 The oils from the WC oilfield were distinguished from other northern oils by relatively high abundances of C_{35} hopanes (C_{35}-H/C_{34}-H= 1.74–1.87) and thioaromatics (DBT/P= 0.55–0.56; Figures A2-5c, 6b, d). They also typically had relatively low Pr/Ph values; high G/C_{31}-hopane ratios and high overall abundances of steranes and hopanes (Figures A2-5a, b; 6f, Table A2-2).

OF-2 Two crude oils from the PC oilfield (i.e., Pu7-111 and Pu7-18) had relatively low Pr/Ph values (0.48–0.50) and high G/C_{31}-hopane values (1.07–1.27; Figure A2-5a, b; Table A2-1 & 2). They also had lower DBT/P ratios (0.13–0.17) and total abundances of hopanes and steranes than OF-1 (Figure A2-5c, f).

OF-3 LT oils had lower G/C_{31}-hopane ratios (0.78–0.79; Figure A2-5b; Table A2-2) and much lower abundances of steranes and hopanes (Figure A2-5f; Figure A2-6d, Table A2-2) than OF-1 and OF-2. They also contained more prominent tricyclic terpanes relative to pentacyclic terpanes (TTs/PTs = 1.23–1.36; Figure A2-4) and diasteranes relative to regular steranes (DiaS/RegS = 0.43–0.76; Figure A2-5e). Thermal cracking at higher maturities may have led to

a reduction of hopanoids/pentacyclic terpanes (Figure A2-4).

OF-4 WL oils were differentiated by relatively high abundances of gammacerane (G/C_{31}-hopane = 0.80–1.61; Figure A2-5b; Table A2-2) and low C_{29}-H/C_{30}-H ratios (0.31–0.36, average 0.33) – except Wen203-63 oil which had a high thermal maturity (R_o = 1.06%). These oils also had generally low DBT/P ratios (0.06–0.21, Ave 0.15; Figure A2-5c, Table A2-2), in noted contrast to the WC oils (0.55–0.56; Figure A2-5c).

OF-5 The south Dongpu Depression Sanchunji (Chun24-1) and Machang (Ma19-30) oils showed typical freshwater lacustrine characteristics including Pr/Ph values > 1 (Figure A2-5a) and G/C_{31}H < 0.3 (Figure A2-5b).

These five oil families represent the full oil suite except for Wei 42-26 and Wei42-21. Assigned as from PC oil field in Table A2-1, these two wells were actually situated in a transitional zone between the PC and WC oilfields (Figure A2-1) and their oil was derived from a self-generating and self-preserving laminal reservoir interbedded and sealed by gypsum-salt rocks. The biomarker characteristics of these two oils included relatively high Pr/Ph, high C_{29}-H/C_{30}-H and low DBT/P values (Figure A2-5a, b and d) likely indicative of a distinctive formation background (Figure A2-5; Table A2-2). The DBTs of these oils also had enriched δ^{34}S values consistent with a major TSR event (see Section 5.2.3).
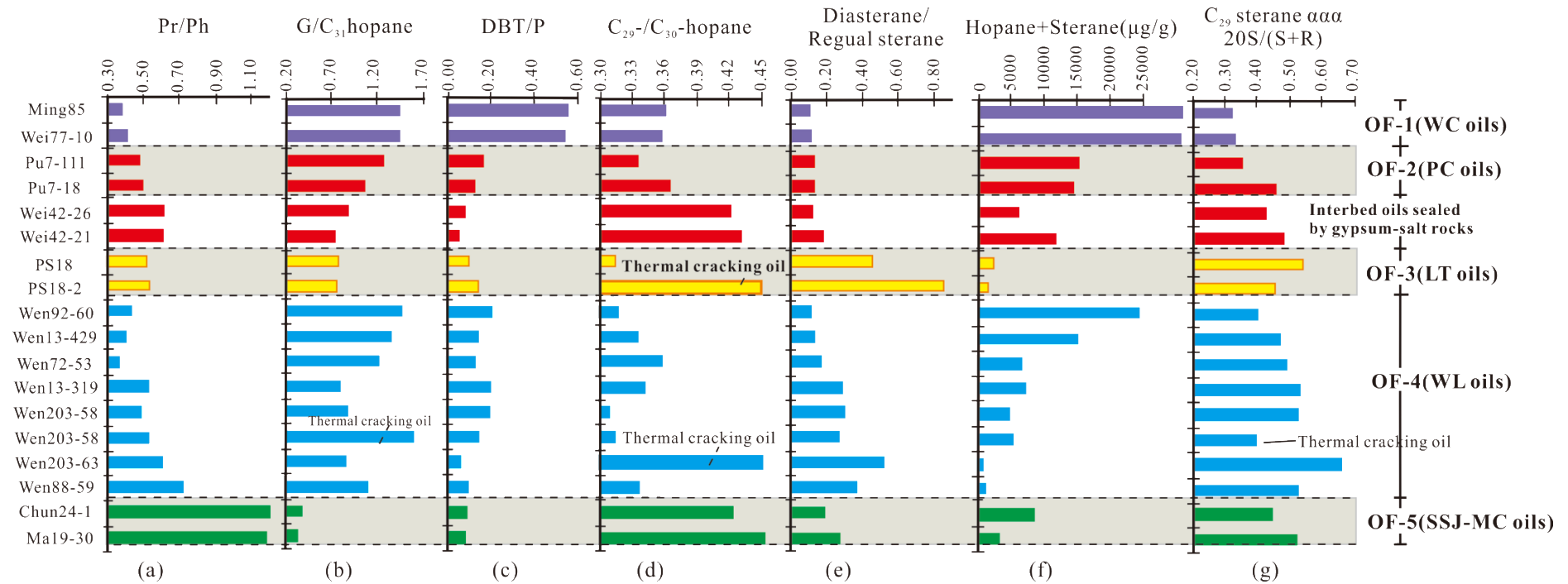
Figure A2-5 Oil-family classification based on hydrocarbon parameters from GC-MS data.

Note: OF-: Oil family 1 (oils from the WC oilfield; data shaded purple); OF-2: Oil family 2 (oils from the PC Oilfield; red data); OF-3: Oil family 3 (oils from the LT Oilfield; orange data); OF-4: Oil family 4 (oils from the WL Oilfield; blue data); OF-5: Oil family 5 (oils from the SSJ-MC Oilfield; green data).
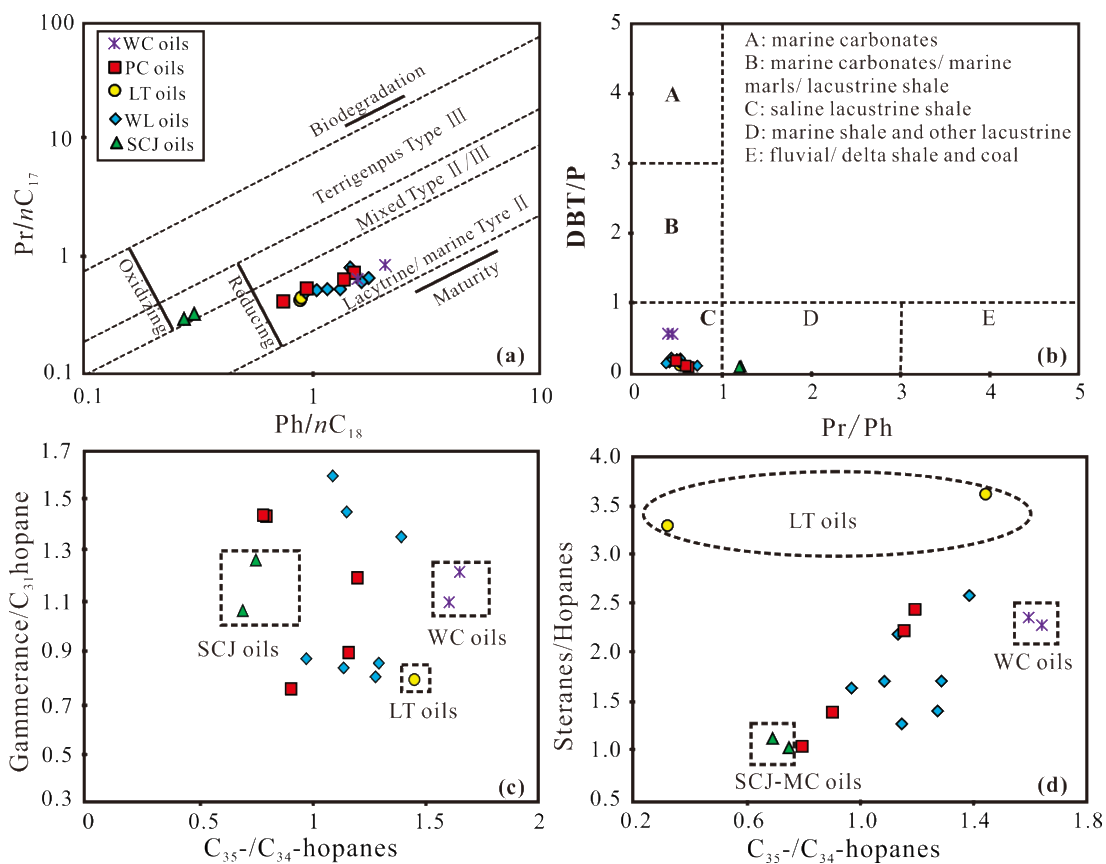
Figure A2-6 Plots of geochemical parameters indicating paleoenvironmental and organic source input of potential source rocks (a) The relationship of Pr/nC$_{18}$ versus Ph/nC$_{17}$; (b) Pr/Ph versus DBT/P; (c) C$_{35}$-/C$_{34}$-hopanes versus gammacerane/C$_{31}$hopane; (d) C$_{35}$-/C$_{34}$-hopanes versus steranes/hopanes.

Table A2-2 Basic geochemical GC-MS parameters of the oil from the Dongpu Depression.

Tectonic Belt	Sample No	Well	Strata	Relative abundance (%) C27	C28	C29	20S	αββ	C31 22S	Ster/ Hop	Dia/ Reg	(C21+C22)/ (C27-C29)	G/ C31H	C35-H/ C34-H	C29-H/ C30-H	T/P	Ste+Hop (μg/g)	MPI1	MPI2	Rc (%)	Ro (%)	DBT/P	mDBT/ mP	4-mDBT/ 1-mDBT
WC	1	Ming85	Es_2^U	35.7	27.8	36.5	0.31	0.28	0.57	2.30	0.10	0.01	1.44	1.87	0.36	0.11	31530	0.46	0.51	0.68	0.71	0.56	0.19	22.14
	2	Wei77-10	Es_4	32.7	29.2	30.8	0.32	0.28	0.57	2.37	0.10	0.01	1.45	1.74	0.36	0.11	31013	0.46	0.53	0.68	0.67	0.55	0.19	28.88
PC	3	Pu7-18	Es_3^M	34.9	27.7	37.4	0.42	0.37	0.60	2.26	0.12	0.01	1.07	1.08	0.37	0.17	14609	0.48	0.55	0.69	0.65	0.13	0.09	17.61
	4	Pu7-111	Es_3^M	32.1	28.7	39.3	0.34	0.32	0.59	2.46	0.12	0.01	1.27	1.43	0.34	0.17	15261	0.45	0.51	0.67	0.62	0.17	0.10	31.80
	5	Wei42-21	Es_3^M	37.7	23.8	38.6	0.45	0.39	0.59	1.05	0.16	0.01	0.75	0.73	0.43	0.18	11973	0.43	0.49	0.66	0.60	0.06	0.05	32.26
	6	Wei42-26	Es_3^M	36.6	27.0	36.4	0.40	0.33	0.59	1.37	0.11	0.01	0.90	0.86	0.42	0.18	6337	0.44	0.51	0.66	0.58	0.08	0.06	24.13
LT	7	PS18	Es_3^M	31.8	30.2	38.0	0.46	0.60	0.76	3.66	0.43	0.07	0.79	1.47	0.31	1.23	2305	0.80	0.89	0.88 (1.82)	0.92	0.11	0.10	53.44
	8	PS18-2	Es_3^M	44.9	23.6	31.5	0.42	0.69	0.72	3.34	0.76	0.10	0.78	4.13	0.86	1.36	1698	0.89	1.00	0.93 (1.77)	0.99	0.15	0.13	39.18
WL	9	Wen92-60	Es_3^U	33.2	27.8	39.0	0.38	0.36	0.60	2.20	0.11	0.01	1.46	2.03	0.32	0.20	24344	0.43	0.51	0.66	0.60	0.21	0.13	29.63
	10	Wen13-281	Es_3^M	33.5	25.5	41.0	0.46	0.53	0.62	1.29	0.26	0.03	0.80	1.02	0.34	0.27	7198	0.47	0.55	0.68	0.62	0.20	0.10	42.89
	11	Wen13-319	Es_3^M	32.0	26.6	40.4	0.46	0.51	0.61	1.41	0.27	0.03	0.87	1.15	0.31	0.29	4744	0.48	0.55	0.69	0.64	0.19	0.10	43.07
	12	Wen13-429	Es_3^U	33.8	26.9	39.3	0.43	0.40	0.61	1.64	0.12	0.01	1.36	1.98	0.34	0.18	15255	0.54	0.68	0.72	0.72	0.15	0.11	29.67
	13	Wen203-58	Es_3^M	30.1	31.8	38.1	0.40	0.67	0.67	2.60	0.23	0.04	1.61	2.00	0.32	0.56	5216	0.51	0.58	0.71 (2.00)	0.66	0.14	0.06	45.18
	14	Wen203-63	Es_3^M	25.6	32.6	41.8	0.50	0.64	0.62	2.52	0.45	0.11	0.86	3.90	0.67	1.81	540	0.94	1.05	0.96 (1.74)	1.06	0.06	0.05	35.52
	15	Wen72-53	Es_3^M	33.4	27.5	39.1	0.45	0.42	0.61	1.72	0.15	0.02	1.22	1.90	0.36	0.23	6499	0.55	0.68	0.73	0.67	0.13	0.09	22.41
	16	Wen88-59	Es_3^M	33.2	28.8	38.1	0.46	0.55	0.65	1.72	0.32	0.05	1.10	1.04	0.34	0.55	1100	1.03	1.17	1.02 (1.68)	1.09	0.10	0.05	45.74
SCJ	17	Chun24-1	Es_3^M	38.9	27.3	33.8	0.42	0.40	0.59	1.13	0.18	0.03	0.39	0.21	0.42	0.28	8385	0.53	0.59	0.72	0.78	0.09	0.05	30.72
MC	18	Ma19-30	Es_3^M	33.0	28.4	38.6	0.47	0.48	0.60	1.05	0.26	0.06	0.32	0.19	0.46	0.46	3065	0.58	0.64	0.75	0.85	0.08	0.05	38.12

Note: C_{27}(%): C_{27} Regular steranes/ (C_{27} Regular steranes+ C_{28} Regular steranes+ C_{29} Regular steranes); C_{28}(%): C_{28} Regular steranes/ (C_{27} Regular steranes+ C_{28} Regular steranes+ C_{29} Regular steranes); C_{29}(%): C_{29} Regular steranes/ (C_{27} Regular steranes+ C_{28} Regular steranes+ C_{29} Regular steranes); 20S: C_{29} steranes 20S/(20R+20S); αββ: C_{29} steranes αββ/(ααα+αββ); C_{31}22S: C_{31} hopanes 22S/(22S+22R); Ster/Hop: Steranes/Hopanes; Dia/Reg: Diasteranes/ Regular steranes; $(C_{21}+C_{22})/(C_{27}-C_{29})$: $(C_{21}+C_{22})$ pregnane/$(C_{27}-C_{29})$ regular sterane; G/C_{31}H: Gammacerane/C_{31}-Hopane; C_{35}-H/C_{34}-H: C_{35}-hopane/C_{34}-hopane; C_{29}/C_{30}H: C_{29}-/C_{30}-hopane; T/P: Tricyclic/pentacyclic terpane; Ste+Hop: The absolute abundance of steranes and hopanes (μg/g oil); MPI_1 = 1.5 × (2–methylphenanthrene + 3–methylphenanthrene)/(1-methylphenanthrene + 9-methylphenanthrene +phenanthrene); MPI_2 = 3 × 2–methylphenanthrene /(1-methylphenanthrene + 9-methylphenanthrene + phenanthrene); Rc: Vitrinite reflectance equivalent calculated from MPI-1 for Ro < 1.35 (Rc=0.6*MPI-1+0.4); Ro: Vitrinite reflectance equivalent predicted by F1 (F1 = (2- + 3-methylphenanthrenes)/(2- + 3- + 1- + 9-methylphenanthrenes)), as defined by Kvalheim et al. (1987) (Ro=-0.166+2.242*F_1). DBT/P: Dibenzothiophene/Phenanthrene; mDBT/mP: methyl-dibenzothiophenes/methyl-phenanthrenes; 4-/1-mDBT: 4-methyldibenzothiophene/1-methyldibenzothiophene.

4.3. Sulfur isotopic composition and oil family classification

4.3.1. $\delta^{34}S$ values of OSCs

The ARO fraction of the oils contained a range of organic sulfur compounds (OSCs). A wide distribution of alkylated ($\leq C_3$) dibenzothiophenes (DBTs) were detected in all oils. Additional series of alkylated (C_2-C_4) benzothiophenes (BTs) were detected in three samples (Wen203-63, Ming85, Wei77-10) and 1-3 caged thiadiamondoids were detected in two oils (Pu7-111 and Pu7-18).

$\delta^{34}S$ measurements (Table A2-3) were generally achievable for the three methyl-DBT resolved peaks (4-m; coeluting 3&2-m; 1-m), three isomerically unassigned dimethyl DBTs (dmDBT$_{i-iii}$) and two isomerically unassigned trimethyl DBTs (tmDBT$_{i-ii}$). The $\delta^{34}S$ analyses of BTs in the three oils they occurred extended to four C_2-BT isomers (C_2BT_i, C_2BT_{ii}, C_2BT_{iii}, C_2BT_{iv}), four C_3-BT isomers (C_3BT_i, C_3BT_{ii}, C_3BT_{iii}, C_3BT_{iv}) and two C_4-BT isomers (C_4BT_i, C_4BT_{ii}). $\delta^{34}S$ analysis of TDs in the PC oils included of one thiaamantane compound (A_i), two thiadiamantane compounds (D_{i-ii}), and five thiatriamantane compounds (T_{i-v}).

The $\delta^{34}S_{OSC}$ data measured in 17 of the Dongpu oils analysed spanned a wide range of values from +10.9‰ to +47.8‰ (Table A2-3).

Table A2-3 Compound specific sulfur isotope values (‰) of Dongpu oils.

No	Well	C_3BT_i	C_3BT_{ii}	C_3BT_{iii}	C_3BT_{iv}	C_4BT_i	C_4BT_{ii}	C_4BT_{iii}	C_4BT_{iv}	C_5BT_i	C_5BT_{ii}	DBT	4m3&2m DBT	1m DBT	dm DBT	dm DBT_i	dm DBT_{ii}	dm DBT_{iii}	tm DBT_i	tm DBT_{ii}	A	D_i	D_{ii}	T_i	T_{ii}	T_{iii}	T_{iv}	T_v	$\Delta\delta^{34}S$ (1-mDBT − 4-mDBT)	$\Delta\delta^{34}S$ (BTs − DBTs)	$\Delta\delta^{34}S$ (TDs − DBTs)
1	Min85,	34.53	39.59	35.82	29.60	27.56	25.98	32.24	28.83	30.82	32.98	19.04	17.62	20.14	23.47	18.60	17.65	22.44	20.62	21.66	-	-	-	-	-	-	-	-	5.85	11.66	-
2	Wei77-10	20.86	-	28.86	39.90	23.97	36.57	-	25.48	30.42	-	21.60	19.62	21.26	26.00	22.47	21.49	25.29	24.97	25.75	-	-	-	-	-	-	-	-	6.38	6.28	-
3	Pu7-18	-	-	-	-	-	-	-	-	-	-	31.44	26.04	27.56	28.93	24.77	25.14	27.37	26.52	27.03	40.82	35.48	34.51	34.92	34.17	33.11	27.73	35.02	2.89	-	7.27
4	Pu7-111	-	-	-	-	-	-	-	-	-	-	33.55	28.63	30.48	32.07	25.12	26.00	30.18	29.27	26.46	45.61	37.71	36.37	36.88	34.39	30.67	20.98	33.10	3.44	-	5.38
5	Wei42-21	-	-	-	-	-	-	-	-	-	-	34.82	29.77	34.24	37.49	23.98	26.30	27.39	25.93	27.76	-	-	-	-	-	-	-	-	7.72	-	-
6	Wei42-26	-	-	-	-	-	-	-	-	-	-	28.65	24.39	27.04	28.25	18.10	22.12	22.52	20.53	20.95	-	-	-	-	-	-	-	-	3.86	-	-
7	Pushen18	-	-	-	-	-	-	-	-	-	-	24.85	22.80	24.77	25.50	22.17	24.08	24.42	24.19	24.28	-	-	-	-	-	-	-	-	2.70	-	-
8	Pushen18-2	-	-	-	-	-	-	-	-	-	-	24.64	22.35	23.88	25.17	21.24	22.86	23.09	22.53	22.41	-	-	-	-	-	-	-	-	2.82	-	-
9	Wen92-60	-	-	-	-	-	-	-	-	-	-	17.30	16.37	18.21	19.34	14.19	15.37	16.92	15.72	16.59	-	-	-	-	-	-	-	-	2.97	-	-
10	Wen13-281	-	-	-	-	-	-	-	-	-	-	18.88	24.42	24.48	26.90	24.01	24.65	26.16	25.46	27.65	-	-	-	-	-	-	-	-	2.48	-	-
11	Wen13-319	-	-	-	-	-	-	-	-	-	-	20.46	25.15	23.91	26.59	25.18	25.17	26.40	26.73	27.27	-	-	-	-	-	-	-	-	1.44	-	-
12	Wen13-429	-	-	-	-	-	-	-	-	-	-	15.16	12.79	15.08	16.62	11.08	10.88	12.07	14.33	12.33	-	-	-	-	-	-	-	-	3.83	-	-
13	Wen203-58	-	-	-	-	-	-	-	-	-	-	15.77	25.77	25.71	28.14	30.80	28.56	29.46	-	-	-	-	-	-	-	-	-	-	2.37	-	-
14	Wen203-63	30.69	-	39.66	47.82	31.89	40.73	30.69	-	39.66	-	20.44	21.21	22.40	24.40	19.24	20.12	24.29	33.85	37.32	-	-	-	-	-	-	-	-	3.19	11.77	-
15	Wen72-53	-	-	-	-	-	-	-	-	-	-	19.18	18.86	20.60	22.40	25.15	21.22	22.74	-	-	-	-	-	-	-	-	-	-	3.54	-	-
16	Wen88-59	-	-	-	-	-	-	-	-	-	-	22.36	26.66	25.87	29.22	25.88	27.15	27.67	25.28	26.49	-	-	-	-	-	-	-	-	2.56	-	-
17	Chun24-1	-	-	-	-	-	-	-	-	-	-	18.45	17.94	19.22	-	19.64	18.74	17.60	18.90	17.05	-	-	-	-	-	-	-	-	-	-	-
19	Y41*											10.70	11.30	11.70		11.80	11.50	13.9	10.1	11.60											
20	Y31*											11.30	13.0	12.7		10.50	10.60	-	-	-											

Notes: Note: C_3BT_i, C_3BT_{ii}, C_3BT_{iii} and C_3BT_{iv} represent three isomers of benzothiophenes with 3 carbon atoms in alkyl group; C_4BT_i, C_4BT_{ii}, C_4BT_{iii}, C_4BT_{iv} represent four benzothiophenes with 4 carbon atoms in alkyl group; C_5BT_i and C_5BT_{ii} represent two isomers of benzothiophenes with 2 carbon atoms in alkyl group; mDBT: methyl dibenzothiophenes, $dmDBT_i$, $dmDBT_{ii}$ and $dmDBT_{iii}$ represent three isomers of dimethyl dibenzothiophenes; $tmDBT_i$ and $tmDBT_{ii}$ represent two isomers of trimethyl dibenzothiophenes; Ai: One adamantane compound; $2D_{i-ii}$: Two diamantane compounds; $3T_{i-v}$: Five triamantane compounds; $\Delta\delta^{34}S_{1-mDBT–4-mDBT}$: $\delta^{34}S_{1-mDBT}–\delta^{34}S_{4-mDBT}$; $\Delta\delta^{34}S_{BTs–DBTs}$: Difference of average $\delta^{34}S$ of benzothiophenes and average $\delta^{34}S$ of dibenzothiophenes; $\Delta\delta^{34}S_{TDs–DBTs}$: Difference of average $\delta^{34}S$ of thiadiamondoids and average $\delta^{34}S$ of dibenzothiophenes. *: Y41 and Y33 were freshwater lacustrine oils collected from Tabei Uplift of the Tarim Basin used for a comparison.

4.3.2. Sulfur isotopic classification of oil families

The δ^{34}S characteristics of the four northern and one southern oil families can be summarized as follows:

OF1 The DBTs in the WC oils had relatively depleted δ^{34}S values (+18 to +25‰; Figure A2-7a; Table A2-3). The BTs were notably more enriched in ^{34}S (δ^{34}S $\approx$ +25 to +40‰). The difference between the average values of alkyl BTs and alkyl DBTs (i. e, $\Delta\delta^{34}$S$_{BTs-DBTs}$) of Ming85 and Wei77-10 in the WC oilfield was 11.7‰ and 6.3‰, respectively (Figure A2-7a; Table A2-3).

OF2 The OSCs measured in the PC oils generally had the heaviest δ^{34}S values (average +30‰) and included very ^{34}S enriched TDs (δ^{34}S approaching 40‰; Figure A2-7b; Table A2-3) indicative of TSR. The sulfur isotope difference between TDs and DBTs was large (Figure A2-7b; Table A2-3) - the $\Delta\delta^{34}$S$_{TDs–DBTs}$ of Pu7-18 and Pu7-111 was 7.3‰ and 5.4‰, respectively. A decline in δ^{34}S values with increasing alkylation (δ^{34}S$_{DBT}$ ~ δ^{34}S$_{mDBT}$ > δ^{34}S$_{C2DBT}$) observed in the two interbedded oils (Wei42-21 and Wei42-26, Figure A2-7f) situated between the WC and PC oilfields, also sometimes typical of TSR altered oils (discussed *infra.*), distinguished these oils from the two other PC oils (OF-2)

OF3 The LT oils (OF-3) had intermediate δ^{34}S values (+21 to +25‰; Table A2-3) showing little variance with alkylation (Figure A2-7c).

OF4 The WL oils showed a relatively broad range, but of mostly intermediate δ^{34}S values (+10.9 to +25.2‰; Table A2-3). The methyl

DBTs in the higher (oil window) maturity WL oils had relatively constant $\delta^{34}S$ values, but all notably more enriched than DBT. Alkyl BTs detected in Wen203-63 were also more ^{34}S enriched than the alkyl DBTs ($\Delta\delta^{34}S_{BTs-DBTs}$= 11.8‰). The alkyl DBTs in two of the lower maturity WL oils (Wen13-429; Wen92-60) had more depleted $\delta^{34}S$ values (Ave = 13.4−16.7‰), slightly more depleted even than the WC oils (OF-1; Ave =20.1−23.2‰). One contrast to the WC oils was the slight depletion in $\delta^{34}S$ with increasing alkylation observed for Wen13-429 and Wen92-60 i.e., $\delta^{34}S_{1-mDBT} > \delta^{34}S_{dmDBTiii} > \delta^{34}S_{tmDBTii}$ (Figure A2-7d). The low maturity Wen72-53 oil showed the opposite trend of enrichment in $\delta^{34}S$ with increasing DBT alkylation which suggests a mixed oil source (Zhang et al., 2017).

OF5 The DBTs in the southern Sanchunji oil (Chun24-1) had quite depleted $\delta^{34}S$ values (Ave 18.4‰), which remained relatively constant with increasing alkylation. We previously observed similar $\delta^{34}S$ distributions of OSCs from two freshwater lacustrine oils from the Tabei Uplift of the Tarim Basin (i.e., Y33 and Y41; Li et al., 2010) and for comparison include these previously unpublished data in Table A2-3 and Figure A2-7e.

There was a general trend of decreasing $\delta^{34}S$ values for oils along a north to south gradient with the PC oils most enriched in ^{34}S, followed by the LT and high maturity WL oils. The low maturity WC and WL oils had similar $\delta^{34}S$ values, and the southern SCJ/MC oils were mostly depleted in ^{34}S (Figure A2-7 & 11). A plot of $\delta^{34}S_{DBT}$ versus

$\Delta^{34}S_{1m-4mDBT}$ (the $\delta^{34}S$ difference between 1-methyl DBT and 4-methyl DBT) provided a good separation of the four northern oil families (Figure A2-5 & 6).
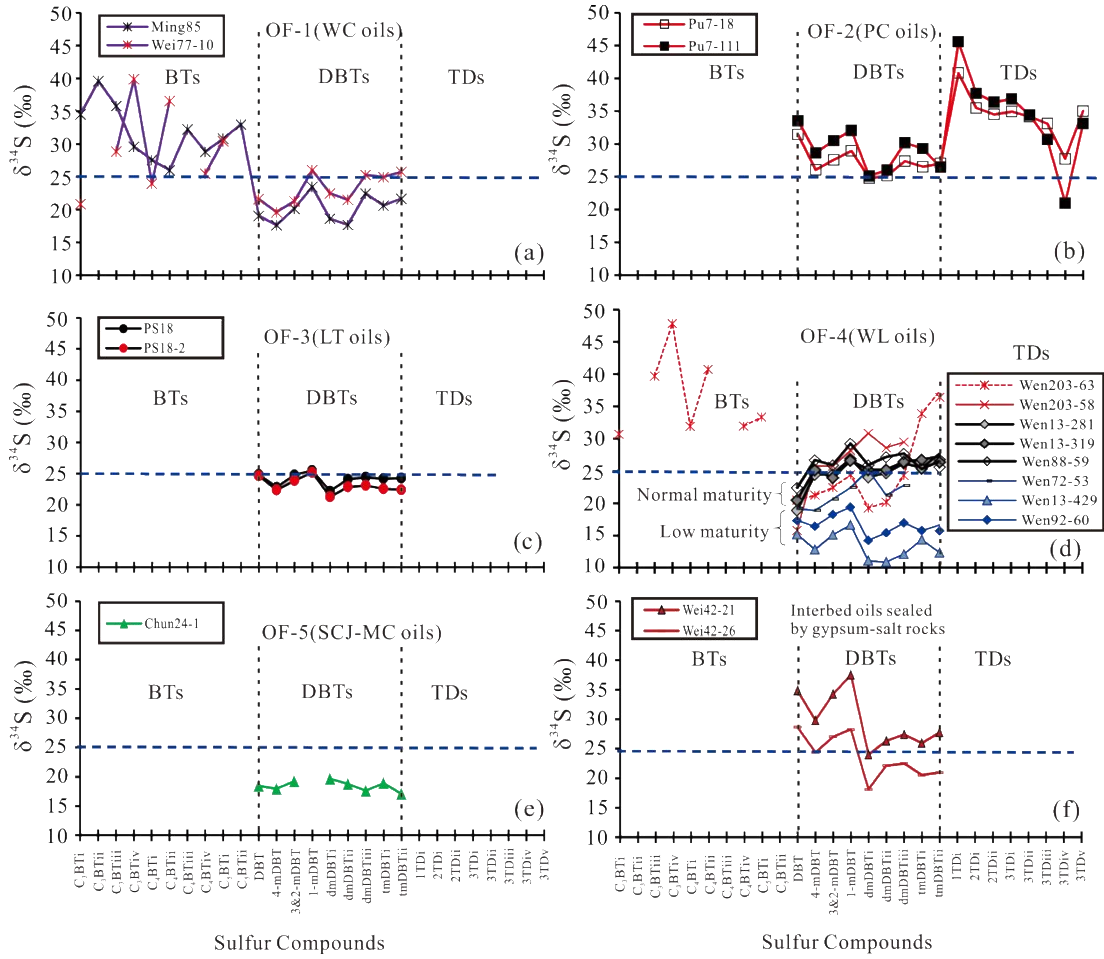
Figure A2-7 Distribution patterns of the compound specific sulfur isotope of the crude oils. Note: Y41 and Y33 were freshwater lacustrine oils collected from Tabei Uplift of the Tarim Basin used for a comparison.
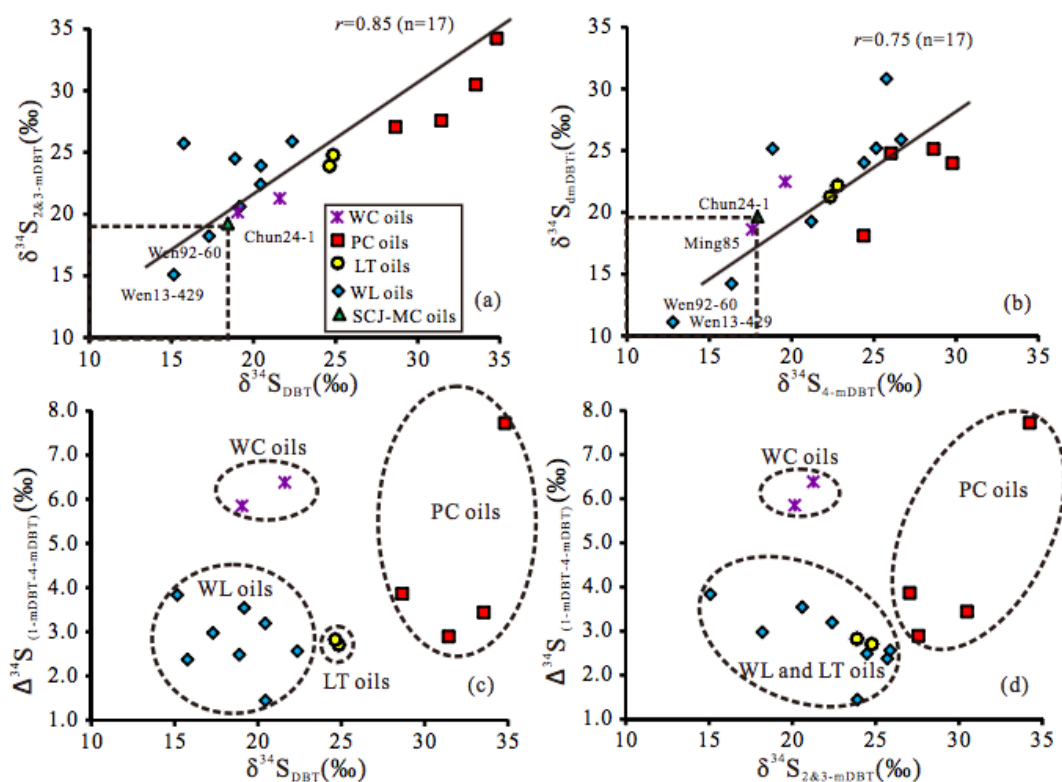
Figure A2-8 Genetic relationship between isomers of sulfur compounds (a) $\delta^{34}S_{DBT}$ versus $\delta^{34}S_{2\&3\text{-mDBT}}$; (b) $\delta^{34}S_{4\text{-DBT}}$ versus $\delta^{34}S_{dmDBTi}$); and classification of the crude oils based on $\delta^{34}S$ values (c) $\delta^{34}S_{DBT}$ versus $\Delta\delta^{34}S_{(1\text{-mDBT-}4\text{-mDBT})}$; (d) $\delta^{34}S_{2\&3\text{-mDBT}}$ versus $\Delta\delta^{34}S_{(1\text{-mDBT-}4\text{-mDBT})}$.

5. Controls and implications of compound specific sulfur isotope

5.1. Sedimentary environment

The $C_{35}\text{-H}/C_{34}\text{-H}$ ratios of the PC and WL oils showed a general trend with $\delta^{34}S_{DBT}$ values and the $C_{35}\text{-H}/C_{34}\text{-H}$ ratios of nearly all oils had an inverse relationship with the $\Delta^{34}S_{1m-4mDBTs}$ (Figure A2-9a and b). Molecular parameters such as $C_{35}\text{-H}/C_{34}\text{-H}$ (and others like Pr/Ph) are sensitive to the salinity and redox conditions of depositional environments (Peters et al., 2005). The S-isotopic relationships identified here with

C_{35}-H/C_{34}-H values suggest that $\delta^{34}S_{OSCs}$ values are strongly influenced by the salinity levels of sedimentary environments. Specifically, a brackish/saline paleo-environment might be conducive to oils with enriched $\delta^{34}S$. This environmental control might also account for the depleted $\delta^{34}S_{OSCs}$ values of the freshwater lacustrine SCJ oil. The bulk $\delta^{34}S$ values of marine carbonates and saline lacustrine crude oils have generally been heavier than those of marine mudstone and freshwater lacustrine oils (Amrani et al., 2005; Zhang et al., 2005; Xue et al., 2014). A similar relationship was not evident between $\delta^{34}S_{DBT}$ and Pr/Ph values (Figure A2-9c) which are sometimes sensitive to salinity, but also strongly responsive to changing redox conditions.

With increasing C_{35}-H/C_{34}-H/salinity the $\delta^{34}S_{OSCs}$ values generally increased (Figure A2-9a), whereas the $\Delta^{34}S_{1m-4mDBTs}$ decreased (Figure A2-9b). This latter trend, evident for all but some WC oils, suggests that with increasing salinity 4-mDBTs were enriched in ^{34}S at a quicker rate than 1-mDBT. This also led to a reduction in the (initial 4‰) isotopic difference between these two mDBT isomers. The $\Delta^{34}S_{1m-4mDBTs}$ parameter did show an increase with the "resin + asphaltene" content of the oils, likely due to the relatively high S-content of these polar fractions, with salinity potentially having less influence on the strong covalently bound S within these moieties.
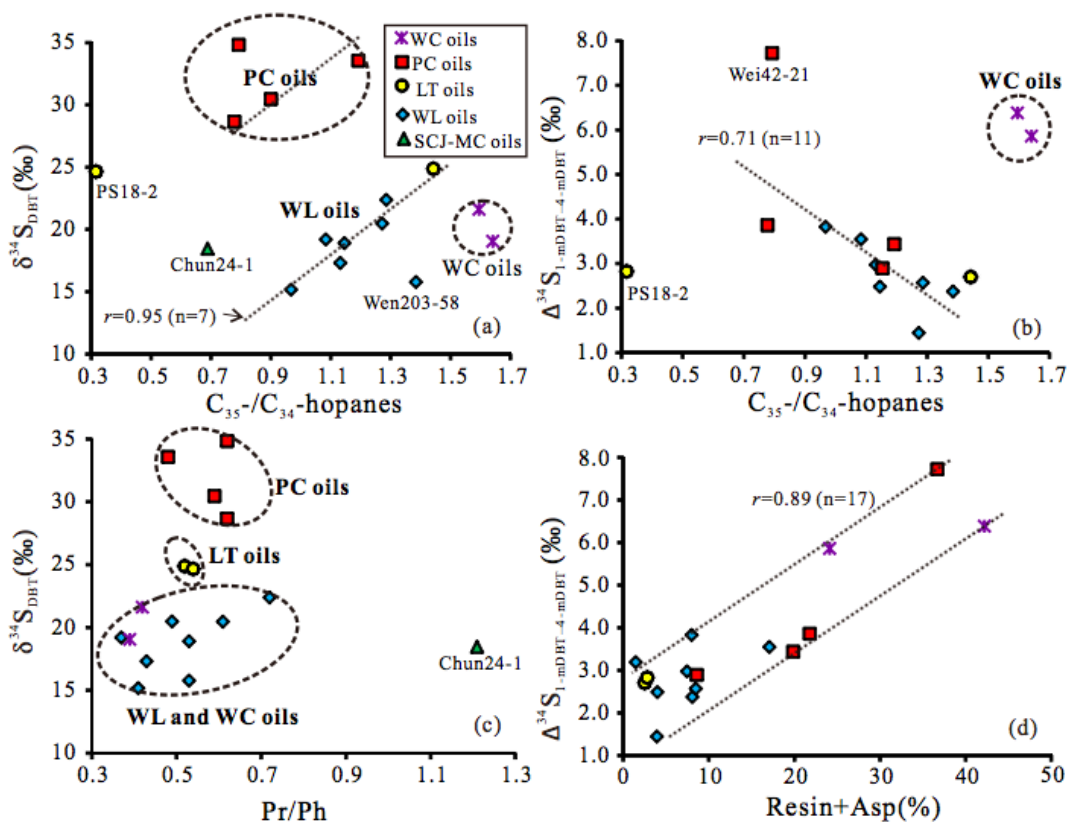
Figure A2-9 Cross plots of sulfur isotopic and hydrocarbon parameters (a) C_{35}-H/C_{34}-Hopane with $\delta^{34}S_{DBT}$; (b) C_{35}-H/C_{34}-Hopane with $\Delta\delta^{34}S_{1-mDBT-4-mDBT}$; (c) Pr/Ph with $\delta^{34}S_{DBT}$ ratios and (d) "resin + asphaltene" with $\Delta\delta^{34}S_{1-mDBT-4-mDBT}$.

5.2. Thermal maturity and $\delta^{34}S$

The $\delta^{34}S_{DBT}$ and $\Delta\delta^{34}S_{1m–4mDBTs}$ values of the oils were compared to established sterane (C_{29} sterane $\alpha\alpha\alpha$20S/(S+R); C_{29} sterane $\alpha\beta\beta$/($\alpha\alpha\alpha$+$\alpha\beta\beta$); diasteranes/regular steranes) and methyl-dibenzothiophene (4-mDBT/1-mDBT) maturity parameters (Figure A2-10). There was a reasonable correlation between these maturity parameters and the $\delta^{34}S_{DBT}$ values of the WL oils (OF-4; Figure A2-10 left). However, the other oils, particularly the PC (OF-2) and WC (OF-1) oils, generally deviated from the

thermal trend suggested for the WL oils. This departure suggests a larger influence of other controls (e.g., depositional environment, TSR) on the $\delta^{34}S_{DBT}$ values of these oils. For instance, the heavy $\delta^{34}S_{DBT}$ values (>29‰) of the PC oils is a typical TSR effect (see 5.2.3).

The difference in the $\delta^{34}S$ values of the 1-mDBT and 4-mDBT isomers of several oils also suggested a potential relationship with the molecular based thermal maturity parameters (Figure A2-10 right). The $\Delta\delta^{34}S_{1m-4mDBTs}$ values showed a strong inverse relationship with the sterane (C_{29} $\alpha\alpha\alpha20S/(S+R)$, $r=0.74$) and mDBT maturity parameters ($r=0.82$) suggesting a certain level of thermal impact on $\delta^{34}S_{mDBT}$ values. A decrease in the magnitude of $\Delta\delta^{34}S_{1m-4mDBTs}$ with increasing maturity can be attributed to the different thermal stabilities of mDBT isomers (4-mDBT > 1-mDBT) and the general homogenization of OSCs with increasing maturity (Amrani, 2014; Ellis et al., 2017). Several samples (e.g., Wei42-21, Wen203-63 and Pu7-18) which deviated from this general trend may have been impacted by TSR - Nb., TSR diagnostic thiadiamondoids were detected in the Wen203-63 and Pu7-18 oils (and also Pu7-111) by GC-MS and at higher sensitivity by Electrospray ionization Fourier transform ion cyclotron resonance mass spectrometry (Unpublished results).

There was no obvious relationship however between $\Delta\delta^{34}S_{1m-4mDBTs}$ and two other sterane maturity parameters (i.e., C_{29} $\alpha\beta\beta/(\alpha\alpha\alpha + \alpha\beta\beta)$ and diasteranes/regular steranes). The complexity of the Dongpu petroleum system is likely responsible for varied relationships observed for particular $\delta^{34}S$ and hydrocarbon-based parameters.
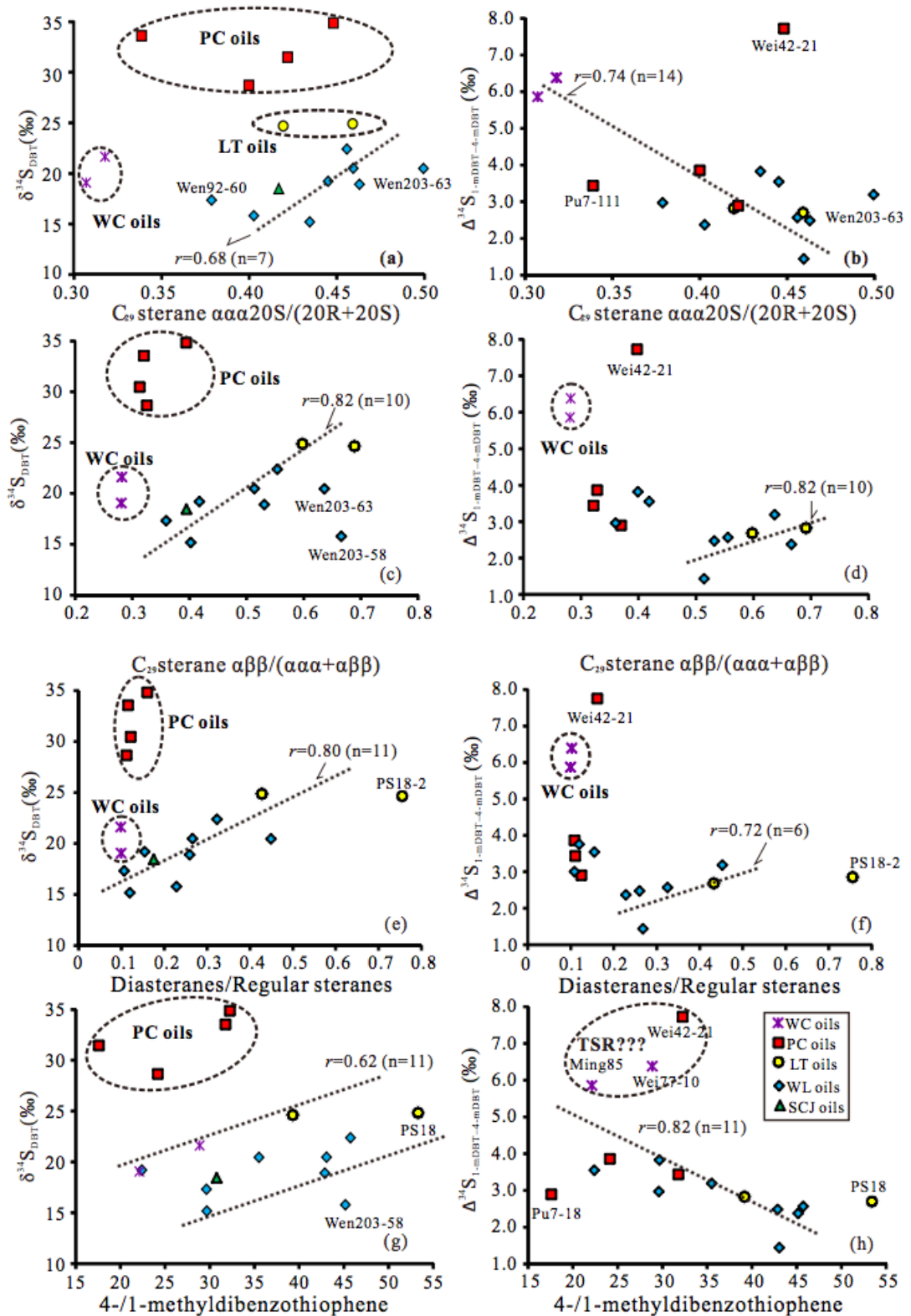
Figure A2-10 Cross plots of sulfur isotopic level with thermal maturity and/or the

relevant parameters.

5.3. Molecular evidence of TSR and its impact on δ^{34}S values

TSR typically occurs at high geological temperatures (> 120°C), although certain conditions can lead to lower temperature initiation (> 120°C; Orr, 1974). Much of the low maturity saline lacustrine oils in the northern Dongpu Depression were sourced from $Es_3 \sim Es_4$ source rocks with a burial depth greater than 3000m (Zhang et al., 2017). Burial history and well-testing data imply the reservoir temperatures at these depths were greater than 110 °C. Fluid inclusion data also indicated temperatures of 125-140 °C for the Wei42-21 and Wei42-26 wells (Jiang et al., 2016). Furthermore, free sulfur and authigenic pyrites, both reagents and products of TSR, have been commonly observed in drill cores from the clastic reservoirs of the Dongpu Depression (Orr, 1974; Zhang et al., 2008).

The $\delta^{34}S_{OSCs}$ data of several WL and PC oils were consistent with TSR impacts. The δ^{34}S values of the C_2–C_4-BT detected in two OF-1 oils (Ming 85, Wei77-10; Figure A2-7a) and one OF-4 oil (Wen203-63; Figure A2-7d) were significantly heavier than the alkyl DBTs in these oils. The $\Delta\delta^{34}S_{BTs–DBTs}$ for Ming85, Wei77-10 and Wen203-63 were 11.66‰, 6.28‰ and 11.77‰ (Table A2-3), respectively. The δ^{34}S values of thiadiamondoids (TDs) detected in the two PC (OF-2) oils were similarly enriched relative to DBTs (Figure A2-7b) - with $\Delta\delta^{34}S_{TDs–DBTs}$ of 7.27‰ (Pu7-18) and 5.38‰ (Pu7-111; Table A2-3), respectively. The δ^{34}S difference between these compound classes has been attributed to their respective stabilities to TSR, with BTs and TDs inheriting the [34]S enriched reduced S of TSR utilized anhydrites at a faster rate than DBTs (Amrani et al., 2012; Gvirtzman et al., 2015). The TDs are themselves diagnostic compounds of TSR (Wei et al., 2012).

The alkyl DBTs of most oils showed some variance in $\delta^{34}S$ values, although the two LT oils (OF-3) and the southern Chun24-1 (OF-1) had a more linear alkyl DBT $\delta^{34}S$ profile (Figure A2-7c). TSR can also lead to large $\Delta\delta^{34}S_{1mDBT-4mDBT}$ values (Ellis et al., 2017) such as observed for several oils across most of the four northern oil families (Ming85, Wei77-10, Wei42-21, Wei42-26, PS18-2, and Wen203-63; Figure A2-10b, d, h).

6. Conclusion

The $\delta^{34}S$ values of OSCs in oils from the Dongpu Depression (Bohai Bay Basin) showed several differences consistent with five biomarker defined oil families, suggesting good potential for the use of compound specific sulfur isotopes in genetic classification of saline and freshwater lacustrine oils. Saline oil samples generally had greater $\delta^{34}S$ values than the freshwater oils and a general trend of increasing $\delta^{34}S$ values along a southerly gradient was consistent with increasing salinity or gypsum development.

The potentially over-lapping influences of S-sources/deposition environment and geochemical processes such as thermal maturity and thermochemical sulfate reduction on the $\delta^{34}S$ values of petroleum S analytes, however, encourages a cautious approach to S-isotopic based oil-source correlations. The $\delta^{34}S$ values of OSCs and a variance in values of different isomers ($\Delta\delta^{34}S_{1mDBT-4mDBT} = \delta^{34}S_{1-mDBT} - \delta^{34}S_{4-mDBT}$) increased by up to several ‰ with increasing oil maturity as indicated by established hydrocarbon and DBT maturity parameters (i.e., C_{29} steranes , Dia/Reg steranes; mDBT index). TSR led to even larger enrichments (up to ~ 10 ‰) of some product groups, with $\Delta\delta^{34}S > 5‰$ between products having a different sensitivity to TSR (e.g., $\delta^{34}S_{BTs-}$

$\delta^{34}S_{DBTs}$; $\delta^{34}S_{TDs}$–$\delta^{34}S_{DBTs}$). A general model of the tectonic belt/oil reservoir setting of the Dongpu Depression and the influences of salinity as well as thermal maturity and TSR on the $\delta^{34}S_{OSC}$ values of the oils is illustrated in Figure A2-11.
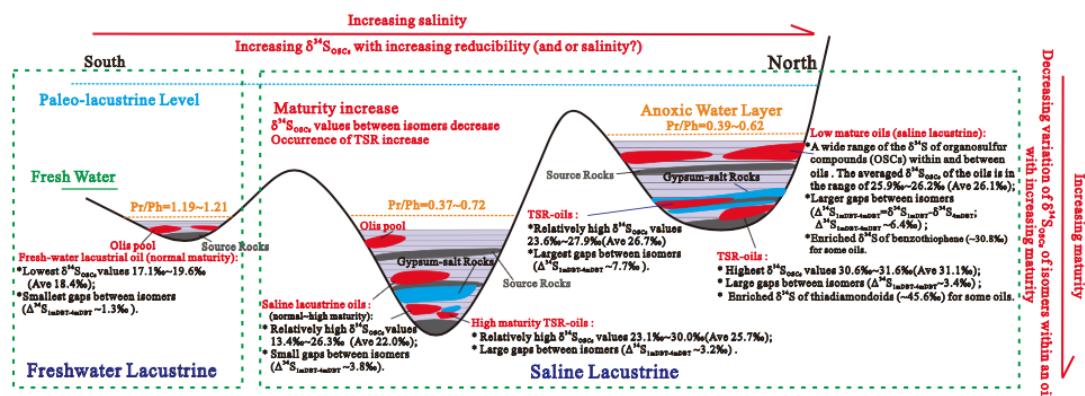
Figure A2-11 A summary model of the distribution characteristics of the compound specific sulphur isotopes in the crude oils from the Dongpu Depression.

Acknowledgement

References

Amrani, A., Lewan, M.D., Aizenshtat, Z., 2005. Stable sulfur isotope partitioning during simulated petroleum formation as determined by hydrous pyrolysis of Ghareb Limestone, Israel. Geochimica et Cosmochimica Acta 69, 5317–5331.

Amrani, A., Sessions, A.L., Adkins, J.F., 2009. Compound-specific δ34S analysis of volatile organics by coupled GC/multicollector-ICP MS. Analytical Chemistry 81, 9027–9034.

Amrani, A., Sessions, A.L., Tang, Y., Adkins, J.F., Hills, R.J., Moldowan, M.J., Wei, Z., 2012. The sulfur-isotopic compositions of benzothiophenes and dibenzothiophenes as a proxy for thermochemical sulfate reduction. Geochimica et Cosmochimica Acta 84, 152–164.

Amrani A., 2014. Organosulfur compounds: molecular and isotopic evolution from biota to oil and gas. Annual Review of Earth and Planetary Sciences 42, 733–768.

Cai, C., Amrani, A., Worden, R.H., Xiao, Q., Wang, T., Gvirtzman, Z., Jia, L., 2016. Sulfur isotopic compositions of individual organosulfur compounds and their genetic links in the Lower Paleozoic petroleum pools of the Tarim Basin, NW China. Geochimica et Cosmochimica Acta 182, 88–108.

Cai, C., Xiang, L., Yuan, Y., Xu, C., He, W., Tang, Y., Borjigin, T., 2017a. Sulfur and carbon isotopic compositions of the Permian to Triassic TSR and non-TSR altered solid bitumen and its parent source rock in NE Sichuan Basin. Organic Geochemistry 105, 1–12.

Cai, C., Xu, C., He, W., Zhang, C., Li, H., 2017b. Biomarkers and C and S Isotopes of the Permian to Triassic Solid Bitumen and Its Potential Source Rocks in NE Sichuan Basin. Geofluids 3, 1–14.

Cai, C., Zhang, C., Worden, R. H., Wang, T., Li, H., Jiang, L., Zhang, B., 2015. Application of sulfur and carbon isotopes to oil–source rock correlation: A case study from the Tazhong area, Tarim Basin, China. Organic geochemistry 83, 140–152.

Chang, Z., Chen, Z., Zhang, Y., Peng, J., Jin, Z., 2007. Investigation on geochemistry characterisitics of crude oil from weicheng-wenmingzhai area in Dongpu depression. Fault-Block Oil Gas Field 14, 1–3 (in Chinese).

Chen, X., Li, S., Zhang, H., Xu, T., Zhang, Y., Wan, Z., Ji, H., Guo, Z., 2018. Controlling Effects of Gypsum-salt on Hydrocarbon Generation of Source Rocks in Dongpu Sag and Its Significance on Petroleum Geology. Geoscience 32, 1125–1136 (in Chinese).

Chen, X., 2017. Hydrocarbon Generation and Accumulation Effect of saline Lacustrine Strata Bearing gypsum-salt Rock in Dongpu Sag, Bohai Bay Basin. PhD dissertation. China University of Petroleum (Beijing), pp. 48–51 (in Chinese).

Connan, J., Cassou, A.M., 1980. Properties of gases and petroleum liquids derived from terrestrial kerogen at various maturation levels. Geochimica et Cosmochimica Acta 4, 1–23.

Ellis, G.S., Said-Ahmad, W., Lillis, P.G., Shawar, L., Amrani, A., 2017. Effects of thermal maturation and thermochemical sulfate reduction on compound-specific sulfur isotopic compositions of organosulfur compounds in Phosphoria oils from the Bighorn Basin, USA. Organic Geochemistry 103, 63–78.

Gao, H., Chen, F., Liu, G., Liu, Z., 2009. Advances, problems and prospect in studies of origin of salt rocks of the Paleogene Shahejie Formation in Dongpu Sag. Journal of Palaeogeography 11, 251–264 (in Chinese).

Gao, H., Zheng, R., Xiao, Y., Meng, F., Chen, F., Bai, G., Luan, Y., Tan, X., Shi, Y., 2015. Origin of the slat rock of Paleogene Shahejie formation in Dongpu sag,

Bohai Bay Basin: evidences from sedimentology and geochemistry. Acta Petroleum Sinica 36, 19–32 (in Chinese).

Greenwood, P.F., Mohammed, L., Grice, K., McCulloch, M., Schwark, L., 2018. The application of compound-specific sulfur isotopes to the oil–source rock correlation of Kurdistan petroleum. Organic Geochemistry 117, 22–30.

Gvirtzman, Z, Said-Ahmad, W., Ellis, G.S., Hill, R. J., Moldowan, J.M., Wei, Z., Amrani, A., 2015. Compound-specific sulfur isotope analysis of thiadiamondoids of oils from the Smackover Formation, USA. Geochimica et Cosmochimica Acta 167, 144–16.

He, N., Grice, K., Greenwood, P.F., 2019. The distribution and δ34S values of organic sulfur compounds in biodegraded oils from Peace River (Alberta Basin, western Canada). Organic Geochemistry 128, 16–25.

Ji, H., Li, S., Greenwood, P., Zhang, H., Pang, X., Xu, T., Shi, Q., 2018. Geochemical characteristics and significance of heteroatom compounds in lacustrine oils of the Dongpu Depression (Bohai Bay Basin, China) by negative-ion Fourier transform ion cyclotron resonance mass spectrometry. Marine and Petroleum Geology 97, 568–591.

Ji, Y., Zhou, S., Cheng, T., 2015. Application of sequence stratigraphy to subtle oil–gas reservoir exploration: take example of the third member Shahejie formation Dongpu Depression. Acta Geologica Sinica 89, 395–395.

Jiang, Y., Fang, L., Liu, J., Hu, H., Xu, T., 2016. Hydrocarbon charge history of the Paleocene reservoir in the northern Dongpu depression, Bohai Bay Basin, China. Petroleum Science 13, 625–641.

Kvalheim, O.M., Christy, A.A., Telnaes, N., Bjørseth, A., 1987. Maturity determination of organic matter in coals using the methylphenanthrene distribution. Geochimica et cosmochimica Acta 51, 1883–1888.

Li, S., Pang, X., Yang, H., Xiao, Z., Gu, Q., Zhang, W., 2010. Geochemical characteristics and families of the crude oils in the Yingmaili Oilfield, Tarim Basin. Geoscience 24(4), 643–653 (In Chinese).

Li, J., Li, S., Xu, T., Guo, Z., Zhang, Y., Ke, C. 2019. Geochemical characteristics and formation mechanism for the lacustrine oils in the South Dongpu Depression. Fault-block oil & gas field. In press (In Chinese).

Li, J., Zhang, J., Liu, S., Fan, Z., Xue, H., Sun, Z., Yu, T., 2016. Sedimentology and sequence stratigraphy of the Paleogene lower second member of the Shahejie Formation, W79 Block, Wenliu Oilfield, Bohai Bay Basin, China. Russian Geology and Geophysics 57, 944-957.

Li, X., Zhang, J., Xie, J., Li, C., Dai, Y., Li, W., Li, S., 2015. Sedimentary and sequence-stratigraphic characteristics of the lower second submember, Shahejie formation, M1 block, Wenmingzhai oilfield, Dongpu depression, China. Arabian Journal of Geosciences 8, 5397–5406.

Liu, L., Ren, Z., 2007. Thermal evolution of Dongpu sag. Petroleum Exploration and Development 4, 419-423 (in Chinese).

Moldowan, J.M., Seifert, W.K., Gallegos, E.J., 1983. Identification of an extended series of tricyclic terpanes in petroleum. Geochimica et Cosmochimica Acta 47, 1531–1534.

Orr, W.L., 1974. Changes in the sulfur content and isotopic ratios of sulfur during petroleum Maturation-study of Big Horn Basin Paleozoic oil. AAPG Bulletin 58, 2295–2318.

Peng, J., Wu, X., He, X., Liu, Y., 2003. Oil and gas accumulating law in Machang area Dongpu Depression. Journal of Shandong University of Science and Technology (Natural Science) 22, 100–112 (in Chinese).

Peters, K.E., Walters, C.C., Moldowan, J.M., 2005. The Biomarker Guide: Biomarkers and Isotopes in Petroleum Exploration and Earth History. Cambridge University Press, Cambridge, New York.

Qi, J., Yang, Q., 2010. Cenozoic structural deformation and dynamic processes of the Bohai Bay basin province, China. Marine and Petroleum Geology 27, 757–771.

Radke, M., Willsch, H., 1993. Generation of alkylbenzenes and benzo [b] thiophenes by artificial thermal maturation of sulfur–rich coal. Fuel 72, 1103–1108.

Radke, M., Vriend, S.P., Ramanampisoa, L.R.., 2000. Alkyldibenzofurans in terrestrial rocks: influence of organic facies and maturation. Geochimica et Cosmochimica Acta 64, 275–286.

Raven, M., Adkins, J., Werne J., Lyons T., Sessions. A. 2015. Sulfur isotopic composition of individual organic compounds from Cariaco Basin, Organic geochemistry 80, 53-59.

Rosenberg, Y.O., Meshoulam, A., Said-Ahmad, W., Shawar, L., Dror, G., Reznik, I.J., Feinstein, S., Amrani, A., 2017. Study of thermal maturation processes of sulfur rich source rock using compound specific sulfur isotopes analysis. Organic Geochemistry 112, 59–74.

Shao X., Pang X., Li H., Hu T., Xu T., Xu Y., Li B., 2018. Pore network characteristics of lacustrine shales in the Dongpu Depression, Bohai Bay Basin, China, with implications for oil retention. Marine and Petroleum Geology 96, 457–473.

Scalan, E. S., Smith, J. E., 1970. An improved measure of the odd-even predominance in the normal alkanes of sediment extracts and petroleum. Geochimica et Cosmochimica Acta 34, 611–620.

Wang, M., Sherwood, N., Li, Z., Lu, S., Wang, W., Huang, A., Peng J., Lu, K., 2015. Shale oil occurring between salt intervals in the Dongpu Depression, Bohai Bay Basin, China. International Journal of Coal Geology 152, 100–112.

Wei, Z., Walters, C.C., Moldowan, J.M., Mankiewicz, P.J., Pottorf, R.J., Xiao, Y., Maze, W., Nguyen, P.T.H., Madincea, M.E., Phan, N.T., Peters, K.E., 2012. Thiadiamondoids as proxies for the extent of thermochemical sulfate reduction. Organic Geochemistry 44, 53–70.

Xue, C., Chi, G., Li, Z., Dong, X., 2014. Geology, geochemistry and genesis of the Cretaceous and Paleocene sandstone-and conglomerate-hosted Uragen Zn–Pb deposit, Xinjiang, China: A review. Ore Geology Reviews 63, 328–342.

Zhang, H., Li, S., Xu, T., Pang, X., Zhang, Y., Wan, Z., Ji, H., 2017. Characteristics and formation mechanism for the saline lacustrine oil from the north Dongpu sag. Geoscience 31, 768–778 (in Chinese).

Zhang, K., Qi, J., Zhao, Y., Chen, S., 2007. Structure and evolution of cenozoic in Dongpu sag. Xinjiang Petroleum Geology 28, 714–717 (in Chinese).

Zhang, S., Zhu, G., Liang, Y., Dai, J., Liang, H., Li, M., 2005. Geochemical characteristics of the Zhaolanzhuang sour gas accumulation and

thermochemical sulfate reduction in the Jixian Sag of Bohai Bay Basin. Organic Geochemistry 36, 1717–1730.

Zhang, T., Amrani, A., Ellis, G.S., Ma, Q., Tang, Y., 2008. Experimental investigation on thermochemical sulfate reduction by H_2S initiation. Geochem. Geochimica et Cosmochimica Acta 72, 3518–3530.

Appendix 3

This page details the rights granted by Elsevier, to the first author of the publication that forms Chapter 3 of this thesis, to reproduce the full article in a thesis or dissertation.

Appendix 4

Statement of Contribution to Co-authored Paper

Chapter 3 includes the co-authored paper "The distribution and δ^{34}S values of organic sulfur compounds in biodegraded oils from Peace River (Alberta Basin, western Canada)" published on Organic Geochemistry. The bibliographic details of the co-authored paper, including all authors are:

Nannan He, Kliti Grice, Paul F. Greenwood. (2019) The distribution and δ^{34}S values of organic sulfur compounds in biodegraded oils from Peace River (Alberta Basin, western Canada). Organic Geochemistry 128, 16–25.

I, Nannan He, as the primary author, conducted all the experimental work and data analysis, including creating figures and tables, and writing and editing the manuscript.

I, as a co-author, endorsed that the level of contribution by the candidate indicated above is appropriate.

Kliti Grice

Paul F. Greenwood

Chapter 4 includes the co-authored paper "Source of organic sulfur in petroleum of the Jinxian Sag (Bohai Bay Basin, China) revealed by compound specific sulfur isotope analysis" to be submitted to Organic Geochemistry. The bibliographic details of the co-authored paper, including all authors are:

Nannan He, Kliti Grice, Paul F. Greenwood. (2020) Source of organic sulfur in petroleum of the Jinxian Sag (Bohai Bay Basin, China) revealed by compound specific sulfur isotope analysis. Paper in preparation for submission to Organic Geochemistry.

I, Nannan He, as the primary author, conducted all the experimental work and data analysis, including creating figures and tables, and writing and editing the manuscript.

I, as a co-author, endorsed that the level of contribution by the candidate indicated above is appropriate.

Kliti Grice

Paul F. Greenwood

Chapter 5 includes two co-authored papers "δ^{34}S characteristics of OSCs in oils from Tazhong Uplift, Tabei Uplift and Southwest Depressions of the Tarim Basin (W. China)" and "δ^{34}S character of organic sulfur compounds in the pyrolysis released asphaltene fraction of a TSR impacted oil" to be submitted to Organic Geochemistry. The bibliographic details of the co-authored papers, including all authors are:

Nannan He, Kliti Grice, Guangyou Zhu, Paul F. Greenwood. (2020) δ^{34}S characteristics of OSCs in oils from Tazhong Uplift, Tabei Uplift and Southwest Depressions of the Tarim Basin (W. China). Paper in preparation for submission to Organic Geochemistry.

I, Nannan He, as the primary author, conducted all the experimental work and data analysis, including creating figures and tables, and writing and editing the manuscript.

I, as a co-author, endorsed that the level of contribution by the candidate indicated above is appropriate.

Kliti Grice

Guangyou Zhu

Paul F. Greenwood

Nannan He, Kliti Grice, Paul F. Greenwood. (2020) δ^{34}S character of organic sulfur

      compounds in the pyrolysis released asphaltene fraction of a TSR impacted

      oil. Paper in preparation for submission to Organic Geochemistry.

I, Nannan He, as the primary author, conducted all the experimental work and data
analysis, including creating figures and tables, and writing and editing the manuscript.

I, as a co-author, endorsed that the level of contribution by the candidate indicated
above is appropriate.

Kliti Grice

Paul F. Greenwood